Client:
Rijkswaterstaat Waterdienst

Hydra-Zoet for the fresh water systems in the Netherlands

Probabilistic model for the assessment of dike heights

Author: C.P.M. Geerse (HKV CONSULTANTS)
In cooperation with: R.M. Slomp (Rijkswaterstaat Waterdienst), J.P. de Waal (Deltares)

PR2168 December 2011

HKV CONSULTANTS

Preface

In my contacts abroad I have often missed a book or report which explains in detail how we carry out the assessment of flood defences in the Netherlands. The books 'Fundamentals on Water Defences' [TAC, 1998] from 1998 and 'Water in the Netherlands, Managing Checks and Balances' [Huisman, 2004] provide a lot of insight in Dutch flood management policy. The only comprehensive English language publication on probabilistic tools to calculate hydraulic loads (the combined effect of water levels and waves) in the Netherlands, is the book 'Probabilistic design of flood defences' from 1990 [CUR/TAW, 1990]. In the 1990's Rijkswaterstaat and institutes started experimenting with probabilistic dike assessment tools such as PC-ring, Peilof and Dijkring. Since 1994 we have already had three generations of probabilistic dike assessment tools, one of the latest of which is the model Hydra-Zoet (PC-Ring has been under development until today as well). The model Hydra-Zoet is the main topic of this report. Currently, we are developing a fourth generation probabilistic model, in which PC-Ring will be combined with Hydra-Zoet.

The most important reasons for having this report written are:

- to show how the probabilistic model Hydra-Zoet works,
- providing a summary on the current probabilistic tools for the formal assessment of flood defences from 2012 until 2017,
- closing a chapter of more than a decade (1997-2011) in the development of the current probabilistic tools,
- laying the foundation for the development of new probabilistic tools, setting a standard and helping people to make choices when they design probabilistic tools,
- making an international review of our work possible by the International Advisory Commission Delta Model, a committee installed to review the work of the Deltamodel (Hydra-Zoet is the main component of the safety assessment in the Deltamodel),
- to provide a documentation of our work in the English language.

The development of Hydra-Zoet has been the work of a lot of people; this report has also been written to honour their work and to make it available to others. My role was mostly limited to setting goals, asking other people how to get there, and finding some of the necessary funding.

A comprehensive book in English on the whole process of the assessment of flood defences, involving much more than just Hydra-Zoet, still has to be written. Translating the books containing the 'Hydraulic Boundary Conditions 2006' [HR, 2006], and the 'Safety Regulations for the Assessment of Primary Flood Defences' [VTV, 2007], is not very useful, since they are tailored to the Dutch situation. Also, they cannot be used without a lot of contextual information. For the most important failure modes, technical reports are available in English on the ENW website: http://www.enwinfo.nl/. However, the Dutch versions precede the English by a number of years.

Robert Slomp
Project leader Flood Defences Assessment and Design tools (TOI), Waterdienst

Robert.slomp@rws.nl

Contents

1 Introduction

1.1 General

According to the Water Act [Waterwet, 2009], the Dutch primary flood defences have to be assessed every six years. To that purpose Hydraulic Boundary Conditions (HBC) are used, consisting of normative water levels and wave conditions. The most recent ones date from the year 2006 (HBC2006). A large part of the Hydraulic Boundary Conditions are determined with so-called Hydra models. These are probabilistic models, implemented in computer programs. They are used to assess the primary flood defences along the major water systems in the Netherlands, i.e. along the rivers Rhine and Meuse and their branches and the river (Overijsselse) Vecht, along the large lakes Lake IJssel and Lake Marken and along the coast.

Two important water systems are the *tidal river area* and the *Vecht and IJssel delta*. The tidal river area is that part of the lower reaches of the Rhine and Meuse where storms on the North Sea have a significant effect on the water levels during high discharge waves. The Vecht and IJssel delta consists of the lower reaches of the Vecht and IJssel (a branch of the river Rhine) where storm surges (generating wind set-up) from Lake IJssel have a significant effect on the water levels during high discharge waves. For the tidal river area the model Hydra-B is available, and for the Vecht and IJssel delta the model Hydra-VIJ. These models have been developed by Rijkswaterstaat Waterdienst (the executive arm of the Ministry of Infrastructure and Environment), and HKV Consultants from 1999 until recently.

The models Hydra-VIJ and Hydra-B, both developed for river deltas, have many similarities, and in the past years it became apparent that these models can be constructed in a more uniform way. All the so-called "slow" stochastic variables in these models, such as discharges and lake levels, can be modelled using the same type of schematisation. It also turned out that the upper reaches of these rivers, as well as the lakes Lake IJssel and Lake Marken, fitted into the general scheme of this model, meaning that all primary flood defences of the fresh water systems could be included in a single new probabilistic model.[1] This model, called Hydra-Zoet, has recently been implemented. Such a single model offers big advantages in terms of clarity, management and maintenance.

The formulas of Hydra-Zoet fall in one of two classes: they can be used for locations along a river where

1. a river discharges into the *sea*, or when
2. a river discharges into a *lake* (in this case also locations along the lake are part of the model).

A water system of the first class is called a *sea delta*, and one of the second a *lake delta*. The tidal-river area is of the first type, whereas the water system Vecht and IJssel delta is of the second. One could argue that a sea delta should be seen as a special case of a lake delta, since a sea can be seen as a (very) big lake. In principle, this is true. The reason to make this distinction is that for the lake delta the wind set-up in Hydra-Zoet *is calculated with a physical model* (like WAQUA), whereas for the sea delta this wind set-up, due to a storm surge, is

[1] To be precise: there are several types of primary flood defences (types a, b, c and d). The mentioned primary flood defences in this case all belong to type a, but an exact definition is not needed here.

handled using the sea level *as a random variable*. This means that for a lake probabilities of elevated water levels due to wind set-up are obtained from statistical information for the wind, whereas probabilities for elevated water levels for the sea are obtained (directly) from statistical information for the sea level.

1.2 Aim of this report

The two types of water systems, sea delta and lake delta, are of a general nature. This makes it plausible that the model Hydra-Zoet could also be used in countries other than the Netherlands. This report has been written with the hope that the model will indeed be used in other countries, and the aim of this report has been to provide, firstly, as much information as needed to judge whether or not the model is applicable elsewhere, and secondly, to provide information about the physical and statistical models and input that is required to make the model Hydra-Zoet work. However, we note, that once these aims are fulfilled, the report also serves as a documentation of Hydra-Zoet for the Dutch users of the model. This documentation is also useful in the development of new and more advanced models for the Dutch water systems.

To fulfil those aims, the report contains detailed statistical and mathematical formulas for the model Hydra-Zoet. It also discusses (but in less detail) the physical models for waves and water levels and the way boundary conditions have to be used in these models to generate proper input for Hydra-Zoet. Also a general method is described to derive hydrographs for river discharges and lake levels. A hydrograph provides the (average) evolution in time of a discharge wave or of a lake-level wave (a hydrograph does not include wind set-up). These hydrographs are needed for a proper schematisation of the time behaviour of discharges and lake levels in the model Hydra-Zoet. Also, a very flexible bivariate correlation model is provided, which can be used to correlate e.g. discharges and lake levels, or wind speeds and storm surges. The hope of the authors is that the account in this report about the way physical calculations are made and about the methods to derive hydrographs and correlation models will be sufficiently clear for people to apply them in countries other than the Netherlands.

To provide a context for the Hydra models, the report starts with an explanation of a part of the Dutch flood management policy and the process of the assessment of flood defences.

1.3 Scope of the report

This report has been written to show how the Hydra-Zoet model was developed, where the main focus is on the *probabilistic* part of the model (and not on physical models used to generate input). The computer program Hydra-Zoet contains several options and failure mechanisms. For transparency, this report only treats the major options and failure mechanisms of this model: *overflow* and *wave overtopping*, used respectively in the calculation of *normative water levels* and *required dike heights*, corresponding to exceedance frequencies given by law. These concepts play an important role in the mandatory assessment of the flood defences every six years. Other options and failure mechanisms, such as the determination of wave conditions for the assessment of dike revetments, are left out of the description.

It is noted that the mathematical parts of the report require a fair amount of statistical and mathematical background, although the most complicated formulas are left out of the main text and put in the appendices.

1.4 Structure of the text

The report has been divided into four parts:

- Part 1: General (Chapters 2 - 8)
  A general part with:
  - the role of Hydra-Zoet for assessment, design and policy,
  - a brief description of the fresh water systems,
  - general information concerning physical models for waves and water levels,
  - general information about statistical descriptions of correlations and the time evolutions of random variables.

- Part 2: Sea delta (Chapters 9 - 12)
  This part describes the physical, statistical and probabilistic aspects of the model Hydra-Zoet for a sea delta, in this case the delta of the rivers Rhine and Meuse. This delta is also denoted as the tidal-river area or simply the tidal area.

- Part 3: Lake delta (Chapters 13 - 16)
  This part describes the physical, statistical and probabilistic aspects of the model Hydra-Zoet for a lake delta, in this case the delta of the Vecht and IJssel.

- Part 4: Appendices
  This part consists of two appendices with mathematical details.

1.5 About the literature

As already mentioned in the preface, very few English language publications are available which deal with the probabilistic tools and models concerning Hydraulic Boundary Conditions and the assessment of flood defences in the Netherlands. One of the main reasons for writing this report is to partly fill this gap. When writing about the development of Hydra-Zoet, and of its predecessor Hydra-B and Hydra-VIJ, we cannot avoid, though, referring to all kinds of reports and publications written in the Dutch language. Because of this 'language problem', we restricted ourselves as much as possible, including only publications strictly needed to understand the text or judge the quality and/or background of the model.

Part 1: General

2 Assessment, and use of Hydra-Zoet for design and policy

This chapter provides a context for the program Hydra-Zoet. First, remarks are made about the current assessment of dikes in the Netherlands. Next, safety approaches are discussed which are currently under investigation. Then it is briefly explained how Hydra-Zoet can be used for design and policy purposes. The chapter concludes with remarks about the various types of input of the model, when using it for (standard) assessments, or for design or policy purposes.

2.1 Assessment

The part of the Netherlands that can be flooded by the sea or by one of the large rivers of the country, is divided into *dike rings*. Every dike ring is enclosed by a continuous line of flood defences (dikes, dunes, high grounds), protecting the area against flooding.

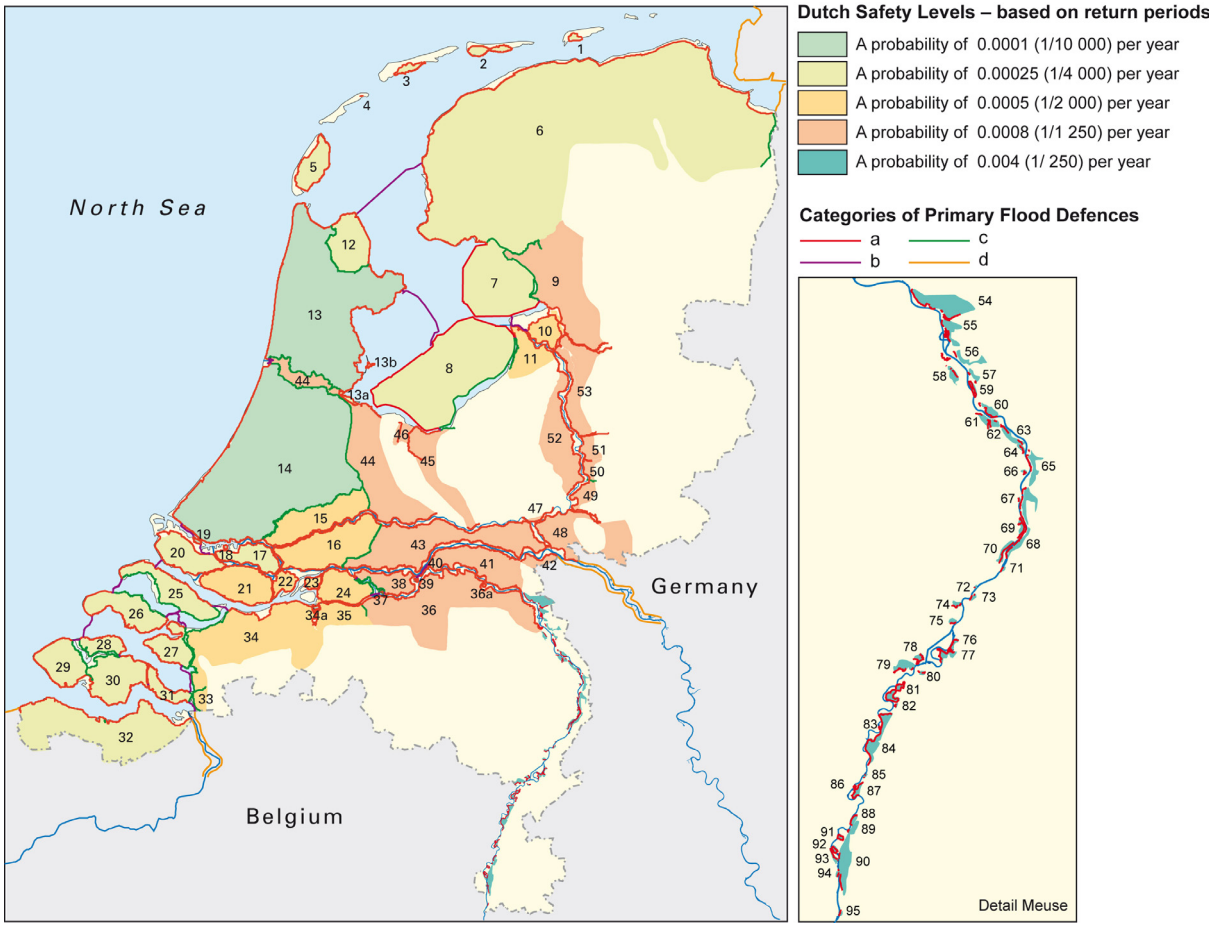

Figure 2-1 The dike rings in the Netherlands with corresponding safety standards according to the Water Act. Note that the panel at the right/below corner applies to the part of the river Meuse in the south-east of the Netherlands.

Every dike ring has its own safety standard, formalised in the Water Act [Waterwet, 2009]. The safety standard of a flood defence is provided in terms of an exceedance frequency (number of times per year) of the water level this flood defence is supposed to be able to withstand. These

safety standards are such that the flood defences should be able to withstand loads (e.g. elevated water levels and wind waves) that are much higher than those encountered over the past century. The dike rings, together with their safety standards, are indicated in Figure 2-1. Note that about 2/3 of the Netherlands is flood prone by the sea or one of the large rivers, whereas about 1/3 consists of high grounds where such floods do not occur.[2]

The Water Act states that the flood defences enclosing dike rings have to be assessed every 6 years: it has to be verified whether they still comply with the safety standards. We note that the Water Act replaces the older Flood Defences Act [Wwk, 1996], which prescribed a 5-yearly assessment period. The new period of 6 years is in line with the period prescribed by the European Flood Risk Directive. Under the older act, there have been three assessment periods: 1996-2001, 2001-2006 and 2006-2011. For each of these periods the Hydraulic Boundary Conditions have been derived and published. The most recent ones, for the period 2006-2011, are denoted as the HBC2006. This assessment period will be succeeded by the periods 2011-2017, 2017-2023 and so on. Most of the statistical information in this report corresponds to the HBC2006.

In the 5- or 6-yearly assessment 'assessment rules' are used for each failure mode to compare the strength of the flood defence with the hydraulic loads that are derived at the normative frequency for the dike ring considered. Examples of 'strength properties' are the present crest height of the dike and the thickness and constitution of its revetment. The hydraulic loads on the flood defences are mainly determined by the water levels and wind waves at the toe of the flood defence. By law, all water boards and Rijkswaterstaat have so-called ledgers which contain all information about the flood defences.[3]

The assessment rules are collected in a report which we denote here as 'Safety Regulations for the Assessment of Primary Flood Defences' (the translation of the Dutch title: 'Voorschrift Toetsen op Veiligheid Primaire Waterkeringen', see reference [VTV, 2007]).

To use these rules, the Hydraulic Boundary Conditions are needed. The most important conditions are *normative water levels*[4], i.e. water levels derived from the normative frequency, and (a range of) *wave conditions* which are relevant at the normative frequency. These wave conditions consist of the significant wave height, a measure for the wave period (e.g. the peak period) and the wave direction. Besides these water levels and wave conditions, some other types of Hydraulic Boundary Conditions are needed, e.g. the (average) time behaviour of the water level thought to be representative during a threatening situation. Some of the Hydraulic Boundary Conditions needed for the assessment are provided in a report (in Dutch: het Hydraulische Randvoorwaardenboek [HR, 2006]), while others are calculated by the computer program Hydra-Zoet for the fresh waters and Hydra-K for the sea and estuaries. The two reports containing (part of) the Hydraulic Boundary Conditions and the assessment rules (VTV), together with Hydra-Zoet and Hydra-K, form the main instruments for the 6-yearly assessment of flood defences.

[2] There are occasions, however, in which water logging or mud flows occur due to extreme rainfall (in the southern part of Limburg).

[3] A ledger is often a combination of digital tools, with as main content a GIS tool in combination with a database; for dike ledger information, IRIS is the database standard.

[4] Normative water levels are used in the 5- or 6-yearly dike assessments, and should reflect the situation at the final year of the assessment period. They are different from the so-called design water levels (used for new or reconstructed flood defences) where such levels represent the (expected) situation at the end of a design period of e.g. 50 or 100 years.

Both the hydraulic loads and the strength properties vary along a dike ring. Therefore a dike ring is divided into a sequence of consecutive dike or dune sections. Those are parts of the dike ring which are uniform regarding load and strength properties. These sections are then assessed separately, with Hydraulic Boundary Conditions determined separately for every section.

So, summarising, in the 6-yearly assessment of the (primary) flood defences, the following information is needed:

- Characteristics of the flood defences, described/stored in ledgers.
- Assessment rules for all failure models, which are collected in a report, called (after translation) 'Safety Regulations for the Assessment of Primary Flood Defences', [VTV, 2007], updated every 6 years.
- Hydraulic Boundary Conditions, updated every 6 year. Part of the Hydraulic Boundary Conditions are published in a report, see e.g. [HR, 2006] for the latest version, and part of them can be calculated with the computer programs Hydra-K and Hydra-Zoet.

2.2 Safety approaches

2.2.1 Different developments and safety approaches

The field of study occupied with the determination of the Hydraulic Boundary Conditions appears to be rather complex and therefore inaccessible. One cause is that the field is the domain of experts, with only a small number of people working in it. A second cause is the wide range of methods used and the diversity of paths along which developments take place. This section comments on the second cause.

In the Netherlands, concerning flood safety, three main paths of developments can be distinguished [Stijnen et al, 2008]:

- *Path 1: current safety approach*
  Within this line of development, the safety of the flood defences has to be guaranteed with assessment tools based on current legislation.
- *Path 2: the evaluation of the flood-safety policy*
  Within this line of development, it is investigated whether the current legislation still is the most proper and adequate approach to assess our safety against flooding, or that adjustments or improvements have to be made.
- *Path 3: long-term developments*
  Within this line of development, expertise is developed in several research projects. Here advanced scientific research is performed by a number of institutes and organisations: Rijkswaterstaat Waterdienst, Deltares, universities, research institutes and consultants.

In each of these development paths four approaches can be considered according to [TAW, 1998] when calculating probabilities or flood risks.[5]

1. overload approach per dike section,
2. overload approach per dike ring,

[5] For the sake of simplicity, we do not consider dunes, since these are not relevant for the main subject of this text.

3. flood (inundation) probability approach,
4. flood (inundation) risk approach.

Without going into details, we provide some comments on these approaches. The first approach originates from the Delta Committee, which was installed just after the storm surge disaster of 1953 which flooded the south-west of the Netherlands. According to the Delta Committee, a dike was said to be overloaded during a threatening event if a certain critical discharge q_{crit} (in litres per metre dike) was exceeded by the water flowing over the dike.[6] Note that overloading in this way does not necessarily mean that the flood defence will collapse; the idea behind this approach is that it is not easy to find out what exactly happens when the overtopping exceeds q_{crit}. The value of q_{crit} is determined in a deterministic way, and depends on a few rough structural characteristics of the dike (e.g. quality of the grass on the inner slope). Once a critical discharge q_{crit} has been established, the annual probability that the loads are such that the actual discharge q exceeds q_{crit} can be calculated. This probability should not exceed the safety levels (norm probabilities) indicated in Figure 2-1.[7]

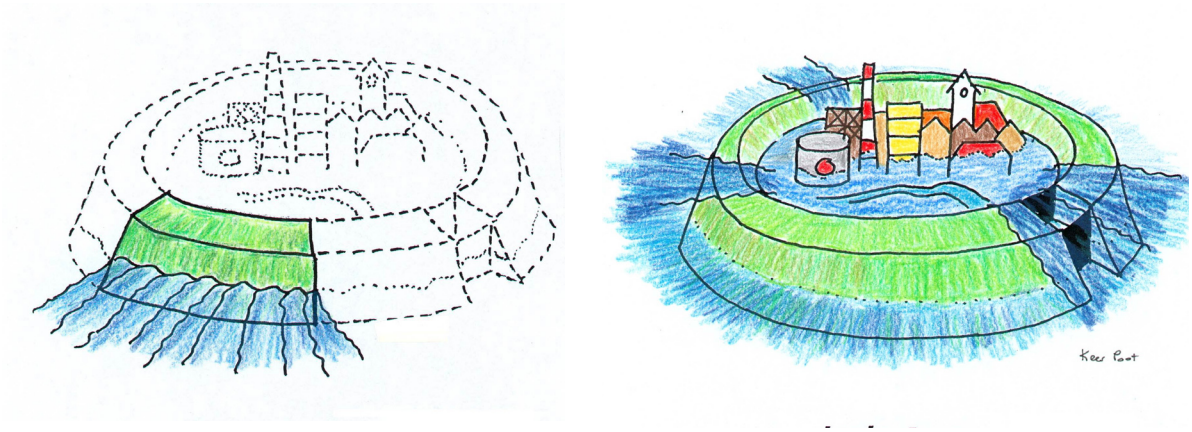

Figure 2-2 Dike section versus dike ring approach. For a dike section (left panel) only threats per section are considered, whereas for the complete ring (right panel) all threats along the ring are considered. Source: Kees Poot, Rijkswaterstaat.

In the second approach, instead of a single dike section, all dike sections of the dike ring area are considered jointly. In practice, this results in crest heights which have to be higher than required according to the first approach. To further clarify this, suppose that all dike sections, numbered i = 1, 2,.., n, satisfy a common safety level (i.e. the norm probability), in the sense that *for every* section i the probability that the overtopping discharge q_i exceeds $q_{crit,i}$ is smaller than the norm probability. In this case the probability that *somewhere* along the ring one of the critical discharges is exceeded can be *larger* than this norm probability, for the reason that the ring as a whole is sensitive to a much larger variety of threats then a single section, see Figure 2-2 (threats can be storm surges, wind storms from different directions, discharges). For instance the ring as a whole might be sensitive (among other things) to eastern as well as to western storms, whereas a particular section might be sensitive only to eastern storms and another section to western storms. If both sections have crest heights according to a norm probability of 1/1000 per year, the exceedance probability of the ring will be larger than 1/1000, since the ring as a whole will be hit by both the eastern and the western storm.

[6] Strictly speaking, the Delta Committee used a criterion in terms of the so-called 2% wave run-up, which later was transformed into a criterion concerning a permissible overtopping discharge.

[7] In fact, we tacitly identify exceedance probabilities with exceedance frequencies here, which is justified for exceedance frequencies smaller than 1/10 per year. For this range of frequencies, these probabilities and frequencies are close to each other, see Appendix A.

The current safety policy, in line with the Water Act, is the one according to the first approach, although occasionally also the second approach is used. The model Hydra-Zoet considers both approaches, at least for the failure mechanisms overflow and overtopping considered in this report.

In the third approach, the flood probability approach, failure corresponds to an impermissible amount of flooding somewhere within the dike ring. Failure here originates from the 'sum' of all possible (failure) mechanisms that lead to impermissible flooding. In this case strength and load both have to be considered in a (semi-) probabilistic manner, whereas in the first and second approach only the loads are treated probabilistically.

The fourth approach, the flood risk approach, considers the risk for an entire dike ring. Important ingredients in this approach are not only the failure probability of the dike ring, but also the number of victims and economic damage. A flood risk approach is a safety consideration in which the consequences of flooding (victims, damage) can vary depending on the location of the breach.

2.2.2 Future developments

The current legislation is based on the first approach (overload per dike section), but there is a broadly shared opinion that in the future the fourth approach should be embraced. A lot of developments in the field of the Hydraulic Boundary Conditions, assessments and design of flood defences investigate the applicability of this approach. One of the most important projects is *Flood Risks and Safety in the Netherlands (Floris)* [Floris, 2005], (*Veiligheid Nederland in Kaart or VNK in Dutch*). In this project the current safety of all the dike rings in the Netherlands is investigated according to the fourth approach. An important instrument in this approach is the computer program PC-Ring [Vrouwenvelder et al, 2003], in which strength and load properties are both handled probabilistically. Due to the vast number of variables the probabilistic calculations can (for practical purposes) only be performed with approximation methods. Also, in PC-Ring time dependent loads (such as lake levels or discharge waves) are modelled in a simplified way, using so-called FBC-models explained in section 8.2.1.

Recently, a new project has been started, the project TOI (in Dutch: Toets- en Ontwerp Instrumentarium). In this project a new model for assessments and design of the primary flood defences is developed, called Hydra-Ring. The aim of this model is to replace the model PC-Ring as well as the Hydra-models, in such a way that the modelling of the loads and strengths is improved [Geerse et al, 2010]. Moreover, new approximation methods will be built into this program [Vrouwenvelder en Courage, 2010]. The new program should incorporate and combine the knowledge obtained from the Floris-project and PC-Ring with those obtained from Hydra-Zoet.

2.3 Hydra-Zoet for design purposes

The assessment of the primary flood defences is carried out every six years. If a flood defence does not pass the assessment, or in case of a physical change of the area to which the defence belongs (e.g. a change in the river bed), a design has to be made for a new flood defence (or a new structural work). On the basis of the technical report about design loads [Van Velzen en Beyer, 2007] and the report with guidelines for designs along the rivers [LR, 2007], the following can be said.

Situation (intended measure)	Usual planning period
widening of the riverbed	50 years
adaptation/construction of a dike with grass cover	50 years
adaptation/construction of a dike in urban area	100 years
adaptation/construction of a structural work	100 years

Table 2-1 Usual planning periods for some intended measures.

A design is made for a planning period of 50 or 100 years (Table 2-1). During this period the implemented design needs to function without radical or costly adjustments. Preferably a design needs to be extendible (flexible): after implementation it should be easy to extend it to comply to more severe (design) demands. This way of designing is part of the concept *robust design*. In the guidelines for designs along the rivers [LR, 2007], three requirements for designs are formulated:

- In the design loads one has to account for the expected increases of river discharges, sea levels and lake levels, on account of climate change during the planning period.
- To account for the uncertainties in water levels, for the upper and lower reaches of the rivers, a standard 'robustness increment' of 0.3 m is taken. In theory, this increment also accounts for other uncertainties, like e.g. those in wave run-up. However, in the design, one may discard this standard increment if a probabilistic analysis, including all kinds of uncertainties, points out that this standard increment is inadequate.
- If a design is not extendible, it is recommended that the design loads are based on more extreme climate scenarios then those used for extendible designs.

The model Hydra-Zoet uses as input for the statistical and physical data information corresponding to the assessment period 2006-2011. Also, some climate scenarios are included in the program, with which design loads can be determined, provided necessary (physical) input is available. In case of the latter type of input, think of water levels and wave characteristics (derived from discharges, lake levels and wind), which change if the considered area is changed by e.g. digging side channels, or river widening or deepening.

2.4 Hydra-Zoet for policy purposes

A number of flood risk analyses on account of flooding have been carried out, or are still being investigated, to support policy purposes. Two of the most important projects are:

- Safety against flooding 21st Century (in Dutch: 'Waterveiligheid 21e eeuw', abbreviated WV21).
- The Delta program, carried out for the water systems: lake area, upper rivers, tidal rivers.

In the following we will comment on these projects, in relation with Hydra-Zoet, or its predecessors.

2.4.1 The project Safety against flooding 21st Century

The project 'Safety against flooding 21st Century' has been carried out. Its purpose was to establish whether the current safety levels indicated in Figure 2-1 are still appropriate, and if not, which safety levels would be adequate. To that purpose a cost benefit analysis has been performed. The Hydra models Hydra-B and Hydra-VIJ (predecessors of Hydra-Zoet) were used to estimate probabilities of flooding for the lake area, upper rivers and tidal rivers. The model Hydra-K, not covered in this report, has been used for the coastal areas.

2.4.2 The Delta program

Coping with climate change is an important issue for the Netherlands. In 2010 a new study, the Delta program, was started to evaluate which flood risk management policy would be the most appropriate (http://www.rijksoverheid.nl/onderwerpen/deltaprogramma). This section briefly describes the context of this program and its main issues.

Large scale flood protection projects usually take about 40 to 60 years to complete. The Netherlands were hit by a storm surge in 1916, resulting in a project in which barrier dams (between Wadden Sea and Lake IJssel) and polders were constructed; these works were finished in 1980. Another major surge, the one of February 1953, flooded a large part of the south-west of the country. This flood initiated the so-called *Delta works*, which were formally finished in 1984. The last storm surge barrier, however, was built in 1997. The Netherlands is spending about 500 million Euros a year on flood protection.

For a new study, the Delta program, the Delta model is being developed. The Delta model currently consists of the Hydra-Zoet model for evaluating flood defences, and of the National Hydraulic Model (in Dutch: 'Nationaal Hydrologisch Instrumentarium (NHI)) for evaluating the distribution of fresh water.

The following policy issues have been declared of national importance:

1. A review of the current safety levels for dike rings in the Netherlands (see section 2.4.1).
2. A review of the national strategy for the supply of fresh water.
3. Deciding on the most adequate target water levels for Lake IJssel (their choices influence the safety of the surrounding dikes and of the water supply for about 1/3 of the country).
4. Deciding on the flood protection of the Rotterdam urban area: should the old harbours and cities be semi- or permanently closed from the sea and the river?
5. A new policy for urban (re-)development.

Three out of the five policy issues (numbers 1, 3 and 4), need the model Hydra-Zoet, or one of its predecessors Hydra-B or Hydra-VIJ.

For the evaluation of future safety provided by flood defences, a number of climate scenarios have to be assessed to determine the scale of possible problems the Netherlands could face. Next, strategies have to be developed to counter the problem of climate change, or increased risk due to economic developments: e.g. new enclosure dams, river enlargement, and the reinforcement of the current flood protection measures, or combinations of these strategies.

2.5 Various types of input for the assessment and for policy and design studies

Evaluating the current situation can be done fairly easily with the Hydra-Zoet model as an assessment tool. For the rivers, lakes and the sea, the model uses all kinds of statistical information, and a large number of calculated water levels and wave variables, calculated with physical models such as WAQUA and SWAN (briefly described in sections 5.2 and 5.3.4). Using the Hydra-model for the current safety levels, i.e. the norm frequencies of Figure 2-1, the normative water levels and required (or desired) dike heights can be determined. A required dike height can then be compared to the existing dike height. A schematic picture is provided in Figure 2-3. The contents of this scheme will be further explained in the remainder of this report.

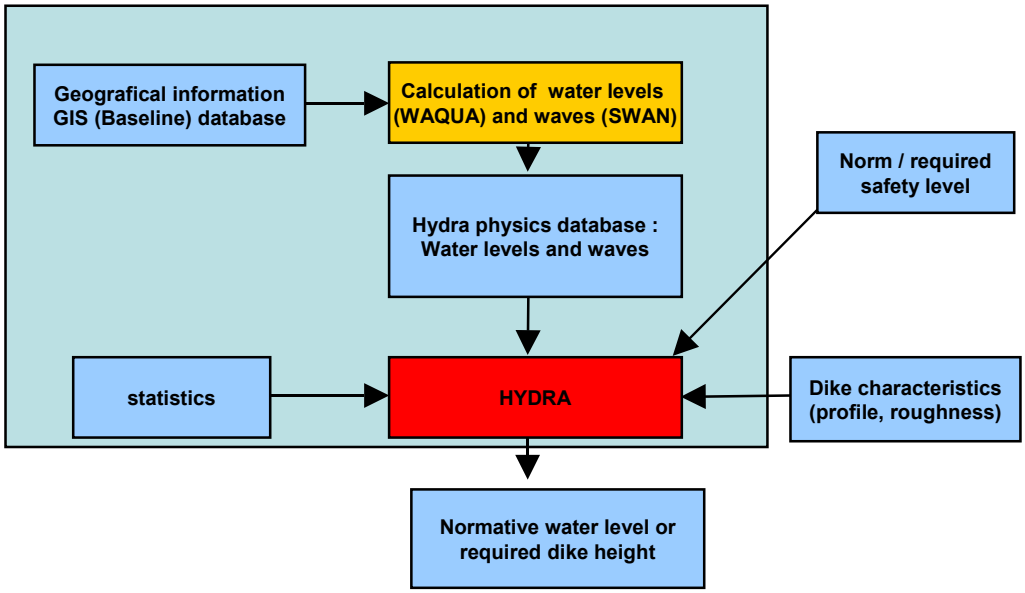

Figure 2-3 Hydra-Zoet, as used in the current assessment.

Instead of considering a single safety level (norm frequency), the Hydra model also determines the water levels and hydraulic load levels for a whole range of exceedance frequencies, yielding so-called *frequency lines* for water levels and hydraulic load levels (Figure 2-4).

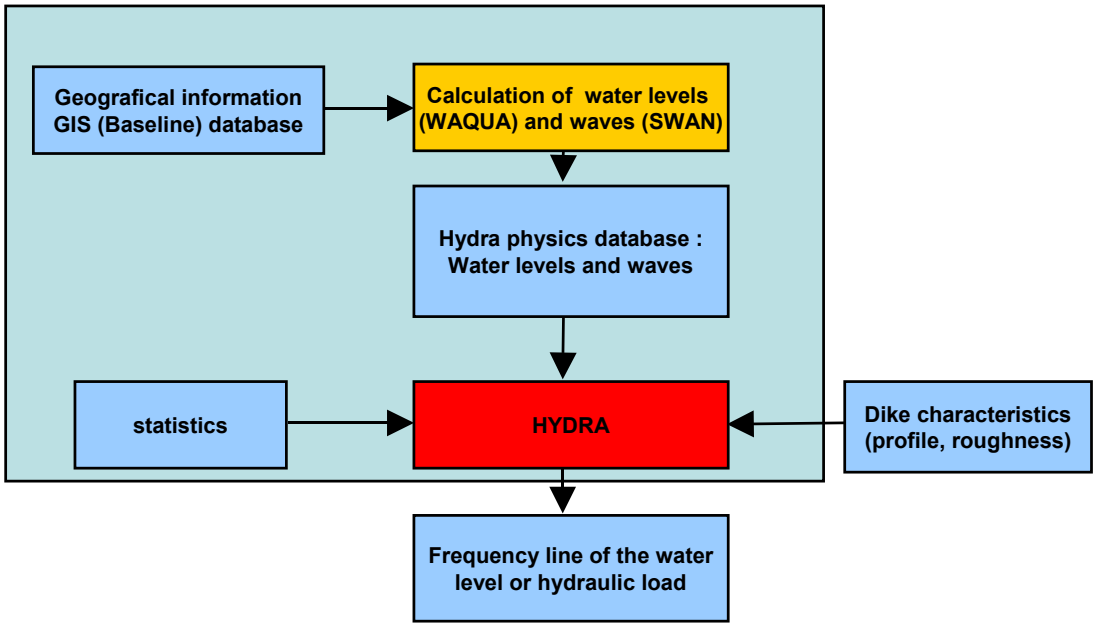

Figure 2-4 Hydra-Zoet, providing for the current situation frequency lines for water levels and hydraulic load levels.

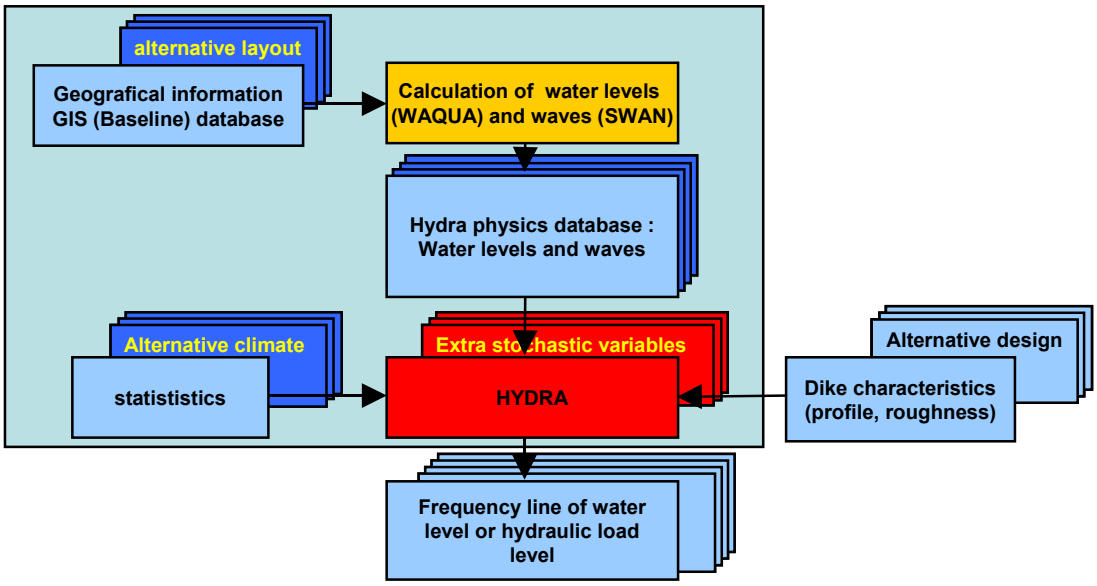

Figure 2-5 Hydra-Zoet, providing frequency lines for water levels and hydraulic load levels for policy and design studies.

When taking into account new enclosure dams or changes in the river bed, changes of the input of Hydra-Zoet are necessary, leading to different "physical databases" of water levels and waves; also, different dike characteristics might have to be used. When considering alternative climate scenarios, changes to the statistical input become necessary. For all kinds of policy studies, such changes to Hydra-Zoet will be necessary, leading to the scheme of Figure 2-5, where also extra random variables are indicated that could be necessary. Note: such alternative random variables, layouts, climate scenarios and dike designs are not treated in this report.

3 Fresh water systems

In the Dutch fresh waters, four water systems are distinguished. They are briefly described in the next section (3.1). All four water systems are considered in Hydra-Zoet, but from a mathematical point of view the Hydra-Zoet formulas fall into just two classes, already mentioned in section 1.1: the class of a *sea delta* and the one of a *lake delta*. These types of deltas are characterised in section 3.2.[8]

3.1 Water systems in Hydra-Zoet

The model Hydra-Zoet incorporates four different water systems, indicated in Figure 3-1. Also shown in this figure are some of the more important rivers, channels and lakes in the Netherlands. The water systems are:

- *upper rivers*, consisting of the upper reaches of the rivers Rhine, Meuse and IJssel (a branch of the Rhine),
- *lakes*, consisting of Lake IJssel and Lake Marken,
- *Vecht and IJssel delta*, consisting of the deltas of the rivers Vecht and IJssel,
- *tidal rivers*, consisting of the lower reaches of the Rhine and Meuse and their branches.

We recall that the failure mechanisms of Hydra-Zoet treated in this report are:

- Overflow, used to calculate water levels at a considered exceedance frequency.
- Wave overtopping, used to calculate required dike heights at a considered exceedance frequency.

	water systems			
	Vecht and IJssel Delta	lake area	tidal rivers	upper rivers
random variables				
Rhine discharge			+	+
Meuse discharge			+	+
Vecht discharge	+			
IJssel discharge	+			+
Lake IJssel	+	+		
Lake Marken		+		
wind speed	+	+	+	+
wind direction	+	+	+	+
sea level			+	
state Maeslant barrier			+	
predictions Maasmond			+	
state Ramspol barrier	+			

Table 3-1 Random variables, used in Hydra-Zoet per water system.

Table 3-1 provides an overview of the random variables used in Hydra-Zoet for each of the water systems. Note that it would theoretically be possible to include *all* random variables of Hydra-Zoet in *every* water system. We could for example consider sea and lake levels in the computations for the upper reaches of the rivers, even though the influence of the sea and lakes can be neglected there. If all variables would be included in a single set of formulas, applicable to all water systems at once, effectively the distinction between water systems would have

[8] We could distinguish a third and a fourth class; the "upper rivers', with only wind and discharge as random variables, and the "lakes", with only wind and lake levels as random variables. But, as explained in section 3.2, the classes of a sea delta and of a lake delta contain these classes as special cases.

vanished. At the moment, due to limitations imposed by memory and speed of computers, such a single model is still out of reach. Also, it would be very inefficient. We also remark that, although Hydra-Zoet considers only the fresh water systems, the sea level has to be included in the formulas, since this variable influences the water levels inland.

The following sections describe which random variables are used in Hydra-Zoet in each water system, and explains (briefly) how the variables result in threats to the dikes for the failure mechanisms overflow and wave-overtopping.

Figure 3-1 Different water systems in Hydra-Zoet.

3.1.1 Upper rivers

The random variables in Hydra-Zoet for the upper reaches of Rhine, Meuse and IJssel are:
- discharge of the Rhine for locations along the Rhine and the IJssel,
- discharge of the Meuse for locations along the Meuse,
- wind speed,
- wind direction.

The threats for the flood defences in this water system primarily result from high discharges, in turn causing high water levels. Next, wind waves cause wave run-up. When too much water flows over the crest of the dike, either through wave run-up or through water levels exceeding the crest of the dike, it can cause erosion of the inner slope. It might also damage the dike due to infiltration into its body, and saturate the soil, causing embankment failure/slip. We note that the wind direction is included in the model for two reasons: firstly, there is a correlation between wind speed and wind direction that has to be accounted for (westerly directions have much higher wind speeds then easterly directions), and secondly only wind directions causing waves 'towards the dike' are important, i.e. wind directions 'coming from land' pose no threat.

For completeness we mention that the probabilistic model Hydra-Zoet also contains an option with a *deterministic* (i.e. a non-probabilistic) method for the assessment of dikes, called Hydra-R. For policy reasons this option still will be used in the dike assessment for the period 2011-2017, though the (better) probabilistic method of Hydra-Zoet is available. This deterministic method is not considered in this report.

3.1.2 Lakes

For this water system, consisting of Lake IJssel and Lake Marken, the random variables are:
- water level of Lake IJssel,
- water level of Lake Marken,
- wind speed,
- wind direction.

The lakes are filled by rivers and pumping stations, discharging into the lakes. Under normal circumstances, the water from the lakes flows into the sea during low tide. High lake levels arise when no, or insufficient, discharge into the sea is possible over prolonged periods with north-westerly winds, causing elevated sea levels.

In Hydra-Zoet the water level of a lake is treated as a spatially averaged level, i.e. it is a measure of the total volume of the water in the lake, without taking into account a possible tilt of the water level due to wind set-up (such a tilt is averaged out to obtain the lake level considered here). We note that the lakes in Hydra-Zoet are treated completely separated from each other: it is assumed that there is no influence of one lake onto the other. The threats to the dikes in these lakes are due to (combinations of) high lake levels, elevated high water levels caused by wind set-up and wind waves causing wave run-up.

3.1.3 Vecht and IJssel delta

In the deltas of the rivers Vecht and IJssel (a branch of the Rhine) the random variables are:
- water level of Lake IJssel,
- discharge of the IJssel (for locations along the IJssel),

- discharge of the Vecht (for locations along the Vecht),
- wind speed,
- wind direction,
- barrier state of the Ramspol storm-surge barrier.

The storm-surge barrier closes off the Vecht delta from Lake IJssel in case of westerly storms, preventing high water levels in the delta which are generated by wind set-up in Lake IJssel. The barrier might fail to close during a (westerly) storm. The probability for this kind of failure is considered in Hydra-Zoet. The water system Vecht and IJssel delta is considered in detail in part 3 of this report (chapter 9-12).

The threats to the dikes in this region are due to (combinations of) high lake levels, elevated high water levels caused by wind set-up or high discharges and wind waves causing wave run-up. Also, failure of closing of the barrier might occur.

3.1.4 Tidal rivers

This water system consists of the lower reaches of the Rhine and Meuse. Here the sea tide influences the water levels, hence the name tidal rivers or tidal area. A precise definition for this water system is that it consists of that part of the branches of the Rhine and Meuse where *during high discharge waves* the water levels are significantly affected by storm surges (generated by wind storms at the North Sea).

We note that without the condition of high discharges, the tidal area would extend further inland, since during low discharges the influence of the sea extends further inland. For safety reasons, further inland high discharges are *always* important, which explains why in the definition of the tidal area one makes the restriction to consider sea influence during *high* discharges only.

In the tidal rivers the random variables of Hydra-Zoet are:
- sea level,
- discharge of the Rhine (for locations along the Rhine or its branches),
- discharge of the Meuse (for locations along the Meuse or its branches),
- wind speed,
- wind direction,
- barrier state of the Maeslant storm surge barrier
- prediction of the water level at Maasmond.

In case of storm surges the Maeslant Barrier closes off the area from the sea.[9] In the operation of the barrier predicted water levels at Maasmond are used. These predictions contain uncertainties, which is why they affect the effectiveness of the closure procedure of the barrier, and why they have to be included in the model. The barrier might fail to close for two reasons: the predicted water levels might have been lower than in reality, so that the barrier has not been closed or was closed too late (wrong prediction). The barrier might also fail to close when it had to (operational failure). Besides the use of predicted water levels, the probability of failure to close is considered in Hydra-Zoet as well. In part 2 of this report the tidal rivers will be considered in detail (chapters 9-12).

[9] Next to the Maeslant Barrier there exists a smaller barrier, the Hartel Barrier in the 'Hartelkanaal' whose operation is linked to the operation of the Maeslant Barrier, For the sake of simplicity, this smaller barrier will be left out in this text.

Threats to the dikes in this water system are due to (combinations of) high storm surges generated by westerly storms over the North Sea, elevated high water levels caused by wind set-up inside the region itself, high discharges, and by wind waves causing wave run-up. Also, failure to close the barrier poses a threat.

3.1.5 Additional increments for water levels and waves

In the 6-yearly assessment all kinds of increments for water levels and waves are used, such as increments to account for local increases of the water level caused by obstacles or bends in the river, various kinds of (harbour) oscillations in the water level caused by wind (e.g. seiches) and wave penetration from the sea to the Europort Area in Rotterdam. Some of the increments are accounted for in Hydra-Zoet, but in order not to complicate matters, these increments are not treated in this report.

3.2 Two main types of water systems

In the preceding text, four water systems have been considered. We note that in Hydra-Zoet there are basically only two sets of probabilistic formulas, corresponding to two different types of river deltas:

1. *lake delta*: a delta with the river discharging into a *lake*, and
2. *sea delta*: a delta with the river discharging into the *sea*.

The water system Vecht and IJssel delta is of the first type, whereas the tidal rivers are of the second type. You could argue that a sea delta can be seen as a special case of a lake delta, since a sea can be considered a (very) big lake. The reason to still make the distinction is that for the lake delta the wind set-up in Hydra-Zoet *is calculated with a physical model* (WAQUA), whereas for the sea delta this wind set-up (due to a storm surge) is handled using the sea level *as a random variable*. For a lake the probabilities of elevated water levels due to wind set-up are obtained through hydraulic computations, which in turn use statistical information of the wind as a boundary condition. Probabilities for sea levels are obtained (directly) from statistical information of the sea level. Maybe in the future we will succeed in treating the sea delta in the same way as a lake delta. This means, however, the use of a model for the entire North Sea, and the availability of statistical information of wind fields extending across the entire North Sea area. At this moment, such information is not available. Note that since a lake is much smaller than the North Sea, the wind field across a lake can be taken as (more or less) uniform over the lake.

	water systems			
	lake delta	lake area	sea delta	upper rivers
random variables				
discharge	+		+	+
lake level	+	+		
wind speed	+	+	+	+
wind direction	+	+	+	+
sea level			+	
barrier state	+		+	
predictions for barrier state			+	

Table 3-2 Random variables for (types of) water systems: lake delta, lake area, sea delta, upper rivers.

The water system *lakes* can, from a computational point of view, be seen as a special case of the water system *lake delta*, in the sense that the random variables for the lakes are a subset of the set of variables used for the lake delta, see Table 3-2. In a similar way, the upper rivers can

be seen as a special case of a lake delta: just remove the lake level and barrier state from the set of variables used for a lake delta. This means that once the probabilistic formulas for the lake delta have been formulated, the formulas for a lake or for (one of the) upper rivers, are obtained by leaving out some of the variables. It should be stressed though, that the lakes and the upper rivers are only special cases of the lake delta *from a mathematical point of view*, i.e. regarding the probabilistic formulas. In these formulas one still has to substitute the proper statistical data for the water system considered. Lake Marken, for example, cannot be considered as a special case of the 'Vecht and IJssel delta', since the statistical data for the Vecht and IJssel delta do not contain the lake level of Lake Marken (compare Table 3-1).

From a mathematical point of view the formulas for the upper rivers are not only a special case of the lake delta, but also of the sea delta: one just has to remove the part of the sea level and the variables related to the barrier (the influence of these variables becomes negligible in the upper river area). Hence, mathematically speaking, the upper rivers are a special case of both a sea delta and a lake delta. In the remainder of this report, since the lakes and upper rivers are special situations of the sea delta and the lake delta, the formulas for lakes and upper rivers are not considered explicitly.

4 Hydra-Zoet features and examples of results

This report is primarily about the probabilistic model Hydra-Zoet, about the statistical input and the probabilistic formulas, and not so much about practical applications of the model. Before turning to the details of the model, it is instructive though, to provide some specific examples of output of the model. The examples are given for a location in the Vecht delta, where the physical and statistical data that are used correspond to the assessment period 2006 – 2011.

This chapter is structured as follows. First different user versions of the model are considered. Then, to help interpret the output of the examples, information about return periods is given for the random variables in the Vecht delta. Next, examples are provided for failure mechanisms overflow and wave overtopping. The chapter concludes with an investigation to what extent discharges, lake levels and wind play a role when the safety standard for the water levels (i.e. the normative water levels) is exceeded.

When looking at the examples in this chapter, a reader may experience the difficulty that some of the concepts are not fully explained here. A full explanation is only given in later chapters. Therefore, some of the readers might prefer to skip (parts of) this chapter, to return to it at a later stage. But since later chapters often focus on details of models and calculations, we want to provide specific examples preceding these chapters. We hope at least some readers will appreciate the examples.

4.1 Versions for normal and advanced users

The computer program Hydra-Zoet can be used in two user modes:

- *Normal user version*
  This version is meant for regular use of the program in the 6-yearly assessment.
- *Advanced user version*
  This version is meant for research and policy purposes. Using the program in this mode requires a good understanding of the background of the model (as provided in the current report). With this version statistical input can be altered. The output is more extensive as well, and can be provided in a (partly) user defined format.

An important application of the second version has been its use during the development of the model to test whether the program yields the proper answers.

There are user guides for both versions of the model [Duits, 2010bc], and a common system documentation [Duits, 2000a]. The examples in this chapter are all carried out with the version for the normal users.

4.2 Return periods for variables in Hydra-Zoet

As an aid to interpret the examples in the remainder of this chapter, recurrence levels, also called quantiles, are provided for the most relevant random variables occurring in Hydra-Zoet. These are given, for return periods 10, 100, 1000 and 10000 years, in Table 4-1 for the Vecht

and IJssel delta, and in Table 4-2 for the tidal area (see for their sources [Geerse, 2010]). Of these, only the results for the Vecht and IJssel delta are used in this chapter.

return period	discharge Dalfsen	discharge Olst	Lake IJssel	potential wind speed Schiphol	
year	m3/s	m3/s	m+NAP	m/s	Beaufort
1	180	800	0.05	20.1	a full 8
10	299	1420	0.40	24.0	transition from 9 to 10
100	419	2040	0.62	28.4	transition from 10 to 11
1000	538	2660	0.85	32.4	transition from 11 to 12
1250	550	2720	0.87	32.8	beginning 12
2000	574	2846	0.91	33.6	12
4000	610	3033	0.98	34.7	12
10000	658	3279	1.07	36.1	a full 12

Table 4-1 Return periods for random variables in the Vecht and IJssel delta.

return period	discharge Lobith	discharge Lith	sea level Maasmond	potential wind speed Schiphol	
year	m3/s	m3/s	m+NAP	m/s	Beaufort
1	5893	1315	2.38	20.1	a full 8
10	9459	2070	2.96	24.0	transition from 9 to 10
100	12675	2824	3.60	28.4	transition from 10 to 11
1000	15706	3579	4.29	32.4	transition from 11 to 12
1250	16000	3652	4.36	32.8	beginning 12
2000	16619	3806	4.50	33.6	12
4000	17531	4033	4.73	34.7	12
10000	18737	4333	5.03	36.1	a full 12

Table 4-2 Return periods for random variables in the tidal area.

Note that the wind information in both tables is the same, because statistical information from the Schiphol station is used for both regions. The wind information consists of so-called potential wind speeds (explained in section 5.3.3), which are transformed to other types of wind speeds at the locations of interest. This is explained in detail later in this report, when discussing hydrodynamic and wave models (section 5.3.3, 10.1.2 and 14.1.3). In the examples of this chapter only information of the potential wind speed at Schiphol is used.[10]

As a further remark on the wind, it is noted that the quantiles in the tables are *omni-directional*, (regardless of wind direction). However, in Hydra-Zoet wind speeds are needed in combination with the wind directions, since (extreme) wind speeds are highly dependent on these directions. The latter is apparent from Figure 4-1, where the quantiles are provided corresponding to the wind directions. Here is an example: for the most extreme direction W, the figure shows a value of 35.8 m/s for T = 10.000 year, which means that there is an annual probability of 0.0001 that a storm occurs with at least one hour for which the wind speed exceeds 35.8 m/s in combination with direction W during that hour. Note also that the most extreme direction W dominates the omni-directional value: the quantiles for direction W are close to those for the omni-directional ones of Table 4-2, although in the omni-directional quantiles also the contributions of the other directions have been incorporated.

[10] For the tidal rivers a small correction on the wind speeds has been applied in Hydra-Zoet, accounting for the fact that the maximum wind speed in a storm does not need to coincide with the maximum water level during a surge. This rather small correction will not bother us here.

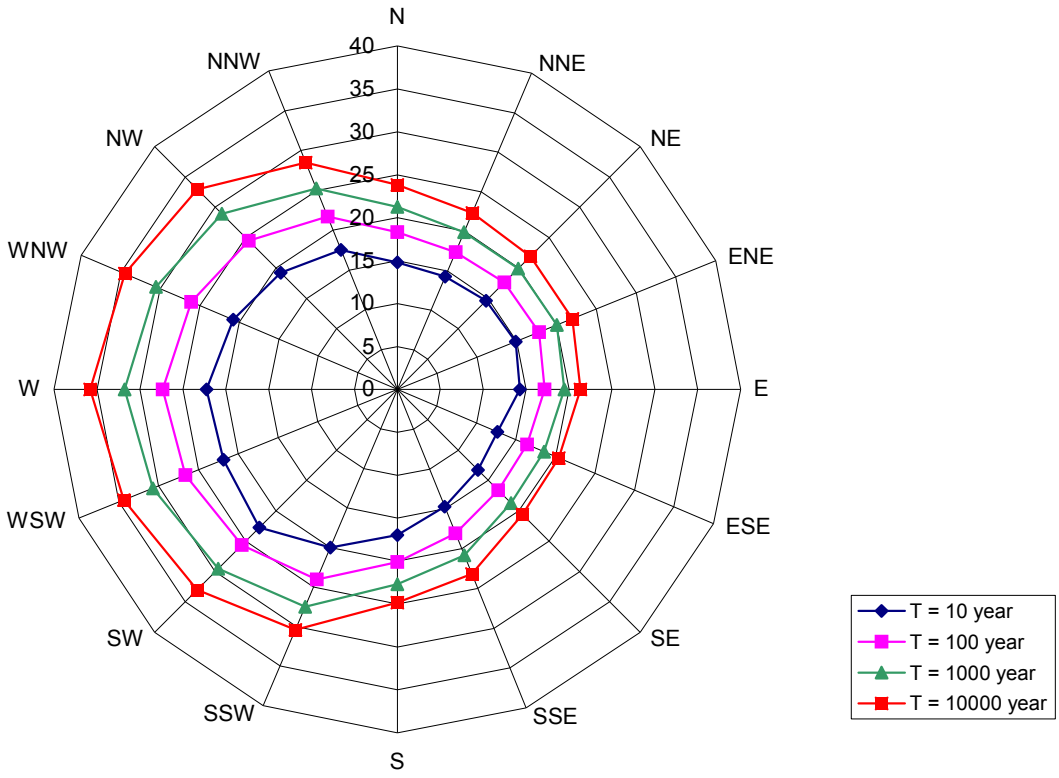

Figure 4-1 Quantiles of potential wind speeds at Schiphol for all wind directions. The wind speeds are displayed for the range of 0 to 40 m/s.

4.3 Failure mechanism overflow: water levels

In this section and the next, dialogue screens of Hydra-Zoet are shown, as well as output of the program. The program is available only in the Dutch language. For this reason the dialogue screens are in Dutch. The output, however, is translated in English.

We note that a predecessor of Hydra-Zoet, the program Hydra-B for the tidal river area, is bilingual: it can be used with the English as well the Dutch language. This program can be downloaded from http://www.helpdeskwater.nl. During the installation, one can choose the preferred language. After installation, both the Dutch and English user manuals become available.

4.3.1 Elementary output for water levels

Figure 4-2 shows the main screen of Hydra-Zoet. Here a database has been loaded for dike ring 9, named Vollenhove (compare Figure 2-1). The red dots indicate shore locations, which are located about 20 to 25 m from the toe of the flood defence. For all these locations it is possible to make calculations. The location of interest here, denoted by "Zwarte Water km 14 Locatie 1", has been marked in yellow. For this location a calculation has been made for three return periods, namely T = 1250, 2000 and 4000 year. Table 4-3 shows part of the output. The normative frequency corresponds to T = 1250 year, for which a (normative) water level is found of 1.85 m+NAP. The output shows that the water levels for T = 2000 and 4000 year do not

differ much: they are (rounded to 1 cm) only 0.06 m and 0.16 m higher than the normative water level.

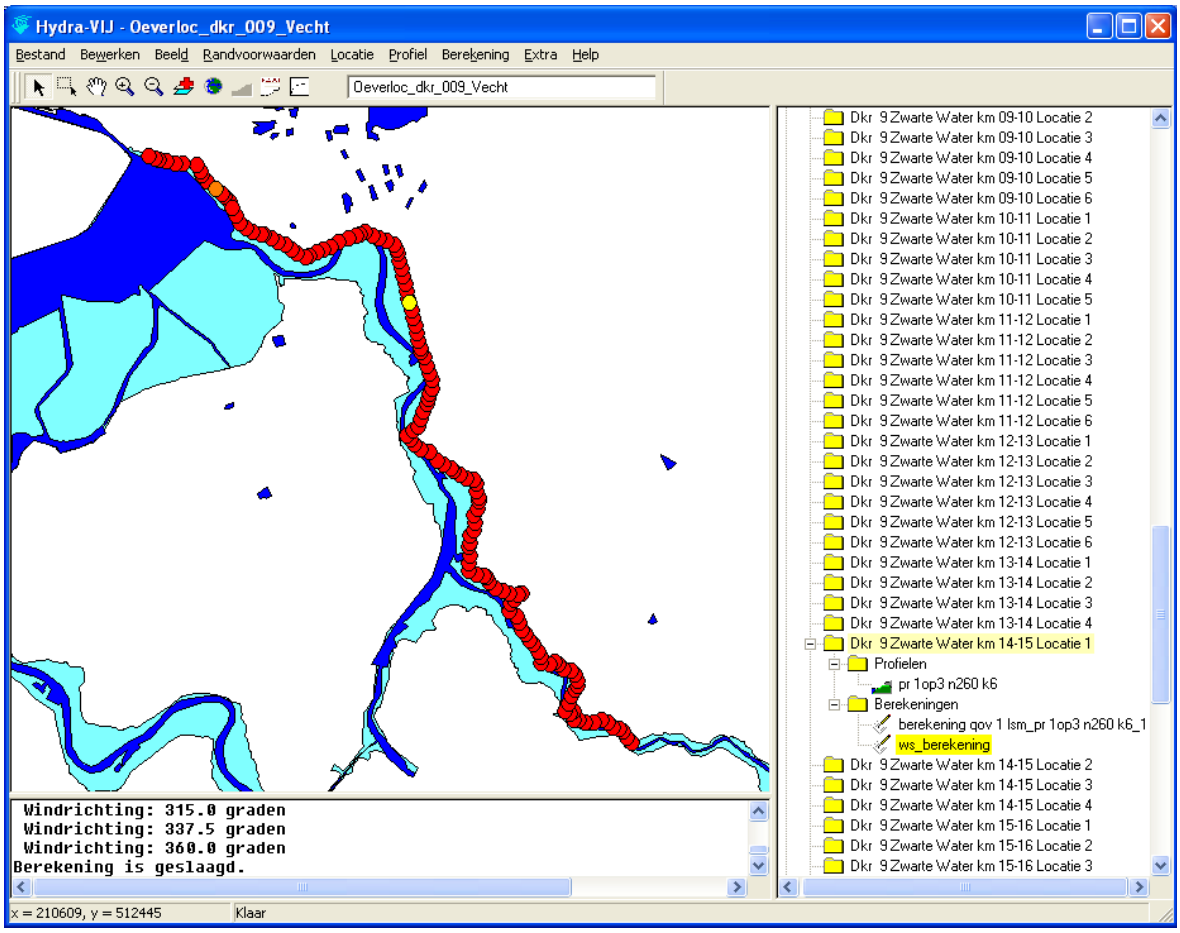

Figure 4-2 The main screen of Hydra-Zoet location Zwarte Water km 14 marked in yellow.

```
Database                                        = Oeverloc_dkr_009_Vecht.mdb
Location                                        = Dkr  9 Zwarte Water km 14-15 Locatie 1
  X-coordinate                                  =  202428 (m)
  Y-coordinate                                  =  515247 (m)

Type of computation                             = Water level

Calculated results:
    Frequency:          Water level
      1/ 1250           1.850 (m+NAP)
      1/ 2000           1.911 (m+NAP)
      1/ 4000           2.009 (m+NAP)

   Return period        Water level
     (year)             (m+NAP)
          0.5           0.797
            1           0.912
            2           1.011
            5           1.134
           10           1.226
           25           1.348
           50           1.439
          100           1.528
          250           1.645
          500           1.732
         1000           1.821
         2000           1.911
         4000           2.009
        10000           2.164
        20000           2.307
```

Table 4-3 Basic Hydra-Zoet output water level calculation Zwarte Water km 14.

4.3.2 Contributions to the exceedance frequency for a water level

With Hydra-Zoet so-called "contributions to the exceedance frequency" can be calculated, which provide information about the probabilities with which discharges, lake levels, wind speeds, wind directions and barrier states occur during a failure event.[11] The contributions are explained for the water level calculation for T = 1250 year of the preceding section, where failure here means the exceedance of the water level 1.85 m+NAP.

The output for the contributions is shown in Table 4-4. There are contributions calculated for:

- barrier state,
- discharge of the Vecht,
- lake level,
- wind speed,
- wind direction.

```
Location                      = Dkr  9 Zwarte Water km 14-15 Locatie 1 (202428,515247)
Type of computation           = Water level
Water level                   =     1.85 (m+NAP)
Return period                 =     1250 (year)
Exceedance frequency          = 8.00E-04 (per year)

Open Ramspol Barrier          =  31.9%
Closed Ramspol Barrier        =  68.1%

Percentiles for Vecht discharge  (m³/s):

 percentage | open+closed| open       |  closed
------------+-------------+-----------+-----------
         5% |          40 |         15 |        202
        10% |          90 |         30 |        336
        25% |         349 |         86 |        397
        50% |         447 |        264 |        451
        75% |         525 |        601 |        505
        90% |         596 |        664 |        550
        95% |         640 |        705 |        573

Percentiles for lake level  (m+NAP):

 percentage | open+closed| open       |  closed
------------+-------------+-----------+-----------
         5% |       -0.27 |      -0.34 |       0.08
        10% |       -0.15 |      -0.30 |       0.39
        25% |        0.44 |      -0.16 |       0.57
        50% |        0.70 |       0.36 |       0.73
        75% |        0.86 |       0.90 |       0.85
        90% |        1.00 |       1.07 |       0.96
        95% |        1.06 |       1.17 |       1.02

Percentiles for wind speed  (m/s):

 percentage | open+closed| open       |  closed
------------+-------------+-----------+-----------
         5% |        13.2 |        8.9 |       15.4
        10% |        14.9 |       12.2 |       16.5
        25% |        17.7 |       15.1 |       18.3
        50% |        20.9 |       23.1 |       20.7
        75% |        25.8 |       27.7 |       24.2
        90% |        29.6 |       29.7 |       29.4
        95% |        33.4 |       31.0 |       36.1
```

Table 4-4 Hydra-Zoet output Zwarte Water km 14 for the contributions, for the water level calculation with T = 1250 year (the normative return period).

Only results for the first four variables are given in Table 4-4; for the wind direction they are provided in the next section. We will explain the interpretation of the numbers, using a few examples. The table displays the number 31.9% for the open barrier state, which means that during failure (exceedance of 1.85 m+NAP) there is a 31.9% probability of an open barrier. Here open amounts to the situations for which (a) no closure was needed, i.e. closure criteria not met during low wind speeds, and (b) the barrier fails to close because of a technical

[11] As will be explained in section 12.2.1, strictly speaking one can not speak of (unique) values of the discharges, lake levels and so on, since these variables may vary during a failure event. But in a pragmatic sense, as explained in section 12.2.1, it is allowed to speak of the (unique) values of the discharges, lake levels and the other variables during failure, which we will do in the remainder of this chapter.

malfunction. Correspondingly, there is a 68.1% chance on a closed barrier during a failure event, which means that the influence of the wind on failure is considerable (recall that the barrier only closes during storms).

Next, consider some numbers for the contributions of the discharges. First look at the 10% numbers 90, 30 and 336 m^3/s, belonging respectively to the columns "open+closed", "open" and "closed". These numbers mean:

- During failure there is a 10% probability of a discharge below 90 m^3/s.
- If during failure the open barrier state occurs, there is a 10% probability of a discharge below 30 m^3/s, i.e. this probability results when conditioning on the open state.
- If during failure the closed barrier state occurs, there is a 10% probability of a discharge below 336 m^3/s, i.e. this probability results when conditioning on the closed state.

The other numbers in Table 4-4 reveal a large range of threatening discharges during failure. For the open state, with 10- and 90-percentiles respectively equal to 90 and 596 m^3/s, there appears to be a probability of 80% that the discharge during failure is between 90 and 596 m^3/s. The first value is not far above the winter discharge of the Vecht (60 m^3/s), whereas the second discharge has a return period above 2000 year.[12]

The contributions for the lake levels and wind speeds can be interpreted in the same manner. Similar to the discharges, the variety of lake levels and wind speeds during failure appears to be exceptionally large: failure can occur during more or less daily lake levels and wind speeds, but also at extreme values of these variables, as well as for values in between. The results in section 4.5 show that this holds for almost all locations in the Vecht delta. Only in the neighbourhood of location Dalfsen, at Vecht km 45, the wind plays a minor role; here the discharges and lake levels are the dominant cause for extreme water levels.

4.3.3 Illustration points for the calculation of a water level

Besides contributions to the exceedance frequency, Hydra-Zoet can also calculate Illustration Points (IP's). In other literature the term "design point" is often used, which is very similar to the IP. Roughly speaking, the IP's provide the most probable circumstances conditional on the occurrence of the calculated water level (or required dike height in the next section). Examples of the interpretation of the IP's are provided in what follows. How they are calculated is treated in section 16.1.

[12] We note that, while the calculation was performed for T = 1250 year, the percentiles can exceed the discharge 550 m^3/s corresponding to 1250 year. A theoretical upper bound for the p-percentile would be the discharge with return period 1250/(1-p). E.g. for p = 90%, this leads to the upper bound of 670 m^3/s, corresponding to T = 12.500 year.

```
Location                    = Dkr  9 Zwarte Water km 14-15 Locatie 1 (202428,515247)
Type of computation         = Water level
Water level                 =     1.85 (m+NAP)
Return period               =     1250 (year)
Exceedance frequency        = 8.00E-04 (per year)

Open Ramspol Barrier
```

r	lake lev. m+NAP	q IJssel m³/s	q Vecht m³/s	wind sp. m/s	wat.lev. m+NAP	exc.freq. *0.001/why	exc.freq. %
NNE	1.16	2265	688	6.0	1.85	0.001	0.1
NE	1.16	2265	688	7.0	1.85	0.001	0.1
ENE	1.16	2265	688	7.0	1.85	0.001	0.1
E	1.16	2265	688	6.0	1.85	0.001	0.1
ESE	1.16	2265	688	5.0	1.85	0.001	0.1
SE	1.16	2265	688	6.0	1.85	0.001	0.1
SSE	1.16	2265	688	6.0	1.85	0.001	0.1
S	1.16	2265	688	7.0	1.85	0.001	0.1
SSW	1.16	2265	688	8.0	1.85	0.001	0.1
SW	1.03	2034	611	14.0	1.85	0.017	2.1
WSW	0.80	1760	520	16.8	1.85	0.064	8.0
W	0.85	1985	595	13.1	1.85	0.097	12.1
WNW	0.85	1985	595	13.0	1.85	0.054	6.7
NW	0.95	2025	608	12.4	1.85	0.014	1.7
NNW	1.13	2168	656	8.0	1.85	0.003	0.3
N	1.14	2229	676	6.0	1.85	0.001	0.1
sum						0.255	31.9

Closed Ramspol Barrier

r	lake lev. m+NAP	q IJssel m³/s	q Vecht m³/s	wind sp. m/s	wat.lev. m+NAP	exc.freq. *0.001/why	exc.freq. %
NNE	--	--	--	--	--	0.000	0.0
NE	--	--	--	--	--	0.000	0.0
ENE	--	--	--	--	--	0.000	0.0
E	--	--	--	--	--	0.000	0.0
ESE	--	--	--	--	--	0.000	0.0
SE	--	--	--	--	--	0.000	0.0
SSE	--	--	--	--	--	0.000	0.0
S	--	--	--	--	--	0.000	0.0
SSW	--	--	--	--	--	0.000	0.0
SW	0.75	1400	400	22.6	1.85	0.050	6.2
WSW	0.74	1430	410	19.8	1.85	0.138	17.3
W	0.65	1550	450	19.0	1.85	0.216	27.0
WNW	0.72	1595	465	17.8	1.85	0.108	13.6
NW	0.77	1655	485	17.8	1.85	0.030	3.8
NNW	0.85	1610	470	20.4	1.85	0.002	0.3
N	1.15	1730	510	19.6	1.85	0.000	0.0
sum						0.545	68.1

```
 Meaning of the data:
 - r         = wind direction
 - lake lev. = spatially averaged water level of Lake IJssel, in m+NAP
 - q IJssel  = discharge IJssel at Olst, in m³/s
 - q Vecht   = discharge Vecht at Dalfsen, in m³/s
 - wind sp.  = potential wind speed Schiphol, in m/s
 - wat.lev.  = water level at the location, in m+NAP
 - exc.freq. = contribution of the wind direction to the exceedance frequency of the water level,
               in average times per winter half year and as a percentage
```

Table 4-5 Hydra-Zoet output Zwarte Water km 14 for the illustration points, for the water level calculation with T = 1250 year.

Some output for IP's is displayed in columns 1 to 6 of Table 4-5, again corresponding to the former calculation of the normative water level 1.85 m+NAP for T = 1250 year. The columns 7 and 8 yield information about the contributions of the wind direction to the exceedance frequency, which facilitates the interpretation of the IP's.

An IP is calculated for every calculation of the barrier state and wind direction, leading to 32 different IP's: 16 for the open and 16 for the closed barrier state. It might happen that a combination of barrier state/wind direction delivers such a small contribution to the failure frequency, that no numbers are displayed in the table.

Now let us explain the content of the table. The first block of 5 lines, appearing also in Table 4-4, yields elementary information about the calculation, and needs no further comment.

The next two blocks contain results for the open and the closed barrier state. The last two columns provide the contributions of the various wind directions to the exceedance frequency, both as absolute numbers, in times per year, and as percentages of the exceedance frequency. The most relevant IP turns out to be the one for direction W and the closed barrier state: it contributes 27.0% to the exceedance frequency. Since direction W contributes 12.1% to the open barrier state, we may conclude that during failure there is a 27.0+12.1 = 39.1% probability of direction W. The results show that for this location failure occurs mainly for the directions WSW, W and WNW, which in total contribute for 84.7% to the exceedance frequency.

We now explain the columns 1 – 6 for the open and closed barrier state. As a first remark: we can discard the results in column 3 for the river IJssel; these numbers are only meaningful for people who generate input for Hydra-Zoet, and are not treated here. The columns 2, 4 and 5 show information, respectively, per wind direction (displayed in column 1), lake level, Vecht discharge and wind speed. The values in these columns are, conditional on the wind direction and barrier state, the most probable ones in the situation that the calculated water level equals 1.85 m+NAP. As a side remark, we note that an IP provides conditions denoted as "just failure", because the calculated water level lies on the boundary of the failure region, where this boundary separates the "safe situations" from the "failure situations". Note the difference here with the contributions to the exceedance frequency: the contributions represent failure events inside the failure region. See for a more detailed explanation of the way IP's and the contributions are calculated chapter 16.

Column 6 shows the water level under consideration (1.85 m+NAP). As already mentioned, the values in columns 2, 4 and 5 are such that they lead to this water level. For the failure mechanism overflow (as considered here), displaying the water level is superfluous, since it equals the (already) calculated water level for all combinations of wind direction and barrier state. For the failure mechanism wave overtopping, however, the water levels for these combinations will be different. This failure mechanism is treated in the following section.

4.4 Failure mechanism overtopping: required dike heights

The failure mechanism wave overtopping is used to calculate a required dike height (or required crest level), for a specified return period. Again location "Zwarte Water km 14" is considered. For this failure mechanism the threatening situations do not only consist of extreme water levels, but also of wave run-up caused by wind waves. In this case so-called hydraulic load levels, in m+NAP, are used in the calculations, where such levels account for the combined effect of water levels and wave overtopping. The precise definitions of the hydraulic load levels are provided in section 5.5. We mention that the wind wave variables, i.e. significant wave height H_s and the peak period T_p, in the example of the current section will be calculated with the formulas of Bretschneider, using effective fetches and bottom levels; these concepts, as well as the formulas needed, are treated in section 5.3.1. The longer the fetches, and the lower the bottom levels (deeper water), the higher the waves and the larger the peak period.

Also a dike cross section (also called dike profile) is needed, since its characteristics determine the amount of wave overtopping: the steeper the dike, the higher the wave run-up an the higher the wave overtopping. Next to the dike cross section, an allowed wave overtopping

discharge, also called critical wave overtopping discharge (q_{crit}), has to be specified, in litre per second per metre (l/s/m) of flood defence. In practice, the critical discharge depends on the quality of the grass revetment of the inner slope: the better the quality, the higher the critical discharge can be chosen. Values often considered in the assessment range from 0.1 to 10 l/s/m. The larger the amount of water that is permitted to overtop the crest, the lower the dike can be, whereas if this critical overtopping discharge is chosen small, the dike should be high to prevent water from flowing over the dike.

4.4.1 Effective fetches, bottom levels and dike properties

Figure 4-3 shows the screen of Hydra-Zoet used to substitute values for effective fetches and bottom levels. The values for the fetches are also graphically shown on the right side: the black lines indicate the fetches; the blue lines the main dikes along the river. See the program's user guide for an explanation of the other elements in the screen.

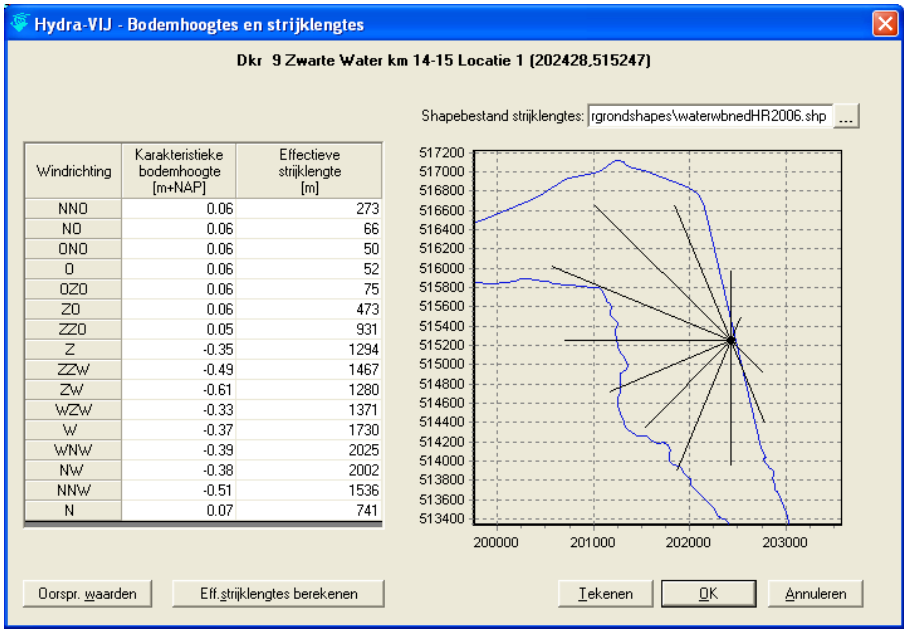

Figure 4-3 Hydra-Zoet input screen for effective fetches and bottom levels.

The database with water levels used as input for Hydra-Zoet, contains default values for the effective fetches and bottom levels (how they are determined, in a standard way, is the subject of section 5.3.2). Based on knowledge of the circumstances of the location, such as the influence of islands, a user of the program is allowed to change these values, either by changing the default values by hand or by using a different map (shape file) with the new river configuration.

A user of the program can specify a dike cross section, using the "cross section editor" of Hydra-Zoet. Different (outer) dike segments can have different slopes and roughnesses. Also, a shoulder (berm) might be specified, or a dam and/or foreshore in front of the dike. How the program treats these elements is explained in section 5.4. Here we choose a very simple cross section with a slope of 1-to-3 and a default roughness of 1, e.g. suitable for a grass cover. We also need to specify the orientation of the dike. A dike-normal of 260° is taken, i.e. pointing in a direction between WSW and W. Finally, a critical overtopping discharge has to be specified. The choice of 1 l/s/m is made. We want to emphasize that most of the values chosen are fictitious: the actual required dike height could differ significantly from the one in this example.

4.4.2 Basic output required dike height

With the information just described, Hydra-Zoet calculates, for the normative return period T = 1250 year, a required crest level of 3.00 m+NAP, see Table 4-6. This means that for this dike height a discharge of 1 l/s/m will flow over the crest of the dike with a probability of 1/1250 per year. The required crest level lies 1.15 m above the normative water level of 1.85 m+NAP calculated for T = 1250 year. We note that the difference between the required crest height and the water level can differ strongly per location.

```
Database                                                = Oeverloc_dkr_009_Vecht.mdb
Location                                                = Dkr  9 Zwarte Water km 14-15 Locatie 1
  X-coordinate                                          =  202428 (m)
  Y-coordinate                                          =  515247 (m)

Fetch and river bed data for the location:
  Wind direction    Effective           Effective
  r                 bottom level        fetch
                     (m+NAP)              (m)
  NNE                  0.06            273.00
  NE                   0.06             66.00
  ENE                  0.06             50.00
  E                    0.06             52.00
  ESE                  0.06             75.00
  SE                   0.06            473.00
  SSE                  0.05            931.00
  S                   -0.35           1294.00
  SSW                 -0.49           1467.00
  SW                  -0.61           1280.00
  WSW                 -0.33           1371.00
  W                   -0.37           1730.00
  WNW                 -0.39           2025.00
  NW                  -0.38           2002.00
  NNW                 -0.51           1536.00
  N                    0.07            741.00

Wave variables are calculated with Bretschneider

Profile                                                 = pr 1op3 n260 k6.prfl
  Crest level present                                   =         6.00 (m+NAP)
  Exterior dike normal                                  =       260.00 (°)

    Coordinates dike profile      Slope roughness
     Distance     Height          factor
       (m)        (m+NAP)          (-)
        0.00       0.00            1.00
       18.00       6.00

Failure mechanism                                       = Wave overtopping
  Critical overtopping discharge                        =         1.00 (l/s/m)

Calculated results:
    Frequency:        Hydraulic load level:
      1/ 1250            2.999 (m+NAP)
      1/ 2000            3.096 (m+NAP)
      1/ 4000            3.253 (m+NAP)

  Return period       Hydraulic load level:
      (year)             (m+NAP)
           0.5           1.426
             1           1.616
             2           1.778
             5           1.969
            10           2.103
            25           2.272
            50           2.398
           100           2.523
           250           2.689
           500           2.820
          1000           2.954
          2000           3.096
          4000           3.253
         10000           3.488
         20000           3.701
```

Table 4-6 Basic Hydra-Zoet output for required dike height Zwarte Water km 14 (based on a typical but non-existing dike).

4.4.3 Contributions to the exceedance frequency for required dike heights

Similar to the computation of the normative water levels, contributions to the exceedance frequency can be calculated for required dike heights, see Table 4-7. The interpretation of the output is analogous to the earlier one in Table 4-4, and is not repeated. Note that failure events for the required dike height occur at somewhat lower discharges and lake levels than failure events for the water level, and at a bit higher wind speeds. As an example: for the water level calculation, for "open+closed", there is an 80% range of 14.9 – 29.6 m/s during failure, whereas this range has been shifted upwards to 23.1 – 37.0 m/s for the required dike height. The latter is plausible. In case of the dike height the wind becomes a more important variable, and in general the more important random variables are the ones attaining the most extreme values during failure. Think about the upper rivers, where the discharge dominates the other variables; the discharges attain extreme values during failure, whereas the wind attains (moderately) low values.[13]

```
Location                    = Dkr  9 Zwarte Water km 14-15 Locatie 1 (202428,515247)
Type of computation         = Hydraulic load level for critical overtopping discharge 1.00 (l/s/m)
Hydraulic load level        =     3.00 (m+NAP)
Return period               =     1250 (year)
Exceedance frequency        = 8.00E-04 (per year)

Open Ramspol Barrier        =  23.7%
Closed Ramspol Barrier      =  76.3%

Percentiles for Vecht discharge  (m³/s):

 percentage | open+closed| open      |  closed
------------+------------+-----------+-----------
         5% |         14 |         8 |        18
        10% |         27 |        14 |        37
        25% |         71 |        35 |       101
        50% |        175 |        77 |       241
        75% |        346 |       139 |       380
        90% |        455 |       214 |       476
        95% |        524 |       281 |       537

Percentiles for lake level  (m+NAP):

 percentage | open+closed| open      |  closed
------------+------------+-----------+-----------
         5% |      -0.35 |     -0.38 |     -0.34
        10% |      -0.32 |     -0.36 |     -0.30
        25% |      -0.23 |     -0.31 |     -0.17
        50% |       0.02 |     -0.21 |      0.17
        75% |       0.44 |     -0.03 |      0.54
        90% |       0.71 |      0.21 |      0.76
        95% |       0.85 |      0.39 |      0.88

Percentiles for wind speed  (m/s):

 percentage | open+closed| open      |  closed
------------+------------+-----------+-----------
         5% |       21.3 |      23.1 |      21.0
        10% |       23.1 |      24.4 |      22.7
        25% |       26.0 |      25.9 |      26.1
        50% |       30.0 |      27.3 |      32.0
        75% |       34.3 |      29.4 |      35.2
        90% |       37.0 |      32.4 |      37.6
        95% |       38.3 |      33.1 |      38.7
```

Table 4-7 Hydra-Zoet output Zwarte Water km 14 for the contributions, for the required dike height with T = 1250 year.

4.4.4 Illustration points for the calculation of a required dike height

We have also determined the IP's corresponding to the calculation of the required dike height, see Table 4-8. Their interpretation is analogous to the former in section 4.3.3 for the normative

[13] Here an exception has to be made for the lake level. Far inland the lake level has almost no influence on the water levels, but due to the rather strong correlation between the discharge and the lake level, at these locations during failure high lake levels occur.

water levels, except that now also the most probable wave variables are provided as part of the IP. These variables are, at the toe of the dike, the significant wave height H_s, the peak period T_p and the wave direction θ. We note, however, that whenever wave variables are calculated with the 1-dimensional formulas of Bretschneider, and no foreshore is present (our current setting), θ simply equals the wind direction (see section 5.3.4 for other wave models, where θ might differ from the wind direction).

```
Location                    = Dkr  9 Zwarte Water km 14-15 Locatie 1 (202428,515247)
Type of computation         = Hydraulic load level for critical overtopping discharge 1.00 (l/s/m)
Hydraulic load level        =     3.00 (m+NAP)
Return period               =     1250 (year)
Exceedance frequency        = 8.00E-04 (per year)

Open Ramspol Barrier
```

r	lake lev. m+NAP	q IJssel m³/s	q Vecht m³/s	wind sp. m/s	wat.lev. m+NAP	Hs m	Tp s	wave dir. graden	exc.freq. *0.001/why	exc.freq. %
NNE	--	--	--	--	--	--	--	--	0.000	0.0
NE	--	--	--	--	--	--	--	--	0.000	0.0
ENE	--	--	--	--	--	--	--	--	0.000	0.0
E	--	--	--	--	--	--	--	--	0.000	0.0
ESE	--	--	--	--	--	--	--	--	0.000	0.0
SE	--	--	--	--	--	--	--	--	0.000	0.0
SSE	--	--	--	--	--	--	--	--	0.000	0.0
S	1.43	2465	755	27.4	2.03	0.70	3.1	180	0.000	0.0
SSW	1.23	2360	720	26.5	1.91	0.70	3.2	203	0.000	0.0
SW	-0.25	480	95	31.5	1.68	0.76	3.3	225	0.021	2.6
WSW	-0.19	367	70	27.4	1.77	0.67	3.1	248	0.025	3.1
W	-0.22	344	65	25.5	1.74	0.66	3.2	270	0.091	11.4
WNW	-0.22	344	65	25.8	1.76	0.69	3.3	293	0.045	5.6
NW	-0.19	389	75	27.6	1.79	0.73	3.4	315	0.008	0.9
NNW	0.35	905	235	27.5	1.94	0.73	3.3	338	0.000	0.0
N	1.45	2371	724	32.8	2.76	0.74	3.1	360	0.000	0.0
sum									0.190	23.7

Closed Ramspol Barrier

r	lake lev. m+NAP	q IJssel m³/s	q Vecht m³/s	wind sp. m/s	wat.lev. m+NAP	Hs m	Tp s	wave dir. degree	exc.freq. *0.001/why	exc.freq. %
NNE	--	--	--	--	--	--	--	--	0.000	0.0
NE	--	--	--	--	--	--	--	--	0.000	0.0
ENE	--	--	--	--	--	--	--	--	0.000	0.0
E	--	--	--	--	--	--	--	--	0.000	0.0
ESE	--	--	--	--	--	--	--	--	0.000	0.0
SE	--	--	--	--	--	--	--	--	0.000	0.0
SSE	--	--	--	--	--	--	--	--	0.000	0.0
S	--	--	--	--	--	--	--	--	0.000	0.0
SSW	--	--	--	--	--	--	--	--	0.000	0.0
SW	-0.13	344	65	32.9	1.64	0.78	3.4	225	0.119	14.9
WSW	-0.25	380	73	34.8	1.54	0.75	3.4	248	0.153	19.2
W	-0.10	571	124	34.7	1.46	0.75	3.5	270	0.260	32.5
WNW	0.55	1321	374	24.0	1.82	0.66	3.2	293	0.067	8.4
NW	0.55	1274	358	27.0	1.80	0.72	3.3	315	0.010	1.3
NNW	0.90	1850	550	24.1	2.06	0.67	3.1	338	0.000	0.0
N	1.39	2300	700	20.8	2.86	0.49	2.5	360	0.000	0.0
sum									0.610	76.3

```
Meaning of the data:
 - r         = wind direction
 - lake lev. = spatially averaged water level of Lake IJssel, in m+NAP
 - q IJssel  = discharge IJssel at Olst, in m³/s
 - q Vecht   = discharge Vecht at Dalfsen, in m³/s
 - wind sp.  = potential wind speed Schiphol, in m/s
 - wat.lev.  = water level at the location, in m+NAP, after a possible transformation across a foreshore
 - Hs        = significant wave height, in m, after a possible transformation across a dam and/or foreshore
 - Tp        = peakperiod, in s, after a possible transformation across a foreshore
 - wave dir. = wave direction, in degrees, after a possible transformation across a foreshore
 - exc.freq. = contribution of the wind direction to the exceedance frequency of the hydraulic load level,
               in average times per winter half year and as a percentage
```

Table 4-8 Hydra-Zoet output Zwarte Water km 14 in the illustration points, for the required dike height with T = 1250 year.

Because most aspects of the IP's are already explained for the calculation of the normative water level treated in section 4.3.3, here we restrict ourselves to some comments specifically of interest for the dike height.

The first remark is that the values for the respective variables at every line in the table (one line for every wind direction and barrier state) result in the calculated hydraulic load level of 3.00 m+NAP. We note that lines containing empty positions indicate the combinations of wind direction and barrier state with a negligible contribution to the exceedance frequency.

A second remark is that the various water levels in the table, contrary to the case for the failure mechanism overflow in Table 4-5, now differ on every line. The reason is that *different* "superpositions" of water levels and waves can result in the *same* hydraulic load level of 3.00 m+NAP.

4.5 Which variables are most important for the normative water levels in the Vecht delta?

We would like to know which variables are the most threatening ones to the dikes throughout the Vecht delta. It is interesting to know, for instance, for which locations discharges are the most threatening, for which locations the wind, and for which locations combinations of both. To that purpose, nine locations have been chosen, scattered throughout the Vecht delta. Only *water levels* have been investigated. Note: for required dike heights the situation would be much more complex, because the cross section and orientation of the dike and its neighbourhood would strongly influence the results; therefore we restrict ourselves to water levels.

For every location results have been calculated, for a fixed return period T = 1250 year. In the following O and C respectively denote the open and closed barrier states. Where results are mentioned for the situation "O", they hold conditional on the open barrier state. Similarly, a result for situation "C" holds conditional on the closed barrier state. Results for the situation "O+C" are without conditioning on the barrier states. For return period T = 1250 year, the following results have been calculated:

- The water level.
- The 10- and 90-percentiles, for situations "O+C" , "O" and "C", of the discharge, lake level and wind speed, resulting in:
    - $q_{10\%}$ and $q_{90\%}$
    - $m_{10\%}$ and $m_{90\%}$
    - $u_{10\%}$ and $u_{90\%}$.

The way these percentiles have been calculated has been explained in section 4.3.2. The results are shown in Table 4-9, and partly in Figure 4-4, where also the geographical positions of the locations can be seen. A first comment on the results is that high discharges always correspond to high lake levels, and low discharges to low lake levels. The origin of this is that discharges and lake levels are strongly correlated: so if one is high, or low, there's a strong probability that the other will be as well. Because of this correspondence between discharges and lake levels, the latter variable will not be mentioned anymore (conclusions for the discharge also hold for lake levels).

		Ommen			Dalfsen						mouth of Vecht			Zwolle		
		Vecht km 36			Vecht km 45			Vecht km 53			Vecht km 60			Zw.Water km 1		
		h = 5.19 m+NAP			h = 4.45 m+NAP			h = 2.82 m+NAP			h = 2.12 m+NAP			h = 2.13 m+NAP		
		O+C	O	C	**O+C**	O	C	**O+C**	O	C	**O+C**	O	C	**O+C**	O	C
	prob, %	**100**	73	27	**100**	93	8	**100**	74	26	**100**	50	50	**100**	50	50
percentiles	q 10%	**409**	560	271	**551**	555	467	**457**	557	331	**347**	177	374	**333**	194	353
	q 90%	**639**	650	554	**631**	633	566	**638**	649	554	**648**	672	550	**648**	672	549
	m 10%	**0.41**	0.54	0.13	**0.52**	0.53	0.44	**0.48**	0.55	0.30	**0.36**	0.08	0.41	**0.34**	0.13	0.37
	m 90%	**0.95**	0.98	0.82	**0.96**	0.96	0.90	**0.98**	1.00	0.89	**1.02**	1.07	0.93	**1.01**	1.07	0.93
	u 10%	**4.8**	4.3	17.6	**3.9**	3.8	15.8	**4.5**	4.1	16.2	**6.8**	4.9	15.7	**6.6**	4.8	15.8
	u 90%	**27.3**	15.8	32.6	**15.9**	13.9	28.6	**23.9**	15.3	30.9	**27.0**	26.7	27.2	**27.0**	26.1	27.5

		near Hasselt			mouth Zw.W			NE side Zw.Meer			near Ramspol		
		Zw.Water km 12			Zw.Water km 19			WsRW39			Zw.Meer WsZL54		
		h = 1.88 m+NAP			h = 1.64 m+NAP			h = 1.54 m+NAP			h =1.31 m+NAP		
		O+C	O	C	**O+C**	O	C	**O+C**	O	C	**O+C**	O	C
	prob, %	**100**	35	65	**100**	35	66	**100**	33	67	**100**	33	67
percentiles	q 10%	**130**	44	362	**84**	27	364	**49**	24	117	**199**	45	349
	q 90%	**628**	688	551	**594**	659	549	**575**	637	542	**583**	643	537
	m 10%	**-0.04**	-0.27	0.44	**-0.15**	-0.30	0.54	**-0.26**	-0.32	-0.12	**0.23**	-0.24	0.66
	m 90%	**1.03**	1.13	0.97	**1.04**	1.15	0.99	**1.04**	1.15	1.00	**1.08**	1.19	0.98
	u 10%	**13.2**	8.5	16.0	**14.3**	12.1	15.6	**14.9**	12.7	15.9	**12.1**	7.5	14.5
	u 90%	**28.4**	29.2	27.0	**28.2**	29.4	25.5	**33.0**	30.3	34.0	**26.4**	28.9	23.1

Table 4-9 *Hydra-Zoet output for the contributions to the exceedance frequency for nine locations in the Vecht delta, for T = 1250 year.*

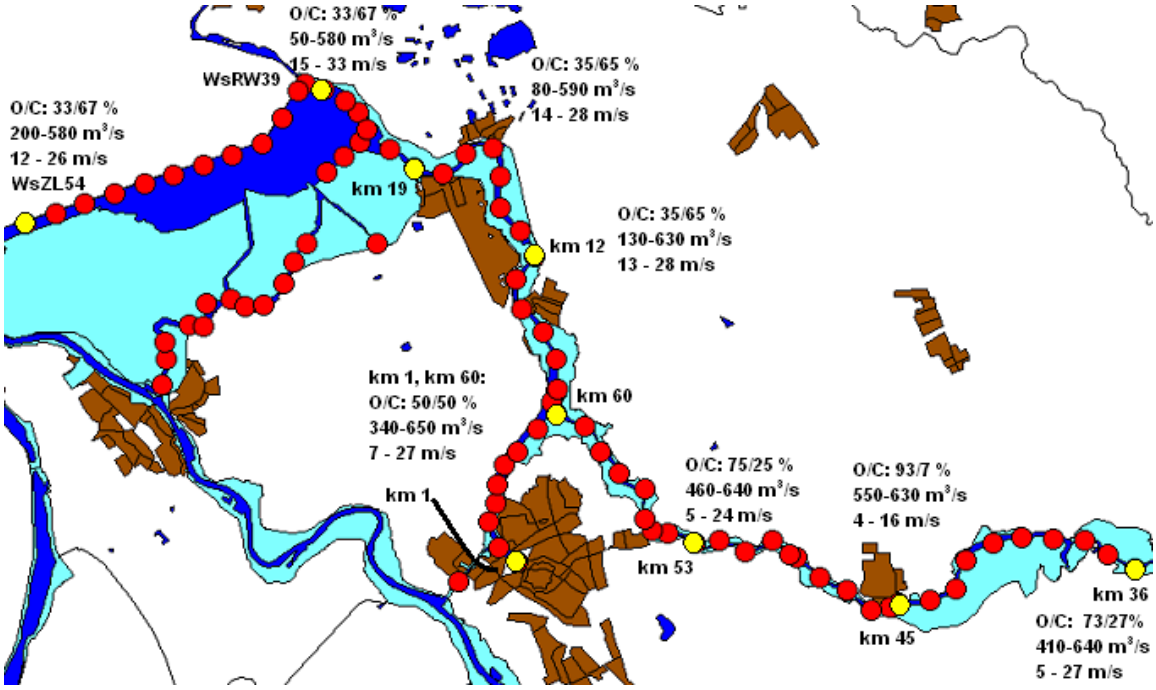

Figure 4-4 *Map of the Vecht delta with the locations of Table 4-9. Displayed are probabilities on the open (O) and closed (C) barrier states. Also shown are the 10- and 90-percentiles of the discharge and wind speed (rounded numbers), corresponding to the situation O+C. The colour light blue indicates regions where during "normal circumstances" no flooding occurs, but only during elevated water levels caused by (combinations) of storm surges and large discharges.*

Based on Table 4-9 and Figure 4-4 the following conclusions are drawn:

1. Everywhere in the area, except near Dalfsen (km 45), there is a broad diversity of circumstances during failure. At almost every location the threat consists of: extreme discharges with little wind, low discharges with extreme wind, and combinations of elevated discharges and wind.

2. The only locations dominated by discharges are those near Dalfsen (km 45). The reason that upstream of Dalfsen the wind becomes more important (at km 36) is that locally generated wind set-up influences the water levels here. (If the river would remain narrow, the wind's influence would not increase further upstream.)

3. There are no locations purely dominated by wind. The role of the wind becomes most prominent at the north-east side of the small lake Zwarte Meer (at WsRW39), where wind set-up from the most relevant westerly directions can be large.

4. Except in the vicinity of Dalfsen (km 45), failure can occur with considerable probabilities for both the open and the closed barrier state. Near Dalfsen, wind poses no threat, explaining why the barrier with high probability remains open (it does not need to close without a storm).

As a final remark, not illustrated with calculations here, we note that the most threatening wind directions throughout the Vecht delta are WSW, W and WNW, again with the exception of locations near Dalfsen, where all wind directions contribute to the exceedance frequency.

5 Physical models

Hydra-Zoet uses input generated by physical models to calculate water levels and wave variables. This chapter introduces these physical models, but since these models are not at the heart of Hydra-Zoet, the explanation will be brief, with the exception of the Bretschneider formulas to calculate wave variables.

Section 5.1 explains that a lot of physical calculations have to be made as input for a probabilistic model such as Hydra-Zoet. Sections 5.2 and 5.3 treat the hydrodynamic models used to calculate water levels and the wave models to calculate wave variables near the dike. The wind waves then have to be transformed towards the toe of the dike if a dam and/or foreshore are present, which is treated in section 5.4 (for a foreshore the water levels are also transformed). Finally section 5.5 describes how the water levels and wave variables at the toe of the flood defence are used to compute the hydraulic load level on the dike, using a physical model to determine wave overtopping.

5.1 Role of physical models in Hydra-Zoet

Physical models for water levels and wave variables are used to generate input for Hydra-Zoet. The program uses a wave overtopping module to compute the hydraulic load levels. We note that the water levels and wave variables have to be calculated for various so-called c*ombinations of boundary conditions*. For Lake IJssel for example, such a combination would consist of values for the lake level, the wind speed and the wind direction. The load level in case of overflow would be the local water level. The details of the way the boundary conditions are chosen is explained for the tidal rivers in chapter 10, and for the Vecht and IJssel delta in chapter 14.

In a probabilistic model such as Hydra-Zoet, the load level has to be known for a lot of combinations, since these combinations should cover the whole range of circumstances occurring in reality; only circumstances with extremely low probabilities of occurrence, say smaller than 10^{-6} per year, can be left out as being irrelevant (they don't contribute to the failure probabilities which are relevant for Hydra-Zoet). Usually a few thousand combinations have to be considered for the more complex water systems. In the probabilistic part of the model Hydra-Zoet, proper probabilities are assigned to the combinations of boundary conditions (and ones obtained by interpolation), eventually providing the exceedance frequencies of load levels. Actually, the probabilistic calculation is more complicated than this, since the model has to take care of different time scales of the random variables: discharges and lake levels vary at much longer time scales than storms and storm surges. So roughly speaking, in a probabilistic model such as Hydra-Zoet, a whole range of boundary conditions has to be used as input for the physical models, where the results of the physical models are then weighed with the proper probabilities of the combinations, at the same time accounting for differences in time scales.

5.2 Water levels

To generate water levels corresponding to a set of boundary conditions for a given water system in Hydra-Zoet, two hydrodynamic models are used, the 2-dimensional model WAQUA and the 1-dimensional model SOBEK. Information about these models can be found on the web sites

http://www.helpdeskwater.nl, created by the Dutch government, provinces, municipalities and the union of local water boards, and on the site http://www.deltares.nl from the knowledge institute Deltares.

When using these models, a program called Baseline is used to convert GIS-data into a database with all the physical characteristics of the lake and/or river bottoms and shores. Next, using this database, a WAQUA (2-d) schematisation or SOBEK 'lay out' (1-d) is built. For the most recent Hydraulic Boundary Conditions, i.e. HBC2006, WAQUA has been used for the lakes, Vecht and IJssel delta and the upper rivers. For the tidal rivers, SOBEK was used, where for the wider parts of the channels sometimes more than one branch was included in the model, to simulate 2-dimensional effects.

The model WAQUA, being a 2-d model, has the advantage of being more accurate than the 1-d model SOBEK, especially for the wider channels and the lakes. For practical purposes, however, a disadvantage of WAQUA is that it requires much more information to build the (schematisation) of the model. Another disadvantage is that a calculation with WAQUA is much more time consuming then one with SOBEK, demanding more computer capacity and time. A disadvantage of SOBEK, besides being less accurate then WAQUA, is that it cannot compute wind set-up perpendicular to the branches of the model: only the component of the wind set-up parallel to a branch can be calculated. If wind set-up cannot be neglected, the component of the set-up perpendicular to a branch is calculated pragmatically using a formula provided in [Leidraad rivierdijken deel 2, 1989]. WAQUA also properly represents the effect of the centrifugal force in river bends on water levels, which is not the case in Sobek.

Generally speaking, if one has to choose between SOBEK or WAQUA (or another 2-d or even 3-d model) to make calculations for a water system, one has to weigh the pros and cons of either choice. In this comparison the following aspects have to be considered:

- the accuracy required,
- the effort to build a functioning model,
- the number of calculations required, in connection with available computer capacity.

The ideal situation for the Hydraulic Boundary Conditions would be to use only WAQUA, and discard the less accurate model SOBEK. At this moment, though, the effort to use WAQUA everywhere in the Netherlands is still too large. As it turns out, to build a 2-d model for the estuaries is a difficult task: one has to account for the difference in density of sea water and river water, storm surges, river discharges, wind set-up and the operation of storm surge barriers.

5.3 Wind waves

To calculate the hydraulic load on a dike, wave variables are needed. In Hydra-Zoet these usually are: the significant wave height, the peak period and the wave direction. Until now, these variables are mostly calculated with the 1-d wave growth formulas of Bretschneider. Only for Lake IJssel and Lake Marken a 2-d model has been used. It is possible, however, to use wave variables derived with 2-d wave models as input for other water systems as well (the program Hydra-Zoet can handle both types of input). In sections 5.3.1-5.3.3 the 1-d Bretschneider formulas are considered in detail, whereas in section 5.3.4 some comments on the 2-d models are made.

5.3.1 Formulas of Bretschneider

Before turning to the details of the Bretschneider formulas, some notation is given:

H_s	significant wave height	m
T_p	peak period	s
T_s	significant wave period	s
$T_{m-1,0}$	mean wave energy period	s
θ	wave direction	degrees relative to the north
F	effective fetch	m
d	effective water depth	m
u_{10}	wind speed at 10 m height above open water	m/s
g	constant of gravitational acceleration (9.81 in the Netherlands)	m/s^2

The formulas of Bretschneider for H_s and T_s, as taken from [Leidraad rivierdijken deel 2, 1989], are given by

$$H_s = \frac{0.283 u_{10}^{\,2} \nu_1}{g} \tanh\left(\frac{0.0125}{\nu_1} \left(\frac{gF}{u_{10}^{\,2}} \right)^{0.42} \right), \qquad \nu_1 = \tanh\left(0.530 \left(\frac{gd}{u_{10}^{\,2}} \right)^{0.75} \right) \tag{5.1}$$

$$T_s = \frac{2.4\pi u_{10} \nu_2}{g} \tanh\left(\frac{0.077}{\nu_2} \left(\frac{gF}{u_{10}^{\,2}} \right)^{0.25} \right), \qquad \nu_2 = \tanh\left(0.833 \left(\frac{gd}{u_{10}^{\,2}} \right)^{0.375} \right) \tag{5.2}$$

Since in Hydra-Zoet usually the mean wave energy period $T_{m-1,0}$ is used instead of T_s, this quantity is pragmatically derived from T_s by[14]

$$T_{m-1,0} = \frac{1.08}{1.10} T_s \tag{5.3}$$

We remark that, when using Bretschneider, the wave direction is taken equal to the wind direction:

$$\text{wave direction } \theta = \text{wind direction } r, \qquad \text{for wave parameters according to Bretschneider} \tag{5.4}$$

In a 2-d wave model this need no longer be the case.

5.3.2 Effective fetches and bottom levels for Bretschneider

For a specific location, wave variables need to be calculated in Hydra-Zoet for several wind directions. These wind directions are actually wind *sectors*, with a width of 22.5°. The considered sectors are numbered as r = 1, 2,..., 16, where the midpoints of these sectors correspond to the familiar 16 wind directions NNE, NE,..., N. Sometimes wind directions are also denoted by their mid-values 22.5°, 45°,..., 360°. E.g. r = 1 is also denoted as direction 22.5°, which really stands for the sector 11.25° - 33.75°.

[14] We note that T_p is derived from T_s using T_p = 1.08 T_s, after which $T_{m-1,0}$ is derived from T_p as $T_{m-1,0} = T_p/1.10$. This results in (5.3). We also note that in older versions of Hydra-Zoet, the output of Hydra-Zoet shows T_p instead of $T_{m-1,0}$, as f.i. in Table 4-8.

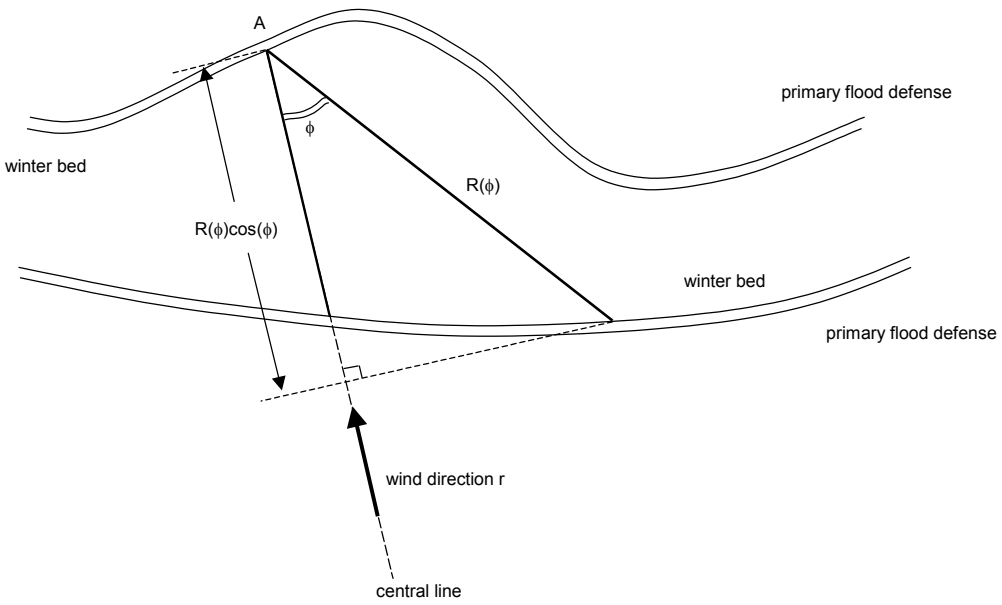

Figure 5-1 Illustration for the calculation of the effective fetch for wind direction r.

Suppose that we observe a water level h_{wl} (wl = water level) at location A for wind direction r (see Figure 5-1). To apply the Bretschneider formulas, the effective fetch F and the effective water depth d are needed, the calculation of which is the subject of this section.

We start with the calculation of the effective fetch F for direction r. It is determined by a sort of weighing over various distances from A towards the primary flood defence at the other side of the river. These distances correspond to angles, with the main direction r (normal to the flood defence at location A) in the centre of the cone of angles. Consider in Figure 5-1 the 'central line' corresponding to direction r, originating from A. Next to this line, a bundle of lines i is considered all originating from A, having angles ϕ_i with the central line. With a fixed step size $\Delta\phi$ = 6°, values $\{\phi_i\}_{i=1,\ldots,15}$ = {-42°,-36°,..., 36°, 42°} are considered, where ϕ_8 = 0° corresponds to the central line. Denote with $R(\phi)$ the distance along direction ϕ from A to the primary flood defence on the other side of the water. Then $R(\phi)\cos(\phi)$ is the length of the projection of this distance onto the central line. The effective fetch for direction r, then, is calculated by:[15]

$$F = \frac{\sum_{i=1}^{15} R(\phi_i)\cos^2(\phi)}{\sum_{i=1}^{15}\cos(\phi)} \qquad (5.5)$$

Note that in this calculation the water level h_{wl} is not used, although strictly speaking the distances $R(\phi)$ depend on this water level, especially if for low levels only the summer bed is flooded. For extreme high-water levels, however, the winter bed is always flooded, in which case $R(\phi)$ hardly depends on h_{wl}.

We also need, corresponding to direction r, an effective water depth d (for which the value of h_{wl} is important). In this case d is calculated by subtracting an effective bottom level h_{bottom} from h_{wl}, i.e.

[15] Note that the finite summations in this formula could be replaced by integrals over ϕ, but here the recipe is given that is currently in use.

$$d = h_{wl} - h_{bottom} \tag{5.6}$$

The effective bottom level is calculated by averaging all bottom levels along the central line. Note that alternatively, this bottom level could be calculated by some kind of weighing as in (5.5).

5.3.3 Potential wind and open water transformation

As input for Bretschneider, the open water wind speed u_{10} at a height of 10 metres above water is needed. Hydra-Zoet, however, uses what are called potential wind speeds, denoted by u. This section briefly explains the meaning of these types of wind speeds, and relates them to each other.

According to [Wieringa en Rijkoort, 1983], the meaning of the potential wind speed is as follows. Suppose that at some location measurements of the wind speed are performed at a certain height. It is possible to convert these measurements to a standard height of 10 m and a standard roughness 0.03 m of a flat and open surrounding landscape (e.g. short grass), resulting in a fictitious wind speed called the potential wind speed. Here the roughness is a measure for the friction that the wind experiences from the ground: the rougher the land, the more the wind slows near the ground. Hence, the potential wind speed is a fictitious wind speed, which would have been observed at a height of 10 metres above the ground if the surrounding landscape would be flat and with a roughness of 0.03 m. The reason to use a potential wind speed is that different wind measurement stations can be compared meaningfully.

Next to land, open water has a roughness which will be smaller than the roughness of land. Therefore, if at high altitudes we have a constant wind speed across an area containing a transition from land to water, because of these differences in roughness the wind above water is slowed down to a lesser extent than above land. For this reason the Bretschneider formulas use the wind speed u_{10} (at 10 metres above open water) instead of the potential wind speed u. The conversion of the potential wind speed u to u_{10} is done with a so-called *open water transformation* [De Waal, 2003], see Table 5-1. For values of u in between the tabulated values, linear interpolation is used to obtain u_{10}. We note that this transformation is a bit pragmatic; transforming wind from land to water turns out to be a difficult problem, as already discussed in [De Waal, 2003], and also in the more recent report [De Waal, 2010].

pot. wind	10 m wind
m/s	m/s
0	0.00
1	1.12
2	2.25
3	3.37
4	4.49
5	5.61
6	6.74
7	7.86
8	8.97
9	10.06
10	11.14
11	12.21
12	13.28
13	14.34
14	15.39
15	16.44
16	17.49

pot. wind	10 m wind
m/s	m/s
17	18.53
18	19.56
19	20.59
20	21.62
21	22.64
22	23.66
23	24.68
24	25.69
25	26.69
26	27.69
27	28.69
28	29.69
29	30.68
30	31.67
31	32.65
32	33.64
33	34.62

pot. wind	10 m wind
m/s	m/s
34	35.59
35	36.56
36	37.53
37	38.50
38	39.47
39	40.43
40	41.39
41	42.34
42	43.30
43	44.25
44	45.20
45	46.14
46	47.08
47	48.03
48	48.96
49	49.90
50	50.83

Table 5-1 Transformation of the potential wind speed u to the open water wind speed u_{10}.

5.3.4 Other wave models

The Bretschneider formulas can be considered a 1-d model to calculate wave variables, in which the flood defence and its surroundings are treated in a simplified manner, using only effective fetches and bottom levels for each direction. Another possibility is to use a 2-d (or 3-d) model to calculate the wave variables. The need for such a model becomes more important if the wind waves threatening the dike are higher, for example in the case of larger bodies of water such as lakes and wider channels. A 2-d model will also perform better than a 1-d model if the surroundings of the flood defence is complex (varying depths as in sea ports and/or large bends in the river). Next to this, a 2-d model allows you, among other things, to take into account the effect of current velocities on the waves, and better modelling of diffraction, refraction and energy dissipation.

Until recently, the 2-d wave model HISWA was used for the lake areas in Hydra-Zoet [Hydra-M, 1999 – deelrapport 6]. Currently this model has been replaced by the more up to date 2-d wave model SWAN. SWAN is public domain software, maintained by Delft University of Technology, see for information about the model the web site http://www.swan.tudelft.nl.

The model SWAN has already been used for the Dutch coast and the estuaries of the Eastern- and Western Scheld. If the 2-d wave model SWAN is used instead of Bretschneider, no effective fetches and bottom levels are needed, since this kind of information is contained in the 2-dimensional schematisation of the SWAN model. We note that the wave variables H_s, T_p and θ are output of the SWAN model, next to other characteristics of the wave period. When using SWAN, the wave direction θ differs from the wind direction, since contrary to the Bretschneider formulas, bending of waves is included in SWAN. Also, no foreshore module is needed if the Hydraulic Boundary Conditions are provided at or near the toe of the dike.

Since wave models are not essential in the understanding of Hydra-Zoet, we will not elaborate on them much further. We conclude with a few remarks regarding other 1-d wave models. Such other models are the 1-d wave growth formulas of e.g. from [Young en Verhagen, 1996] and

[Wilson, 1965]. We note that using different wave models certainly yields different outcomes for required dike heights: depending on the location, differences of order decimetres can easily result [Duits, 2005], indicating that quite a lot of uncertainty is involved when accounting for the effect of wave overtopping. According to [De Waal, 2008], the formulas of Bretschneider have a reputation to yield relatively large wave variables (i.e. probably too large), particularly in the case of short fetches. This reference also demonstrates that Bretschneider usually provides more severe wave conditions than those by [Young en Verhagen, 1996].

5.4 Transformations from open water to the toe of the dike

The preceding section described how wave variables for 'open water' can be derived with Bretschneider, or another wave model. If between this open water and the toe of the dike a dam and/or foreshore is present, the wave variables have to be transformed from open water to the toe, as illustrated in Figure 5-2. The modules used in Hydra-Zoet for these transformations are described in the report [Hydra-M, Deelrapport 9], written by De Waal. The following sections briefly comment upon these modules. The figures in the remainder of this chapter are adaptations of the ones in the report just mentioned.

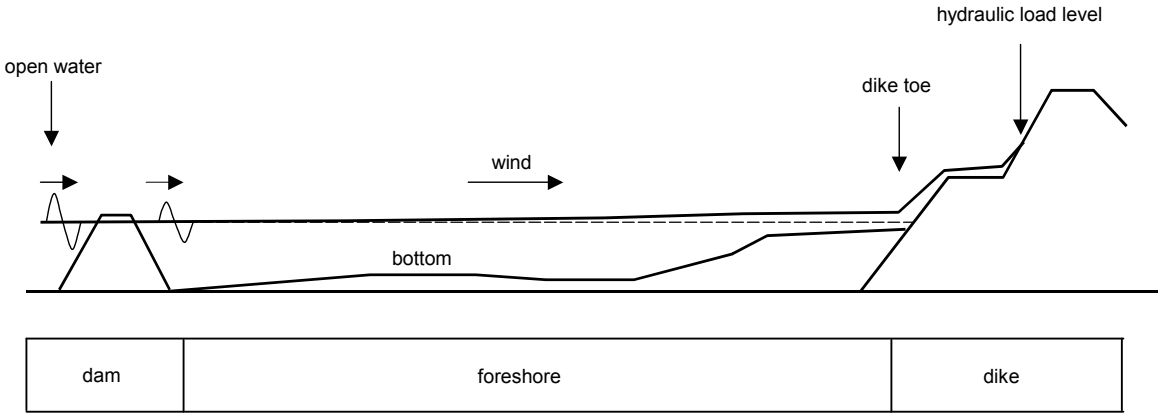

Figure 5-2 Overview of dam, foreshore and dike; the 'open water' is at the left of the figure.

5.4.1 Transformation module for a dam

In the dam module the wave variables from outside the dam are transformed to new variables at the landside of the dam, using formulas for wave transmission. This transmission mainly decreases the wave height. The formulas used in the module are based on [Goda, 1969] and [Seelig, 1979]. The formulas currently used in the module only affect the wave height, whereas the wave period, wave direction and water level remain unaltered.

A dam in Hydra-Zoet has to be characterised by two characteristics. The first is the type of dam: a trapezoidal shape, a caisson or a vertical wall (Figure 5-3). The second is the crest height, in metres + NAP. The significant wave height directly behind the dam is assumed to be influenced by wave transmission across the dam only – wave penetration through holes in the dam is neglected. Strictly speaking, the latter contradicts the assumption of equal water levels in front and behind the dam if between the dam and the dike there is a closed basin and the dam has no holes (a non-porous dam). The actual assumption is: regarding the water level the

dam contains openings, with equal water levels before and after, while regarding the waves the dam contains no holes.

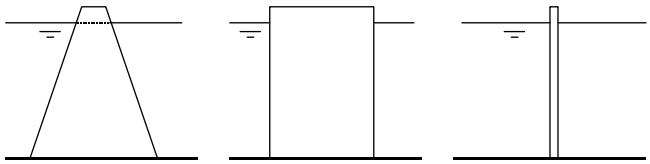

Figure 5-3 Types of dams: dam, caisson and vertical wall.

5.4.2 Transformation module for a foreshore

If a foreshore is present in front of the dike, the wave variables at the beginning of the foreshore have to be transformed to ones at the toe of the dike. This transformation is done in the foreshore module with the model ENDEC (acronym for Energy Decay), developed by the institute WL|Delft Hydraulics (nowadays part of the Deltares institute). ENDEC calculates changes in wave height and wave direction, but not of the wave period, due to:

- refraction (bending of waves as a consequence of changes in bottom levels),
- shoaling (changes in wave height due to changes in bottom levels),
- energy loss by breaking of waves,
- energy loss by bottom friction,
- energy gain caused by wave growth due to wind.

ENDEC also calculates the (usually small) changes of the water level as a consequence of wave set-up and wave set-down, whereas changes in the wave period (decrease by breaking or increase by wind) are neglected.

In the original ENDEC model, no changes of the water level caused by wind set-up have been taken into account. For some situations this could lead to an underestimation of the water level and waves at the toe of the dike. Therefore the wind set-up was built in into the foreshore module at a later stage, as described in [Ris, 1997]. In the module first the wind set-up is calculated for the specified cross section of the bottom. Afterwards, the ENDEC calculation is performed.

When using ENDEC, it is important to note that the model is 1-dimensional, and therefore of limited accuracy. This (lack of) accuracy is commented upon in [Hydra-M, Deelrapport 9].

5.5 Hydraulic load levels

If the failure mechanism wave overtopping is used in Hydra-Zoet, the wave variables at the toe of the dike have to be transformed into a hydraulic load level on the dike. This load level, in metres + NAP, depends on the wave variables, but also on the allowed critical overtopping discharge q_{crit} (see section 4.4). The better the quality of the grass cover of the inner slope, the larger q_{crit} can be. Larger values of q_{crit} result (for fixed wave variables) in lower hydraulic load levels on the dike. This means that dikes with good grass cover can have lower required crest heights then dikes with poor grass cover.

It is useful to provide some definitions, the first taken from [TAW, 2002], the second and third from [De Waal, 1999b].

1. The *overtopping discharge* is measured as an average discharge per metre along the dike, e.g. in m^3/s per m, or in l/s per m. This overtopping discharge is calculated at the location of the *outer crest* line of the dike (see Figure 5-4), where it is assumed that the water passing the outer crest also reaches the inner crest and the inner slope of the dike.

2. For a given overtopping discharge, the *wave overtopping height*, in m, is defined as the height relative to the local water level where this specified discharge occurs. More precisely, the wave overtopping height is the difference between the level of the outer crest and the local water level, provided the outer crest has a height chosen such that it corresponds to a discharge equal to the specified overtopping discharge.

3. The *hydraulic load level*, in m+NAP, equals the sum of the local water level and the wave overtopping height.

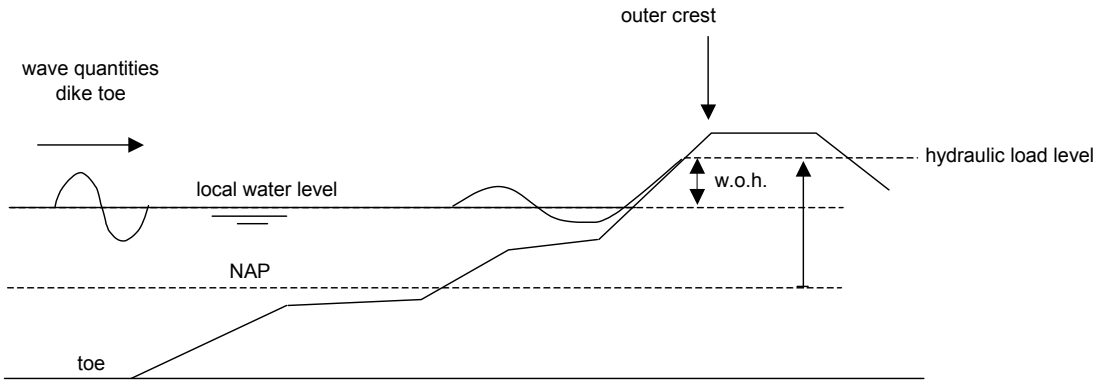

Figure 5-4 Illustration of the concepts wave overtopping height (w.o.h) and hydraulic load level.

After a possible transformation by the dam and/or foreshore module, the (wave) variables at the toe of the dike in Figure 5-4 consist of:

- local water level,
- significant wave height H_s,
- peak period T_p,
- wave direction θ.

For the calculation of the wave overtopping height in Hydra-Zoet, the module PC-Overslag is used, based on the work of Van der Meer [TAW, 2002]. The formulas are not discussed here. We only mention that in PC-Overslag the wave period $T_{m-1,0}$ is used. In Hydra-Zoet (when T_p is calculated with Bretschneider) is pragmatically obtained from T_p by using the relation $T_{m-1,0} = T_p/1.1$.

6 Derivation of standard waves for discharges and lakes

In the remainder of this report hydrographs for discharges and lake levels are needed. Hydrographs are schematised shapes of the average time evolution of discharge or lake level waves. They are determined with what is called the *scaling method*.

For use in Hydra-Zoet the hydrographs obtained are parameterised by trapeziums (compare Figure 6-6). Such a parameterisation has the advantage that the hydrograph can be described with only a few parameters, without the need to tabulate the values as a function of time. Since the results of Hydra-Zoet appear to be rather insensitive to the precise shape of the hydrograph, such a parameterisation is permissible. (Note that the trapezium is a further simplification of the hydrograph, which itself is a simplification of the time evolution of the variable under consideration.)

In this chapter the scaling method is explained using the discharge of the river Rhine as an example. Next, results are given for Lake IJssel. We end with some references and comments on the method.

6.1 The scaling method, applied to the Rhine

6.1.1 How to derive a normalised discharge wave with the scaling method

To illustrate the scaling method, measurements of the discharge of the river Rhine are considered during the period Jan-01-1901 until May-25-2005. The discharges are daily measurements (one measurement each day, which will be treated as a daily average). Since very high discharges (and also lake levels and wind speeds) are much more probable in the 'winter months' October - March then in the 'summer months' April - September, the analysis is restricted to data of the winter months. We note that all calculations and statistical data in Hydra-Zoet are based on winter months, based on the assumption that extreme water levels and extreme hydraulic loads in summer months may be ignored.[16]

The scaling method consists of the following steps, which are illustrated below with several figures. Each of the steps are then elaborated on afterwards.

1. Waves are selected for which the peak exceeds some *threshold* ω, in such a way that no higher peaks are present in a window running from z days before until z days after the selected peak; z = called the *sight duration*. For the remainder of the analysis, only the part of a selected wave within this window is considered.

2. Since every measurement represents a daily average, a correction is made to ensure that every peak lasts at least one day.

[16] We mention that drought may still affect the safety of a flood defence in summer.

3. Next to the main peak, there may be secondary peaks which we want to transform into a single peak. This is done in such a way that within the resulting single peak the total exceedance duration of every level remains the same as in the original (multiple) peaks. This transformation is done separately for the part of the selected wave(s) before the main peak and the part after the main peak.

4. The (adapted) waves are normalised such that their peak values become equal to 1. Here it is assumed that all relevant discharges exceed a minimum value q_{min}, and all discharges q(t) at time t within a wave with peak value k are normalised such that q(t) is replaced by the value $(q(t) - q_{min})/(k - q_{min})$. In the analysis q_{min} = 750 m^3/s is chosen.

5. For every (normalised) discharge level v, where $0 \leq v \leq 1$, the N exceedance durations of this level for the N available waves are averaged. Actually, this is done separately for the increasing part of the waves and for the decreasing parts. These durations are respectively denoted as $L_{front}(v)$ and $L_{back}(v)$. These two variables completely determine the normalised standard shape.

An un-normalised standard shape with peak value k can be obtained by 'scaling back' this standardised shape, as will be explained below. But first the above steps will be explained (the accompanying figures are provided after the explanation).

Step 1
A threshold ω = 9740 m^3/s is chosen, for which waves are selected such that the selected peaks exceed this threshold and are separated in time by at least z = 15 days. This results in N = 20 waves, see Figure 6-1 (the red trapeziums in the subplots will be explained later). The peaks of the selected waves were all put together at time t = 0. The actual dates of the peak are indicated above each subplot. For clarity, all selected waves have been put together in a single figure (Figure 6-2).

Step 2 and 3
The results of these steps are shown in Figure 6-3.[17] Note that after these steps, every wave has an increasing front flank, a top duration of (at least) 1 day, and a decreasing back flank.

Step 4
The results of the normalisation are shown in Figure 6-4 and need no further comments.

Step 5
For a fixed relative discharge level v, we can split the duration of the exceedance of level v in the i-th normalised adapted wave into two parts: the duration before t = 0 and the duration after t = 0. Denote these durations respectively by $L_{front,i}(v)$ and $L_{back,i}(v)$, see Figure 6-5. Averaging over the N waves we then obtain

$$L_{\text{front}}(v) = \frac{1}{N}\sum_{i=1}^{N} L_{\text{front},i}(v)$$
$$L_{\text{back}}(v) = \frac{1}{N}\sum_{i=1}^{N} L_{\text{back},i}(v) \qquad (6.1)$$

[17] The discharge waves start half a day later and end half a day sooner, which is an artefact of the program code used, but will not influence the final results.

The results of this procedure are given in Figure 6-6 (the trapezium in this figure is discussed later). Of course, the total exceedance duration of level v in this standard wave is given by

$$L(v) = L_{\text{front}}(v) + L_{\text{back}}(v) \tag{6.2}$$

The normalised standard wave is now completely specified.

In principle we could use (rescaled versions of) this default wave in Hydra-Zoet for the modelling of the time evolution of discharge waves. Note, however, that the standard wave looks just like a trapezium, which suggests that we might just as well use a simple trapezium shaped standard wave. Various analyses have revealed that the results of Hydra-Zoet for the failure mechanisms overflow and wave overtopping are very insensitive to the details of the shape of the discharge waves: e.g. using waves which are wider or narrower around the peak practically yield the same results for the normative water levels and required dike heights. For this reason we have chosen to replace the obtained standard shape by a trapezium as indicated in Figure 6-6. This trapezium has a top duration of 1 day.

We note, however, that discharge waves are only suitable to model the time evolution of relatively high discharges (exceeding the once per year value: approximately 6000 m^3/s for the Rhine). For the lower discharges, which are much more frequent, the time evolution is so irregular that proper discharge waves cannot be discerned. In Chapter 8 we will explain how this problem is solved in Hydra-Zoet.

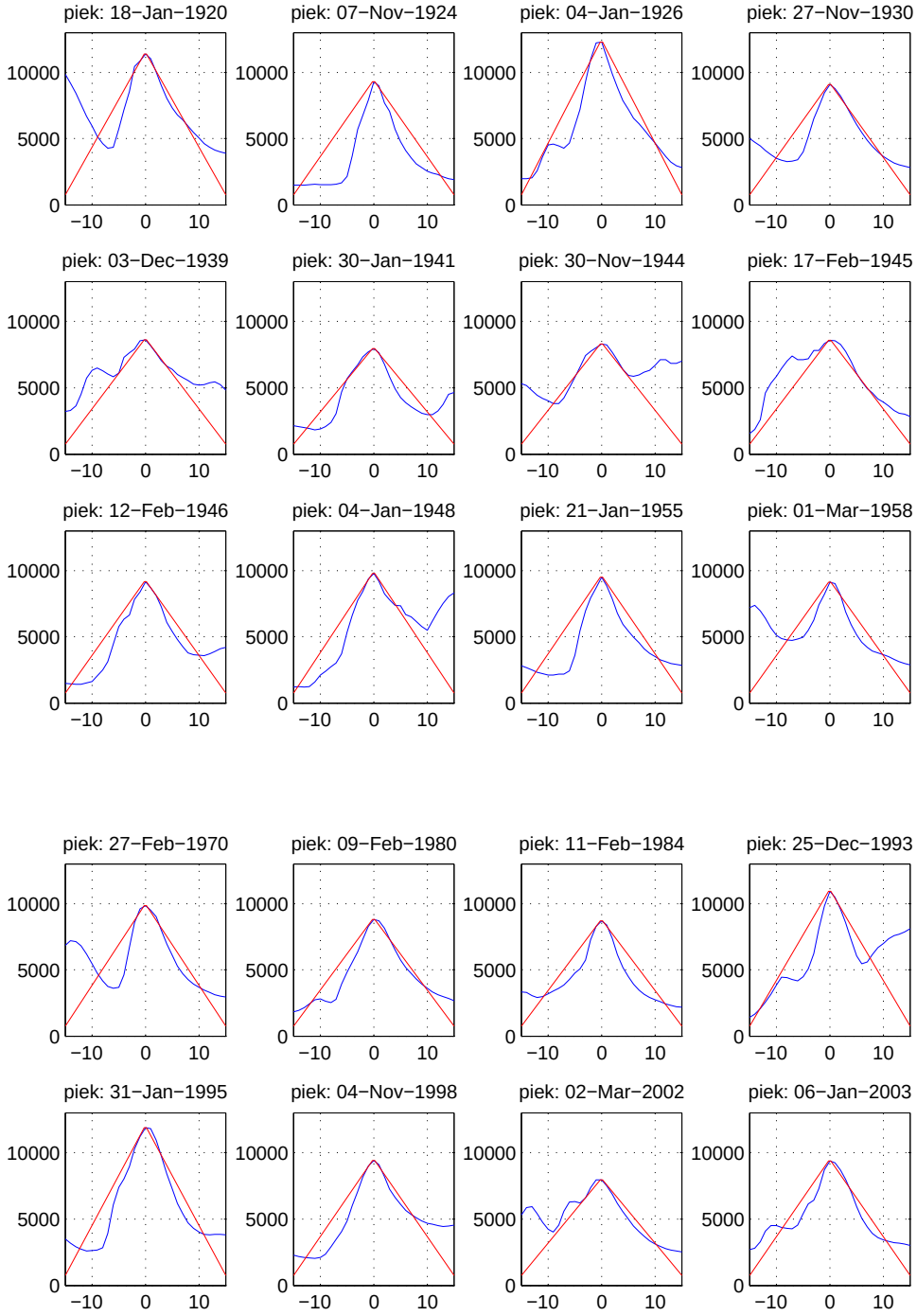

Figure 6-1 Selected discharge waves for station Lobith, with peaks exceeding ω = 7940 m^3/s, resulting in N = 20 waves. Horizontal axis: time t in days, from t = -15 until t = 15 days. Vertical axis: discharge in m^3/s.

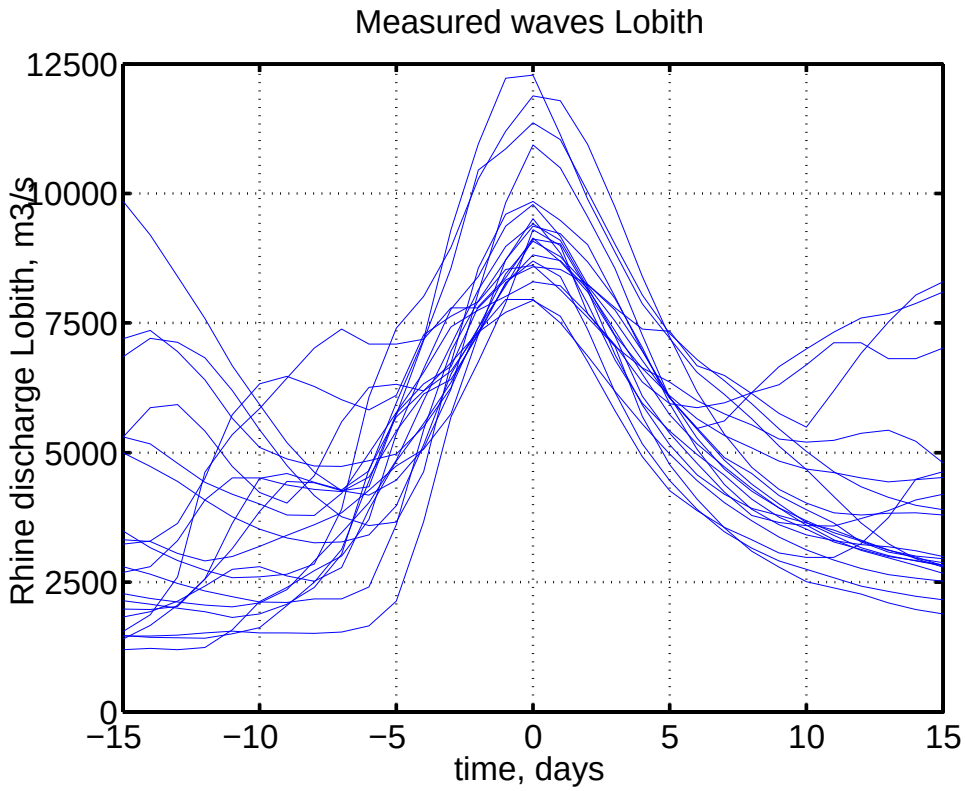

Figure 6-2 Selected discharge waves at Lobith.

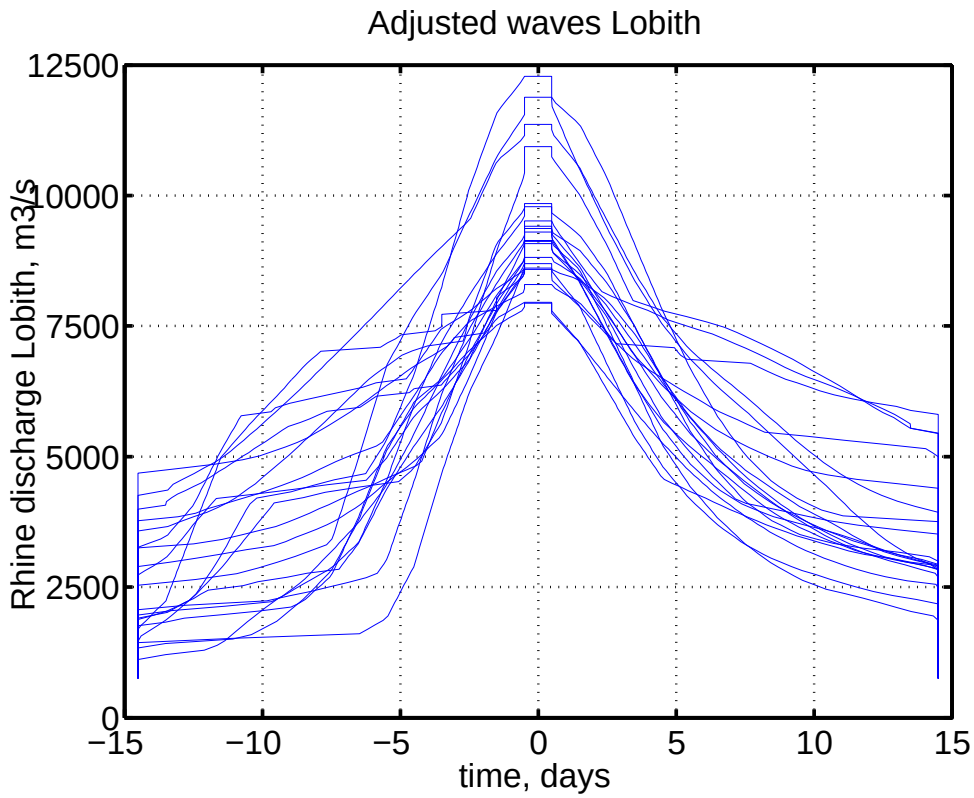

Figure 6-3 *The waves of Figure 6-2, but now with corrections such that peaks obtain a duration of 1 day and possible secondary peaks are 'glued' to the main peak, thereby retaining their total duration and volume.*

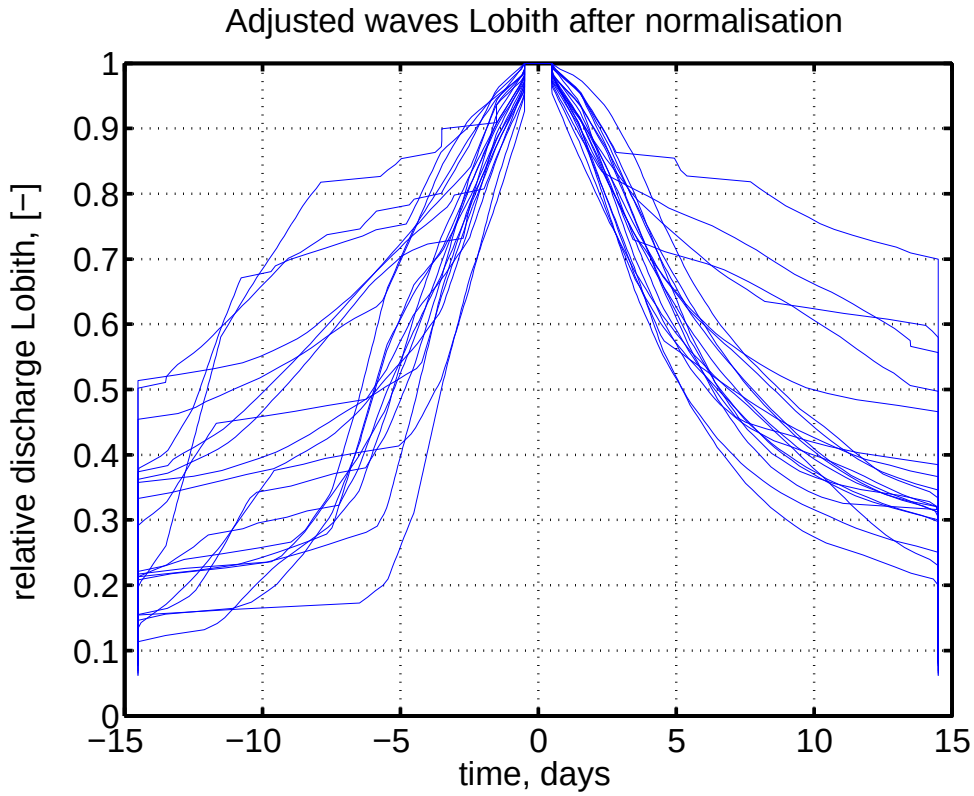

Figure 6-4 *The waves of Figure 6-3 after normalisation.*

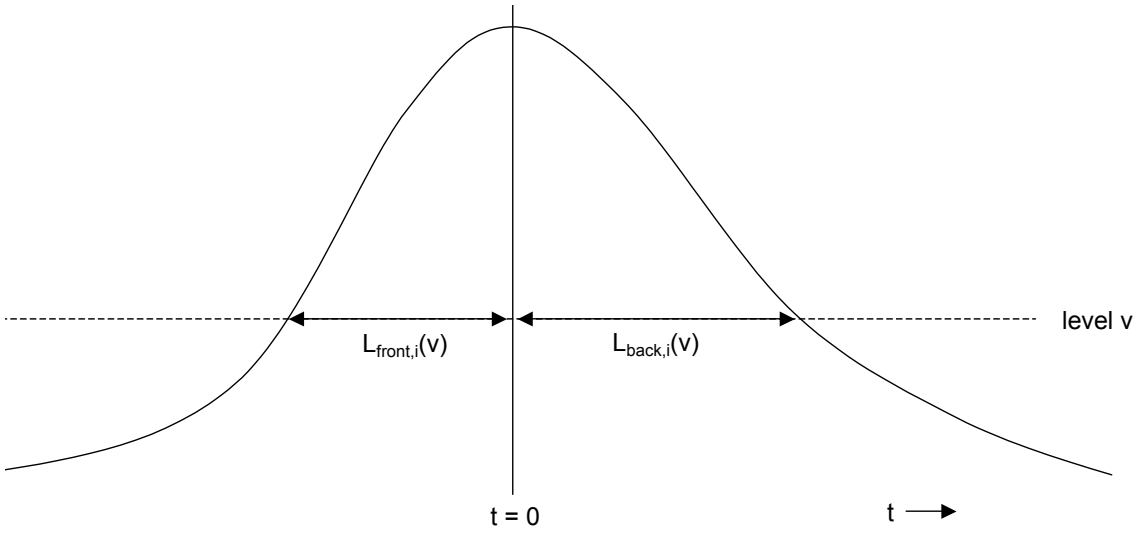

Figure 6-5 Illustration of $L_{front,i}(v)$ and $L_{back,i}(v)$ within an adjusted, normalised (hypothetic) wave i.

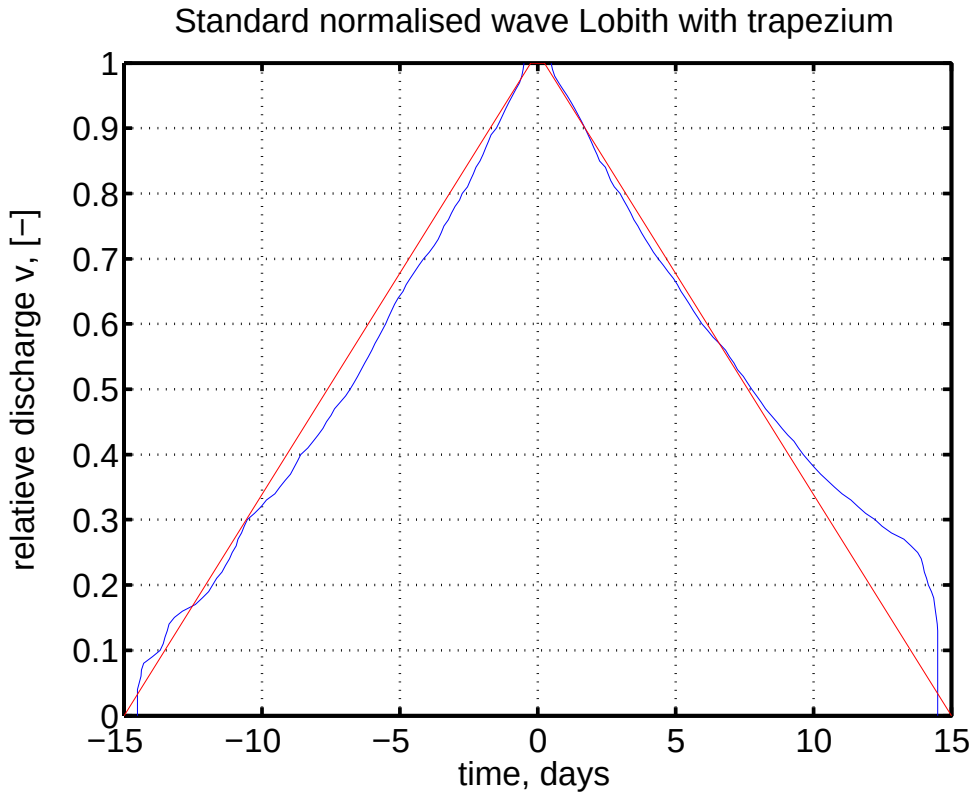

Figure 6-6 The standard normalised wave, obtained from averaging, at every considered relative discharge v, over the durations in the waves of Figure 6-4. Also the trapezium used to model the standard shape is indicated.

6.1.2 Scaling back to obtain an un-normalised shape

It will be explained how an *un*-normalised discharge wave with peak value k is obtained from the normalised trapezium shape. This is done simply by 'vertically rescaling back' the trapezoidal shape in such a way that it attains the peak value k. We have to be a bit careful concerning the role of the minimum discharge q_{min}, so here is the recipe.

Say we want an un-normalised trapezium wave with peak value k. Let v(t) denote the relative discharge in the standard trapezium at time t, and $\alpha(t,k)$ the discharge in the desired un-normalised wave with peak value k (with $\alpha(t=0,k) = k$). Then $\alpha(t,k)$ is obtained as

$$\alpha(t,k) = q_{\min} + (k - q_{\min})v(t). \tag{6.3}$$

Next to the observed selected waves, the trapezoidal waves $\alpha(t,k)$ are indicated in Figure 6-1. They seem to fit the upper half of the observed waves rather well. It should be mentioned though, that the fit can only be judged to be adequate because it is known that the results of Hydra-Zoet for the failure mechanisms overflow and overtopping are very insensitive to the shapes of the discharge waves. For other failure mechanisms, this does not need to be true, in which case a more refined modelling of the waves would be necessary, possibly with different shapes, each with their own probabilities.

6.2 Results for Lake IJssel

The scaling method was explained for an example using discharges of the Rhine, but the method appears to work satisfactory for lake levels as well. Here we provide the results for Lake IJssel. The data period used is Jan-01-1976 until Sep-31-2005, consisting of daily measurements, of which only the winter months are used.[18] The selected lake level waves, together with the trapeziums used to model the waves, are shown in Figure 6-7, which is analogous to Figure 6-1. As threshold for the selection of the lake levels ω = 0.05 m+NAP was used, resulting in N = 24 waves. We note that just as for the discharges, sensitivity analyses with Hydra-Zoet show that for failure mechanisms overflow and wave overtopping the results for normative water levels and required dike height are very insensitive to the precise shape of the waves. Because of this, the 'fit' of the trapeziums to the observed waves is judged to be adequate.

The trapeziums begin and end at the minimum lake level m_{min} = -0.40 m+NAP and have, for the peak values considered here, peak durations of 4 days (lower trapeziums have longer peak durations, as will be treated in section 8.3). The trapeziums are not meant to describe the lower lake levels in an adequate way; they only need to describe the upper half of the waves with sufficiently high peak values, say values > 0.05 m+NAP. How the lower lake levels are treated in Hydra-Zoet will become clear in Chapter 8.

[18] In 1976 a dam halfway Lake IJssel was built, the 'Houtribdijk', connecting dike ring 13 with dike ring 8, see Figure 2-1. This created Lake IJssel to the north of this dam and Lake Marken to the south. For this reason, measurements for Lake IJssel can only be used from 1976 onwards.

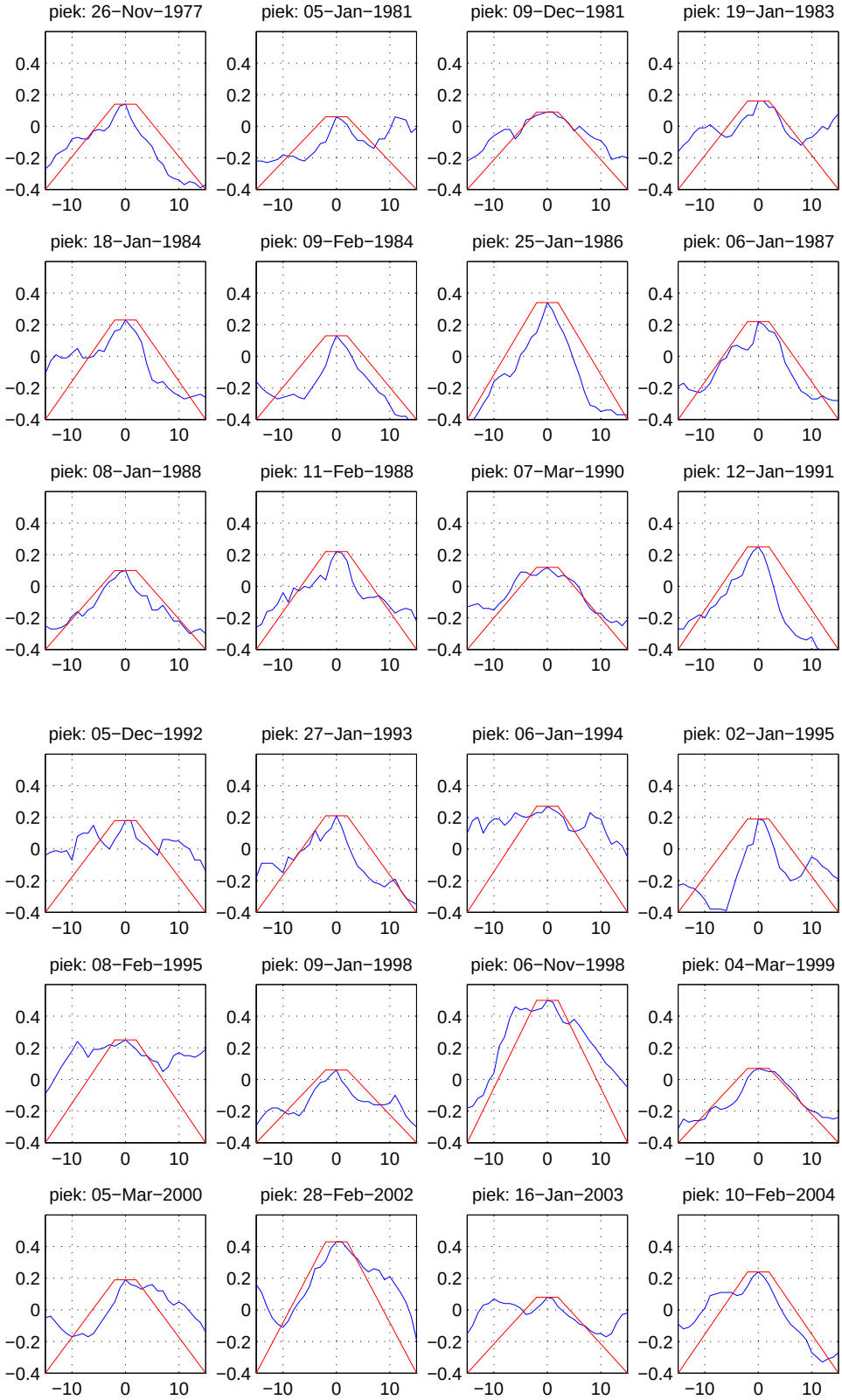

Figure 6-7 Selected waves for Lake IJssel, with peaks exceeding ω = 0.05 m+NAP, resulting in N = 24 waves. Horizontal axis: time t in days, from t = -15 until t = 15 days. Vertical axis: lake level in m+NAP.

6.3 Comments on the scaling method

6.3.1 Computer code used for the scaling method

The above results of the scaling method, applied to discharges and lake levels, have been calculated with Matlab code, written by Beijk and Geerse [2004a]. The method has been used before to derive standard discharge waves for the Rhine and Meuse [Klopstra en Duits, 1999; Klopstra en Vrisou van Eck, 1999]. In the earlier derivation a computer program has been built for this purpose, called the 'wave shape generator' (in Dutch: 'golfvormgenerator'). This program gives results which differ in some respects from those obtained with the Matlab code. The reason is that for the application of the scaling method some subjective choices have to be made concerning the part of the selected wave used in the analysis. The program from 1999 considers a longer part of the selected waves then the Matlab code. Also, choices have to be made with respect to secondary waves (are they 'glued together' with the main peak, and if so, how is this performed?).

The different, and subjective, choices regarding these aspects appear not to be important for the higher parts of the waves (the highest 30% in a wave), but do effect the lower parts. Fortunately, only the modelling of the upper parts of the waves turns out to be critical, as will be clarified in Chapter 8.

As a side remark we note that the Matlab code has been written to obtain a more flexible program then the program of 1999. The 'wave shape generator' program can only be used for discharges, not for lake levels. Also, the scaling method within the Matlab code has been applied to wind speeds (not treated in this text), which is not possible with the program from 1999.

6.3.2 Discharge waves for different stretches of the river

In Hydra-Zoet a standard discharge wave for the Rhine is used, derived from measurements for the station Lobith. This station lies close to the eastern border of the Netherlands with Germany, where the Rhine enters the Netherlands. It is known that a (high) discharge wave going downstream does not change shape too much for a considerable stretch of the river: there is only a limited amount of broadening of the wave, accompanied with a slight decrease of the peak value, at least, provided the dikes along the river are not breached. This is true for the Rhine, because no significant lateral discharge inflow occurs and there are no parts of the rivers where it suddenly widens. An exception has to be made for the river IJssel, a branch of the Rhine, where there is a significant lateral inflow. For this reason, in Hydra-Zoet a separate standard wave downstream of Olst along the IJssel is used.

For the Meuse, also different standard discharge shapes have to be used, one for the upper part of the Meuse (beginning at the border with Belgium), and one for the lower part of the river. Of course, we have to compromise here, since at a particular location we have to jump from one shape of the discharge wave to another. For the Meuse, this transition was made at the village Lith, but Mook could have been chosen as well.

The important point to note here, is that different stretches of the river may require different standard shapes of the discharge waves. When applying a model such as Hydra-Zoet, proper choices have to be made about the stretches of rivers where a single shape might be used. Usually, for stretches of the river of about 100 to 150 kilometres a single discharge wave can be used.

7 Correlation models

In Hydra-Zoet correlation models are used, e.g. to describe the correlation between the river IJssel and Lake IJssel, or the correlation between the sea level and the wind speed (conditional on the wind direction). This chapter treats two types of models, the model HOS (from homoscedastic variance, i.e. constant variance) and the model HES (from heteroscedastic variance, i.e. varying variance). Actually, the model HOS is an improved and extended correlation model from a model often used in the program PC-Ring [Vrouwenvelder et al, 2003].

The models HOS and HES are explained in this chapter, together with specific examples, without providing all mathematical details. Most of these details can be found in the paper [Diermanse and Geerse, 2010], written in English, and the remaining ones in the Dutch report [Geerse, 2004]. Actually, the model HOS is a special case of the model HES, but since HOS has some properties not possessed by the general model HES, the model HOS is treated separately.

7.1 General setting

Consider two random variables V and W, which are statistically dependent, and assume that there are paired data available, of the form (v_i, w_i), i = 1, 2,..., N. Assume also that the marginal probability densities (pdf's) $f_V(v)$ and $f_W(w)$ *are already available*, as is often the case if Hydraulic Boundary Conditions have to be determined. The aim in both the models HOS and HES is to provide a bivariate density $f_{V,W}(v,w)$ with the properties:

1. The marginal densities of $f_{V,W}(v,w)$ correspond exactly with the prescribed densities $f_V(v)$ and $f_W(w)$.
2. The amount of variance modelled by $f_{V,W}(v,w)$ describes the scatter in the data points (v_i, w_i), i = 1, 2,..., N, sufficiently accurate. (As a check: for every value v, the standard deviation of $f_{W|V}(.|v)$ can be compared with the scatter in the data values w_i for those i for which v_i is close to v.)

We denote the cumulative distributions (cdf's) of V and W by $F_V(v)$ and $F_W(w)$. In the correlation model, V and W are transformed to random variables X and Y, with cdf's $F_X(x)$ and $F_Y(y)$. Regarding the notation, if no confusion can arise, the subscripts V, W, X and Y are left out for brevity.

In the literature it is common to use a certain trick to satisfy property 1, using a transformation in which V and W are transformed separately to specific random variables X and Y (the nature of this transformation will become clear below). In this transformed space a certain $f_{X,Y}(x,y)$ is then assumed. By reversing the transformation it turns out that f(v,w) has the desired property 1. Whether property 2 is satisfied to a sufficient degree of accuracy then still needs to be assessed. It appears that the model HOS, corresponding with a fixed standard deviation in the transformed space, is often applicable in the context of the derivation of the Hydraulic Boundary Conditions. Sometimes, however, it is not, in which case the model HES, is often applicable.

In the transformations not only the distributions are transformed, but also the data. The (x,y)-space resulting after this transformation is called the *transformed space*, whereas the original (v,w)-space is called the *physical space*.

7.2 Model with constant variance (HOS)

7.2.1 Theory for model HOS

For the sake of simplicity, in this chapter a simplified version of the model HOS is considered, in which the probability density $\lambda_\sigma(t)$ that is used in the model, see (7.3), equals a normal density. However, a more general situation could be considered, with only minor changes in the formulas, for which $\lambda_\sigma(t)$ can be any density satisfying $\int dt\, e^t \lambda_\sigma(t) < \infty$.

First consider, for given marginals f(v) and f(w), a bivariate density function f(v,w) possessing these marginals. In that case we can write

$$f(v,w) = f(v)f(w \mid v) \tag{7.1}$$

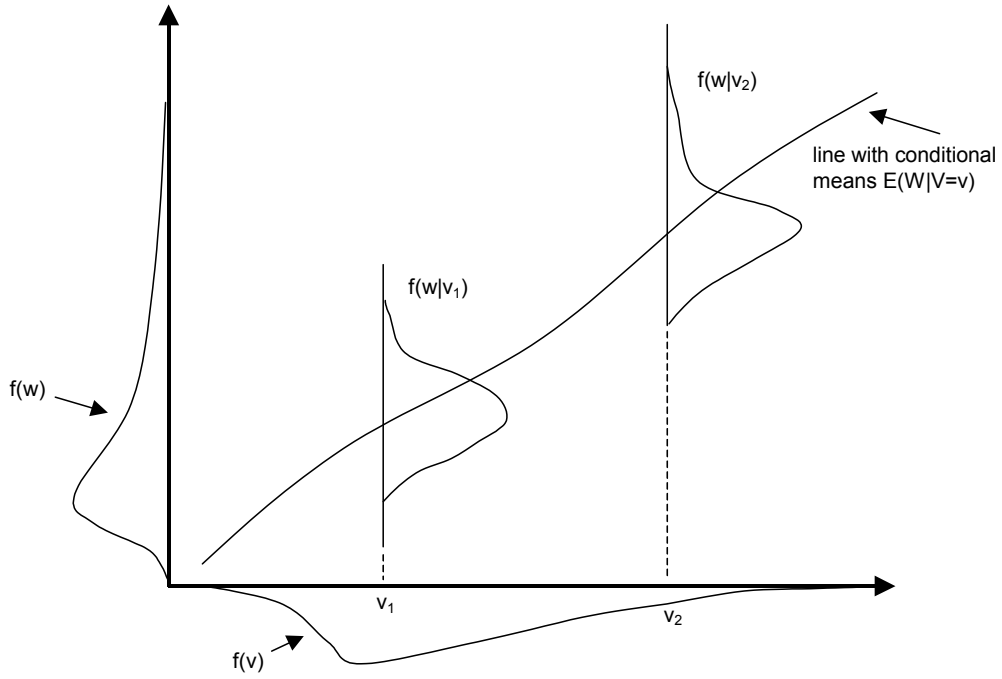

Figure 7-1 Aspects of the bivariate density f(v,w).

Figure 7-1 illustrates in a schematic way some points of interest:

- the marginals f(v) and f(w),
- for two values v_1 and v_2, the conditional densities $f(w|v_1)$ and $f(w|v_2)$,
- the line displaying the conditional means E(W|V=v) for given values V = v.

Observe that f(v,w) is completely determined once f(v) and f(w|v) are known. At that point also f(w) is known. (Note that Figure 7-1 not only applies to the model HOS, but holds in general.)

The specification of the model HOS is done in the transformed space, in which the model is of the form shown in Figure 7-2. A standard exponential density is taken for f(x):

$$f(x) = \exp(-x), \quad x \geq 0 \tag{7.2}$$

and for f(y|x) a normal density with standard deviation σ and mean $\mu = x-\sigma^2/2$. If $\lambda_\sigma(t)$ denotes the normal density with mean 0 and standard deviation σ, we can write

$$f(y \mid x) = \lambda_\sigma(y - x + \sigma^2/2) \tag{7.3}$$

This means that f(y|x) is, apart from a translation, equal to the standard normal density function with mean 0 and standard deviation σ, where the conditional means E(Y|X=x) are located on the line $y = x-\sigma^2/2$. This is shown in Figure 7-2. Note that f(y) can be calculated as

$$f(y) = \int_0^\infty dx\, e^{-x} f(y \mid x). \tag{7.4}$$

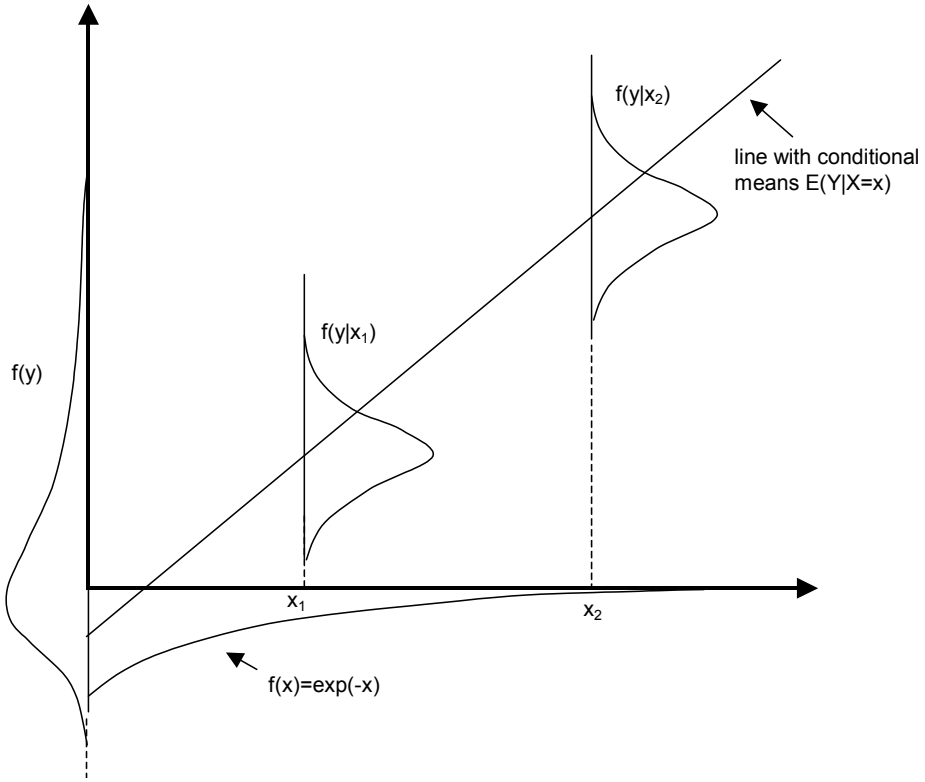

Figure 7-2 Illustration of the bivariate density f(x,y).

The transformations coupling (v,w) to (x,y) are found by equating the cumulative distributions of V and X on the one hand and W and Y on the other (see Figure 7-3):

$$\begin{aligned} F_V(v) &= F_X(x) \\ F_W(w) &= F_Y(y) \end{aligned} \tag{7.5}$$

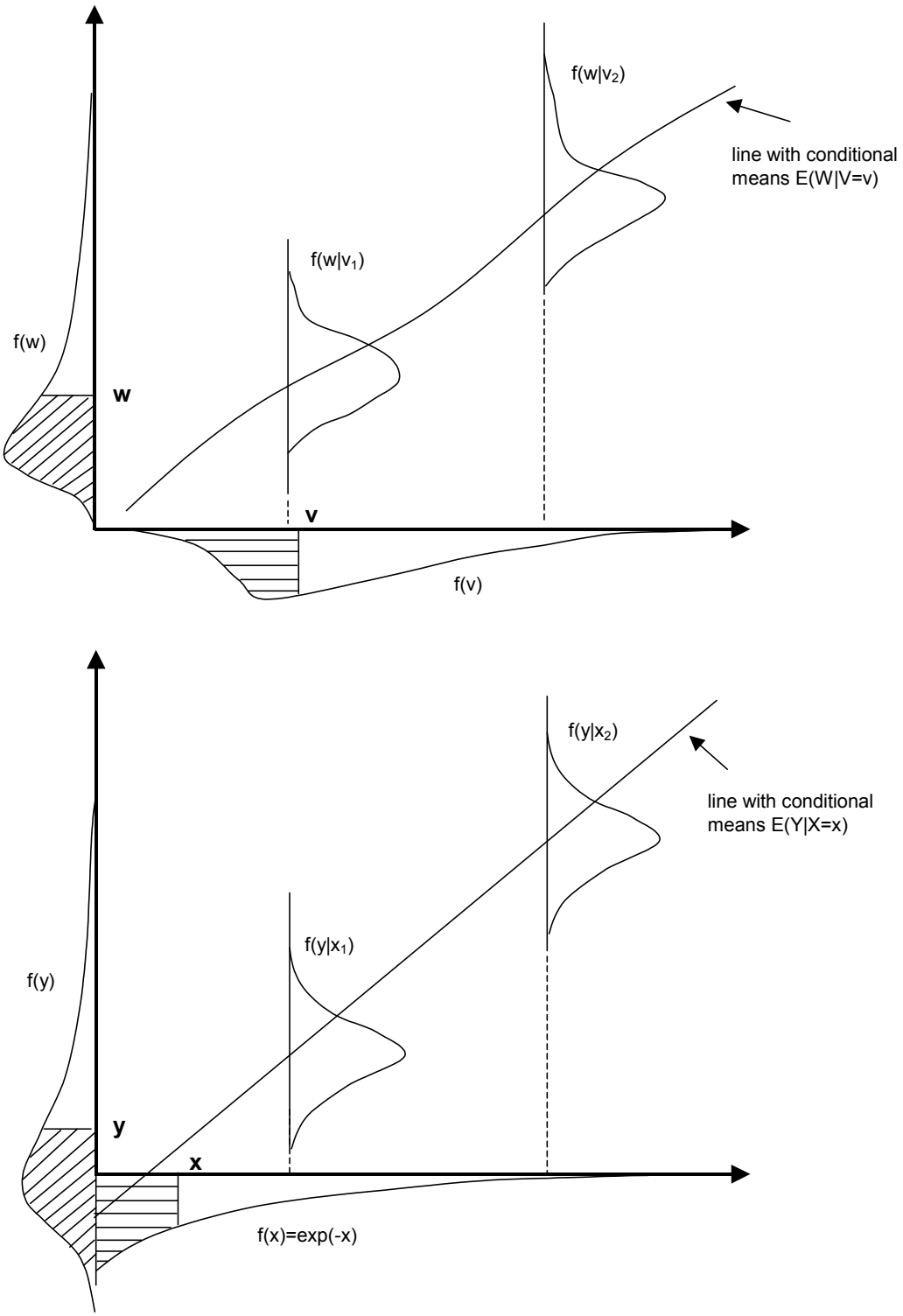

Figure 7-3 Coupling of v to x and of w to y using the transformations (7.5): the obliquely shaded parts have equal surfaces, as do the horizontally shaded parts.

From (7.2) and (7.3) it follows that

$$f(x,y) = \exp(-x)\lambda_\sigma(y - x + \sigma^2/2) \tag{7.6}$$

Under the transformations (7.5) the density f(x,y) in the (x,y)-space is transformed in the density f(v,w) in the (v,w)-space. It can be shown that the resulting f(v,w) is such that it has the prescribed marginals f(v) and f(w). Once again, it is stressed that the formulation of the model HOS as in Figure 7-2 does not guarantee that f(v,w) in the (v,w)-space describes the scatter in the observed data well. Whether this is the case needs to be established for every practical application. If the model does apply, a suitable value of σ has to be obtained. Often, this is done simply by visual inspection, see f.i. section 7.2.2.

We conclude with some remarks, the proofs of which are given in [Geerse, 2004]:
1. The function f(y) of (7.4) is asymptotically standard exponential.
2. In the limit $\sigma \to \infty$ the density f(v,w) becomes equal to the product f(v)f(w), meaning that V and W become statistically independent.

7.2.2 Application of model HOS

As an example for the model HOS we use data for the North Sea water level and wind speed, from the period 1979 until 2002. For this period storms are selected for the wind sector 315° - 345°. The data points (N = 89) consist of the maximum water level within this wind sector during the storm, coupled with the wind speed at the moment this maximum is attained. (Note that the wind sector has a width of 30°, which is larger than the width of 22.5° usually considered in Hydra-Zoet.[19]

The data are shown in Figure 7-4, together with the so-called 10, 50 and 90 percentile lines resulting from the model HOS, applied with σ = 1.4. For a given percentage p, the p percentile line consists of the collection of p percentiles of the probability densities f(w|v), when ranging over all values of v. The precise definition is as follows: the p percentile line, consisting of points $(v,w_p(v))$, is such that $w_p(v)$ satisfies the equation $P(W< w_p(v)|V=v) = p/100$.

This means that roughly 50% of the data points should be below the 50 percentile line, and roughly 50% above this line; outside of the outer lines there should be roughly 20% of the data points. The value of σ was chosen by visual inspection. The corresponding picture in the transformed space is displayed in Figure 7-5. The assumption of constant variance in the transformed space, together with a normal conditional density f(y|x), seems reasonable here. So indeed the model HOS can be used to describe the data. The choice is made based on visual inspection.

[19] The results in the example in this section are not used in Hydra-Zoet, since for historical reasons in Hydra-Zoet a conditional f(y|x) is used that differs from the normal density.

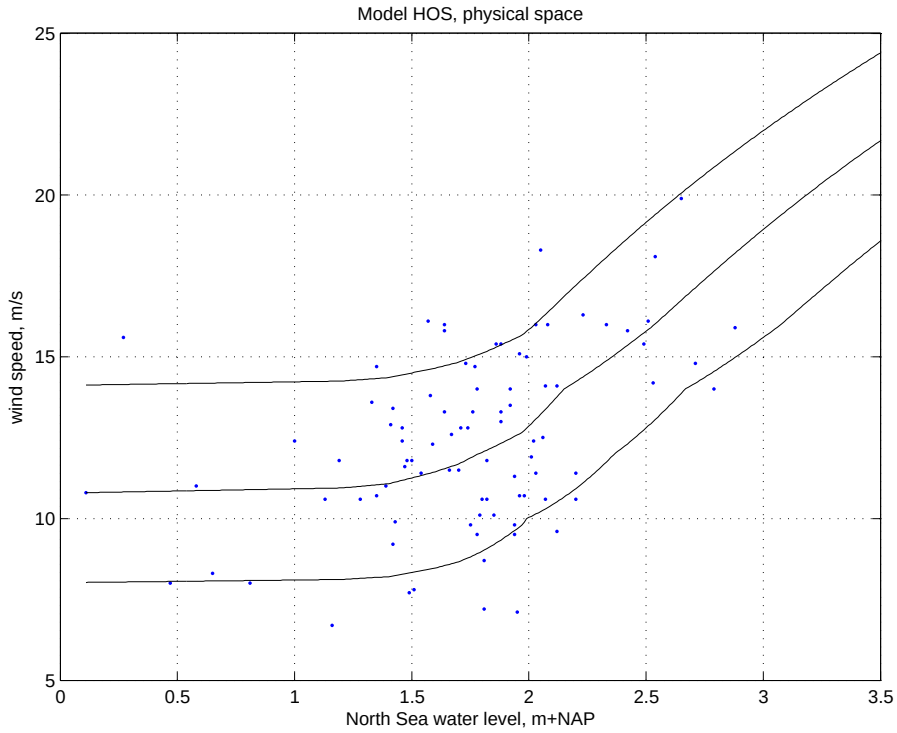

Figure 7-4 Data of North Sea level and wind speed, for wind sector 315° - 345°, with 10, 50 and 90 percentile lines. The model HOS is applied with σ = 1.4.

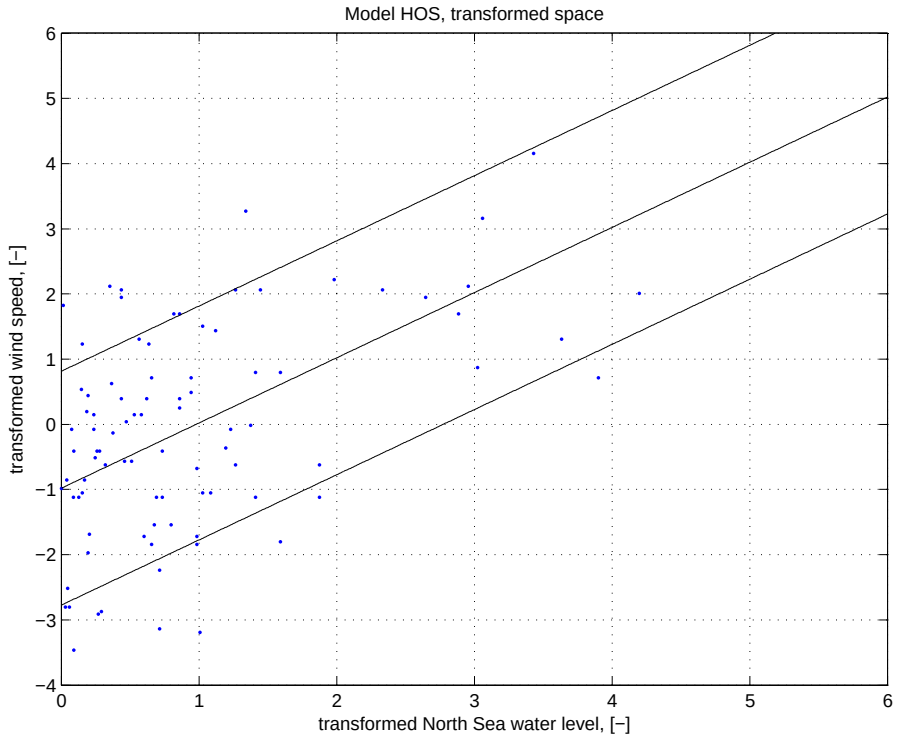

Figure 7-5 Transformed data and percentile lines of Figure 7-4.

7.3 Model with varying variance (HES)

7.3.1 Theory for model HES

The model HES is a straightforward extension of the model HOS. For HES we allow the standard deviation of the normal conditional density f(y|x) to vary with x, i.e. instead of (7.3) we take

$$f(y \mid x) = \lambda_{\sigma(x)}(y - x + \sigma(x)^2 / 2) \tag{7.7}$$

The formulas (7.2), (7.4) and the transformations (7.5) remain unaltered. It is evident that model HOS is a special case of the model HES.

7.3.2 Application of model HES

For an example of the model HES, data are used for the discharge of the river IJssel and the lake level of Lake IJssel, from the period 1981 until 2005. For this period discharge peaks are selected, in a window of 15 days before until 15 days after the peak of the discharge. Within this window the maximum of the lake level is considered, which is then correlated with the discharge peak.

The data are shown in Figure 7-6 for the physical space and in Figure 7-7 for the transformed space. Also shown are the 10, 50 and 90 percentile lines according to the model HES, where here, by visual inspection, $\sigma(x) = 0.2 + 1.5x$ is chosen. Note that because of the increase of the scatter in the data, the model HOS would be less appropriate here. We remark that in Hydra-Zoet the (older) model HOS is still used, which can be justified with a sensitivity analysis, showing that the results of Hydra-Zoet for normative water levels and dike heights are not very sensitive to the precise way the correlation is modelled. We note, however, that if the correlation would be completely ignored, results would become very inaccurate.

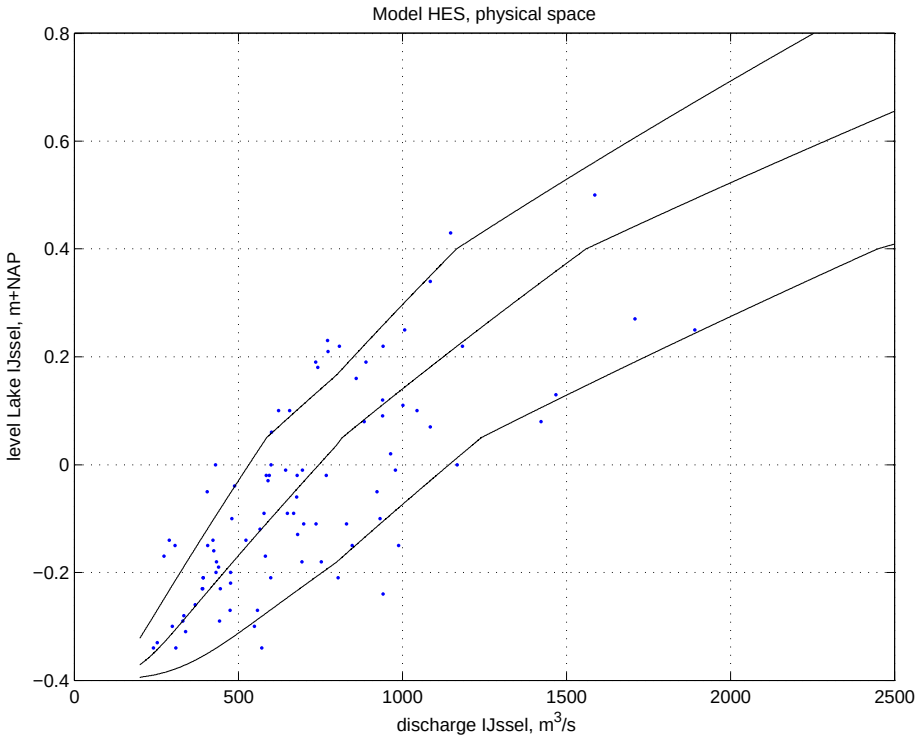

Figure 7-6 Data of lake IJssel and the river IJssel, with 10, 50 and 90 percentile lines. The model HES is applied with $\sigma(x) = 0.2 + 0.30x$.

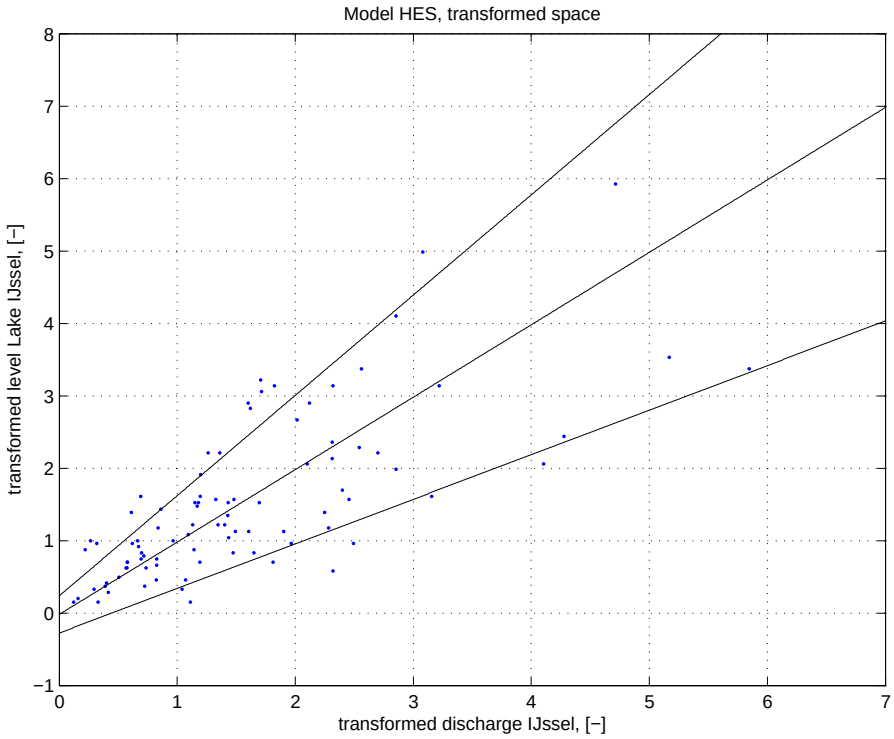

Figure 7-7 Transformed data and percentile lines of Figure 7-7.

8 Time evolution of slow and fast random variables

In Hydra-Zoet a distinction is made, depending on the way they vary in time, between *slow* and *fast* changing random variables. Among the slow ones are discharges and lake levels, whereas among the fast ones are wind speed, wind direction and sea levels. It turns out that only for the slow variables a true time modelling is needed, and actually only for the higher levels. This means that no (explicit) time modelling is needed for (a) the fast variables and (b) the lower levels of the slow variables.

It also turns out that for the lower levels of the slow variables the so-called *momentaneous* probabilities should be accounted for in the model correctly. A momentaneous probability is a probability at a single instant in time, or more precisely: it concerns the probability in a period that is so short that the variable of interest can be regarded constant during this period. For instance the momentaneous exceedance probability P(M>m) for the lake level is the probability that at an arbitrary instant of time the lake level exceeds m. It can also be interpreted as the fraction of time for which the random variable M exceeds level m.

In section 8.1 it is explained why a proper time modelling is only necessary for the higher levels of the slow variables. Next, in section 8.2, is shown how this time modelling is done in Hydra-Zoet, using the trapeziums from chapter 6 as simplified hydrographs. In section 8.3 it is shown how the proper momentaneous probabilities are obtained.

8.1 On the combination of slow and fast random variables

The aim of sections 8.1.1 and 8.1.2 is to demonstrate that for the *lower levels* of slow variables in Hydra-Zoet one can do without a description of the time evolution. It does turn out to be important, though, that the *momentaneous* probabilities of the slow variables are accounted for in the model (in particular for the lower levels).

8.1.1 Choice of time base for the fast variables

In Hydra-Zoet a characteristic period b is used, which more or less corresponds with the duration of the time fluctuations of the fast variables (wind speed, wind direction and sea level). For all fast random variables b = 12 hours is chosen. It is assumed that every 12 hourly period these variables assume new values, independently from the values in the preceding period, i.e. successive periods are taken *statistically independent*. Of course, this is an approximation. But it seems to yield rather accurate results, although in reality successive periods with this duration certainly will not be independent. Another point worth noticing is that a 'complete' wind storm or storm surge in reality definitely has a longer duration (say about 30 – 50 hours) than 12 hours. On theoretical grounds it can be motivated that the results of Hydra-Zoet are rather insensitive to the choice of b, as long as b is chosen in such a way that during this period the slow variables do not vary too much. A proper motivation is however beyond the scope of this report.

8.1.2 Combination of the slow and fast variables lake level and wind speed

As mentioned before, we have to show that for relatively low values of the slow variables the time modelling of these variables does not necessarily need to be included in Hydra-Zoet, provided the momentaneous probabilities for these variables are correctly accounted for in the model. For the sake of simplicity, we will only consider the case of the slow variable lake level M and the fast variable wind speed U.

In Hydra-Zoet only the winter half year (October – March) is considered, which is assumed to consist of 180 days. This means that there are N = 360 'wind blocks' of duration b = 12 hours, which are numbered i = 1, 2,..., N. Corresponding to these periods we have random variables $\{U_1, U_2,..., U_N\}$ and $\{M_1, M_2,..., M_N\}$. Random variables are denoted by capital letters and realizations of these variables with small letters. E.g. for wind block i we write (u_i,m_i) for the realizations of the random variables (U_i,M_i).

Since the lake level is a slow variable, a realization m_i can be interpreted as the average of the lake level during the period b (there is only little variation within b = 12 hours). The wind speed might vary a lot during 12 hours. We can expect – at least for the failure mechanisms overflow and wave overtopping considered here – that the most threatening situation occurs if the wind speed obtains its maximum during the period of 12 hours. We therefore choose u_i to be the maximum of the wind speed during the 12-hourly period.

Every realization (u_i,m_i) leads to a load h_i in the i-th block:

$$h_i = H(u_i, m_i) \tag{8.1}$$

Recall that for the failure mechanism overflow, H simply represents the local water level at the location of interest, whereas for mechanism wave overtopping it equals the sum of the local water level and the wave overtopping height. Actually, (8.1) is an approximation, since in reality the load level not only depends on the average lake level m_i and the maximum wind speed u_i in block i, but also on the complete time evolution of the wind speed (and to a lesser extent of that of the lake level) in block i. The way (8.1) is actually calculated in Hydra-Zoet will become clear in later chapters. Here we just assume that there is a well defined load level h_i in every block, which is a function of (u_i,m_i).

The basic calculation in Hydra-Zoet is the one of the exceedance frequency $F_H(h)$ of a load level h, i.e. the average number of exceedances of the random variable H of the level h, in times per year. (Note that F, to be consistent with earlier literature about Hydra-Zoet, denotes an exceedance frequency, whereas it denoted a cumulative distribution function in Chapter 7.) An exceedance of level h might be caused by an extreme lake level, an extreme wind speed, or by a combination of an increased lake level and an increased wind speed. In a qualitative way, remarks can be made about the durations of the exceedances.

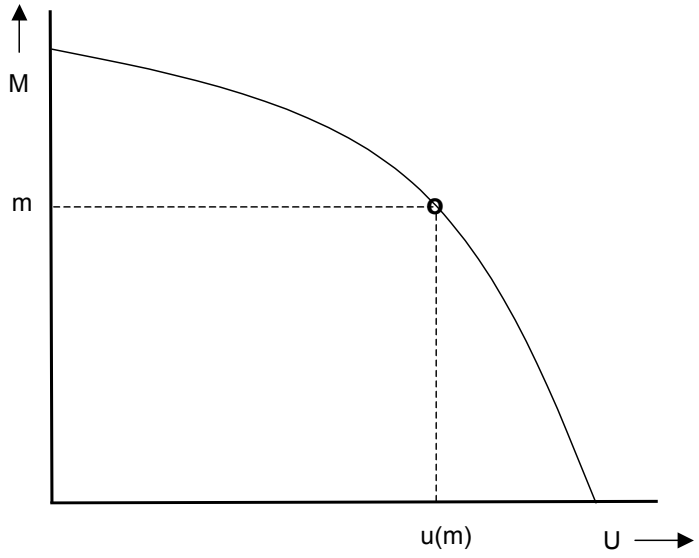

Figure 8-1 Contour line of level h, with a point (u(m),m) located on this line.

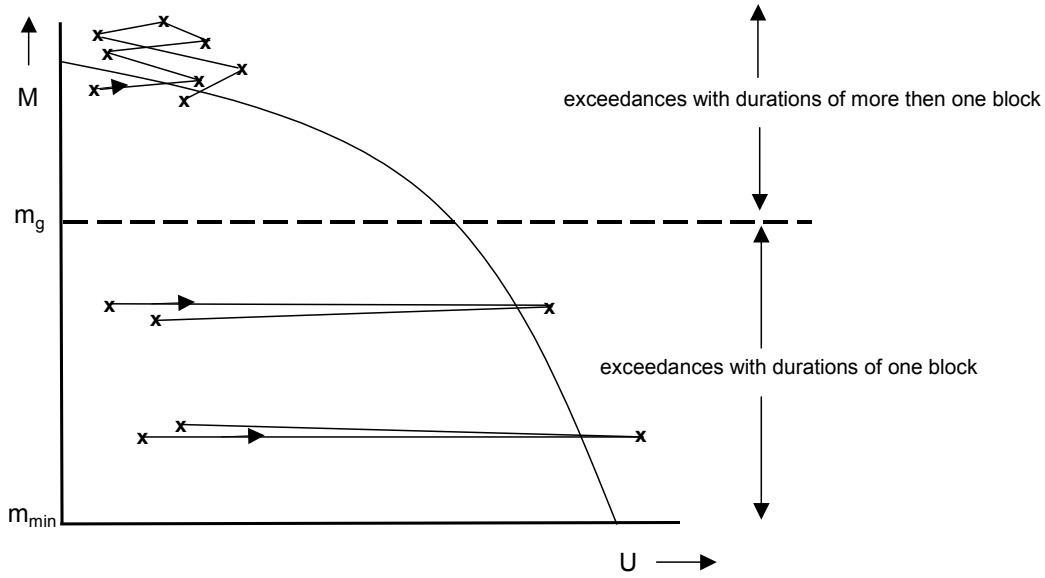

Figure 8-2 Schematic display of 3 exceedance events over time; m_{min} denotes the minimum lake level, and m_g the boundary between exceedances of short and long durations.

Consider a contour line of level h, consisting of the points (u,m) for which H(u,m) = h, indicated in Figure 8-1. The next figure (8-2) shows three exceedances of this line, where the crosses indicate outcomes (u_i,m_i). Connected crosses belong to the same exceedance, also called failure events, where the arrow denotes the direction of time: the exceedance starts directly to the left of the arrow, and ends at the end of the connected line segments.

The longest failure duration is the event in the upper left corner of Figure 8-2, starting at a high lake level just below h, which then increases slowly and next decreases slowly until the load level has decreased to a value smaller then h. During the exceedance, the wind speed varies considerably: because successive wind blocks are assumed to be statistically independent, in each block a 'new' wind speed occurs, which can differ significantly from the previous one. The other two failure events occur at relatively low lake levels. For such lake levels, failure can occur

only at extreme wind speeds, for if both the lake level and the wind speed are (relatively) low, no threatening situation would happen. Because of the high wind speed during failure, and because wind blocks are assumed statistically independent, the probability that two consecutive wind blocks with extreme wind speeds occur can be neglected.

Strictly speaking, no definite 'boundary level' for the lake level can be given, separating events with a short duration (one block period) from the ones with a long duration (two or more periods). With the lowest lake level, there is still a probability of an exceedance lasting longer than a single block. But more or less we can assume there is a boundary value m_g separating durations of one block from the events with longer durations. The precise value of m_g is of no concern at this point. What is interesting here, is that the contribution to $F_H(h)$ from lake levels smaller than m_g can be calculated easily. We write this contribution as $F_H(h,m<m_g)$. Denote the minimum lake level that can occur by m_{min}, and the wind speed on the contour of level h corresponding to m by u(m), see Figure 8-1. The momentaneous probability density of M is written as g(m), and the conditional exceedance probability of level h, given M=m, as P(H>h|m). Note that, since U and M are assumed to be independent, the latter probability equals P(U>u(m)).

For an arbitrary block period, the probability that h is exceeded in combination with a lake level smaller than m_g, is now given by

$$P(H > h, M < m_g) = \int_{m_{\min}}^{m_g} dm\, g(m) P\left(H > h \mid m\right) = \int_{m_{\min}}^{m_g} dm\, g(m) P\left(U > u(m)\right) \tag{8.2}$$

Because the failure events corresponding to (8.2) only last one block period, the contribution of such events to the exceedance frequency is then given by

$$F_H(h, m < m_g) = N \int_{m_{\min}}^{m_g} dm\, g(m) P\left(H > h \mid m\right) \tag{8.3}$$

where it is recalled that N = 360 denotes the number of 12-hourly blocks in a winter half year.

If the right hand side (r.h.s.) of (8.3) would be used for the whole range of lake levels to calculate $F_H(h)$, i.e. if we take $m_g = \infty$, this exceedance frequency would be overestimated. The reason is that the r.h.s. of (8.3) then yields the average number of all 'separate' blocks per year for which failure occurs, which is too large: for failure events lasting longer than a single block, the successive exceedances within such an event should not be counted separately, but be counted as *just one* exceedance.

Formula (8.3) is not used in Hydra-Zoet. It merely serves here to show that for relatively low values of the slow variable lake level, no detailed information concerning the time evolution is needed. The formula shows that only the momentaneous probability for the lake level needs to be accounted for in the model. For the slow variable discharge a similar reasoning can be given.

8.1.3 Why there is no need for a time modelling of fast variables

In the above treatise no time modelling of the fast variable wind speed has been used. Only the maximum wind speed occurred in the calculation, which does not require the detailed time behaviour of the wind speed. Other fast natural variables in Hydra-Zoet are the wind direction

and the sea-water level. In a 12-hourly block the *vectorially averaged* direction over the 12 hours is taken as a representative value for the wind direction, whereas for the sea water level the maximum water level during the 12 hours is taken. Hence, for these variables again no modelling of the temporal behaviour (or, behaviour over time) is needed.

8.2 Time evolution of slow random variables

8.2.1 Modelling of time evolution by trapezia

The slow variables in Hydra-Zoet, i.e. discharges and lake levels, can be modelled by trapeziums, as was explained in chapter 6. In Figure 8-3 these trapezia are shown. In this case a base duration B = 30 days is taken for the trapeziums, to model the slow variables for the Vecht and IJssel delta. Here the slow variables are Lake IJssel and, depending on the location, either the discharge of the Vecht or the IJssel.

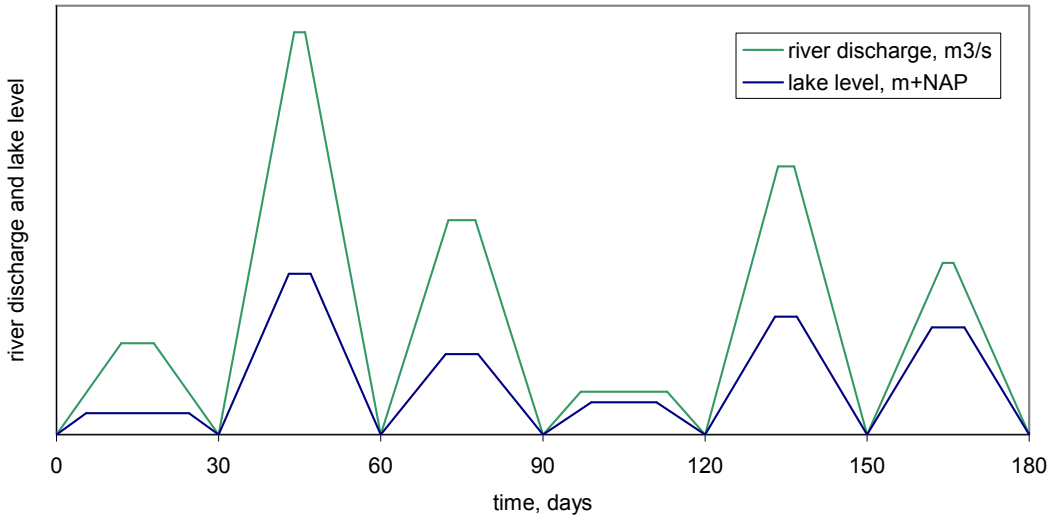

Figure 8-3 Modelling of discharges and lake levels using trapezia.

In the following, peak values of discharges are denoted by k and those of lake levels by s. The corresponding random variables are denoted by K and S. In Hydra-Zoet probability densities f(k) and f(s) are used for K and S respectively, which are related to a single base duration B. In principle, these densities can be chosen differently in every one of the 6 durations in the winter half year in Hydra-Zoet, but in this report we will assume that all durations have the same densities f(k) and f(s).

The trapeziums and the densities f(k) and f(s) should be chosen in such a way that some properties are satisfied. To formulate these properties, we denote the discharge and the lake level corresponding to a return period T = 1 year by k_1 and s_1. In other words: k_1 and s_1 are the once per year levels of K and S (the relation between T and P(K>k) and P(S>s) will be explained in section 8.2.3). The required properties are the following:

1. The trapeziums with peak values $k > k_1$ and $s > s_1$, should be such that their parts exceeding the levels k_1 and s_1 provide a proper modelling of the (average) time evolution within discharge and lake level waves.

2. For peak values $k > k_1$ and $s > s_1$, the densities f(k) and f(s) should represent the proper number of peaks per winter half year.

3. The trapeziums with peak values $k < k_1$ and $s < s_1$ need not describe the true time evolution within waves adequately, and also f(k) and f(s) need not be realistic for these values.
   The trapeziums and the densities f(k) and f(s) should be such however, that the proper momentaneous probabilities are reproduced in the model, since as explained in section 8.1.2, the calculation of $F_H(h)$ only involves momentaneous probabilities (time evolution of the lake, as well as peak values of trapezia are absent in this calculation).

It has been shown in the literature about Hydra-Zoet that these conditions can always be satisfied for the slow variables occurring in Hydra-Zoet. For point 1, this was illustrated in section 6.1 for the Rhine and partly for Lake IJssel in section 6.2. Points 2 and 3 will be illustrated in section 8.3.

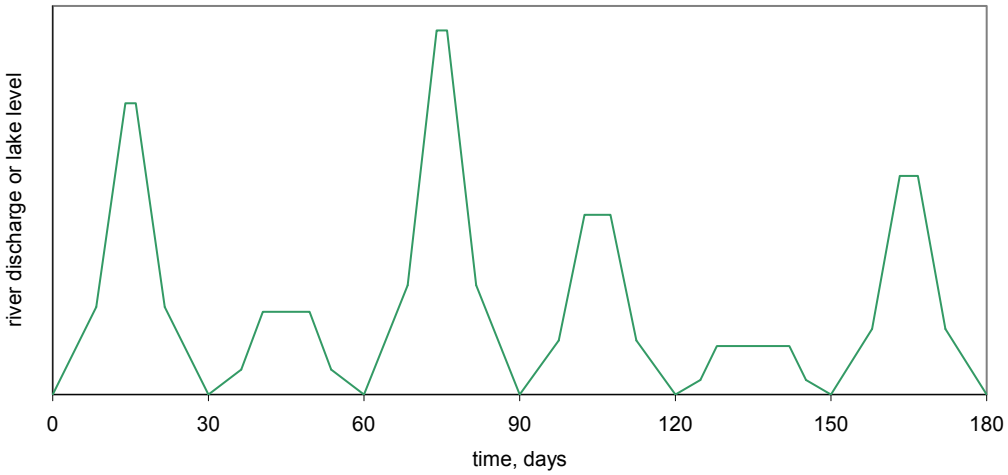

Figure 8-4 Deformed trapezia to model discharges or lake levels.

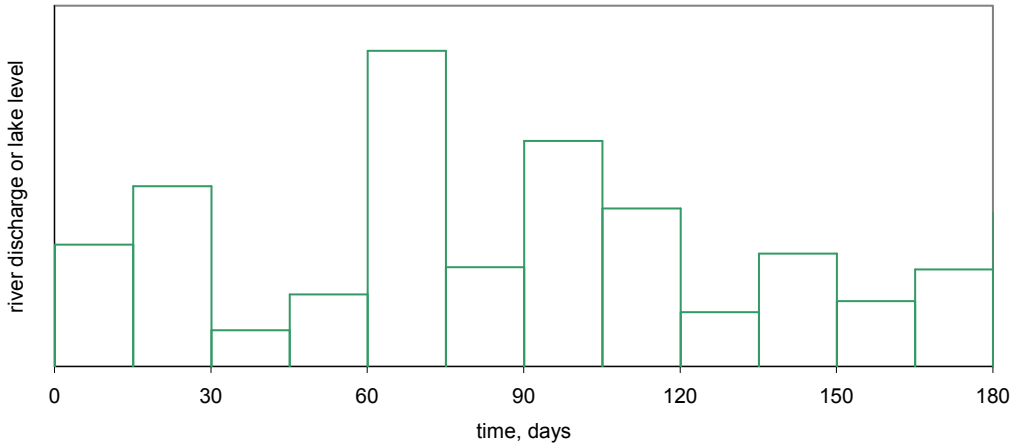

Figure 8-5 Rectangular blocks to model discharges or lake levels (FBC model).

We note that in Hydra-Zoet more general shapes for waves are possible, see Figure 8-4 for example, where trapeziums are made narrower. Also trapezia which are made wider can be considered. Next to this, as a special case of trapezia also 'rectangular blocks' can be considered

(Figure 8-5), which have been introduced in [Ferry Borges and Castanheta, 1971] as a type of load model. These models are called FBC-models. They are often used in the model PC-Ring, which was mentioned in section 2.2.2.

In this report the deformed trapezia and the FBC blocks are not considered further. We only note that these alternative schematisations have been used in sensitivity analyses to verify that – at least for failure mechanisms overflow and wave overtopping – the results of Hydra-Zoet are rather insensitive to the precise way discharge and lake waves are modelled in time.

8.2.2 Correlations and phases between discharges and lake level

In reality, a phase shift between two slow variables can exist, for example between the discharge wave of the river IJssel and the lake wave of Lake IJssel. Such a phase shift is accounted for in Hydra-Zoet by shifting all the trapezia in the winter half year by a fixed time displacement, as indicated in Figure 8-6. The choice of this phase shift appears not to be critical: Hydra-Zoet results are not very sensitive to the particular choice of this shift. If on the contrary, this choice would have been important, the shift should have been treated as a random variable.

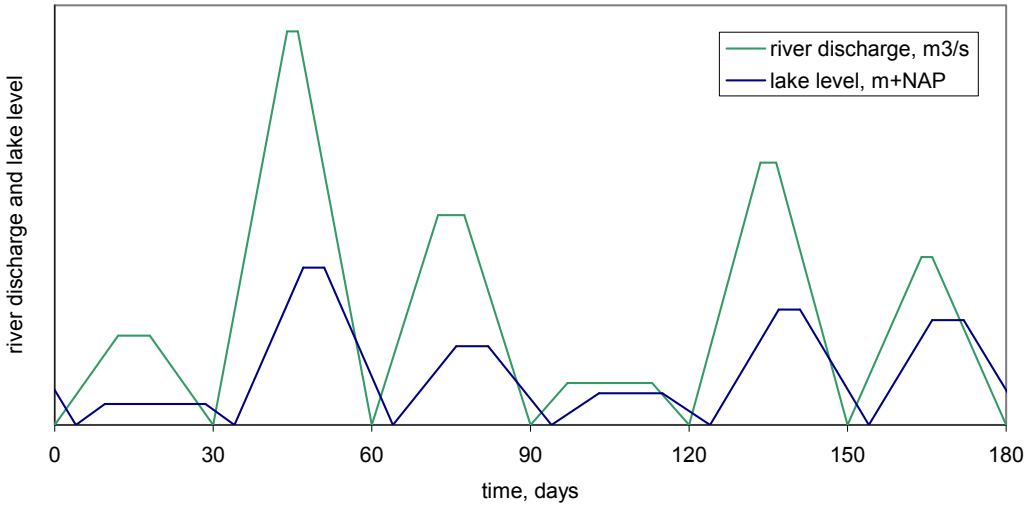

Figure 8-6 Discharges and lake level trapezia with a phase shift.

Given a (deterministic) shift, slow variables can be correlated, as is the case for the discharge of the IJssel and the level of Lake IJssel. This correlation is modelled using a bivariate probability density derived with one of the models treated in chapter 7. This means that, if the peaks of the slow variables are denoted by K and S, we use a bivariate density f(k,s), which is such that its marginals are the prescribed f(k) and f(s), with the correlation between measurements (k_i,s_i) properly accounted for by f(k,s).

8.2.3 Exceedance frequency versus probability density for the base duration

In applications usually exceedance frequencies of the slow variables are available for sufficiently high levels, say for levels with return periods of at least T = 1 year. The reason that they are not available for lower levels, is that for the lower levels no longer proper waves can be

discerned: the propagation in time for these levels is too irregular. If, for sufficiently high peak values, the time propagation of a slow variable is schematised with trapezia, the probability density of the peak value of the trapezia is used in Hydra-Zoet. In what follows, the relation between the exceedance frequency and this probability density is explained, where it is assumed that the exceedance frequency is available above the once per year value.

Denote by $F_S(s)$ the exceedance frequency of level s, available for $s > s_1$ (with s_1 the once per year level). We want to know how the exceedance probability P(S>s) related to duration B can be calculated. Recall that threatening situations in the summer half year are supposed to be absent. Since there are 6 discharge trapezia in the winter half year, we then must have $F_S(s) = 6\ P(S>s)$. More generally, if there are N_{trap} trapezia considered in a year, we obtain

$$F_S(s) = N_{trap} P(S > s), \qquad s \geq s_1 \tag{8.4}$$

In particular, for the once per year level s_1 it follows that $P(S>s_1) = 1/6$. We note that sometimes the return period T(s) of level s is used, which by definition is given by

$$T(s) = \frac{1}{F_S(s)} \tag{8.5}$$

At this stage the variables $F_S(s)$ and P(S>s) are available for $s \geq s_1$. For use in Hydra-Zoet they also need to be available for the levels between the minimum level s_{min} and s_1. The extension of the exceedance frequency to these lower levels has to be such, as explained before, that the proper momentaneous probabilities are reproduced. How this reproduction is achieved (and verified) is explained in the next section.

8.3 Reproduction of momentaneous probabilities for the slow variables

In this section we will show how points 2 and 3 of section 8.2.1 can be verified. This will be done here only for Lake IJssel, although these verifications have been done for all slow random variables in Hydra-Zoet. Restricting ourselves to Lake IJssel, points 2 and 3 amount to the following:

a) For peak value $s > s_1$, with s_1 the lake level with return period T = 1 year, the density f(s) should represent the proper number of peaks $F_S(s)$ per winter half year.

b) The trapezia and the density f(s) should be such that the proper momentaneous probabilities P(M>m) are reproduced.

Starting with point a) we have to consider the exceedance frequency $F_S(s)$ first. The one used in Hydra-Zoet for Lake IJssel is shown in Figure 8-7, together with the available data, belonging to the period 1976 – 2005.[20] The peaks are selected here using a threshold of –0.2 m+NAP, in such a way that the duration between successive peaks is at least 15 days.

The exceedance frequency in the figure consists of three exponential parts, given by

[20] These are the same data as in section 6.2, apart from a slight trend correction, which makes the data representative for the year 2011; the details of this trend correction do not bother us here.

$$F_S(s) = \exp\left(-\frac{s-b}{a}\right)$$

with:

$$\begin{aligned} a &= 0.250, \quad b = 0.05, \quad \text{for } -0.40 \le s < 0.05 \text{ m+NAP} \\ a &= 0.152, \quad b = 0.05, \quad \text{for } 0.05 \le s < 0.40 \text{ m+NAP} \\ a &= 0.097, \quad b = 0.177, \quad \text{for } s \ge 0.40 \text{ m+NAP} \end{aligned} \tag{8.6}$$

We note that for the range $s > s_1$ the frequency line is derived as a proper fit for the exceedance peaks in the measurements (note that s_1 = 0.05 m+NAP). From $F_S(s)$ the probability density f(s) follows from (8.4) as

$$f(s) = -\frac{1}{N_{trap}}\frac{dF_S(s)}{ds} \tag{8.7}$$

Since $F_S(s)$ gives a proper description of the peaks in the lake levels, the same holds for f(s), which means that point a) is satisfied.

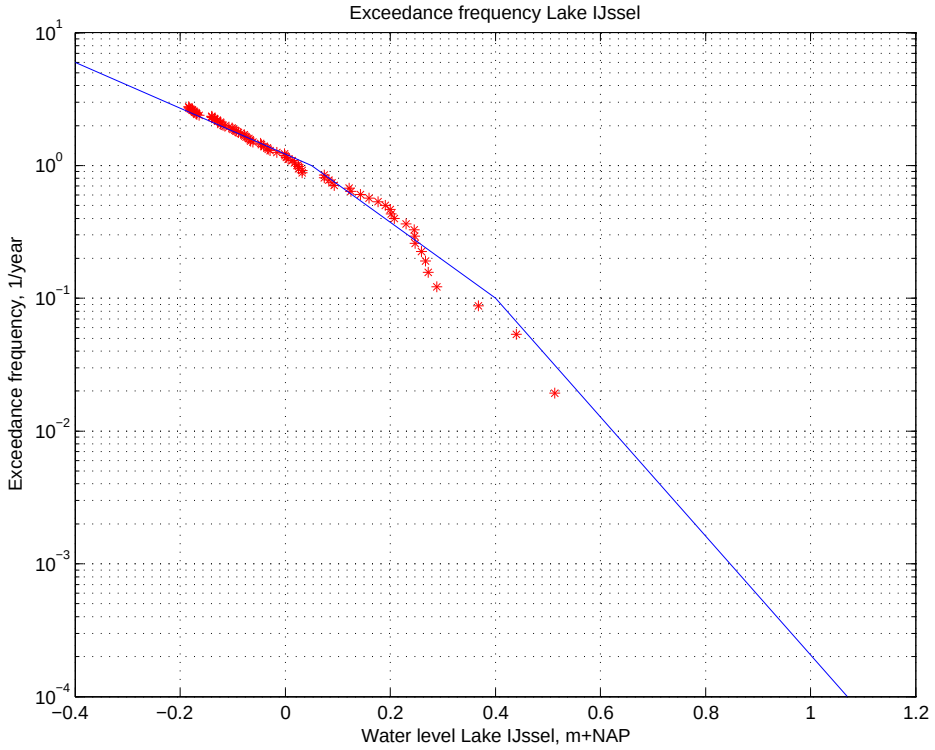

Figure 8-7 The exceedance frequency $F_S(s)$ for Lake IJssel (blue line), together with the data (situation for the year 2011).

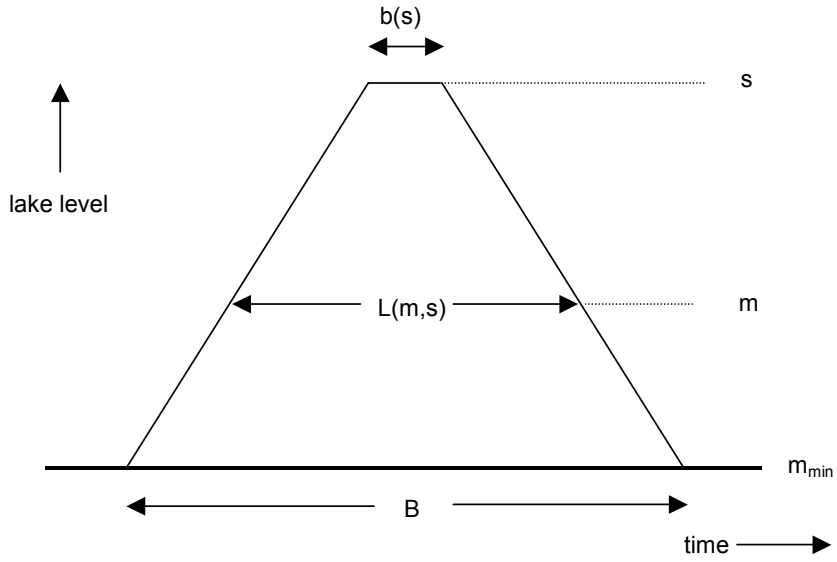

Figure 8-8 Notation used in connection with trapezia; note that m_{min} = -0.40 m+NAP is the minimum level that can occur in the winter half year.

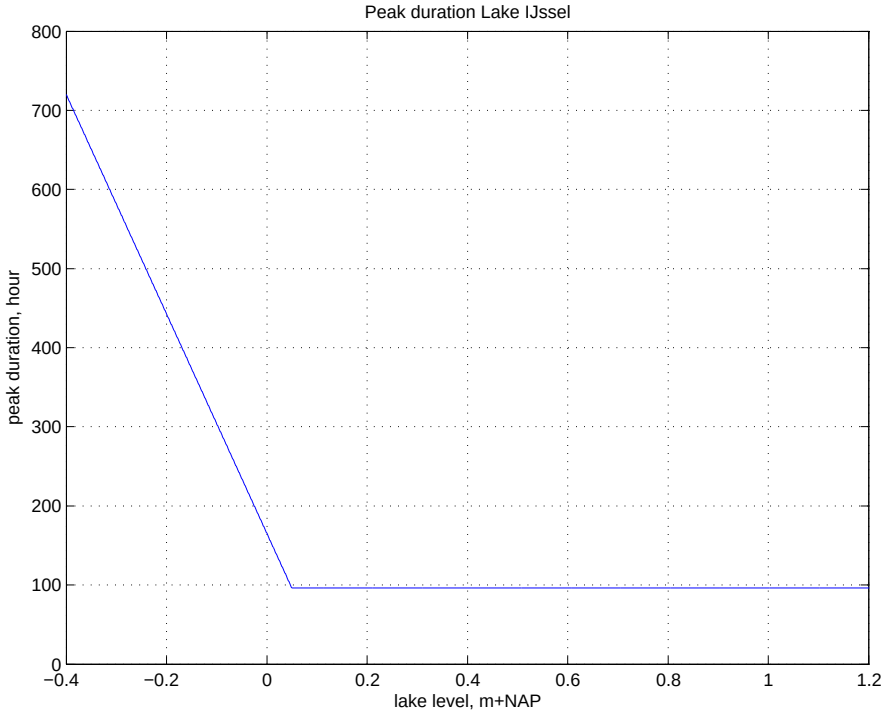

Figure 8-9 Peak duration trapezia for Lake IJssel.

Regarding point b), we will check that the momentaneous probabilities P(M>m) are reproduced. First note that, as is easy to verify, P(M>m) can be calculated from f(s) and the trapezia as

$$P(M > m) = \frac{1}{B}\int_{m}^{\infty} ds\, f(s) L(m,s), \quad m \geq m_{\min} \tag{8.8}$$

where L(m,s) denotes the duration of level m inside the trapezium with peak value s (see Figure 8-8). The peak duration b(s) for Lake IJssel is chosen in Hydra-Zoet as in Figure 8-9: $b(m_0) = B = 720$ hours, or 30 days, decreasing linearly until b(m=0.05) = 96 hours, or 4 days, and then staying on this fixed value for higher lake levels.

With (8.8) P(M>m) can be calculated, with the result shown in Figure 8-10. This figure also shows the so-called empirical version of P(M>m), as obtained from the data. In that case P(M>m) is obtained by counting the number of days with lake level exceeding m, and dividing this number by the total number of days in the data set. For m < 0.2 m+NAP, both lines are close to each other, indicating that for these levels the density f(s) and the duration L(m,s) considered in Hydra-Zoet are chosen in an appropriate way. For m > 0.2 m+NAP, the lines differ. But note firstly that statistical noise for these larger levels becomes important, and secondly that for levels exceeding the highest measurement, P(M>m) always becomes 0 according to the data. The latter means that the tail of the data line most likely will be below the calculated line in the region of the highest measurements.

To get a feeling for the amount of statistical noise (or uncertainty) present, in Figure 8-11 the calculated frequency line is compared with the data line based upon the shorter period 1990 - 2005. The data line now differs considerably for the higher lake levels. In view of the amount of statistical noise, the line according to the calculation reproduces the line according to the data sufficiently well.

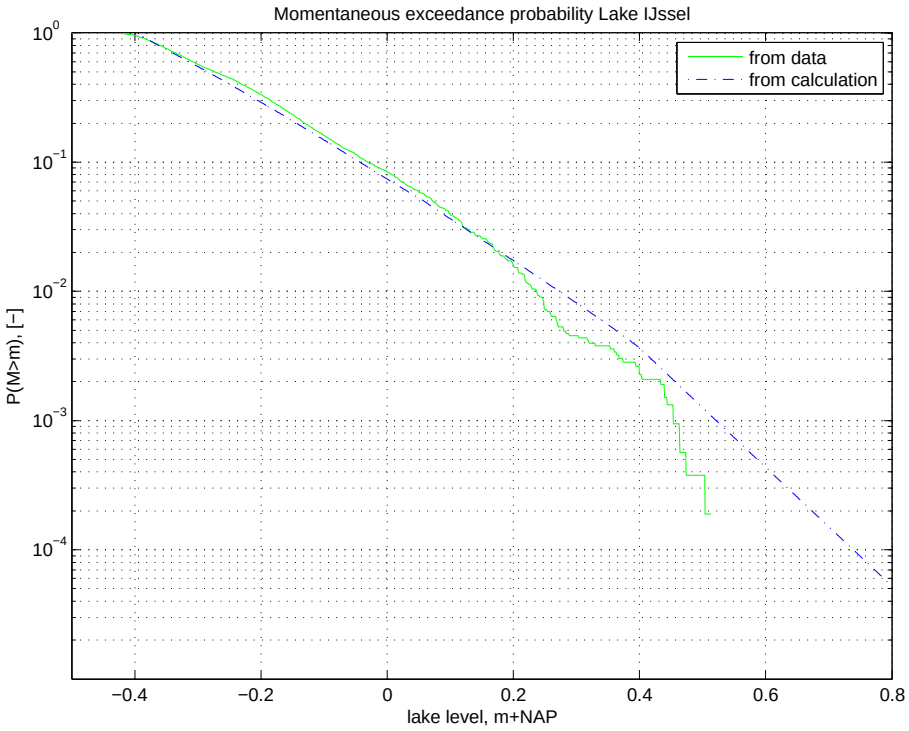

Figure 8-10 Momentaneous probabilities for Lake IJssel according to the calculation and the data from 1976-2005 (trend corrected to situation 2011).

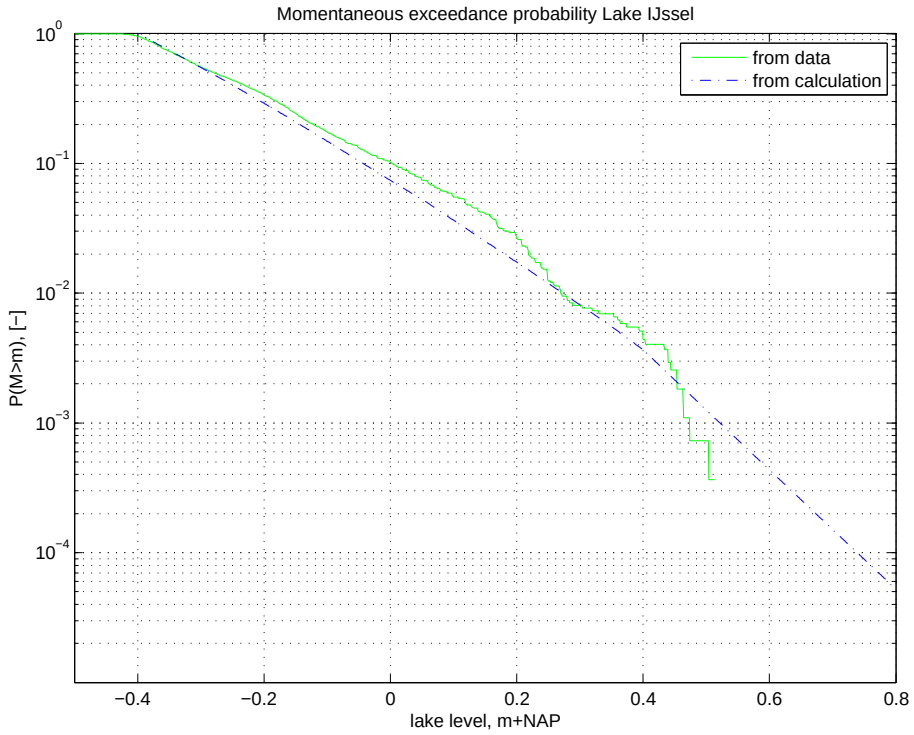

Figure 8-11 Momentaneous probabilities for Lake IJssel according to the calculation and the data from the restricted period 1990-2005 (trend corrected to situation 2011).

We note that for the lower lake levels, the variables f(s) and L(m,s) could have been chosen differently, yet again reproducing the empirical P(M>m) sufficiently accurately, i.e. the choice for f(s) and L(m,s) is not unique. We also mention (once again) that an analysis as described here was performed for every slow variable in Hydra-Zoet, where proper choices of the probability density for the peak value and the trapezium parameters could easily be found.

Part 2: Sea delta

9 Introduction tidal rivers (Rhine and Meuse delta)

As mentioned in section 3.2, the basic formulas of Hydra-Zoet fall into two categories: a sea delta or a lake delta. This part of the report(chapters 9 to 12), is about a sea delta, which here is the 'Rhine and Meuse delta', also denoted as the 'tidal rivers' or 'tidal area'. This water system was already briefly introduced in chapter 3.

The current chapter provides a more extensive description. First the area is described as well as the random variables used for this area. Then the main purpose of Hydra-Zoet is given, followed by an explanation of the influence and importance of the various random variables. The chapter concludes with a diagram summarising the structure of the Hydra-Zoet model for the tidal rivers. Part of this diagram is also used to explain, at a very basic level, the structure of the computer program Hydra-Zoet.

As a short historical note, we mention that the Hydraulic Boundary Conditions 2001 and 2006 (HBC2001 and HBC2006) for the tidal area were determined with Hydra-B, the predecessor of Hydra-Zoet for this area. The determination of the HBC2001 was described in [Slomp et al, 2005], whereas a lot of aspects concerning the HBC2006 were treated in [De Waal, 2007].

Where in the explanation of Hydra-Zoet, in chapters 9 to 12, models or model parameters are mentioned, they are taken from HBC2006.

9.1 The area and the random variables used in the model

The tidal rivers are shown in Figure 9-1. The map shows the so-called 'axis locations' in the area, which are located in the axes of the river branches 1 kilometre apart from each other. Note that the wider channels in the enclosed estuary (Haringvliet and Hollandsch Diep) contain more than one "axis". Complementary to the axis locations Hydra-Zoet also contains a great number of 'shore locations' along the toe of the flood defences with approximately 100 metres between. For the latter locations, dike assessments can be done and required crest levels can be calculated with Hydra-Zoet.

In case of storm surges, generated by storms over the North Sea, the Maeslant Barrier (see Figure 9-1 closes off the area from the sea. The barrier is operated using predicted water levels at location Maasmond, which is why these predictions (containing uncertainties), are included in the model. The barrier might fail to close for two reasons: firstly, the predicted water levels might have been underestimated, so that the barrier has not been closed or was closed too late; secondly, the barrier might fail to close due to technical malfunction. Besides the predicted water levels, the probability of failure to close the barrier is considered in Hydra-Zoet as well.

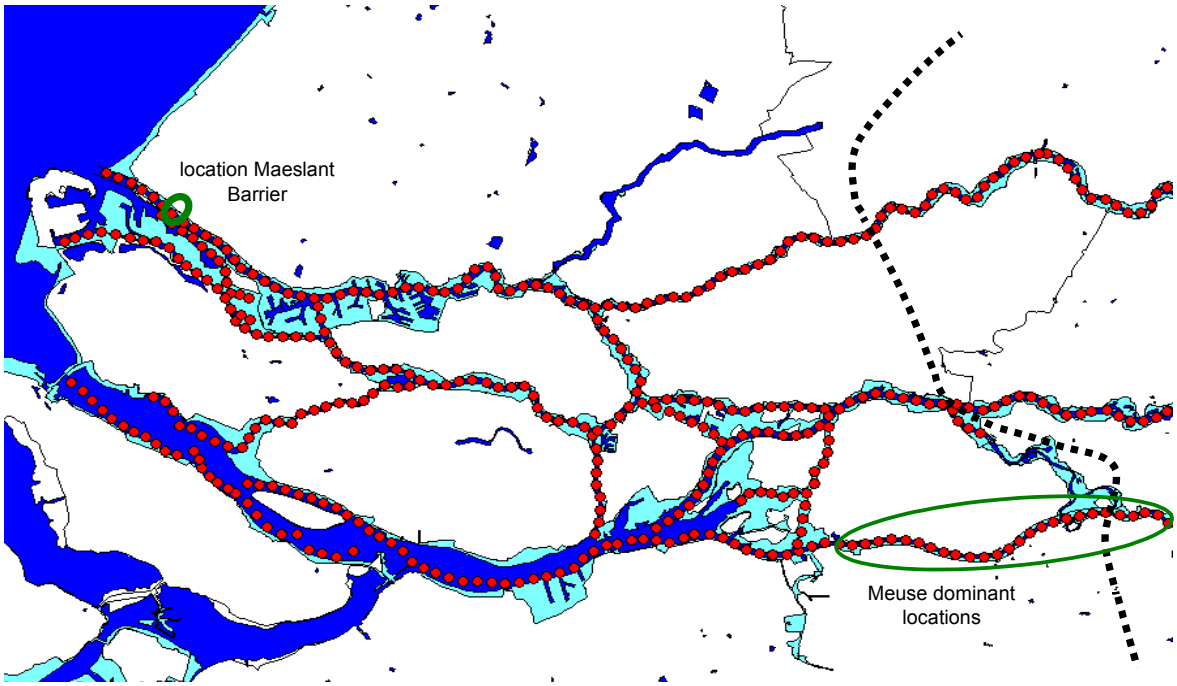

Figure 9-1 Axis locations in the tidal rivers are situated to the west of the dotted line. The Maeslant Barrier and the locations which are dominated by the Meuse discharge are also indicated; all other locations are dominated by the Rhine discharge (see section 10.1.3 for an explanation).

The random variables in Hydra-Zoet for this region have already been listed in section 3.1.4. For the convenience of the reader they are mentioned again, here with their symbol used in the formulas:

- sea level M,
- discharge Q (for locations along the Rhine or one of its branches, this is the Rhine discharge, along the Meuse it is the Meuse discharge),
- wind speed U,
- wind direction R,
- barrier state of the Maeslant Barrier Ω,
- prediction of the water level at Maasmond V.

9.2 Main purpose of Hydra-Zoet

At this point it is useful to recall, within the scope of the report, the main purpose of Hydra-Zoet. The failure mechanisms included are:

- overflow,
- wave overtopping.

The first one is used to calculate the exceedance frequency $F_H(h)$ of a water level h, where here the random variable load level H consists simply of the local water level. The second mechanism is used to calculate the exceedance frequency $F_H(h)$ of a dike height h, where here H consists of the local water level plus the wave overtopping height for a specified critical overtopping discharge, as explained in section 5.5. Once $F_H(h)$ is known for a range of values h_1, h_2,..., h_n, the level h corresponding to a fixed (normative) exceedance frequency F_{norm} can be calculated using interpolation. The value h corresponding to F_{norm} then is used in the assessment of the flood defence.

In this part of the report the following points will be discussed:

- How to calculate the exceedance frequency $F_H(h)$ for a load level h, for the failure mechanisms overflow and wave overtopping.
- How to calculate Illustration Points (IP's), yielding the most probable circumstances once a level h is attained (see for examples chapter 4).
- How to calculate the contributions to the exceedance frequency, yielding the probabilities with which outcomes of random variable occur once a level h is exceeded (see for examples chapter 4).

The formulas for these calculations will be given in the following chapters for a single location or *dike section*, located somewhere along a dike ring. We will also provide the formulas for an entire dike *ring*, which follow quite easily once they are established for a dike section.

9.3 Classification into three areas

Concerning the threats caused by river discharges, sea levels and wind, the area can roughly be divided into three subareas: the *Sea area S* where the sea is most important, the *Transition area T* where both the sea and river discharge are important, and the *River area R* where the discharges of the rivers are most important. Besides these influences, the wind plays a role everywhere. Depending on the location and the failure mechanism considered, its influence is minor or large.

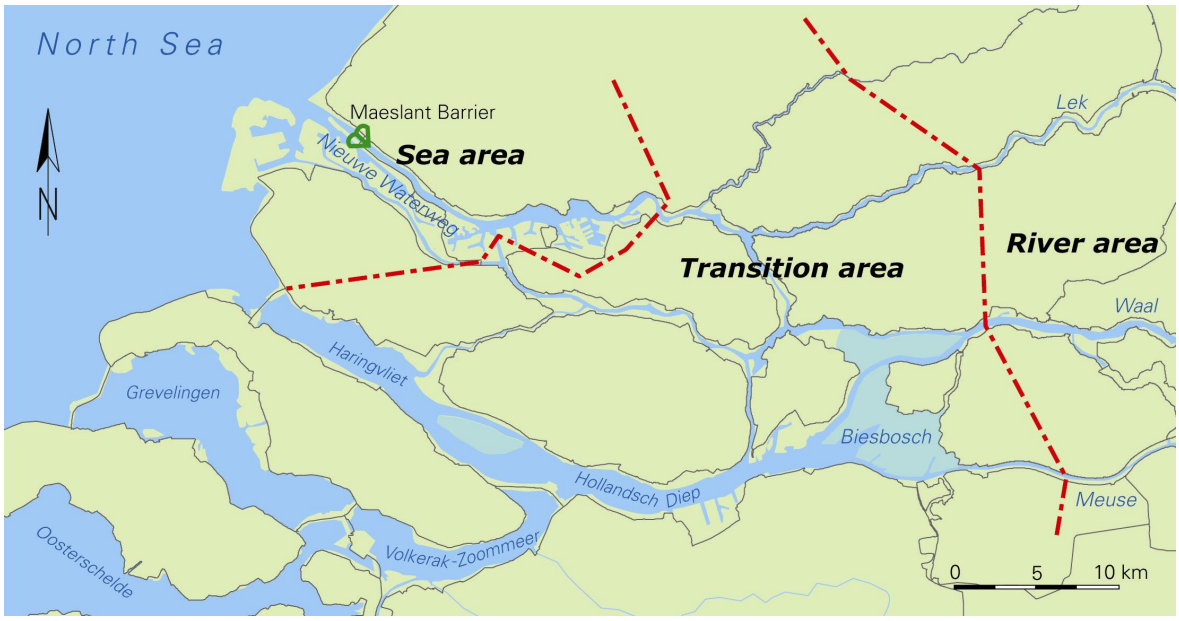

Figure 9-2 The tidal river area, subdivided into the Sea area, Transition area and River area.

The subareas can briefly be characterised as follows:

- *Sea area*
  Water levels are mainly determined by storm surges in combination with failure to close the Maeslant Barrier. These storm surges occur together with high wind speeds, which means that dikes are threatened by wave action.

- *Transition area*
  Here water levels are determined by combinations of storm surges and discharges, where

also failure of the Maeslant Barrier is important. Just as in the Sea area, wind accompanying a storm surge causes high wind waves, which especially are important for the dikes along the wider channels in the south-west of the area.

- *River area*
  Here extreme discharges are the cause for high water levels: storm surges do not reach so far inland, and the wind set-up generated inside the area turns out to be marginal. Since storm surges can be neglected, no high wind speeds occur (at least not with a high probability during extreme discharges). However, also wind waves generated at lower wind speeds are important, but due to these lower wind speeds and relatively short fetches, these waves are less important than in the other areas. Maximum wave heights rarely exceed 1 metre.

9.4 Schematic structure of the model

This section discusses a diagram showing the relation between different parts of the probabilistic model/computer program Hydra-Zoet (Figure 9-3). These parts will be explained in detail in the following chapters; here we only give a brief explanation of the different parts and the way they are connected. In order not to complicate matters, the diagram only shows the calculation of the hydraulic load level for the failure mechanism wave overtopping, for a shore location where wave variables are obtained with the 1-dimensional Bretschneider formulas, and not with the 2-dimensional model SWAN.

The general structure of the diagram is as follows. All data, delivered by the Ministry of Infrastructure and Environment, are used as input for the model (left block in the diagram of Figure 9-3). For the assessment of the flood defence, the user of the model enters data which are specific to the location considered (right block in the diagram). The blocks in the middle of the diagram show the flow of the data, and at which point in the model the probabilistic calculation is executed.

We now briefly describe the individual components of the diagram. The block 'PHYSICAL MODELS/DATA' describes water level calculations and location-specific data for fetches and bottom levels. For a total of 6768 combinations of boundary conditions, consisting of discharges Q, sea levels M, wind speeds U, wind directions R and barrier states Ω, water levels have been calculated with a hydrodynamic model such as SOBEK, for a great number of locations throughout the area. Since the 1-d model SOBEK cannot calculate wind set-up perpendicular to a SOBEK-branch, as mentioned in section 5.2, an appropriate "perpendicular" wind set-up is added to the water level at a shore location. For these locations also effective fetches and bottom levels (required for the Bretschneider formulas), are determined.

The data for the shore locations are stored in a database (the block 'HYDRA-ZOET DATABASE'). Actually, because of the size of this database, it has been divided into a number of 'sub databases', one for each dike ring to be assessed, and distributed by the Ministry of Infrastructure and Environment to the users of Hydra-Zoet.

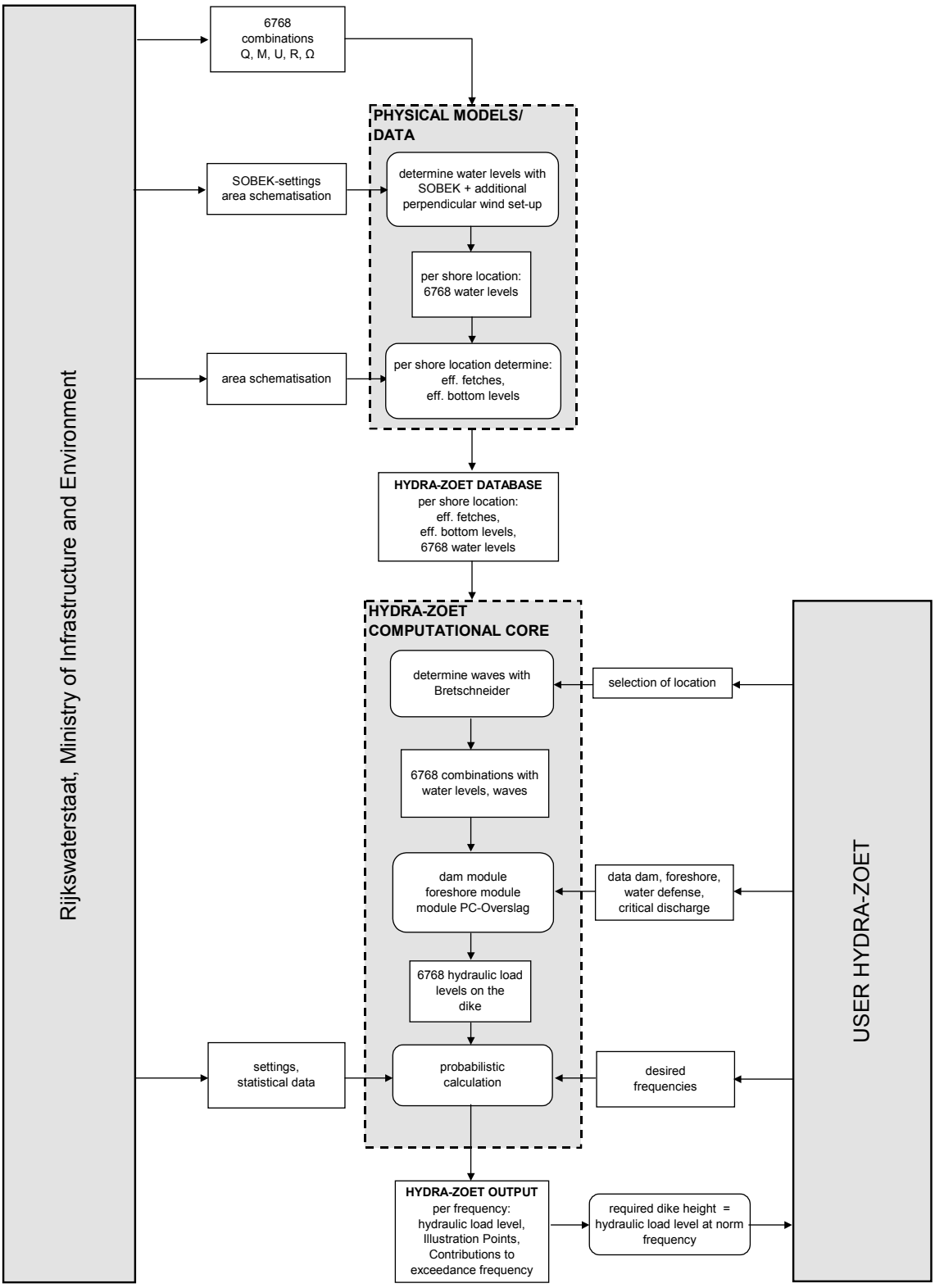

Figure 9-3 Diagram for a shore location in the tidal rivers, for failure mechanism wave overtopping.

The block 'HYDRA-ZOET COMPUTATIONAL CORE' represents the actual model code of Hydra-Zoet (the former data are only input for the model). In advance of the probabilistic calculation executed in this block, the available data has to be used to calculate the hydraulic load level in every one of the 6768 combinations, as explained in sections 5.3 until 5.5. We briefly repeat the steps. First, for every combination the wave variables H_s and T_p are calculated with Bretschneider. At this stage of the program, water levels and waves are known at 'open water' near the toe of the dike. If necessary, they are transformed by the dam and/or foreshore module, to water levels and waves directly in front of the dike toe. The module PC-Overslag transforms the conditions at the toe of the dike to a hydraulic load level on the dike. Note that the load levels in this block not only depend on the data stored in the Hydra-Zoet database, but also on the information supplied by the user of the program. In addition to the information for a possible dam and/or foreshore, these contain the dike orientation, the geometry of the dike (shoulders/berms, slopes and their roughnesses) and the critical wave overtopping discharge.

At this point of the program the load levels are known for all of the 6768 combinations. Using the probability distributions of discharges, sea levels, wind speeds, wind directions and barrier states, a probabilistic calculation now yields the hydraulic load levels at the user-specified (normative) exceedance frequencies.

The block 'HYDRA-ZOET OUTPUT' shows the most relevant output of the program. Next to the hydraulic load levels just mentioned, this output contains Illustration Points and contributions to the exceedance frequencies, which have been explained earlier in chapter 4.

10 Hydraulic load levels tidal rivers

This chapter describes the computations with physical models, needed as input for Hydra-Zoet. It is also describes how these computations are used to obtain the hydraulic load level for every combination of boundary conditions that is considered. Only the physical calculations themselves are considered in this chapter. Their probabilities and exceedance frequencies are subject of the remaining chapters.

From the diagram in Figure 9-3, in this chapter the following parts are considered:

- the block 'PHYSICAL MODELS/DATA',
- the block 'HYDRA-ZOET DATABASE',
- the block 'HYDRA-ZOET COMPUTATIONAL CORE', with the exception of the part "probabilistic calculation".

10.1 Water level calculations with SOBEK

To build the Hydra-Zoet database, a lot of combinations of discharges, sea levels, wind speeds and wind directions have to be used as input for SOBEK. It is a 1-dimensional model, consisting of branches and nodes, shown in Figure 10-1. The small blue plusses, as well as the nodes, are the calculation points of the model, for which water levels are calculated. The green circles and/or names denote the boundaries of the model as they existed in 2001, to be discussed in sections 10.1.1 and 10.1.3.

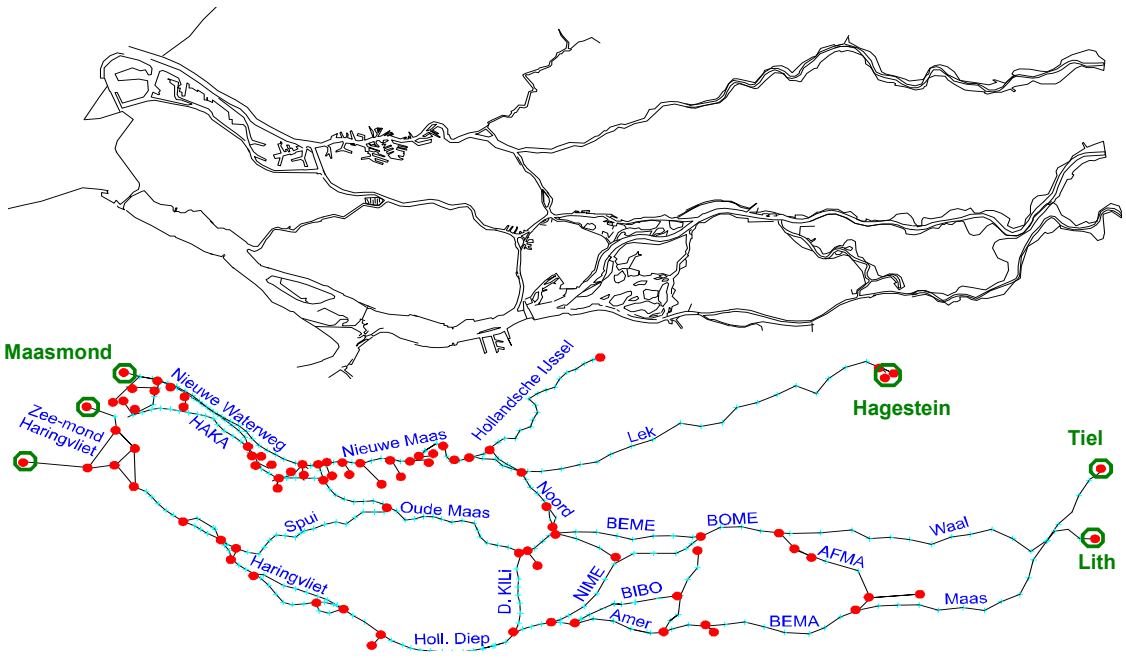

Figure 10-1 The tidal rivers with the branches and nodes (in red) of the SOBEK model.

We will not comment on the equations and computational schemes used in SOBEK, since these are beyond the scope of this report (more details about the model can be found in [De Deugd, 2002] and the references therein). For a proper understanding of Hydra-Zoet, however, it will be important to look in some detail on how precisely the boundary conditions are imposed on the model.

The result of a SOBEK calculation is a time series of water levels for a large number of calculation points on the SOBEK branches. Only the maximum water level from the series is used at each calculation point. The water levels per calculation point are interpolated to SOBEK points on the middle of the river (for each kilometre). A problem is that the available SOBEK points are not located near the shore, where dike assessment takes place. Therefore the maximum water levels at the branch points have to be transposed to the shore locations. In this transformation wind set-up perpendicular to the branch is added, as described in section 5.2. After this transformation, local (maximum) water levels become available, for the axis as well as the shore locations, for every combination of boundary conditions imposed on the model. Note that 2-dimensional effects such as higher water levels in outer bends of the river, or lower water levels in inner bends, are neglected.

The combinations used as input for SOBEK are given in Table 10-1. The information looks a bit complicated, but will become clear in the subsequent sections.

Random variable		**Chosen values imposed on SOBEK**									**Number**
Western sector											
sea level	m+NAP	1.11	2.00	3.00	4.00	5.00	6.00				6
wind direction		SW	WSW	W	WNW	NW	NNW	N			7
wind speed	m/s	0	10	20	30	42					1 + 4
Rhine dominant situation:											
Rhine discharge	m3/s	600	2000	4000	6000	8000	10000	13000	16000	18000	9
corresponding Meuse disch.	m3/s	55	217	687	1156	1626	2095	2800	3504	3974	
Meuse dominant situation:											
Meuse discharge	m3/s	10	327	855	1382	1909	2437	3228	3700	4546	9
corresponding Rhine disch.	m3/s	600	2000	4000	6000	8000	10000	13000	14790	18000	
barrier state		open	closed								2
Total number of calculations for western sector: 6 * (1 + 4*7) * (9 + 9) * 2 =											**6264**
Oostelijke sector											
sea level	m+NAP	1.3 (high tide)									1
wind direction		NNE	NE	ENE	E	ESE	SE	SSE	S	SSW	9
wind speed	m/s	0	10	20	30						1 + 3
Rhine dominant situation:											
Rhine discharge	m3/s	600	2000	4000	6000	8000	10000	13000	16000	18000	9
corresponding Meuse disch.	m3/s	55	217	687	1156	1626	2095	2800	3504	3974	
Meuse dominant situation:											
Meuse discharge	m3/s	10	327	855	1382	1909	2437	3228	3700	4546	9
corresponding Rhine disch.	m3/s	600	2000	4000	6000	8000	10000	13000	14790	18000	
barrier state		open									1
Total number of calculations for eastern sector: 1 * (1 + 3*9) * (9 + 9) * 1 =											**504**
Total number of calculations for western + eastern sector:											**6768**

Table 10-1 Combinations used in SOBEK, together with the number of calculations.

10.1.1 Sea levels

At the western side of the model, SOBEK has three sea boundaries: one in the north at Maasmond (the mouth of the Nieuwe Waterweg), and two in the south (outside the sluices of the Haringvliet).

It is assumed that storm surges only pose significant threats for one of the 7 wind directions SW, WSW,..., N, briefly denoted as the *westerly directions*. From the other directions, the nine *easterly directions* NNE,NE,... SSW, significant storm surges do not occur (the wind either blows away the sea from the land, or, for S and SSW, cannot develop a surge due to limited fetches). For the westerly directions, a (more or less) trapezium shaped time evolution of the surge is superimposed on the time-averaged tide evolution.[21] The trapezium is parameterised by three parameters, the maximum surge height h_s, the surge duration t_s and the phase f_s between the moment of the astronomical high tide and the maximum surge, as indicated in Figure 10-2 and Figure 10-3. The latter figure shows how the time evolution of the sea level is obtained by adding the surge level to the astronomical water level. The astronomical tide is different for the three boundaries of the SOBEK model, since the tide changes along the coast.

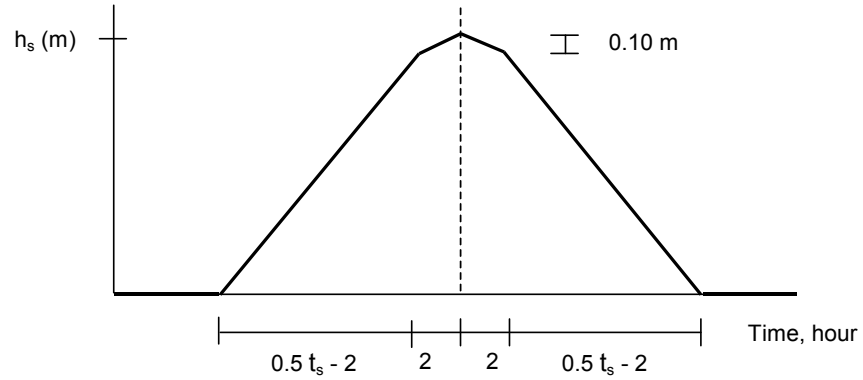

Figure 10-2 The storm surge, parameterised by the parameters h_s and t_s.

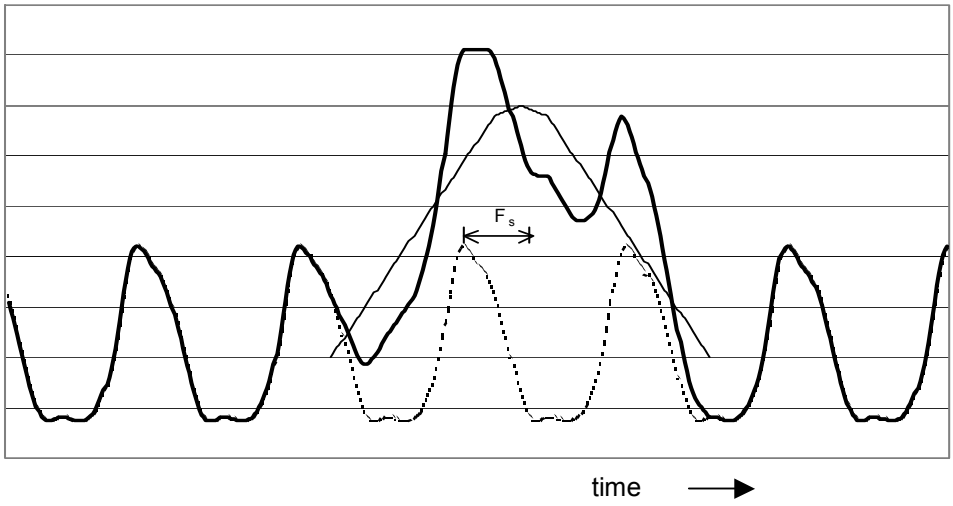

Figure 10-3 Schematised time evolution of the sea level, obtained by superimposing the surge on the time-averaged tide.

[21] Neap and spring tides are ignored, since the effects of the surge are much more important then the details of the tide. We remark that the phase and duration of the surge are not treated stochastically. This is a pragmatic choice to simplify the model.

The parameters for the duration and the phase are taken as t_s = 29 hour and f_s = 4.5 hours (the peak of the surge occurs 4.5 hours later than astronomical high tide). We will not comment much on these choices, except for the remark that contrary to what one might think, the phase is not uniformly distributed. This is due to the fact that surges develop easier at lower water depths, occurring near low tide. Also, recent investigations suggest that the duration of the surge should be taken longer than 29 hours.

The value h_s depends on the particular SOBEK-combination considered. Note that Table 10-1 shows that a number of 6 sea levels m are considered: m = 1.1, 2.0,..., 6.0 m+NAP. In the boundary conditions of the model, these levels are imposed at location Maasmond (see Figure 10-1). For every considered value m, h_s is chosen in such a way that the maximum of the water level obtained by superimposing the surge on the tide equals the value of m.

We note that instead of Maasmond, another location at sea could have been chosen. This location should on the one hand be so far away from land that the effect of the discharges on the water levels can be neglected, and on the other hand is close enough near land so that the "additional" wind set-up generated between this location and the land can be neglected. Also, of course, statistical information for this location has to be available. The location Maasmond satisfies these conditions.

For the 9 easterly directions NNE, NE,..., SSW, for which no surges are considered, a single value m_{ST} for the sea boundary is used, obtained by the time evolution of the *spring tide* instead of the average tide. Note that this is a slightly conservative approach. But the amount of conservatism is limited, since the Hydra-Zoet results for locations where the sea poses a threat for the dikes appear to be dominated by the *westerly* directions.

10.1.2 Wind speed and wind direction

In SOBEK the speed and direction of the wind are assumed to be spatially uniform, aside from the fact that for the smaller rivers *hiding factors* are used to reduce the wind speed. These factors take into account that wind across smaller rivers is decreased as a consequence of the 'roughness' of the surrounding landscape.

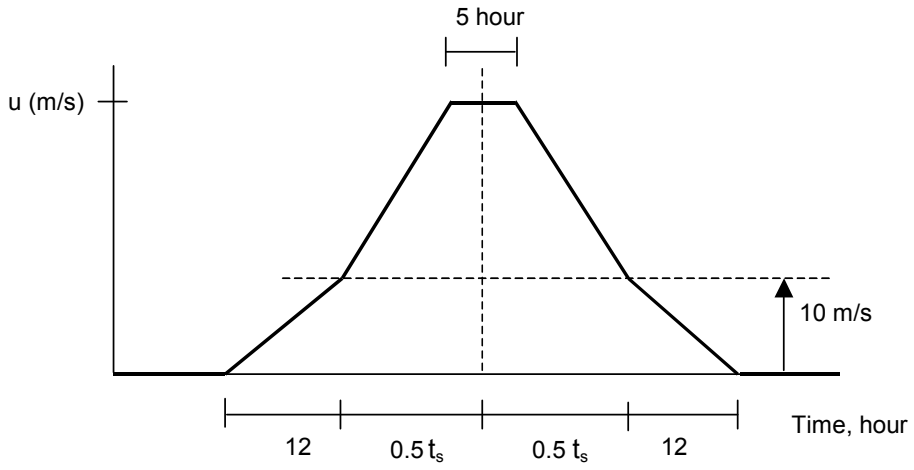

Figure 10-4 Schematised time evolution of the wind speed.

Figure 10-4 shows the assumed schematisation of the wind speed in time: front and back flanks of 12 hours to reach a wind speed of 10 m/s. Above 10 m/s a trapezium with peak duration of 5

hours is used. The base of the trapezium is equal to the base duration of the surge, i.e. t_s = 29 hours. The wind speeds mentioned in Table 10-1 correspond to the *maximum* of the schematised wind pattern, in Figure 10-4 denoted as u. The centre of the pattern coincides in time with the centre of the surge, i.e. the centre of the wind pattern occurs f_s = 4.5 hours after astronomical high tide.

10.1.3 Discharges and Rhine and Meuse dominant locations

At the eastern side of the model are three discharge boundaries (see Figure 10-1): on the river Lek at location Hagestein, on the Waal at Tiel and on the Meuse at Lith. The SOBEK calculations are made for different discharge levels of the Rhine and Meuse. To understand the information of Table 10-1, some explanation is needed.

The locations in the tidal river area can be divided into two categories: *Rhine dominant locations*, for which the Rhine has the most influence on the safety of flood defences, and *Meuse dominant locations* for which the Meuse has the most influence on this safety (see Figure 9-1). The majority of the locations, as has been shown by sensitivity calculations, belongs to the Rhine dominant set. For this category, statistical information of the Rhine is used in Hydra-Zoet. For every Rhine discharge a corresponding representative Meuse discharge is considered, equal to the median of all possible Meuse discharges that can occur at the considered Rhine discharge. For the Meuse dominant locations the role of Rhine and Meuse are interchanged.

Theoretically, it would be possible to include both the Rhine and the Meuse discharge as statistically dependent random variables into the model. This would lead to a more accurate model, however, at the cost of increasing the number of SOBEK calculations by a factor 4.5, leading to 30456 calculations (see the explanation in section 11.4.2). Earlier investigations suggest that the lack of accuracy by not treating both rivers 'fully probabilistic', is limited to 0.05 m for the normative water levels, while for the majority of the locations the error will be much smaller, see [Geerse, 2003; De Deugd, 1998].

Because of the two categories of locations, two types of SOBEK calculations are considered:

- as input for Rhine dominant locations: 9 Rhine discharges, with corresponding median Meuse discharges,
- as input for Meuse dominant locations: 9 Meuse discharges, with corresponding median Rhine discharges.

The discharges are imposed on the model as *stationary* values, i.e. they do not vary in time. The reason for this approximation is that the discharges vary so slowly over time, that it does not matter much whether a water level is calculated for a constant discharge q, or whether the water level is calculated at the moment the value q is attained in a front or a back flank of a discharge wave. Strictly speaking, the water level at discharge q will depend on the 'history in time' of the discharges preceding the moment of time q is attained. The error made here is neglected.[22]

We note that on the Meuse some lateral inflow occurs. The amount of lateral inflow is directly (deterministically) related to the level of the Meuse discharge, and is accounted for in the SOBEK model. The inflows do not appear in the formulas of Hydra-Zoet.

[22] For the upper rivers the model WAQUA is used to calculate water levels. In that case non-stationary discharge waves are used.

10.1.4 Maeslant Barrier

For the western directions storm surges can occur. During a surge the Maeslant Barrier might function properly or might fail to close. So both barrier states have to be accounted for in the model, which means that SOBEK calculations are required for both states. For the easterly directions it is assumed that surges do not occur, so that for these directions the barrier never needs to close. Hence for these directions only the open barrier state has to be considered.

10.2 Wind waves

The wave variables, i.e. significant wave height H_s, wave period $T_{m-1,0}$ and wave direction θ, are determined in every one of the 6768 combinations of boundary conditions in the diagram of Figure 9-3, by 1-dimensional wave growth formulas like the one from Bretschneider or by a 2-dimensional model such as SWAN (as explained in section 5.3).

If wave growth formulas are used, as is done in HBC2006, effective fetches and bottom levels are needed. If a 2-dimensional model is used, there is no need for them, since the 2-dimensional schematisation in SWAN then contains detailed geometrical information, from which SWAN can calculate the wave variables.

10.3 Hydraulic load levels

Using SOBEK and a wave model the local water level and wave variables are now available in every one of the 6768 combinations in the diagram of Figure 9-3, for both the axis and the shore locations. Consequently, in every combination the hydraulic load level H can be calculated. For axis locations (not located at a dike toe) this can only be done for the failure mechanism overflow, whereas for shore locations this can be done for mechanisms overflow as well as wave overtopping. For the latter locations, if a dam and/or foreshore are present in front of the dike, the waves at open water still have to be transformed using the dam and/or foreshore module. The details have been explained in section 5.5.

For clarity we express the load level H as a function of the load variables that are relevant for the probabilistic formulas in later chapters. H is a function of the discharge q, sea level m, wind speed u, wind direction r and barrier state ω, i.e. H = H(q,m,u,r,ω). Denote the local (maximum) water level by h_{wl}. Then for failure mechanism overflow, we have

$$H(q,m,u,r,\omega) = h_{wl}(q,m,u,r,\omega) \tag{10.1}$$

For mechanism wave overtopping we need the wave overtopping height $h_{overtop}$, with unit metres, which has been defined in section 5.5, corresponding to a specified critical overtopping discharge. For this mechanism we have

$$H(q,m,u,r,\omega) = h_{wl}(q,m,u,r,\omega) + h_{overtop}(q,m,u,r,\omega) \tag{10.2}$$

In Hydra-Zoet H is not only required for the 6768 combinations of Table 10-1, but also for arbitrary combinations (q,m,u,r,ω). To obtain the load levels for these combinations, linear interpolation is used between the results of the 6768 combinations.

11 Probabilistic formulas tidal rivers

This chapter introduces the basic probabilistic formulas of Hydra-Zoet for the tidal rivers. First, the statistical information for the discharge, sea level and wind are described. Next, formulas are given for some probabilities related to the shortest time scale of the model. These probabilities are then used to calculate the exceedance frequency at a given location. The chapter concludes with a section providing formulas for entire dike rings, consisting of a number of (consecutive) locations.

11.1 Statistical information

This section discusses statistical information for the tidal rivers. Since most of the locations are Rhine dominant (section 10.1.3), only the information for the Rhine is provided, while the information for the Meuse is left out. We do not provide all statistical details here, but provide only the information necessary to understand the probabilistic formulas of Hydra-Zoet.

11.1.1 Statistical information Rhine at Lobith

The statistical information for the Rhine, at location Lobith, consists of the following information (compare sections 6.1, 8.2 and 8.3):

- Minimum discharge q_{min} and base duration B of the trapezia that are used to model the time evolution of the discharge.
- Peak duration b(k) of the trapezia, where k denotes the peak value k of the trapezia.
- Exceedance probabilities P(K>k) for the peak value k of the trapezia.

The minimum discharge is chosen as q_{min} = 750 m^3/s. As base duration B = 720 hour (30 days) is chosen, corresponding to 6 trapezia in the winter half year.

The peak duration b(k) consists of two linear portions: a top duration of 720 hours at the minimum discharge k = 750 m^3/s, decreasing linearly to a duration of 12 hours at k = 6000 m^3/s, and remaining at this constant value for all k > 6000 m^3/s.

peak discharge Lobith	exceedance probability
750	1
1000	0.97
1500	0.8
3500	0.3
4500	0.22
5893.3	1.667E-01
7017	8.333E-02
10850	6.667E-03
16000	1.333E-04

Table 11-1 Points (k_i, $P(K>k_i)$) characterising the exceedance probability of the peak value of the trapezia for station Lobith.

The quantity P(K>k), depicted in Figure 11-1, is built of a number of exponential portions, where each portion is of the form

$$P(K > k) = \exp\left(-\frac{k-b}{a}\right) \tag{11.1}$$

Stated otherwise: the logarithm of P(K>k) consists of a number of linear portions as a function of k. Table 11-1 contains the begin and end points of the exponential portions. E.g. the second portion runs from k = 1000 until k = 1500 m^3/s, where P(K>1000) = 0.97 and P(K>1500) = 0.8. The latter probabilities determine the values of a and b in formula (11.1) for this portion; these values can of course be calculated, but do not bother us here. The last exponential portion, running from 10850 until 16000 m^3/s, is extended beyond 16000 m^3/s.

We recall from (8.4) that the once per year discharge k_1 corresponds to $P(K>k_1) = 1/6$, implying by Table 11-1 that k_1 = 5893.3 m^3/s. The parameters a and b in (11.1) for $k > k_1$ are chosen in such a way that they adequately describe the frequency of observed peaks in the measurements. Below k_1, the line in Figure 11-1 looks a bit odd. The reason for this is that for $k < k_1$ the portions constituting the line have to be chosen in such a way that together with the trapezia they reproduce the momentaneous probabilities P(Q>q) prescribed by the measurements, using the procedure that was explained for lake levels in section 8.3. This reproduction turned out to be possible using the odd looking line below k_1. We recall however, as explained in section 8.2.1, that below k_1 the exceedance probability does not have a physical meaning.

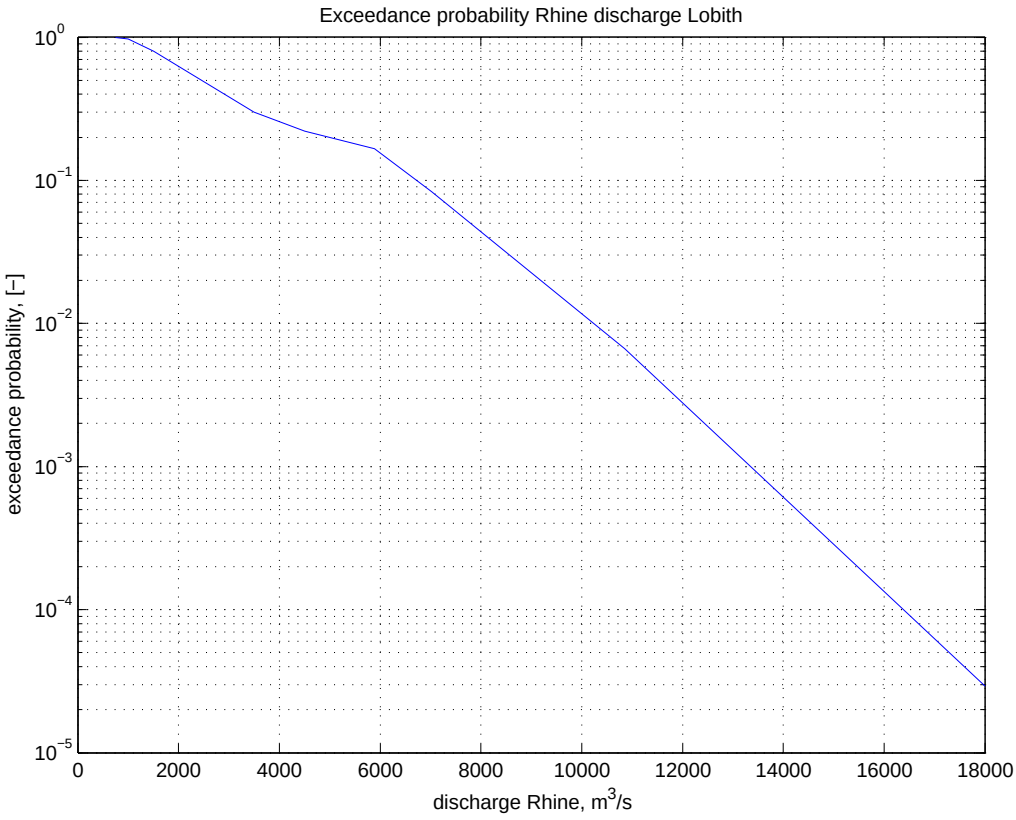

Figure 11-1 The exceedance probability P(K>k), related to the base duration B = 30 days.

11.1.2 Sea levels, wind and their correlation

As explained in section 8.1, the time base for the fast variables sea level M, wind speed U and wind direction R equals b = 12 hours. In this period b, M is taken to be the maximum water level, U the maximum wind speed, and R the vectorially averaged wind direction.

For the 9 eastern directions NNE, NE,..., SSW it is assumed no surges do occur, which means that for these directions only statistical information for the wind has to be available, represented in Hydra-Zoet by a probability density g(u,r). For the 7 westerly directions SW, WSW,..., N, a probability density g(m,u,r) is used. The details of this multivariate density will be skipped. We only mention that for the westerly directions a version of the model CS (see section 7.2) was used to derive, conditional on a westerly direction r, a bivariate density g(m,u|r). Multiplying this density with the probability g(r) on direction r, the density g(m,u,r) then is obtained, for the details see [Geerse et al, 2002].

11.1.3 Predicted sea water levels at Maasmond

The Maeslant Barrier is operated using predicted values for the discharges of the Rhine and Meuse, wind speeds, wind directions and sea water levels at Maasmond. These predictions are used to calculate the water levels at locations throughout the area with the model SOBEK; the resulting water levels then also are predictions. If these predictions are such that for two 'key locations' certain critical levels are exceeded, a command to close the barrier is ordered. These key locations are Rotterdam and Dordrecht, with critical levels respectively 3.0 m+NAP and 2.9 m+NAP.

The predicted values for the discharges of the Rhine and Meuse, wind speeds, wind directions and sea water levels at Maasmond all have uncertainties, as does the model SOBEK used to calculate predicted water levels throughout the area. For the safety against flooding, the most important uncertainty happens to be the one for the predicted water levels of Maasmond. This uncertainty is accounted for in Hydra-Zoet.

Denote the predicted sea water level at Maasmond by V. Given an *actual* occurring water level m at Maasmond, the predictions are modelled with a normal density:

$$g(v \mid m) = \frac{1}{\sigma\sqrt{2\pi}} \exp\left\{-\frac{1}{2}\left(\frac{v-(m+\mu_{MM})}{\sigma_{MM}}\right)^2\right\}$$
$$\mu_{MM} = -0.09 \text{ m} \qquad (11.2)$$
$$\sigma_{MM} = 0.18 \text{ m}$$

where the *negative* value for μ_{MM} means that the predictions are on average 0.09 m too low. The latter might be puzzling: why should the error in the predictions, on average, not be zero? The reason is that a prescribed procedure/model is used to generate these predictions, which later turned out to have a bias. One way to solve for this bias is to shift the predictions upwards by 0.09 m, another way is to account for this bias by choosing μ_{MM} as in (11.2), which is done in Hydra-Zoet. (If this bias would not be accounted for, the outcomes of Hydra-Zoet would be non-conservative, with Hydraulic Boundary Conditions that could be too low.)

11.2 Probability for the shortest time scale

11.2.1 Structure of the probability density for shortest time scale

In the probabilistic formulas of Hydra-Zoet a probability density is needed for the shortest period b = 12 hours that is considered in the model. For the easterly directions NNE, NE,..., SSW, this density is g(q,u,r). Since the discharge is assumed to be independent of the wind, we have

$$g(q,u,r) = g(q)g(u,r) \tag{11.3}$$

where g(q) = -dP(Q>q)/dq, with P(Q>q) the momentaneous exceedance probability of level q.

For the westerly directions SW, SSW,..., N, the probability density g(q,m,u,r,ω) is needed. Because the discharge is assumed statistically independent of all other variables, we can write

$$g(q,m,u,r,\omega) = g(q)g(m,u,r)g(\omega \mid q,m,u,r) \tag{11.4}$$

Here g(m,u,r) was introduced in section 11.1.2. The quantity g(ω|q,m,u,r) denotes the probability on barrier state ω, conditional on q,m,u,r. The formula to calculate g(ω|q,m,u,r) is the subject of the next section. In the derivation we use the following notation for the open and the closed barrier state:

$$\omega = \begin{cases} 0 & \text{if the barrier remains open during a storm surge} \\ 1 & \text{if the barrier closes during the storm surge} \end{cases} \tag{11.5}$$

11.2.2 Operation and probabilities of closure Maeslant Barrier

This section explains how the (conditional) probabilities on the barrier states can be calculated. First a 'criterion' random variable E is needed, defined as

$$E = \begin{cases} 1, & \text{if } q,v,u,r \text{ are such that the Maeslant Barrier has to be closed} \\ 0, & \text{otherwise} \end{cases} \tag{11.6}$$

We will explain how P(E=1|q,m,u,r) is calculated, i.e. the probability that a 'closure command' is ordered, given the occurrence of (q,m,u,r), see Figure 11-2. The figure corresponds to a fixed value u and to one of the westerly directions r. The horizontal axis gives the discharge q and the vertical the prediction v. The figure contains three lines:

1. The contour of critical level 3.0 m+NAP for location Rotterdam, as derived by interpolation from the SOBEK calculations for the open barrier state (these calculations are part of the ones described in Table 10-1).

2. The contour of critical level 2.9 m+NAP for location Dordrecht, as derived by interpolation from the SOBEK calculations for the open barrier state (these calculations are part of the ones described in Table 10-1).

3. The so-called closure function $v_E(q,u,r)$ for the Maeslant Barrier, which equals for a given q the minimum of the lines in 1 and 2.

Note that the contours in 1 and 2 are determined for the *open* barrier state: since one needs to know whether for the *open* situation the criteria for closure are attained (if not, no closure information is needed). If for given q,u,r the prediction v is such that $v \geq v_E(q,u,r)$, a closure command is ordered, since in that case the criteria for Rotterdam and/or Dordrecht are exceeded or just attained.

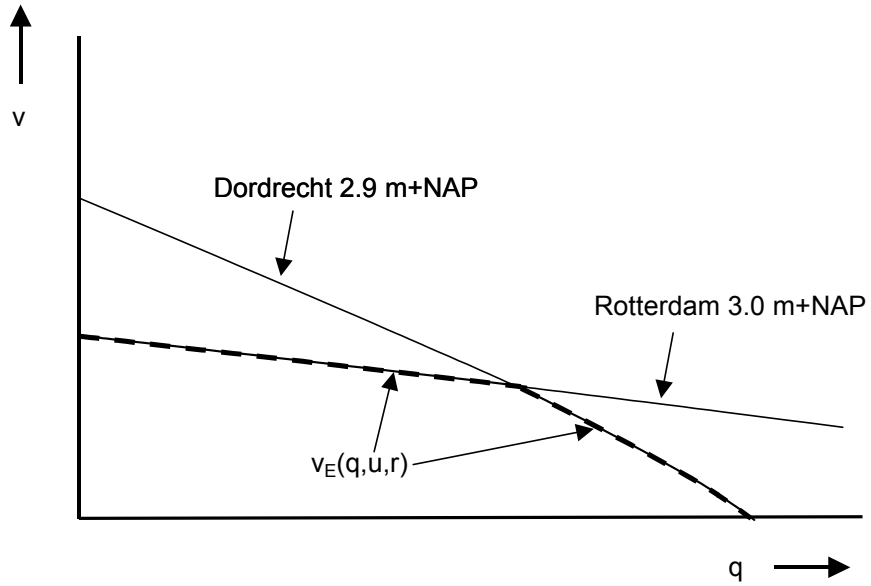

Figure 11-2 Illustration of the closure function $v_E(q,u,r)$ for the Maeslant Barrier, given by the dashed line (u and r are fixed here). The contours for Rotterdam and Dordrecht are determined for the open barrier.

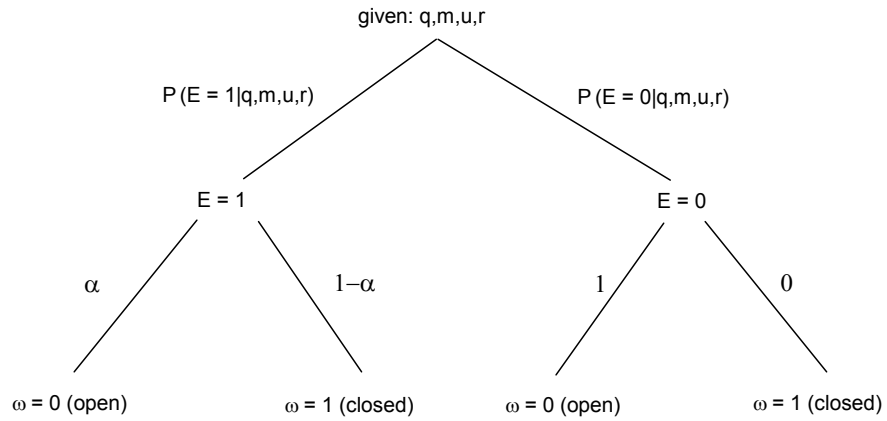

Figure 11-3 Tree diagram for the calculation of the probabilities for the open and closed barrier state.

Conditional on q,m,u,r, the probabilities on the predictions v can be calculated using g(v|m) of (11.2).[23] The probability P(E=1|q,m,u,r) then is given by

$$P(E=1 \mid q,m,u,r) = \int_{v_E(q,u,r)}^{\infty} dv\, g(v \mid m) \qquad (11.7)$$

[23] Note that the error in the prediction, is as an approximation, assumed to be independent of q,u,r; otherwise we should have considered g(v|q,m,u,r) instead of g(v|m).

while P(E=0|q,m,u,r) of course equals 1 minus this probability. The probability that the barrier fails to close, once a closure command has been ordered, is denoted by α (a value of 0.01 is used in the Hydraulic Boundary Conditions 2006). Using the tree diagram of Figure 11-3 we then obtain, respectively for the closed and the open state,

$$\begin{aligned} g(\omega=1\,|\,q,m,u,r) &= (1-\alpha)\int\limits_{v_E(q,u,r)}^{\infty} dv\, g(v\,|\,m) \\ g(\omega=0\,|\,q,m,u,r) &= 1-g(\omega=1\,|\,q,m,u,r) \end{aligned} \tag{11.8}$$

For the easterly directions, since no surges are assumed, no closure will occur, so that the probability on the closed state is 0 and the one for the open state is 1.

11.2.3 Exceedance probability of the load

In the remainder of this report, as some kind of building block in various formulas, often the probability P(H>h|q) is needed, i.e. the probability that the hydraulic load level H exceeds the value h, given a discharge q, in the period b = 12 hours. Denoting the 16 wind directions by r = 1, 2,..., 16, this probability is given by

$$P(H>h\,|\,q)=\sum_{r=1}^{16}\sum_{\omega=0,1}\int\limits_{(q,m,u,r,\omega):H(q,m,u,r,\omega)>h} du\, g(m,u,r,\omega\,|\,q)P(H>h\,|\,q,m,u,r,\omega) \tag{11.9}$$

where it is understood that the integral is 0 if for a combination (r,ω) there are no points (q,m,u,r,ω) satisfying H(q,m,u,r,ω)>h.

To rewrite (11.9), note that for the easterly directions r = 1, 2,..., 9, only ω = 0 can occur, while the value of m is equal to the fixed value m_{ST} denoting spring tide. This means that in this situation H = H(q,m_{ST},u,r,ω=0) and also that we can replace g(q,m,u,r,ω=0) by g(q,u,r). Moreover, from (11.3), we observe that g(u,r|q) = g(u,r). For the westerly directions r = 10, 11,..., 16, it follows from (11.4) that g(m,u,r,ω|q) = g(m,u,r)g(ω|q,m,u,r), with H = H(q,m,u,r,ω). Now (11.9) can be rewritten as

$$\begin{aligned} P(H>h\,|\,q) = &\sum_{r=1}^{9}\int\limits_{(q,u,r):H(q,m_{ST},u,r,\omega=0)>h} du\, g(u,r) \\ &+\sum_{r=10}^{16}\sum_{\omega=0,1}\int\limits_{(q,m,u,r,\omega):H(q,m,u,r,\omega)>h} dm\,du\;\; g(m,u,r)g(\omega\,|\,q,m,u,r) \end{aligned} \tag{11.10}$$

where we recall that g(m,u,r) is discussed in section 11.1.2 and g(ω|q,m,u,r) is given by (11.8). So all parts on the r.h.s. of (11.10) are known, meaning that this formula can be used for the actual calculation of P(H>h|q).

11.3 Exceedance frequency for the load level

We now turn to the calculation of the exceedance frequency $F_H(h)$ of load level h, given in times per year. The quantity $F_H(h)$ will also be called the *failure frequency*. Recall that exceedances in the summer half year are neglected, and that the winter half year is 'filled' with N_{trap} = 6 trapezia of base duration B = 30 days. Let us denote by $P_B(H>h)$ the probability that in a base duration B failure occurs at least once, where here failure means exceedance by H of level h. Then we must have

$$F_H(h) = N_{trap} P_B(H > h) \tag{11.11}$$

We recall that f(k) denotes the probability density for the peak value k of the discharge trapezia. Then we can write

$$P_B(H > h) = \int dk\, f(k) P_B(H > h \mid k) \tag{11.12}$$

where $P_B(H>h|k)$ denotes the failure probability in duration B, conditional on the peak value k of the trapezium.

To calculate this probability, the time is partitioned in intervals of 12 hours, yielding n(B) = B/b = 60 'time blocks'. Denote the average discharge in the j-th block by q(j|k). Since by assumption, see section 8.1.1, the fast variables in different time-blocks are statistically independent, it follows:

$$\begin{aligned} P_B(H > h \mid k) &= 1 - \text{probability that } H < h \text{ in all time blocks} \\ &= 1 - \prod_{j=1}^{n(B)} \left(1 - P\left[H > h \mid q(j \mid k)\right]\right) \end{aligned} \tag{11.13}$$

where the probabilities on the r.h.s. are obtained from (11.10).

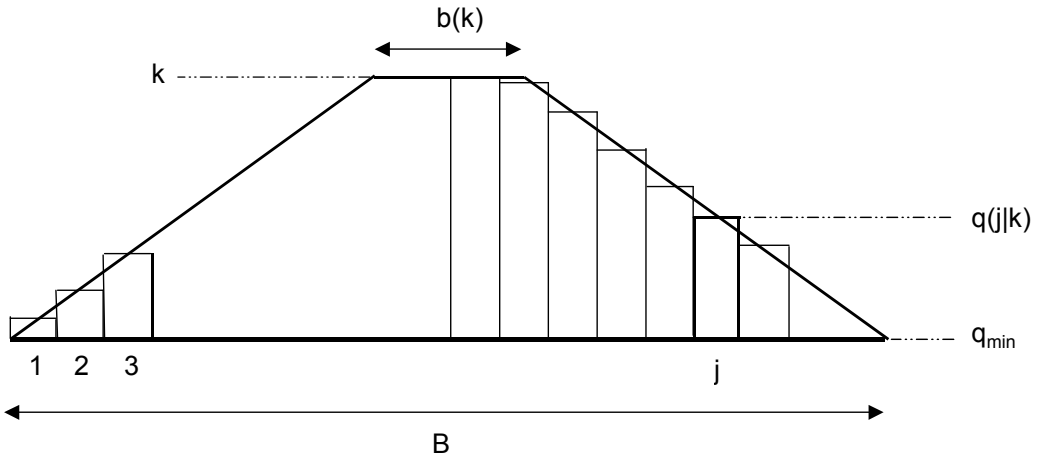

Figure 11-4 Discretisation of duration B in blocks of b = 12 hours.

11.4 Treatment of dike rings

11.4.1 Rings with either Rhine dominant or Meuse dominant locations

The preceding formulas are dealing with single locations. If this is a Rhine dominant location, the discharge Q in the model is the Rhine discharge at Lobith, and for a Meuse dominant location, Q is the Meuse discharge at Lith. This section provides a formula to calculate the exceedance frequency for a complete dike *ring*, a continuous enclosed line of flood defences, when the dike heights along the ring are known. It is required though, that all locations along the ring are either Rhine dominant or Meuse dominant. A ring with 'mixed' locations is not allowed. This means that e.g. dike ring 24 in Figure 2-1 cannot be considered. How to deal with this problem of mixed rings will be dealt with in section 11.4.2.

Let us now consider a ring consisting of either Rhine dominant or Meuse dominant locations. For the Rhine dominant ring, Q is the Rhine discharge, while for a Meuse dominant one Q is the Meuse discharge. Assume the ring consists of i = 1, 2,..., n dike sections, with given dike heights h_1, h_2,..., h_n. Denote the hydraulic load level for the i-th location by

$$H_i = H_i(q,m,u,r,\omega) = \text{hydraulic load level dike section i (m+NAP)} \tag{11.14}$$

We now define an 'effective' hydraulic load level H as the maximum over all locations i of the difference between the load level of the location and the dike height present there:

$$\begin{aligned} H = H(q,m,u,r,\omega) &= \max_{i=1,2,\ldots,n} \left(H_i(q,m,u,r,\omega) - h_i \right) \\ &= \text{effective hydraulic load level dike ring (m)} \end{aligned} \tag{11.15}$$

Note that if $H_i(q,m,u,r,\omega) - h_i$ is positive, the load level in the combination (q,m,u,r,ω) exceeds the crest height at location i, which means that this combination then is 'unsafe' for location i. If on the other hand $H_i(q,m,u,r,\omega) - h_i$ is negative, the load level is below the crest height, which means that the combination is a 'safe' one at this location. In fact, definition (11.15) implies that the ring fails for combination (q,m,u,r,ω) if and only if $H(q,m,u,r,\omega) > 0$, where here failure of the ring means *failure of at least one of the locations*. To explain this, assume that $H(q,m,u,r,\omega) > 0$. Then for at least one location i we must have $H_i(q,m,u,r,\omega) - h_i > 0$, which means that this location, and hence the ring, fails. So $H(q,m,u,r,\omega) > 0$ implies failure of the ring. Next, assume failure of the ring, meaning failure of at least one location i. In that case $H_i(q,m,u,r,\omega) - h_i > 0$, implying $H>0$.

The exceedance frequency $F_{H,ring}$ of the ring, in times per year, can now be calculated by the formulas applicable to a single location, using the effective load level H from (11.15) while considering level h = 0:

$$F_{H,ring} = F_H(h=0) \tag{11.16}$$

Here the r.h.s. is calculated with (11.11).

11.4.2 Rings with Rhine and Meuse dominant locations

The proper way to treat rings with Rhine and Meuse dominant locations would be to consider both the Rhine and Meuse as random, correlated variables. The formulas to do that are available. They would be analogous to the ones for the Vecht and IJsseldelta considered in Chapters 13 - 16 (in the latter formulas one should replace the slow variable lake level by a discharge, yielding two slow discharge variables). There are practical reasons why this has not been done. At present, when considering 9 discharges for the dominant river, with corresponding median values for the non-dominant river, 6768 SOBEK calculations are used as input for Hydra-Zoet (compare Table 10-1). If both discharge are treated the same way, this number of calculations would increase with a factor $9^2/(9+9) = 4.5$, yielding 30456 calculations. This means a large number of calculations. Although with the present computer capacity this number would be feasible, this approach of treating Rhine and Meuse as correlated random variables, has not been implemented.

At this moment, if ring calculations are needed, a simple approximate approach can be used as follows. Partition the ring in a part R_1 of Rhine dominant locations and a part R_2 of Meuse

dominant ones, yielding two exceedance frequencies $F_{H,ring\ 1}$ and $F_{H,ring\ 2}$. As a conservative approximation, we simply can take

$$F_{H,ring} = F_{H,ring1} + F_{H,ring2} \tag{11.17}$$

The reason this answer is conservative, is that failure events (exceedances somewhere along the ring) occurring on the r.h.s. may be counted twice: if during such an event a location along the Rhine fails as well as one along the Meuse, two events are counted in (11.17), although it should account for a *single* failure event for the ring. So the r.h.s. provides an upper bound for the 'true' ring frequency $F_{H,ring}$.

A lower bound is given by the maximum of $F_{H,ring\ 1}$ and $F_{H,ring\ 2}$. If this maximum is close to (11.17), the exceedance frequency of the ring can be calculated accurately; if not, the calculation is less accurate. Note however that the error in (11.17) is bounded by a factor 2, corresponding to the worst case, where all failure events are counted twice. Since an error might be judged of limited importance, compared to all kinds of uncertainties not taken care of in the model, like uncertainties in the water and wave calculations, statistical distributions, the SOBEK-schematisation, the allowed critical overtopping discharge, numerical uncertainties, etcetera.

12 Additional output for the tidal rivers

The preceding chapter treated the basic formulas of Hydra-Zoet, used to calculate the exceedance frequency $F_H(h)$ for a single location or its analog for a dike ring. The current chapter provides additional formulas, used in the program Hydra-Zoet to generate additional output concerning firstly *Illustration Points* (IP's) and secondly *contributions to the exceedance frequency*. This kind of output provides information about the circumstances during failure event. For both kinds of output, examples were provided in chapter 4.

Section 12.1 treats the IP's section 12.2 the contributions. The mathematics used in the latter section is a bit complicated, but we hope the reader will grasp (at least) the main ideas. The most complicated proofs are put aside in an appendix.

12.1 Illustration points: the most probable circumstances in the case of "just failure"

12.1.1 Failure set and failure surface

Before the Illustration Points can be defined, we need some (elementary) definitions. For a considered load level h, the *failure set* is defined as the set of points (q,m,u,r,ω) for which $H(q,m,u,r,\omega) \geq h$, and the *failure surface*, also called *limit state*, as the set of points constituting its boundary, i.e. the set of points for which $H(q,m,u,r,\omega)=h$. The safe set is the complement of the failure set, for which $H(q,m,u,r,\omega) < h$.

In the following subsections, often a fixed combination (r,ω) is considered. For such a fixed combination, an illustration of the failure surface is given in Figure 12-1. Points above and including this surface constitute the failure set, points below this surface the safe set.

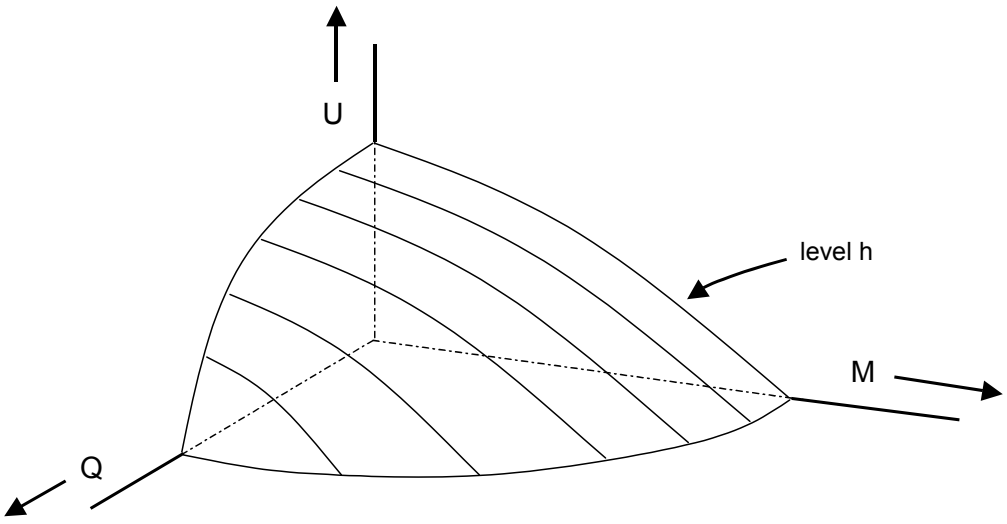

Figure 12-1 Example of a failure surface, also called limit state, for a given combination (r,ω).

12.1.2 Choice of probability density

Suppose that the exceedance frequency $F_H(h)$ has been calculated for load level h. How should we define for this calculation the Illustration Point (IP) for a given combination (r,ω)? An obvious definition seems to be: the IP equals the point on the failure surface for which the probability density of the variables (q,m,u), when considered conditional on (r,ω), attains its maximum. The problem here is that, because of the different time scales of the variables, $F_H(h)$ is not calculated as a straightforward integration of a probability density over the failure region (compare the formulas in section 11.3).

As a *pragmatic choice* in Hydra-Zoet, the probability density $g(q,m,u,r,\omega)$ of (11.4), related to the shortest duration b in the model is taken. For reasons explained below in section 12.1.4, this density as well as the failure surface are first translated with the so-called Rosenblatt transformation. In the following section we will first introduce, for pedagogical reasons, what the definition of the IP would be without this transformation.

12.1.3 Illustration Point without transformation

The procedure to determine the IP for a fixed combination (r,ω), related to the calculation of $F_H(h)$, is as follows:

1. Determine the failure surface, consisting of the points (q,m,u) for which $H(q,m,u,r,\omega) = h$.

2. Find the point $(q,m,u) = (q_{IP}, m_{IP}, u_{IP})$ on this surface for which $g(q,m,u|r,\omega)$ attains its maximum.

Here the conditional probability of point 2 is given by

$$g(q,m,u \mid r,\omega) = \frac{g(q,m,u,r,\omega)}{g(r,\omega)} \tag{12.1}$$

where the numerator on the r.h.s. was discussed in section 11.2, and $g(r,\omega)$ is obtained by integrating out the variables q,m,u in $g(q,m,u,r,\omega)$.

We note that the IP is by definition a point on the failure surface, and *not in the interior* of the failure set. The requirement that it is on the failure surface is for practical purposes, since we want the point to exactly yield the hydraulic load level h. Note that a point in the interior would lead to a load level exceeding h.

12.1.4 Illustration Point with Rosenblatt transformation

The preceding calculation of the IP is not used in Hydra-Zoet, but only the transformed version using the Rosenblatt transformation. In this transformation the distributions of q, m and u are transformed to standard normal ones. An advantage of this approach is that the IP thus obtained is less sensitive to irregularities in $g(q,m,u|r,\omega)$, which in practice might occur as a consequence of numerical imperfections. Another advantage is that the use of this transformation, at least in our opinion, leads to a more natural IP.

Let us illustrate the latter using a very simplified example, considering just one variable and ignoring the failure surface. Figure 12-2 shows a (highly fictional) probability density with a small but high peak near the right tail of the distribution, with the most probable point, i.e. the

mode of the probability density, located at x_1. The Rosenblatt transformation in this simplified situation would be such that the probability density would be transformed to a standard normal density. In this transformation x is mapped onto the point y(x) determined by $P(X<x) = \Phi(y(x))$, with Φ denoting the cumulative standard normal distribution. In the transformed (normal) space, the mode would lie at the centre of the normal density at y = 0, which would correspond in the original space, since $P(X<x_2) = \Phi(y=0) = 0.5$, *to the median of the original distribution*, denoted by x_2 in the figure. So when using the transformed version of the probability density, the IP would, in this simplified example, correspond to x_2. The value x_2 seems to us a more natural one then the value x_1, resulting without applying a transformation. As a side remark, note that this example shows that the most probable point of a distribution (the mode) is not invariant under transformations, implying that the very concept of an IP is not a very robust one: the phrase "most probable circumstances" does not have an absolute meaning. (Such an absolute meaning can only be attributed to outcomes of a *discrete* random variable.)

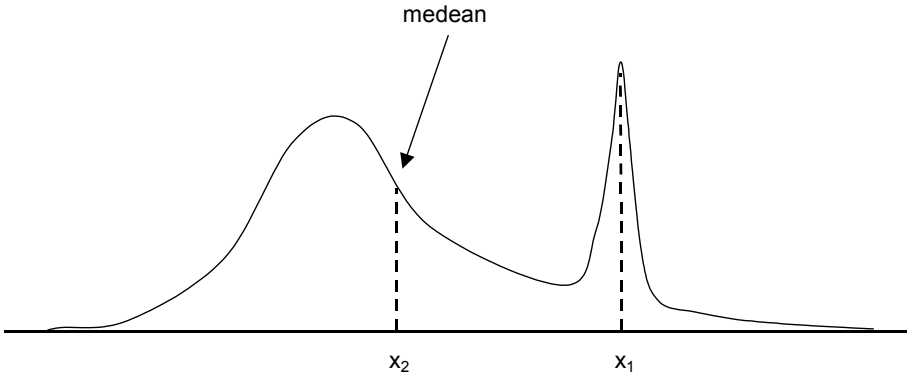

Figure 12-2 Illustration of the benefits of the Rosenblatt transformation.

We now turn to the details of the procedure to determine the IP using the Rosenblatt transformation. This transformation, as applied in Hydra-Zoet, is of the following form:[24]

$$\begin{aligned} x &= x(q,r,\omega) = \Phi^{-1}\left(P(Q<q \mid r,\omega)\right) \\ y &= y(q,m,r,\omega) = \Phi^{-1}\left(P(M<m \mid q,r,\omega)\right) \\ z &= z(q,m,u,r,\omega) = \Phi^{-1}\left(P(U<u \mid q,m,r,\omega)\right) \end{aligned} \tag{12.2}$$

where the probabilities on the r.h.s. are calculated using $g(q,m,r|r,\omega)$. As is well known, see e.g. Chapter 7 of [Ditlevsen en Madsen, 1996], after this transformation the random variables X, Y and Z thus defined become statistically independent standard normal ones, with cumulative density $\Phi(x,y,z) = \Phi(x)\Phi(y)\Phi(z)$. In this transformation the failure surface is transformed as well, leading to a surface in (x,y,z)-space.

The procedure for the determination of the IP corresponding to the combination (r,ω) consists of the following steps:

1. Determine the failure surface consisting of points (q,m,u) for which $H(q,m,u,r,\omega) = h$.

[24] One could transform the variables in a different order, which can give different results. This again shows that the concept of an IP is not a very robust one.

2. Transform the variables q,m,u to the variables x,y,z in the normal space using (12.2). Under this transformation the limit state, i.e. failure surface, in (q,m,u)-space is mapped into a surface in (x,y,z)-space.

3. Look on the transformed surface for the point (x_{IP}, y_{IP}, z_{IP}) with the highest probability in the normal space, which is the point with the shortest distance to the origin (note that $\Phi(x,y,z)$ is a decreasing function of the distance $(x^2+y^2+z^2)^{1/2}$ to the origin).

4. Transform the point (x_{IP}, y_{IP}, z_{IP}) with the inverse of the Rosenblatt transformation to the point (q_{IP}, m_{IP}, u_{IP}) in the original physical space. This point then is taken as the IP.

12.2 Contributions of the random variables to the exceedance frequency

12.2.1 On the nature of the contributions

Once the failure frequency $F_H(h)$ is calculated, often there is the need for extra information concerning the calculation. Such information is provided by the IP's just discussed, which give the most probable circumstances attaining the limit state. This information however is still very limited. Say e.g. it appears that in some calculation the most probable Rhine discharge thus found equals 15000 m^3/s. Then it would be interesting to know whether also much lower or much higher discharges contribute to the failure frequency as well. Such information is provided by what are called the *contributions to the exceedance frequency*. These contributions yield the probabilities with which outcomes q,m,u,r,ω occur, conditional on the occurrence of a failure event. Examples of these contributions were given in Chapter 4.

Before turning to the rather intricate formulas for the calculation of the contributions, we need to stress that strictly speaking it is not possible to speak of definite values of the variables discharge, sea level, wind speed, wind direction and barrier state during failure. Figure 12-3 shows a fictional evolution in time of the load level h(t). Of course, once a failure event occurs, it lasts for some time. During the failure event the variables just mentioned will vary in time. So we cannot speak of *definite* values of these variables during failure.

Next to this, there is another reason why we cannot speak of a definite value of these variables during failure: it may happen that during a single discharge wave (here a trapezium), failure occurs during different time blocks b of 12 hours. For instance, failure could occur at a relatively low discharge in the front flank of a discharge trapezium, and also during the peak of the trapezium. These two failure events are counted as a single failure event in the formula for $P_B(H>h|k)$, but with the consequence that this single failure event cannot be ascribed to a definite values of the discharge, sea level, wind speed, wind direction and barrier state.

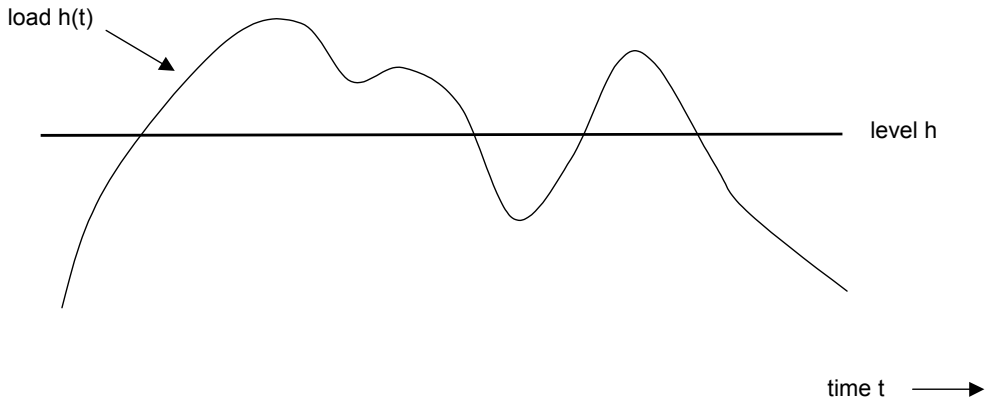

Figure 12-3 The hydraulic load h(t), exceeding a fixed level h for some duration.

Summarizing, during failure one cannot speak of definite values of the variables discharge, sea level, wind speed, wind direction and barrier state, for two reasons:

1. During failure the variables just mentioned may vary in time.
2. Failure might happen more than once during a discharge wave, i.e. in different time blocks b, yielding different values of the variables just mentioned during these different failure events.

It appears possible, though, to use a pragmatic kind of 'weighing recipe', with which contributions to the exceedance frequency can be determined in a sensible way. In the following subsections the formulas are given for this recipe to determine the contributions, where for the more complex proofs we refer to Appendix B.

12.2.2 Continuous version probabilistic formulas

A basic formula of the model is (11.13) for the calculation of $P_B(H>h|k)$. This formula has a 'discrete character', since the r.h.s. contains a product over a discrete number of n(B) probabilities, where here n(B) is the number of time blocks fitting in the base duration B. We will provide in this section a 'continuous version' of this formula. The reason to do that is that this other version makes the formulas for the weighing recipe more transparent.

In the continuous version of the formula for $P_B(H>h|k)$ the discrete product is replaced by a continuous integration over time t. The formulas are best formulated using a rescaled time parameter $\tau = t/b$, meaning that τ equals the (continuous) time, but measured in units of the shortest duration b of the model. If one wants to rewrite the formulas in terms of t, one just has to substitute τ by t/b in the formulas below, after which the dependence of the results on b becomes apparent.

Denote by $\alpha(\tau,k)$, in m^3/s, the discharge at time τ in the trapezium of base duration B with peak value k. As indicated in Figure 11-4 its base duration is partitioned in n(B) time blocks of duration b. Assume that the trapezium starts at $\tau = 0$ and thus ends at $\tau = n(B)$. From (11.13) we obtain, approximating the discrete summation in a standard way by an integral,

$$\ln\left[1-P_B(H>h\mid k)\right]=\sum_{j=1}^{n(B)}\ln\left(1-P\left[H>h\mid q(j\mid k)\right]\right)\cong\int_0^{n(B)}d\tau\ \ln\left(1-P\left[H>h\mid\alpha(\tau,k)\right]\right) \tag{12.3}$$

where the probabilities on the r.h.s. are calculated with (11.10). This formula shows that

$$P_B(H>h\mid k)\cong 1-\exp\left\{\int_0^{n(B)}d\tau\ \ln\left(1-P\left[H>h\mid\alpha(\tau,k)\right]\right)\right\} \tag{12.4}$$

This approximation is accurate if the probability P[H>h|$\alpha(\tau$,k)] is a smooth function of τ, i.e. does not vary in time very fast. But it could be argued as well that the r.h.s. of (12.4) yields an even better answer for the 'true' value of P_B(H>h|k) then the discrete version (11.13), since in (12.4) the actual continuous time evolution of the discharge is included, whereas in the discrete version the discharge follows the artificial pattern of a 'staircase' indicated in Figure 11-4.

In the remainder of this chapter, the continuous version for the calculation of P_B(H>h|k) will be used, where to avoid confusion the r.h.s. of (12.4) will be denoted by G_B(H>h|k):

$$G_B(H>h\mid k)=1-\exp\left\{\int_0^{n(B)}d\tau\ \ln\left(1-P\left[H>h\mid\alpha(\tau,k)\right]\right)\right\} \tag{12.5}$$

We then obtain as the continuous version of formula (11.12) for P_B(H>h):

$$G_B(H>h)=\int dk\ f(k)\,G_B(H>h\mid k) \tag{12.6}$$

whereas the continuous version for the exceedance frequency in (11.11) becomes

$$F_H(h)=N_{trap}\,G_B(H>h) \tag{12.7}$$

12.2.3 Contributions of the discharges

As mentioned before, a pragmatic weighing recipe is used to determine the contributions to the exceedance frequency. This section describes how this recipe works for the case where only contributions for the discharge are considered. The general situation for all the variables is treated in the next section.

Consider a fixed interval [q_1,q_2] of discharges. Then we want to find a sensible recipe to determine the contribution of this interval to the exceedance probability F_H(h). Denote this contribution by F_H(h;[q_1,q_2]). Its interpretation is that this number equals the average number of failure events per year *that occur for discharges q belonging to the interval [q_1,q_2]*. As a consequence, these contributions should have the property (among other things) that for any value q_2' satisfying $q_1<q_2'<q_2$

$$F_H(h;[q_1,q_2])=F_H(h;[q_1,q_2'])+F_H(h;[q_2',q_2]) \tag{12.8}$$

and, since all contributions together should yield the 'total' exceedance frequency,

$$F_H(h)=F_H(h;[q_{\min},\infty]) \tag{12.9}$$

where we recall that q_{min} denotes the minimum discharge that can occur.

To find a sensible recipe, we first obtain a recipe for the contributions inside $[q_1,q_2]$ if failure occurs during the base duration B, conditional on the trapezium with peak value k. This contribution is denoted by $A(h;[q_1,q_2]|k)$. Integrating over k, this then yields the contribution $A(h;[q_1,q_2])$ for the interval unconditional on k. Finally, multiplying this quantity by the number N_{trap} of trapezia in the winter half year, the desired quantity $F_H(h;[q_1,q_2])$ is obtained.

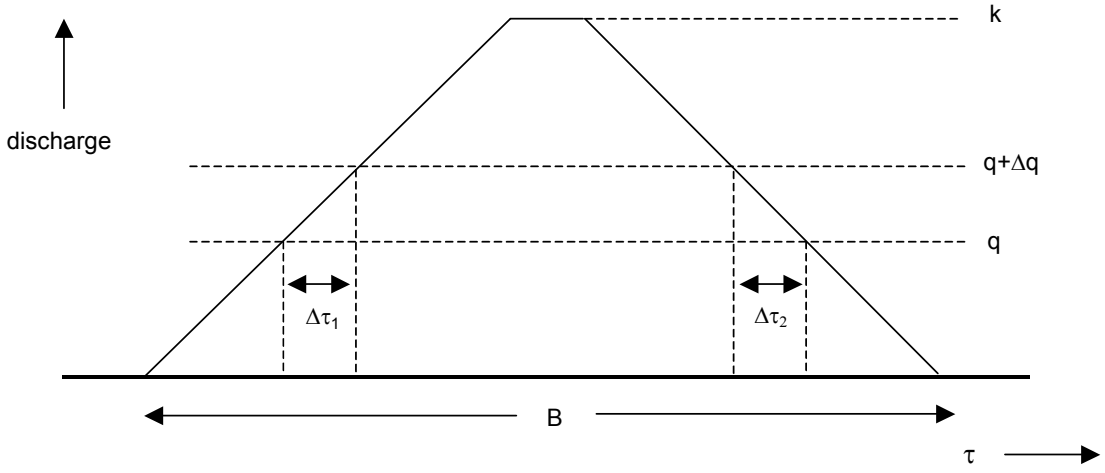

Figure 12-4 The intervals $\Delta\tau_1$ and $\Delta\tau_2$ in the trapezium $\alpha(\tau,k)$.

We turn to the details. We first treat the case for the contributions of a very narrow (infinitesimal) interval $[q,q+\Delta q]$ to the exceedance probability $G_B(H>h|k)$, where the conditioning is on the peak value k of the trapezium $\alpha(\tau,k)$. As a sensible recipe for the contributions of discharges belonging to $[q,q+\Delta q]$ we require that the contributions are proportional to:

- the failure probability $P(H>h|q)$ related to the shortest time duration b, and to
- the duration $\Delta\tau(q,k) = \Delta\tau_1 + \Delta\tau_2$ that the discharge $\alpha(\tau,k)$ is in the interval $[q,q+\Delta q]$, see Figure 12-4.

This implies that we should put

$$A\left(h;[q,q+\Delta q]\,|\,k\right) = J(k)P(H>h\,|\,q)\,\Delta\tau(q,k) \tag{12.10}$$

where J(k) is a proportionality constant that still has to be determined in such a way that after adding the contributions of all discharge intervals the 'full' probability $G_B(H>h|k)$ is obtained. Then requirement (12.9) will be satisfied. At a later stage we will show that the choice according to (12.10) also implies the validity of (12.8).

In order to determine J(k), partition the complete range of discharges within the trapezium, i.e. the interval $[q_{min},k]$, into n-1 intervals of width Δq, with $q_1=q_{min}$, $q_2= q_{min}+\Delta q$, $q_3= q_{min}+2\Delta q$,..., $q_n=q_{min}+(n-1)\Delta q$, where $k=q_n$. Then J(k) should satisfy

$$G_B\left(H>h\,|\,k\right) = J(k)\sum_{i=1}^{n-1} P(H>h\,|\,q_i)\Delta\tau(q_i,k) \tag{12.11}$$

The summation over discharges on the r.h.s. can be replaced by a summation over time durations: instead of partitioning the discharge in steps Δq one can partition the time in steps $\Delta\tau$, provided Δq and $\Delta\tau$ are small enough. In good approximation we then obtain

$$\sum_{i=1}^{n-1} P(H > h \mid q_i)\Delta\tau(q_i,k) = \sum_{j=1}^{m-1} P\big(H > h \mid \alpha(\tau_j,k)\big)\Delta\tau \tag{12.12}$$

where the base duration running from τ=0 until τ=B is partitioned in m-1 intervals of width $\Delta\tau$: t_1=0, τ_2=$\Delta\tau$, τ_3=2$\Delta\tau$,..., τ_m=B. The summation over the time interval, in turn, can be replaced by an integral over time if we take the limit $\Delta\tau\downarrow 0$, in which case (12.11) becomes

$$G_B\big(H > h \mid k\big) = J(k)\int_0^{n(B)} d\tau\, P\big(H > h \mid \alpha(\tau,k)\big) \tag{12.13}$$

Note that the r.h.s. of this formula is no longer an approximation of G_B(H>h|k), since (12.12) has become an exact expression in the limit $\Delta\tau\downarrow 0$, which is equivalent to $\Delta q\downarrow 0$.

Now introduce as an abbreviation for the integral on the r.h.s. of (12.13)

$$\bar{G}_B\big(H > h \mid k\big) = \int_0^{n(B)} d\tau\, P\big(H > h \mid \alpha(\tau,k)\big) \tag{12.14}$$

Then the proportionality constant J(k) is given by

$$J(k) = \frac{G_B(H > h \mid k)}{\bar{G}_B\big(H > h \mid k\big)} \tag{12.15}$$

which means that, for infinitesimally small Δq, the contribution (12.10) of the interval [q,q+Δq] to the failure probability G_B(H>h|k) is given by

$$A\big(h;[q,q+\Delta q] \mid k\big) = J(k)P(H > h \mid q)\Delta\tau(q,k) = \frac{G_B(H > h \mid k)}{\bar{G}_B\big(H > h \mid k\big)}\, P(H > h \mid q)\Delta\tau(q,k) \tag{12.16}$$

Instead of an infinitesimal small interval, we now consider an arbitrary interval [q_1,q_2]. The contributions of the latter interval can be obtained by adding the contributions of the infinitesimal intervals constituting it. Analogous to (12.12) and (12.13) it follows that

$$A\big(h;[q_1,q_2] \mid k\big) = J(k) \int_{\tau\in[0,n(B)]:\ \alpha(\tau,k)\in[q_1,q_2]} d\tau\, P\big(H > h \mid \alpha(\tau,k)\big) \tag{12.17}$$

These contributions are conditional on the peak value k of the trapezium. To obtain the unconditional contributions A(h;[q_1,q_2]) to the failure probability G_B(H>h), we need to integrate over k with respect to the probability density f(k):

$$A\big(h;[q_1,q_2]\big) = \int dk\, f(k) A\big(h;[q_1,q_2] \mid k\big) \tag{12.18}$$

This quantity yields the contributions of the interval [q_1,q_2] to the failure probability G_B(H>h) related to the base duration B. To obtain the contributions from the interval [q_1,q_2] to the exceedance frequency, representing failure events in a winter half year, we have to multiply (12.18) by the number of trapezia in a winter half year:

$$\begin{aligned} F_H(h;[q_1,q_2]) &= N_{trap} A\big(h;[q_1,q_2]\big) \\ &= N_{trap} \int dk\, f(k) J(k) \int\limits_{\tau\in[0,n(B)]:\ \alpha(\tau,k)\in[q_1,q_2]} d\tau\, P\big(H>h \mid \alpha(\tau,k)\big) \end{aligned} \tag{12.19}$$

This is the formula we were looking for. We will check that indeed (12.9) is satisfied, and to that purpose rewrite, using respectively (12.19), (12.14), (12.15), (12.6) and (12.7),

$$\begin{aligned} F_H(h;[q_{\min},\infty]) &= N_{trap} \int dk\, f(k) J(k) \int_0^{n(B)} d\tau\, P\big(H>h \mid \alpha(\tau,k)\big) \\ &= N_{trap} \int dk\, f(k) J(k) G_B(H>h \mid k) \\ &= N_{trap} \int dk\, f(k) G_B(H>h \mid k) \\ &= N_{trap} G_B(H>h) \\ &= F_H(h) \end{aligned} \tag{12.20}$$

which is (12.9). The check of (12.8) is postponed to the following section.

12.2.4 General formula for the contributions

The former section deals with contributions of discharges to the exceedance frequency. The treatment can be extended to contributions of the other variables, i.e. sea levels, wind speeds, wind directions and barrier states. The result is an extension of (12.19), containing again some integral over the time τ (formula (12.23) below). The formula thus obtained looks a bit awkward, but it appears that it can be rewritten in a more elegant form (formula (12.26) below), where the integral over time has been replaced by an integral over discharges. This rewritten version is implemented in Hydra-Zoet. In the following we only state the results, where for the proofs we refer to Appendix B.

First some definitions are needed. Denote the 'most detailed' contributions corresponding to all the variables by

$$\begin{aligned} &F_H(h;[q_1,q_2],[m_1,m_2],[u_1,u_2],r,\omega) \\ &= \text{simultaneous contributions of discharges in } [q_1,q_2],\ \text{sea levels in } [m_1,m_2], \\ &\quad \text{wind speeds in } [u_1,u_2],\ \text{wind direction } r \text{ and barrier state } \omega \end{aligned} \tag{12.21}$$

The failure set G is given by

$$G = \big\{(q,m,u,r,\omega) \mid H\big(q,m,u,r,\omega\big) \geq h\big\} \tag{12.22}$$

where the characteristic function of this set is denoted by $\chi_G(q,m,u,r,\omega)$: it equals 1 for points inside the set and 0 otherwise.

As discussed in Appendix B, the extension of (12.19) to all the variables is given by

$$\begin{aligned} &F_H\big(h;[q_1,q_2],[m_1,m_2],[u_1,u_2],r,\omega\big) \\ &= N_{trap} \int dk\, f(k) J(k) \int\limits_{\substack{\tau\in[0,n(B)]: \\ \alpha(t,k)\in[q_1,q_2]}} d\tau \int_{m_1}^{m_2} dm \int_{u_1}^{u_2} du\, g\big(m,u,r,\omega \mid \alpha(\tau,k)\big)\, \chi_G\big(\alpha(\tau,k),m,u,r,\omega\big) \end{aligned} \tag{12.23}$$

This formula provides the most detailed contributions. By 'aggregating' variables, we can obtain the contributions to a subset of all the variables. E.g. the contributions of discharges as in (12.19) can be obtained as

$$\begin{aligned}
&\sum_{r=1}^{16}\sum_{\omega=0}^{1} F_H\left(h;[q_1,q_2],[m_1=-\infty,m_2=\infty],[u_1=0,u_2=\infty],r,\omega\right) \\
&= N_{trap}\int dk\, f(k)J(k) \int\limits_{\substack{\tau\in[0,n(B)]:\\ \alpha(t,k)\in[q_1,q_2]}} d\tau \int_{-\infty}^{\infty} dm \int_{0}^{\infty} du\, g\left(m,u,r,\omega \mid \alpha(\tau,k)\right)\chi_G\left(\alpha(\tau,k),m,u,r,\omega\right) \qquad (12.24)\\
&= N_{trap}\int dk\, f(k)J(k) \int\limits_{\substack{\tau\in[0,n(B)]:\\ \alpha(t,k)\in[q_1,q_2]}} d\tau\; P_B\left(H>h \mid \alpha(t,k)\right)
\end{aligned}$$

which indeed is equal to (12.19).

As mentioned, the time integration in (12.23) can be rewritten as an integral over discharges. To that purpose we first define

$$\tilde{v}(q) = -\frac{\partial}{\partial q}\int_{q}^{\infty} dk\, f(k)J(k)L(q,k) \geq 0 \qquad (12.25)$$

where L(q,k) denotes the duration that level q is exceeded in the trapezium with peak value k; we note that this definition is analogous to the one for L(m,s) illustrated in Figure 8-8. Then according to Appendix B, (12.23) can be rewritten as

$$F_H\left(h;[q_1,q_2],[m_1,m_2],[u_1,u_2],r,\omega\right) = N_{trap}\int_{q_1}^{q_2} dq \int_{m_1}^{m_2} dm \int_{u_1}^{u_2} du\; \tilde{v}(q)g(m,u,r,\omega \mid q)\chi_G(q,m,u,r,\omega) \qquad (12.26)$$

The r.h.s. is an integration of $N_{trap}\tilde{v}(q)g(m,u,r,\omega|q)$ over the failure set in (q,m,u,r,ω)-space, which means that $N_{trap}\tilde{v}(q)g(m,u,r,\omega|q)$ looks like a kind of a *frequency density*. Unfortunately, it cannot be interpreted as an actual frequency density of the variables Q, M, U, R, Ω, since the expression depends on the level h, because $\tilde{v}(q)$ and the failure set G depend on h.

We still have to verify that our recipe to calculate the contributions does satisfy requirement (12.8). But this is immediate from (12.26), since on the r.h.s. of this formula an integral over discharges occurs.

12.2.5 Wind and/or storm surge dominant locations

It is instructive to look at a limiting situation of the formulas, in which the threatening situations are dominated by wind and/or storm surges. An example of such a location is Rotterdam: failure here can almost exclusively be the result of an extreme storm (surge) in combination with a relatively low discharge. As can be calculated by (12.26), the normative water level at this location is exceeded with at least 95% probability during wind speeds exceeding the once per year value (20.1 m/s). Physically, locations are dominated by wind and/or storm surges if the load level H is much more sensitive to changes in the wind speed and/or sea level then it is for changes in the discharge, as is the case for Rotterdam.

For the wind/surge dominant locations considered here, we can guess what the formula for $F_H(h)$ should be. Following the line of reasoning of section 8.1, we should expect that failure events for wind/surge dominant locations, with high probability have a duration of a single time

block of b = 12 hours (note that although section 8.1 was about lake levels and wind, the explanation can also be applied to the slow variable discharge and the fast variables sea level and wind). During such a short failure event the slowly varying discharge can be assumed constant in time, with a probability governed by the momentaneous density g(q). We now should expect, following the reasoning leading to (8.3) and since (all) failure events with high probability only last one block duration, that

$$F_H(h) = N \int_{q_{\min}}^{\infty} dq\, g(q) P\big(H > h \mid q\big) = N\, P(H > h) \tag{12.27}$$

where, if B is expressed in units of b, N = N_{trap}B is the number of time blocks in the winter half year.

The content of (12.27) is that the failure frequency for wind/surge dominant locations can be calculated by multiplying the failure probability in a single time block with the total number of time blocks in a winter half year. It will be shown that, making the proper approximations for the locations at hand, the general formula (12.26) for the contributions indeed will yield (12.27) .

First we will show that for the locations considered here, the quantity J(k) of (12.15) approximately equals 1. Consider to that purpose $G_B(H>h|k)$ in (12.5), in which the probability $P(H>h|\alpha(\tau,k))$ appears. The assumption of a wind/surge dominant location means that in failure events only relatively low values of k are involved: since always rather severe winds and/or surges are needed for failure, there "is not much probability left to be occupied by discharges". E.g., as can be calculated with (12.26), if the normative water level at Rotterdam is exceeded, then this happens with at least 90% probability for discharges below the once per year value (roughly 6000 m^3/s).

This means that for the relevant (rather small) values of k, and for all τ, the probability $P(H>h|\alpha(\tau,k))$ should be small: for if it would not be, the storm and/or surge leading to failure would not be severe. Using the approximations $\ln(1+x) \cong x$ and $1-\exp(-y) \cong y$, valid for x and y close to 0, (12.5) can be rewritten as

$$\begin{aligned} G_B(H > h \mid k) &= 1 - \exp\left\{ \int_0^{n(B)} d\tau\, \ln\Big(1 - P\big[H > h \mid \alpha(\tau,k)\big]\Big) \right\} \\ &\cong \int_0^{n(B)} d\tau\, P\big[H > h \mid \alpha(\tau,k)\big] \\ &= \bar{G}_B(H > h \mid k) \end{aligned} \tag{12.28}$$

where in the last step definition (12.14) was used. Now (12.15) shows

$$J(k) \cong 1, \qquad \text{for wind and/or storm surge dominant locations} \tag{12.29}$$

From (12.25), recalling that L(q,k) denotes the exceedance duration of level q within $\alpha(\tau,k)$, we now obtain from the analogue of (8.8) for discharges

$$\begin{aligned}\tilde{v}(q) &\cong -\frac{\partial}{\partial q}\int_{q}^{\infty} dk\, f(k)L(q,k) \\ &= -B\frac{\partial}{\partial q}P(Q>q) \\ &= B\,g(q)\end{aligned} \tag{12.30}$$

Substituting this in (12.26) and integrating/summing out all the variables q,m,u,r,ω, we obtain

$$\begin{aligned}F_H(h) &= \sum_{r=1}^{16}\sum_{\omega=0}^{1} F_H\left(h; q\in[q_{\min},\infty], m\in[-\infty,\infty], u\in[0,\infty], r,\omega\right) \\ &\cong N_{trap}\,B\sum_{r=1}^{16}\sum_{\omega=0}^{1}\int_{q_{\min}}^{\infty} dq \int_{-\infty}^{\infty} dm\int_{0}^{\infty} du\; g(q)g(m,u,r,\omega\,|\,q)\chi_G(q,m,u,r,\omega) \\ &= N\,P(H>h)\end{aligned} \tag{12.31}$$

So indeed for the type of locations considered here, we arrive at formula (12.27) which we anticipated.

Finally, an interesting question is how many locations are wind and/or surge dominant as considered here. Investigations have shown that in the tidal area there are many: roughly all locations to the west of Dordrecht satisfy this property, i.e. about half of the locations. For these locations the Hydra-Zoet results could also be calculated with (12.27) instead of (11.11), up to an accuracy of about 0.01 m.

Part 3: Lake delta

13 Introduction Vecht and IJssel delta

This preceding part of the report was about a *sea delta*. The current part, consisting of chapters 13 - 16, is about a *lake delta*, where a river discharges into a lake (recall if necessary the discussion in section 3.2). This lake delta in the following chapters will be the 'Vecht and IJssel delta', already briefly introduced in chapter 3.

The treatment of this water system will be analogous to that of the tidal rivers. Since many aspects of the formulas are alike, the treatment for the Vecht and IJssel delta will be more concise than the former for the tidal rivers. We will mainly focus on the differences for both water systems.

13.1 The area and the random variables used in the model

The area consists of Vecht dominant locations, for which statistical information of the Vecht is used, and of IJssel dominant ones, for which statistical information of the IJssel river is used. As for the tidal rivers, there are *axis* as well as *shore* locations. The Vecht dominant axis locations are shown in Figure 13-1 and the IJssel dominant ones in Figure 13-2.

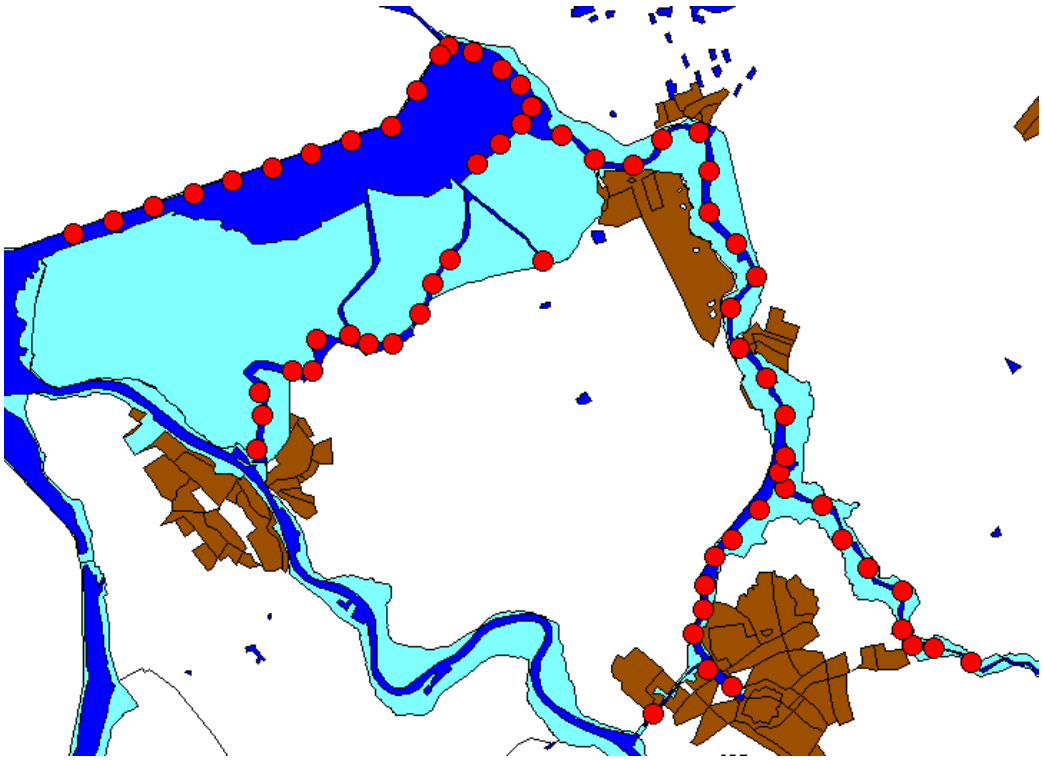

Figure 13-1 Vecht dominant axis locations (located at or in the neighbourhood of dike ring 10 in Figure 2-1).

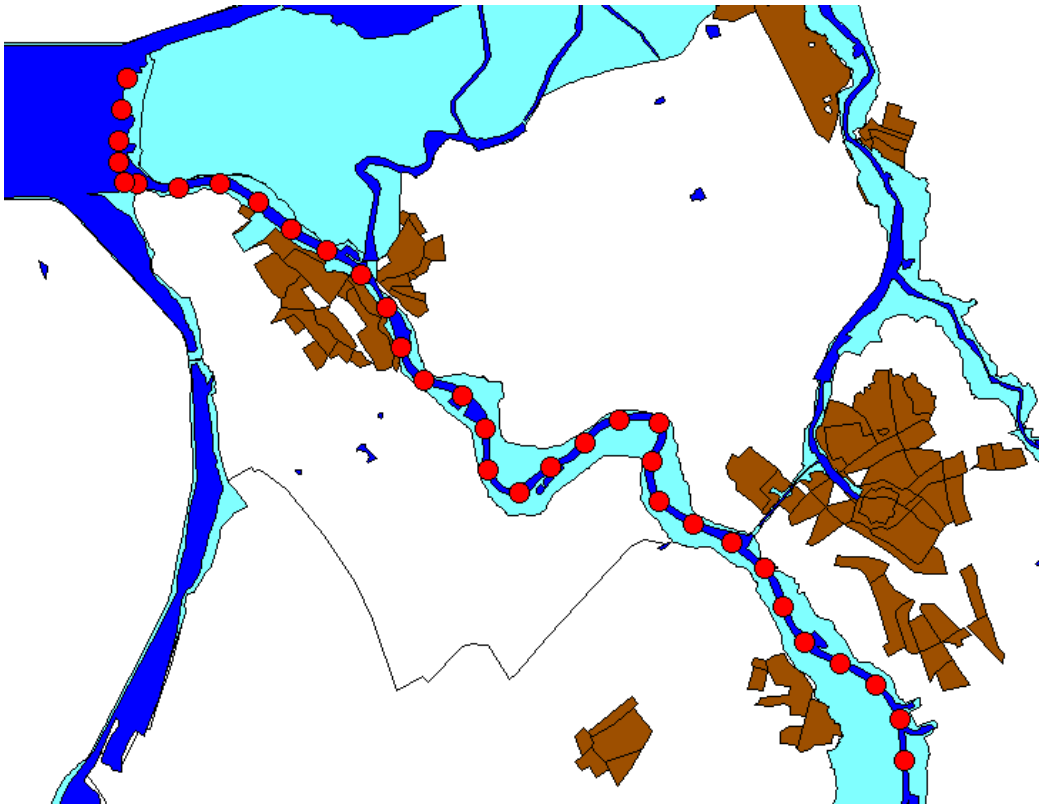

Figure 13-2 IJssel dominant axis locations.

The random variables in Hydra-Zoet for this area where already listed in section 3.1.3. For the convenience of the reader they are mentioned again, here with their appropriate symbol:

- lake level of Lake IJssel M,
- discharge Q (either Vecht or IJssel discharge),
- wind speed U,
- wind direction R,
- barrier state of the Ramspol storm surge barrier Ω.

The Ramspol Barrier is operated differently from the Maeslant Barrier located in the tidal rivers. Contrary to the situation for the tidal rivers, no predicted water levels are needed to operate the Ramspol Barrier: the latter barrier is operated using real time water level measurements directly in front of the barrier. Moreover, no (random) error is assumed in these measurements.

13.2 Schematic structure of the model

We now treat a diagram that is analogous to the one in Figure 9-3 for the tidal rivers. The new diagram (Figure 13-3) again concerns the calculation of the hydraulic load level for failure mechanism wave overtopping, for a shore location with wave variables obtained with the 1-dimensional Bretschneider formulas. Since the diagram is much alike the former, here the exposition will be very brief, focussing mainly on the differences between the current and the earlier version of the diagram.

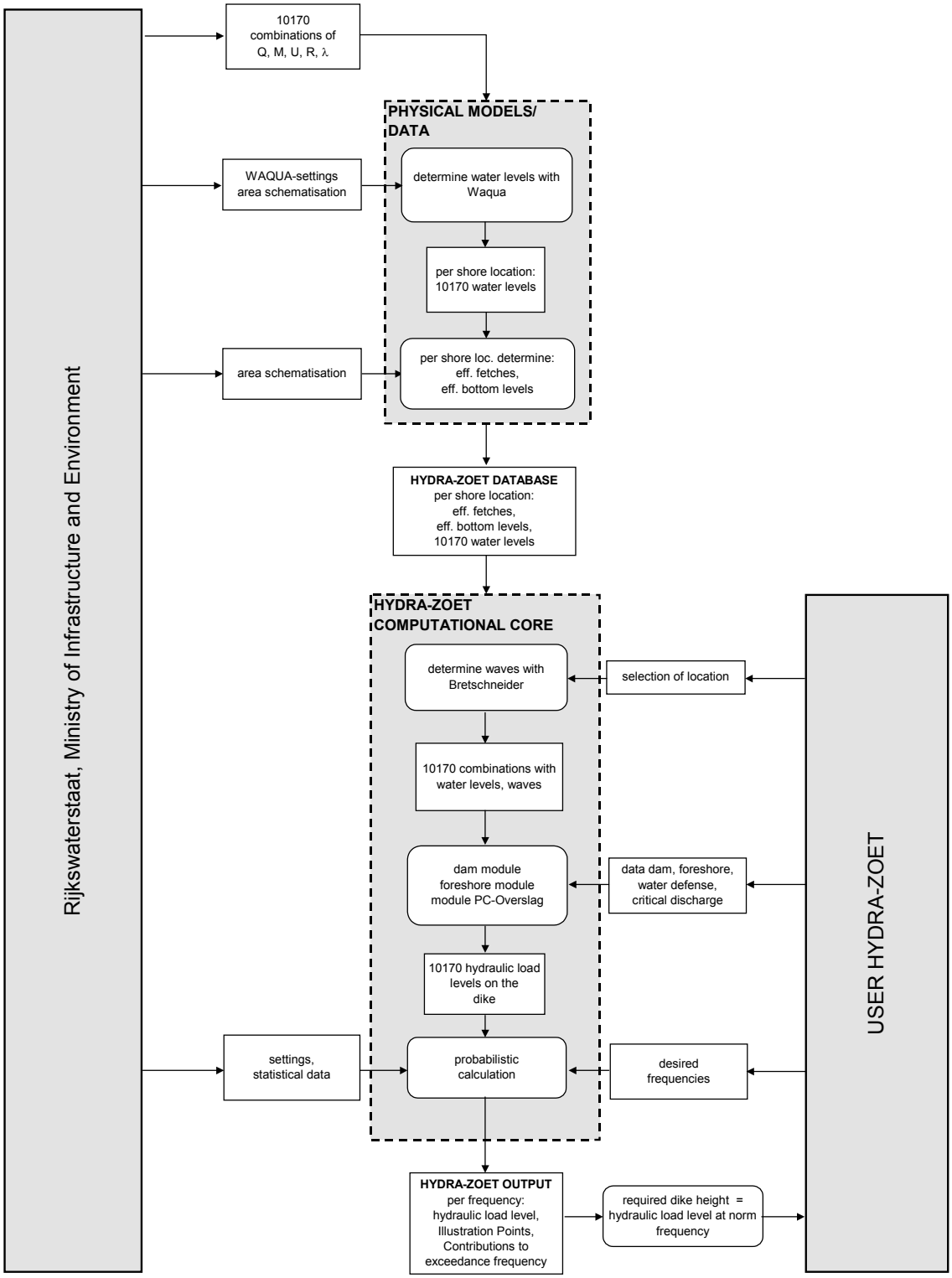

Figure 13-3 Diagram for a shore location in the Vecht and IJssel delta, for failure mechanism wave overtopping. We note that the barrier state here is denoted by λ instead of Ω, for reasons explained in section 14.1.4.

The block 'PHYSICAL MODELS/DATA' deals with water level calculations and location-specific data for fetches and bottom levels. For a total of 10170 combinations of boundary conditions, consisting of discharges Q, lake levels M, wind speeds U, wind directions R and barrier states Ω, water levels have been calculated with the 2-d (i.e. 2-dimensional) hydrodynamic model WAQUA, for a great number of locations throughout the area. We note that, contrary to the 1-d model SOBEK, the 2-d WAQUA model can calculate wind set-up from all directions (WAQUA has a 2-d schematisation without branches). So in WAQUA there is no need to account for wind set-up perpendicular to branches of the model, as was needed in the SOBEK model for the tidal rivers. WAQUA also properly represents the effect of the centrifugal force in river bends on water levels, which is not the case in Sobek.

The data for the shore locations are stored in a database (the block 'HYDRA-ZOET DATABASE'). Just as for the tidal rivers, because of the size of this database, it has been divided into a number of 'sub databases', per dike ring to be assessed delivered by the Ministry of Infrastructure and Environment to the users of Hydra-Zoet.

The block 'HYDRA-ZOET COMPUTATIONAL CORE' is the actual model Hydra-Zoet (the former data are only input for the model). Apart from the number of combinations of boundary conditions, its content is exactly the same as the corresponding block for the tidal rivers in Figure 9-3. So no comments are needed.

The content of the block 'HYDRA-ZOET OUTPUT' is completely the same as the corresponding one for the tidal rivers, and needs no comment.

14 Hydraulic load levels Vecht and IJssel delta

This chapter describes computations with physical models, needed as input for Hydra-Zoet. It is also described how these computations are used to obtain the hydraulic load level for every combination of boundary conditions that is considered. Only physical calculations are treated, while probabilities and frequencies are the subject of remaining chapters.

In the current chapter, from the diagram in Figure 13-3 the following parts are considered: the block 'PHYSICAL MODELS/DATA', the block 'HYDRA-ZOET DATABASE' and from the block 'HYDRA-ZOET COMPUTATIONAL CORE' the components until and including '10170 hydraulic load levels on the dike'.

14.1 Water level calculations with WAQUA

To build the Hydra-Zoet database, a large number of discharges, lake levels, wind speeds and wind directions have to be used as input for the 2-d hydrodynamic model WAQUA, both for a proper functioning storm surge barrier as well as for the open barrier state. The calculations are described in detail in [Beijk, 2006; Jansen et al, 2005]. Here we will only consider aspects that are important for a proper understanding of Hydra-Zoet. In particular we will not comment on the equations and computational schemes used in this model, or on the schematisation used. But for a proper understanding of Hydra-Zoet it is important to look in some detail on how the boundary conditions are imposed on the model.

Vecht- and IJssel discharges		Lake IJssel	wind speed	wind direction	barrier state
Vecht, m3/s	IJssel, m3/s	m+NAP	m/s	[-]	[-]
10	100	-0.4	0	SW	no failure
100	500	-0.1	10	WSW	failure
250	950	0.4	16	W	
400	1400	0.9	22	WNW	
550	1850	1.3	27	NW	
700	2300		32	NNW	
850	2750		37	N	
925	2975		42		
1000	3200				

Table 14-1 Combinations of boundary conditions used in WAQUA. Barrier state 'no failure' means a proper functioning barrier, while 'failure' means that the barrier remains open during a storm.

The combinations used as input for WAQUA are given in Table 14-1. For every combination, and for a great number of locations throughout the area, the result of a WAQUA calculation is a time series of water levels at every location. Of such a time series only the maximum water level of the sequence is used as input for the Hydra-Zoet database. We will comment on the content of the table in the subsequent sections.

As a side remark we note that in a 1-d model like SOBEK, used in the tidal rivers, the locations of the model are located on the SOBEK-branches, so that the water levels still had to be transformed to shore locations. Such a complication is not present in WAQUA, since this 2-d model contains the necessary information at every desired location in the area (the model uses

a grid of 25 by 25 m). Next to this, it is recalled that contrary to SOBEK, no perpendicular wind set-up needs to be added to the WAQUA results: every 'kind of wind set-up' is automatically included in the WAQUA results.

14.1.1 Vecht and IJssel discharge

For the tidal rivers, hydrodynamic calculations were made for Rhine dominant as well as for Meuse dominant locations, as explained in section 10.1.3. In principal, since for the Vecht and IJssel delta the locations also fall into two categories, either Vecht or IJssel dominant, we could use the same method again. This would mean that for a Vecht dominant location we should associate with every Vecht discharge the median value of all possible IJssel discharges that could occur for this Vecht discharge. For an IJssel dominant location, the other way round, we would use for every IJssel discharge considered, the median Vecht discharge. This would lead to two types of calculations, one set for Vecht dominant locations with median values of the IJssel, and one set for IJssel dominant locations with median values for the Vecht.

It turns out that the latter type of calculation is not needed. For IJssel dominant locations the influence of the Vecht discharge on the water levels can be neglected, because of two reasons:

- As can be seen in Figure 13-2, the Vecht can hardly influence the IJssel locations since the mouth of the Vecht is far downstream of the Ijssel's mouth in the lake area.
- The discharges of the Vecht are much lower than the ones from the IJssel (by about a factor 5).

It is of some importance, though, that for Vecht dominant locations a representative IJssel discharge is considered. Firstly, because the IJssel discharges are much higher than those from the Vecht, and secondly, because the dikes in the downstream part of the IJssel at the north side of the river are so low that they can be overtopped when high IJssel discharges occur; this concerns the dike stretch from IJsselmuiden to Ramspol, as shown in Figure 14-1. In the latter case, part of the IJssel discharge flows into a part of the Vecht delta, a polder called Kampereiland, which has been given a lower safety level than the rest of the Vecht delta: the polder Kampereiland may be flooded with frequency 1/500 per year from the IJssel, with the aim to 'relieve' the IJsseldelta, which has a higher safety level of 1/2000 per year.[25] This means that, to model the amount of flooding sufficiently accurate, for every Vecht discharge a proper IJssel discharge has to be chosen.

Table 14-1 shows which pairs of discharges are used as boundary conditions in WAQUA. As just explained, these pairs *provide the proper coupling of discharges of both rivers when applied to Vecht dominant locations*. For IJssel dominant locations these couplings are incorrect, but as explained the values of the Vecht discharges for these locations need not be sensible.

[25] When flooded from the Vecht delta, the area Kampereiland has been given an even lower safety level then 1/500 per year; in that case safety levels of 1/50 and 1/100 per year are used. This area is allowed to flood regularly. Houses are often build on artificial mounds.

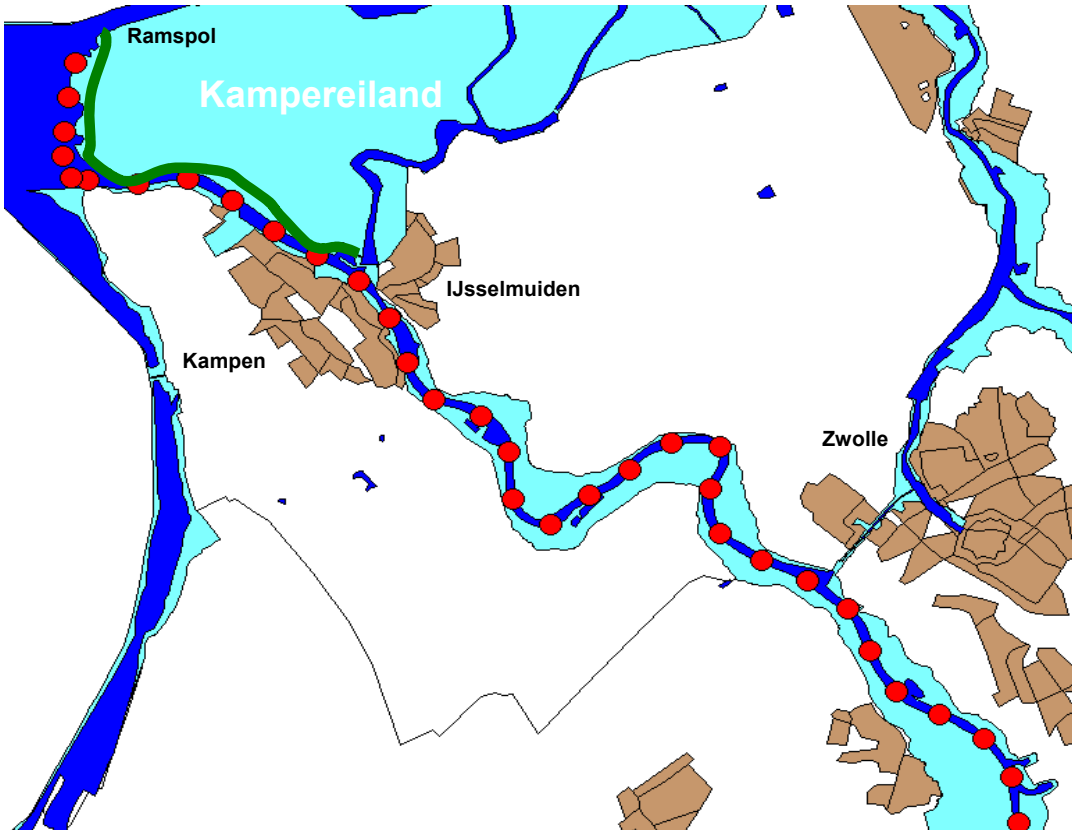

Figure 14-1 The IJssel delta, with the dike stretch IJsselmuiden – Ramspol (indicated in green) adjacent to the area Kampereiland.

In WAQUA the 9 discharges of the Vecht and the 6 lowest ones of the IJssel are imposed on the model as stationary values: they do not vary in time. This simplifying assumption of stationarity was made for the tidal rivers as well, for reasons explained in section 10.1.3. The 3 highest IJssel discharges, however, are imposed as standard discharge waves (hydrographs), which vary in time. As just mentioned, some dikes near the mouth of the IJssel are so low that they can be overtopped, causing an inflow from the IJssel into the polder Kampereiland belonging to the Vecht delta. Because of this, no stationary discharge can be imposed: that would lead to a permanent inflow into the polder Kampereiland, leading to non-realistic water levels in there. So proper discharge waves, whose details do not bother us here, are used in this situation, meaning that only flooding around the peak of the wave can occur. Note: the moment the wave reaches its maximum is chosen in such a way that the wind set-up, caused by the non-stationary wind field imposed, reaches its maximum at approximately the same time as does the discharge wave: so their maxima coincide in time (at least for the locations where the dike could be overtopped).

14.1.2 Lake level

In the WAQUA calculations, 5 lake levels m are used (Table 14-1); these are imposed on the model as stationary values. The assumption of stationarity can be motivated in the same way as provided for the discharges in section 10.1.3: lake levels vary so slow in time that the water level at a location is mainly determined by the level m considered, and hardly depends on the history in time of the lake level until the value m is reached.

14.1.3 Wind speed and direction

Only the directions SW, WSW,..., N are used in the WAQUA calculations (Table 14-1). For the other directions it is assumed that no threatening situations can occur in the area due to wind set-up. For the latter directions the results for wind speed 0 are used: the effect of negative wind set-up, yielding lower water levels than wind speed 0, is not taken into account, since these (non-threatening) situations are judged irrelevant for the safety against flooding. As an example of negative wind set-up, we mention that in 2010, due to a prolonged south-easterly wind, the water level at Kampen dropped with about 0.6 m. But evidently, such a situation is not relevant for safety against flooding (at least not for failure mechanisms overflow and wave overtopping).

Next to wind speed 0 m/s, 7 values of the wind speed are considered for the directions SW,..., N. These are potential wind speeds (see the explanation in section 5.3.3), for which statistical information is used of station Schiphol. Before they are imposed on WAQUA, these wind speeds are transformed to open water wind speeds using the transformation discussed in section 5.3.3, and at the same time are transformed from Schiphol to the area considered. The reason for the latter is that the statistical information for Schiphol is not completely representative for the Vecht and IJssel delta.

The wind speed is taken *spatially* homogeneous: at a given instant of time, everywhere in the area the same wind speed and wind direction occurs. The wind speed is *not* stationary with respect to time. A time pattern like the one in Figure 14-2 is used: a front flank of 23 hours, a peak duration of 2 hours, and a back flank of 23 hours. The only parameter characterising the pattern is the maximum wind speed. This pattern is based on statistical analyses reported in [Geerse, 2006], and is meant as an adequate description of the average time evolution *for the higher wind speeds within the storm*; the lower part of the pattern, say the lower half of it, needs not describe the wind speed during storms properly. We note that, since the wind set-up is mainly determined by the higher wind speeds during the storm, maximum water levels calculated by WAQUA hardly depend on the lower half of the wind pattern. The wind direction in every calculation is taken constant, both in space and time.

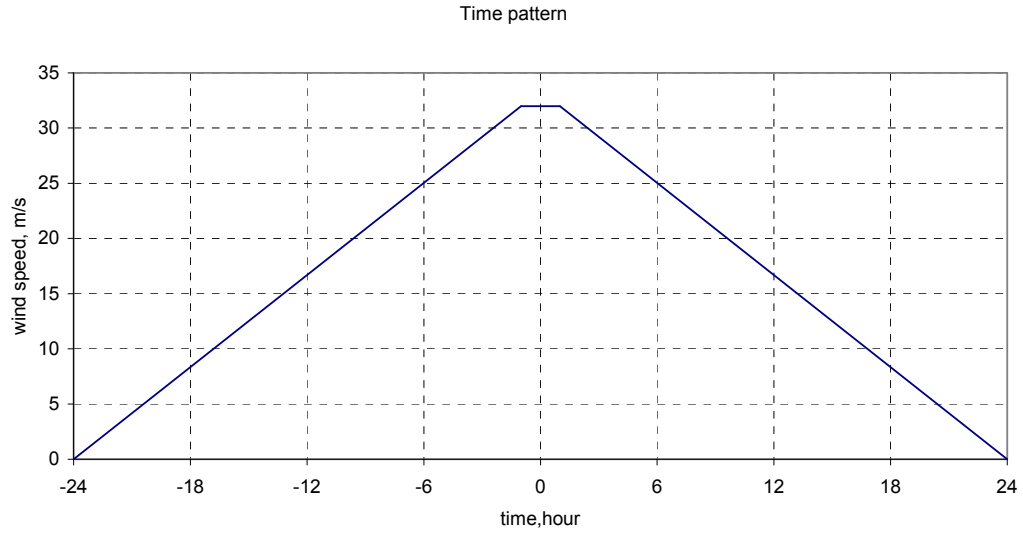

Figure 14-2 Pattern in time for the wind speed, with in this case 32 m/s as the maximum wind speed.

14.1.4 Ramspol storm surge barrier

The Ramspol Barrier is meant to shut off the Vecht delta from Lake IJssel during a westerly storm, to prevent a storm surge generated above Lake IJssel to flow into the area. During a storm the barrier will be closed if the local water level, measured in the vicinity of the barrier, exceeds 0.50 m+NAP and at the same time the direction of the flow is from west to east, i.e. water flowing from Lake IJssel into the Vecht delta. After it has been closed, the barrier opens again as soon as the water level at the eastern side of the barrier exceeds the water level at the western side. After opening, the water then flows from east to west, relieving the Vecht delta again.

In the WAQUA calculations two barrier states λ are considered:

- The state $\lambda = \lambda_{NF}$ denoting 'no failure'. This means that a properly functioning barrier is built in in WAQUA, which closes when it should.
- The state $\lambda = \lambda_{F}$ denoting 'failure'. This means that the barrier in WAQUA never closes, and hence remains open during a storm.

It is important to make a distinction between the symbol λ, used to label the type of WAQUA calculation, and the symbol ω used to characterise the open or closed barrier state in the probabilistic model. There is not a one to one relation between λ and ω: the state $\lambda = \lambda_{F}$ certainly means an open barrier, but $\lambda = \lambda_{NF}$ does not necessarily mean a closed barrier. In the latter situation the barrier will only be closed during a storm if the criteria for closure are met, but otherwise remains open. Note in particular that the water levels calculated by WAQUA for both states λ will be exactly the same if for a boundary condition the closure criteria are *not* met: the water levels then correspond to the open barrier state.

Note that for the tidal rivers there was no need, for the Maeslant Barrier, to make a distinction between barrier states in the hydrodynamic model (i.e. SOBEK) and the ones in the probabilistic model. The reason for this is that if the closure operation is considered in SOBEK, the Maeslant Barrier *always* closes.

14.1.5 Number of calculations and treatment of easterly directions

In Table 14-1 the boundary conditions are listed for which WAQUA calculations are made. We will comment on the number of calculations, but first need to comment on the way the easterly directions NNE,..., SSW are treated.

As mentioned in section 14.1.3, for these directions water levels corresponding to wind speed 0 m/s are taken, which results then are stored in the Hydra-Zoet database (compare the diagram in Figure 13-3). More precisely, this means the following. For every location water levels have to be stored in the database for wind speed 0 m/s and for the 7 positive wind speeds 10, 16, 22, 27, 32, 37, 42 m/s (compare Table 14-1). For every positive wind speed in combination with an easterly direction, then, the water levels corresponding to the calculation with wind speed 0 m/s are taken. Stated otherwise: for the easterly directions the water levels corresponding to wind speed 0 m/s are duplicated to the other wind speeds.

Concerning the number of calculations we now have:

- Directions SW,.., N:

  - 9 discharges, 5 lake levels, 7 positive wind speeds, 7 directions, 2 barrier states, leading to 9*5*7*7*2 = 4410 calculations,
  - for wind speed 0 m/s: 9 discharges, 5 lake levels, 2 barrier states, leading to 9*5*2 = 90 calculations.
- Directions NNE,..., SSW:
  - Wind speed 0 m/s is duplicated to every one of the 7 positive wind speeds, where the 7 wind speeds are combined with 9 discharges, 5 lake levels, 9 directions, 2 barrier states, leading to 7*9*5*9*2 = 5670 calculations. Note that the latter results are denoted as calculations, although they are simply duplicated from already available results.

The total number of calculations becomes 4410+90+5670 = 10170. The latter number occurs in the diagram in Figure 13-3.

14.2 Wind waves

The wave variables significant wave height H_s, wave period T_p and wave direction θ are determined in every one of the 10170 combinations of boundary conditions as explained in section 5.3, by 1-d wave growth formulas like the one from Bretschneider or by a 2-d model like SWAN. If wave growth formulas are used, effective fetches and bottom levels are needed. If a 2-d model is used, they are not, since the schematisation in SWAN contains detailed geometrical information.

For clarity, we note that although water levels for the easterly directions are duplicated, wave variables are not. They have to be calculated for every one of the 10170 combinations of boundary conditions that occur in the database.

14.3 Hydraulic load levels

Using WAQUA and a wave model, in every one of the 10170 combinations the local water level and the wave variables have become available, for the axis as well as the shore locations. Now in every combination the hydraulic load H can be calculated. For axis locations (not located at a dike toe) this can only be done for the failure mechanism overflow, whereas for shore locations this can be done for mechanisms overflow and wave overtopping. For the shore locations, if a dam and/or foreshore are present in front of the dike, the waves for open water still have to be transformed using the dam and/or foreshore module. The details of this calculation are explained in section 5.5.

For clarity, we express the load level H as a function of the variables that are relevant for the probabilistic formulas in later chapters. H is a function of the discharge q, sea level m, wind speed u, wind direction r and operational barrier state λ built in in WAQUA, i.e. H=H(q,m,u,r,λ). Denote the local (maximum) water level by h_{wl}. Then for failure mechanism overflow, we have

$$H(q,m,u,r,\lambda) = h_{wl}(q,m,u,r,\lambda) \tag{14.1}$$

For mechanism wave overtopping we need the wave overtopping height $h_{overtop}$, with unit metres, which was defined in section 5.5, corresponding to a specified critical overtopping discharge. For this mechanism we have

$$H(q,m,u,r,\lambda) = h_{wl}(q,m,u,r,\lambda) + h_{overtop}(q,m,u,r,\lambda) \quad (14.2)$$

The load level H is not only needed in Hydra-Zoet for the 10170 combinations of Table 14-1, but for arbitrary combinations (q,m,u,r,λ) as well. To obtain the load level for these combinations, linear interpolation is used between the results available for the 10170 combinations.

15 Probabilistic formulas Vecht and IJssel delta

This chapter treats the basic probabilistic formulas of Hydra-Zoet for the Vecht and IJssel delta. Just as for the tidal rivers, locations are assumed to be dominated by a single river, in this case the Vecht or the IJssel. In the calculations for a single location, only the statistical information of the dominating river is used. For this reason, we can limit ourselves to the consideration of a single river, which below will be the Vecht.

In section 15.1 the statistical information is listed that is needed in Hydra-Zoet for the Vecht dominated locations. Section 15.2 deals with the exceedance probability of the load for the shortest time scale in the model (b = 12 hours). The results of this section are used in section 15.3 to obtain the failure frequency $F_H(h)$, given in times per year. Section 15.4 concludes with some remarks concerning dike rings instead of single locations.

As a short historical note, we mention that the Hydraulic Boundary Conditions 2006 (HBC2006) for the Vecht delta were determined with Hydra-VIJ, the predecessor of Hydra-Zoet for this area. The determination of the HBC2006 was described in [Beijk, 2007]; this reference also provides a "non-official" variant of the HBC2006 for the IJssel delta. It is noted here that the model Hydra-VIJ completely coincides with Hydra-Zoet if the latter model is restricted to the area Vecht and IJssel delta.

15.1 Statistical information

The slow random variables, i.e. the river discharge of the Vecht and the lake level of Lake IJssel, are schematised in time using trapezia, together with a phase shift, as was explained in section 8.2 and, for the convenience of the reader, again illustrated in Figure 15-1. We will now list the statistical information needed in Hydra-Zoet, concerning, next to the slow variables, the information for the wind.

1. Lake IJssel
   1.1. Trapezium parameters: base duration B, minimum lake level m_{min}, peak duration b(s).
   1.2. Exceedance probability P(S>s), from which f(s) follows by differentiation.

2. Vecht discharge
   2.1. Trapezium parameters: base duration B, minimum discharge q_{min}, peak duration b(k).
   2.2. Exceedance probability P(K>k), from which f(k) follows by differentiation.

3. Correlations between Vecht and Lake IJssel
   3.1. Value for the phase φ between the discharge and the lake level trapezia.
   3.2. Value for the standard deviation σ in the (transformed) model CS used for the bivariate density f(k,s), which has marginals f(k) and f(s). Recall that the model CS was treated in section 7.2.

4. Wind
   4.1. Exceedance probabilities P(U>u|r) for the 12-hourly maximum wind speed U, given wind direction R = r (where r = NNE, NE,..., N).
   4.2. Probabilities g(r) for the wind directions r.

Here are some comments on this list. How to obtain the variables for Lake IJssel was described earlier in the text: from section 8.3 it follows B = 30 days, m_{min} = -0.40 m+NAP, with b(s) given in Figure 8-9, whereas P(S>s) and f(s) are obtained from (8.4), (8.6) and (8.7).

The variables for the Vecht are obtained in a similar way, and will not be discussed here, apart from the remark that again B = 30 days is considered.

A proper value for the phase shift between the discharge and the lake level trapezia is φ = 3.5 days, as was investigated in [Geerse, 2006]. Here we use the convention that a *positive* value of φ means that the lake level is 'delayed' by φ days, compared to the discharge, as indicated in Figure 15-1. S0 the choice φ = 3.5 days, means that the centre of the lake level occurs 3.5 days later then the centre of the discharge trapezium. In [Geerse, 2006] also a value for the standard deviation for the model CS was derived, which is σ = 1.2 (dimensionless quantity in the transformed space).

The information for the wind is given in [Geerse, 2006] and will not be discussed here. We only note that if g(r) and P(U>u|r) are available, the probability density g(u,r), which is needed in the following sections, simply follows as g(u,r) = –g(r)dP(U>u|r)/du.

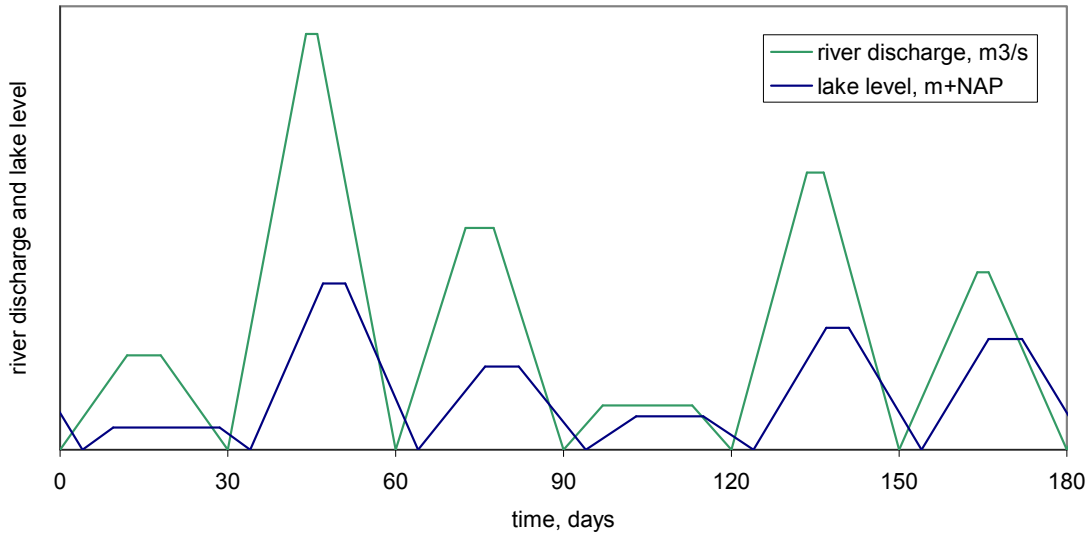

Figure 15-1 Discharges and lake level trapezia with a phase shift.

The following correlation structure is assumed in the model:

- The discharge and the lake level are correlated (this is done by correlating peak values of the trapezia and using a time shift between trapezia, as described in point 3 above).
- The wind speed and wind direction are correlated.
- No correlation is assumed between wind and discharge and between wind and lake level.

15.2 Probability for the shortest time scale

15.2.1 Structure of the probability density for the shortest time scale

For the shortest time period b = 12 hours, a probability density is used in Hydra-Zoet that is of the following structure:

$$g(q,m,u,r,\omega) = g(\omega \mid q,m,u,r)g(q,m)g(u,r) \tag{15.1}$$

where it is recalled that q,m,u,r,ω respectively denote the discharge (of the Vecht), lake level, wind speed, wind direction and barrier state. Here g(q,m) is the momentaneous bivariate probability density of the discharge and lake level, g(u,r) the bivariate probability density of the wind speed and direction, while g(ω|q,m,u,r) is the probability on the barrier state ω, given q,m,u,r. Note that the form of (15.1) is a consequence of the assumed correlation structure just mentioned.

In section 15.1 it is mentioned how g(u,r) is obtained. The functions g(q,m) and g(ω|q,m,u,r) will be treated in the next sections.

15.2.2 The bivariate momentaneous probability density of discharge and lake level

In the derivation of g(q,m), the probability density f(k,s) of the peak values k and s of the discharge and lake level trapezia are needed, together with the parameterisation of the trapezia. The density g(q,m) can be calculated, using trapezia in a single base duration B, as now described.

First, assume discharge and a lake level trapezia with peak values k and s are given, as indicated in Figure 15-2. Denote by L(q,k,m,s) the duration such that at the same time level q is exceeded in the discharge trapezium and level m in the lake level trapezium. This duration need not consist of just one interval of consecutive hours, but may consist of more than one interval. L(q,k,m,s) has the same unit as B, i.e. either hours or days. It is not hard to verify that the momentaneous probability of exceeding q as well as m is given by

$$P(Q > q, M > m) = \frac{1}{B}\int_q^\infty dk \left(\int_m^\infty ds\, f(k,s)L(q,k,m,s) \right) \tag{15.2}$$

Using partial differentiation with respect to (-q) and (-m), it follows

$$g(q,m) = \frac{\partial^2 P(Q > q, M > m)}{\partial q \partial m} \tag{15.3}$$

which is the desired formula for g(q,m).

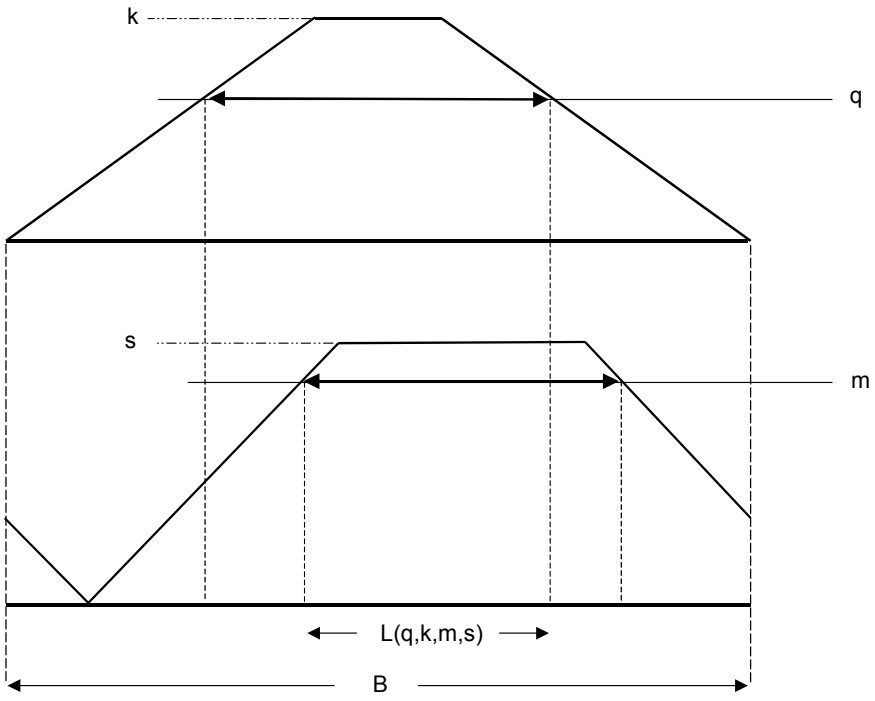

Figure 15-2 Illustration of the duration L(q,k,m,s).

15.2.3 Probabilities for the barrier states

We will treat the calculation of g(ω|q,m,u,r), where here q,m,u,r are the values, within duration b, of respectively the discharge, the lake level, the (maximum) wind speed, and the wind direction (the latter equals the vectorially averaged direction over the hourly values within period b). For this calculation we need a criterion variable C, which equals 1 if during a storm the closure criteria are met (see section 14.1.4) and 0 of the barrier remains open:

$$C(q,m,u,r)=\begin{cases}0 & \text{if } (q,m,u,r) \text{ is such that the closure criteria are not met}\\ 1 & \text{if } (q,m,u,r) \text{ is such that the closure criteria are met}\end{cases} \tag{15.4}$$

For ω we will use the notation

$$\omega=\begin{cases}0 & \text{if the barrier is open during the entire storm}\\ 1 & \text{if the barrier closes during the storm}\end{cases} \tag{15.5}$$

The probability α of failure for closing the barrier is included in Hydra-Zoet. It is equal to α = 0.0035 = 1/286 per closure request, i.e. if the barrier needs to close, it fails on average 1 out of 286 times. The definitions (15.4) and (15.5) then imply

$$g(\omega\,|\,q,m,u,r)=\begin{cases}\alpha & \text{for } \omega=0 \text{ and } C(q,m,u,r)=1\\ 1 & \text{for } \omega=0 \text{ and } C(q,m,u,r)=0\\ 1-\alpha & \text{for } \omega=1 \text{ and } C(q,m,u,r)=1\\ 0 & \text{for } \omega=1 \text{ and } C(q,m,u,r)=0\end{cases} \tag{15.6}$$

15.2.4 Exceedance probability of the load

In the remainder of this report, often the probability P(H>h|q,m) is needed, denoting the probability that the load exceeds level h during duration b, given a discharge q and lake level m within this duration. In this calculation we need g(u,r,ω|q,m), which according to (15.1) is given by

$$g(u,r,\omega \mid q,m) = \frac{g(\omega \mid q,m,u,r)g(q,m,u,r)}{g(q,m)} = g(\omega \mid q,m,u,r)g(u,r) \tag{15.7}$$

In the calculation of P(H>h|q,m) we need to be careful about the distinction between ω and λ, discussed in section 14.1.4, where ω stand for the "actual state" of the barrier, and λ labels the type of operation of the barrier in the WAQUA calculations. Recall that $\lambda = \lambda_{NF}$ denotes a properly functioning barrier in WAQUA, whereas $\lambda = \lambda_F$ denotes an always open barrier in WAQUA. Note that if the closure criteria are not met, i.e. C(q,m,u,r) = 0, the following property holds:

$$H(q,m,u,r,\lambda_{NF}) = H(q,m,u,r,\lambda_F), \qquad \text{if } C(q,m,u,r) = 0 \tag{15.8}$$

since in this case in the WAQUA calculation the barrier remains open.

We now turn to the calculation of P(H>h|q,m). From (15.7) and (15.6) it follows

$$\begin{aligned}
P(H>h \mid q,m) &= \sum_{r=1}^{16}\sum_{\omega=0}^{1}\int_{u\geq 0} du\, P(H>h \mid q,m,u,r,\omega)g(u,r,\omega \mid q,m) \\
&= \sum_{r=1}^{16}\sum_{\omega=0}^{1}\int_{u\geq 0:C(q,m,u,r)=1} du\, P(H>h \mid q,m,u,r,\omega)g(\omega \mid q,m,u,r)g(u,r) \\
&\quad + \sum_{r=1}^{16}\sum_{\omega=0}^{1}\int_{u\geq 0:C(q,m,u,r)=0} du\, P(H>h \mid q,m,u,r,\omega)g(\omega \mid q,m,u,r)g(u,r) \\
&= \alpha\sum_{r=1}^{16}\int_{u\geq 0:C(q,m,u,r)=1} du\, P(H>h \mid q,m,u,r,\omega=0)g(u,r) \\
&\quad + (1-\alpha)\sum_{r=1}^{16}\int_{u\geq 0:C(q,m,u,r)=1} du\, P(H>h \mid q,m,u,r,\omega=1)g(u,r) \\
&\quad + \sum_{r=1}^{16}\int_{u\geq 0:C(q,m,u,r)=0} du\, P(H>h \mid q,m,u,r,\omega=0)g(u,r)
\end{aligned} \tag{15.9}$$

Consider P(H>h|q,m,u,r,ω=0). The conditioning on $\omega = 0$, i.e. the always open state, means that H is derived using WAQUA calculations with $\lambda = \lambda_F$, as also expressed by (15.15). So the load level is of the form $H = H(q,m,u,r,\lambda_F)$. Then, given the condition (q,m,u,r,ω=0), there are only two possibilities: either $H(q,m,u,r,\lambda_F) > h$ or $H(q,m,u,r,\lambda_F) \leq h$. This means that P(H>h|q,m,u,r,ω=0) is an indicator function:

$$P(H>h \mid q,m,u,r,\omega=0) = \begin{cases} 1 & \text{if } H(q,m,u,r,\lambda_F) > h \\ 0 & \text{if } H(q,m,u,r,\lambda_F) \leq h \end{cases} \tag{15.10}$$

A similar reasoning shows:

$$P(H>h \mid q,m,u,r,\omega=1) = \begin{cases} 1 & \text{if } H(q,m,u,r,\lambda_{NF}) > h \\ 0 & \text{if } H(q,m,u,r,\lambda_{NF}) \leq h \end{cases} \tag{15.11}$$

Using this results, formula (15.9) can be rewritten as,

$$\begin{aligned} P(H>h\,|\,q,m) = \alpha \sum_{r=1}^{16} \int_{u\geq 0: C(q,m,u,r)=1;\, H(q,m,u,r,\lambda_F)>h} du\, g(u,r) \\ + (1-\alpha) \sum_{r=1}^{16} \int_{u\geq 0: C(q,m,u,r)=1;\, H(q,m,u,r,\lambda_{NF})>h} du\, g(u,r) \\ + \sum_{r=1}^{16} \int_{u\geq 0: C(q,m,u,r)=0;\, H(q,m,u,r,\lambda_F)>h} du\, g(u,r) \end{aligned} \tag{15.12}$$

With the aid of (15.8), the last term on the r.h.s. can be rewritten as

$$\begin{aligned} &\sum_{r=1}^{16} \int_{u\geq 0: C(q,m,u,r)=0;\, H(q,m,u,r,\lambda_F)>h} du\, g(u,r) \\ &= \alpha \sum_{r=1}^{16} \int_{u\geq 0: C(q,m,u,r)=0;\, H(q,m,u,r,\lambda_F)>h} du\, g(u,r) + (1-\alpha) \sum_{r=1}^{16} \int_{u\geq 0: C(q,m,u,r)=0;\, H(q,m,u,r,\lambda_{NF})>h} du\, g(u,r) \end{aligned} \tag{15.13}$$

Combining this with (15.12), we obtain:

$$P(H>h\,|\,q,m) = \alpha \sum_{r=1}^{16} \int_{u\geq 0: H(q,m,u,r,\lambda_F)>h} du\, g(u,r) + (1-\alpha) \sum_{r=1}^{16} \int_{u\geq 0: H(q,m,u,r,\lambda_{NF})>h} du\, g(u,r) \tag{15.14}$$

It appears that the final formula to calculate P(H>h|q,m) has a rather simple structure. Apart from the factor α, the first term on the r.h.s. equals the probability that H exceeds h when H is obtained from WAQUA results for the open barrier; the second term on the r.h.s. equals, apart from the factor 1-α, the probability that H exceeds h when H is obtained from WAQUA results for the properly functioning barrier. Apparently, both probabilities have to be weighed by the probability α of failure to close the barrier. This result might seem plausible, but is in fact a bit odd: the integral in the first term on the r.h.s., which term obtains weight α, contains also wind speeds and directions for which the barrier need not close at all. So why should this weight α include such situations? The reason for the simple form (15.14) is the use of (15.8), which enables us to simplify the calculation of (15.12). Note that in the final formula (15.14) we need no longer know for which q,m,u,r we have C = 0 or C = 1, whereas this information is needed in (15.12).

Sometimes we want to treat H(q,m,u,r,λ) introduced in section 14.3 as a function of ω instead of λ, as will be useful in chapter 16 and Appendix B. Note that for ω=0 the loads are calculated using H(q,m,u,r,λ=λ_F), and for ω=1 using H(q,m,u,r,λ=λ_{NF}). So if we define $\lambda(\omega)$ as

$$\lambda(\omega) = \begin{cases} \lambda_F & \text{if } \omega = 0 \quad \text{(barrier needs not to close or fails)} \\ \lambda_{NF} & \text{if } \omega = 1 \quad \text{(barrier closes)} \end{cases} \tag{15.15}$$

the load H(q,m,u,r,$\lambda(\omega)$) becomes, next to q,m,u,r, a function of ω instead of λ.

15.3 Exceedance frequency for the load level

We now turn to the calculation of the exceedance frequency $F_H(h)$ of load level h. This calculation is similar to the one for the Vecht and IJssel delta treated in section 11.3, the main

difference being that instead of a single slow random variable, we now have to consider two slow random variables. Anyway, we provide the details.

Recall that exceedances in the summer half year are neglected, and that the winter half year is 'filled' with N_{trap} = 6 trapezia of base duration B = 30 days. The quantity $P_B(H>h)$ denotes the probability that in a base duration B failure occurs at least once, where here failure means exceedance by H of level h. Then we have

$$F_H(h) = N_{trap} P_B(H > h) \tag{15.16}$$

We introduce the quantity $P_B(H>h|k,s)$, which denotes the failure probability within the base duration B, conditional on the peak values k and s of the discharge and lake level trapezia. Then $P_B(H>h)$ can be calculated by integrating over the peak values k and s w.r.t. the bivariate probability density f(k,s):

$$P_B(H > h) = \int dk\, ds\, f(k,s)\, P_B(H > h \mid k,s) \tag{15.17}$$

where the integration extends over all possible values of k and s (in this case k>0 m^3/s and s > -0.40 m+NAP).

We now turn to the calculation of $P_B(H>h|k,s)$. To calculate this quantity, the base duration B is discretised in time intervals of b = 12 hours, yielding n(B) = 60 consecutive 'time blocks'. Denote the average discharge and average lake level in the j-th block respectively by q(j|k) and m(j|s), as illustrated in Figure 15-3. Now it is *assumed* that the wind in consecutive time blocks is statistically independent, in which case we obtain

$$\begin{aligned} P_B(H > h \mid k,s) &= 1 - \text{probability that } H < h \text{ in every 12 hour period} \\ &= 1 - \prod_{j=1}^{n(B)} \left(1 - P\left[H > h \mid q(j \mid k), m(j \mid s)\right]\right) \end{aligned} \tag{15.18}$$

where the probabilities P[H>h|q(j|k),m(j|s)] are calculated using (15.14). This concludes the calculation of (15.16).

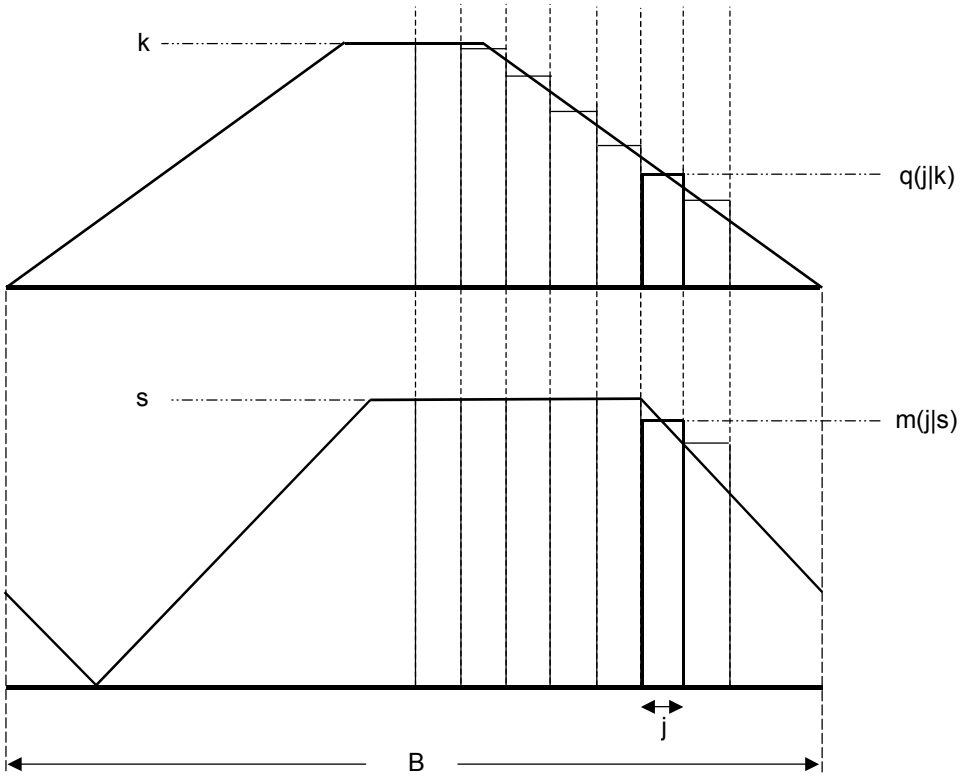

Figure 15-3 Discretisation of duration B in blocks of b = 12 hours, for the discharge and lake level trapezia.

15.4 Treatment of dike rings

In the preceding calculations dike *sections* were considered. We now consider the case of dike *rings*, whose treatment is very similar to the case for the tidal rivers (see section 11.4). Because of this similarity, it is not needed to provide the formulas again. We only note, because of the distinction between the actual barrier state ω and the operating state λ in WAQUA, which distinction was absent for the tidal area, that in formula (11.14) and (11.15) the symbol ω has to be replaced by λ. Apart from this, the ring formulas for the Vecht and IJsseldelta are completely analogous to the ones for the tidal area.

Recall also that the calculation for a ring is only permitted if all the locations along the ring are dominated by the same river, in this case either the Vecht or the IJssel. If a ring contains locations dominated by the Vecht and also ones dominated by the IJssel, only an approximate calculation can be made, as explained in section 11.4.2.

16 Additional output Vecht and IJssel delta

In chapter 4 examples were given for illustration points (IP's) and contributions to the exceedance frequency. For the tidal rivers, the formulas to calculate these contributions, are given in chapter 12. The current chapter provides the analogous formulas for the Vecht and IJsseldelta. Since these formulas are very similar to the ones for the tidal rivers, the treatment will be brief, referring, if necessary, to Appendix B for proofs.

16.1 Illustration points

We recall that the IP's, corresponding to the exceedance frequency $F_H(h)$, provide the most probable circumstances during failure, where failure means "attaining the load level h". We recall, as explained in section 12.1.2, that due to differences in time scales, $F_H(h)$ cannot be calculated by integrating a given probability density over the failure region. Therefore a pragmatic choice has been made for the probability density to use in the calculation of the IP's: for the tidal rivers the momentaneous probability density related to the shortest time scale b = 12 hours was made. For the Vecht and IJssel delta the same approach is chosen, which means that $g(q,m,u,r,\omega)$ described in section 15.2.1 will be used to calculate IP's.

Next we recall that this probability density can be used directly, or that a transformed version can be used, obtained from the Rosenblatt-transformation. The formulas for the calculation of both kinds of IP's are almost identical to the ones given in section 12.1.3 for the untransformed version and section 12.1.4 for the transformed versions. Those formulas will not be repeated. We have to mention, though, that where in the former sections the failure surface is given by the points (q,m,u,r,ω) for which $H(q,m,u,r,\omega) = h$, the failure surface for the Vecht and IJssel delta has to be calculated using the equation $H(q,m,u,r,\lambda(\omega)) = h$, where $\lambda(\omega)$ is given by formula (15.15).

16.2 Contributions to the exceedance frequency

For the tidal rivers the contributions to the exceedance frequency were considered in section 12.2. Recall that these contributions provided the probabilities with which outcomes q,m,u,r,ω occur during failure events. In the following the formulas to calculate these contributions are given for the Vecht and IJsseldelta. The ideas behind the recipe for the calculation of these contributions were explained in section 12.2. Here we will be brief, and provide only the basic formulas. If necessary, we will refer to Appendix B for the proofs of the statements.

16.2.1 Continuous version probabilistic formulas

The calculational recipe for the contributions is based on the continuous version of the probabilistic formulas underlying the calculation of $F_H(h)$. These continuous versions were also given for the tidal rivers, in section 12.2.2. The derivation of the analogous formulas for the Vecht and IJssel delta is similar. So additional proofs will not be given, but only the results.

First the quantity $P_B(H>h|k,s)$ of (15.18) is considered. Its continuous version is denoted by $G_B(H>h|k,s)$. In the same way (12.5) was derived, we obtain

$$G_B(H > h \mid k,s) = 1 - \exp\left\{ \int_0^{n(B)} d\tau \, \ln\left(1 - P\left[H > h \mid \alpha(\tau,k), \beta(\tau,s)\right]\right)\right\} \tag{16.1}$$

with

$$G_B(H > h \mid k,s) \cong P_B(H > h \mid k,s) \tag{16.2}$$

We recall that τ in (16.1) is the time, measured in units of b, that n(B) = B/b denotes the number of time blocks within the base duration, and that $\alpha(\tau,k)$ denotes the discharge at time τ in the discharge trapezium with peak value k. Analogously, $\beta(\tau,s)$ denotes the lake level at time τ in the lake level trapezium with peak value s.

As the respective analogues of (15.17) and (15.16) we then write

$$G_B(H > h) = \int dk\, ds\, f(k,s)\, G_B(H > h \mid k,s) \tag{16.3}$$

and

$$F_H(h) = N_{trap}\, G_B(H > h) \tag{16.4}$$

The formulas (16.1), (16.3) and (16.4) constitute the continuous versions of the probabilistic formulas for the Vecht and IJsseldelta in Hydra-Zoet.

16.2.2 Contributions to the exceedance frequency

For the tidal river area we considered two (mathematically equivalent) formulas for the calculational recipe for the contributions. The first formula (12.23) contained an integral over the time τ, whereas in the second formula (12.26) this integral was replaced by one over the discharge, which is the slow variable in the model for the tidal rivers. For the Vecht and IJssel delta an analogous formula with an integration over τ can be established. This formula can be rewritten, as was the case for the tidal rivers, into an equivalent formula where the τ-integration is replaced by an integration over the slow variables discharge and lake level. In what follows, only the latter formula is given. The formula with the τ-integration is given in Appendix B, together with the proof that this formula is equivalent with the alternative one below in (16.10).

In order to formulate the formula for the contributions, with an integration over q and m instead of τ, some definitions are needed. First we define, as the analogues of (12.14) and (12.15) for the tidal rivers, the quantities

$$\overline{G}_B(H > h \mid k,s) = \int_0^{n(B)} d\tau \, P\left(H > h \mid \alpha(\tau,k), \beta(\tau,s)\right) \tag{16.5}$$

and

$$J(k,s) = \frac{G_B(H > h \mid k,s)}{\overline{G}_B(H > h \mid k,s)} \tag{16.6}$$

We also need the quantity

$$\tilde{v}(q,m) = \frac{\partial^2}{\partial q \partial m} \int_q^\infty dk \int_m^\infty ds\, f(k,s) J(k,s) L(q,k,m,s) \geq 0 \tag{16.7}$$

where it is recalled that the duration L(q,k,m,s) was defined in section 15.2.2. We note, however, that in this context, just as τ is expressed in units of b, L(q,k,m,s) should be expressed in units of b. The failure region is given by

$$G = \left\{ (q,m,u,r,\omega) \mid H\left(q,m,u,r,\lambda(\omega)\right) \geq h \right\} \tag{16.8}$$

and its characteristic function by $\chi_G(q,m,u,r,\omega)$. This function equals 1 if (q,m,u,r,ω) belongs to G and is 0 otherwise.

We are now ready to give the general formula for the contributions. Denote the contributions by

$$\begin{aligned} &F_H(h;[q_1,q_2],[m_1,m_2],[u_1,u_2],r,\omega) \\ &\quad = \text{simultaneous contributions to the exceedance frequency of discharges in } [q_1,q_2], \\ &\qquad \text{lake levels in } [m_1,m_2], \text{wind speeds in } [u_1,u_2], \text{wind direction } r \text{ and barrier state } \omega. \end{aligned} \tag{16.9}$$

Then we obtain, as is shown in Appendix B, that these contributions can be calculated with the formula

$$\begin{aligned} &F_H\left(h;[q_1,q_2],[m_1,m_2],[u_1,u_2],r,\omega\right) \\ &\quad = N_{trap} \int_{q_1}^{q_2} dq \int_{m_1}^{m_2} dm \int_{u_1}^{u_2} du\ \tilde{v}(q,m) g(u,r,\omega \mid q,m) \chi_G(q,m,u,r,\omega) \end{aligned} \tag{16.10}$$

This formula is the one that is implemented in Hydra-Zoet.

Referenties

[Beijk en Geerse, 2004]
Bivariate correlatiemodellen gebaseerd op exponentiële marginale verdelingen. Beschrijving en werking MATLAB-programmatuur. V.A.W. Beijk en C.P.M. Geerse. RIZA-Werkdocument 2004.109x. Rijkswaterstaat-RIZA. Lelystad, May 2004.

[Beijk, 2007]
Achtergrondrapport HR2006 voor de Vecht- en IJsseldelta. Hydraulische randvoorwaarden 2006 voor de Vechtdelta en Thermometerrandvoorwaarden 2006 voor de IJsseldelta. V.A.W. Beijk, 2007. Rijkswaterstaat RIZA Rapport 2007.024.

[CUR/TAW, 1990]
Probabilistic design of flood defences. CUR/TAW. Report No. 141, Gouda, The Netherlands.

[Diermanse en Geerse, 2010]
Correlation models in flood risk analysis. F.L.M Diermanse en C.P.M. Geerse. To appear in the proceedings of ESREL 2010, European safety and reliability conference, September 6-9, 2010, Rhodos, Greece.

[De Deugd, 1998]
Samenhang afvoer Bovenrijn en Maas. H. de Deugd. Memo WST-98.142. RIZA Dordrecht, October 12, 1998.

[De Deugd, 2002]
Waterloopkundige berekeningen in het Benedenrivierengebied voor het Randvoorwaardenboek 2001. H. de Deugd. RIZA-Werkdocument 2002.203x. RIZA Dordrecht.

[Duits, 2005]
Hydra-BT – Testrapport. M.T. Duits. HKV Lijn in Water, March 2005.

[Duits, 2010a]
Hydra-Zoet - Systeemdocumentatie - versie 1.0 [HKV-rapport PR1858]. M.T. Duits. HKV Lijn in Water. Lelystad, August 2010.

[Duits, 2010b]
Hydra-Zoet - Gebruikershandleiding - versie 1.0 [HKV-rapport PR1858]. M.T. Duits. HKV Lijn in Water. Lelystad, August 2010.

[Duits, 2010c]
Hydra-Zoet - Handleiding geavanceerde gebruikers - Versie 1.0 [HKV-rapport PR1858]. M.T. Duits. HKV Lijn in Water. Lelystad, August 2010.

[Ditlevsen en Madsen, 1996]
Structural reliability analysis. O. Ditlevsen, H.O. Madsen. John Wiley & Sons, Chichester, England 1996.

[Ferry Borges and Castanheta, 1971]
Structural safety. J. Ferry Borges and M. Castanheta. Laboratorio National de Engenharia Civil, course 101, 2nd edition, Lisbon.

[Floris, 2005]
Flood Risks and Safety in the Netherlands (Floris). Floris study – Full report. Ministerie van Verkeer en Waterstaat, report DWW-2006-014, November 2005.

[Geerse, 2003]
Probabilistisch model hydraulische randvoorwaarden Benedenrivierengebied. C.P.M. Geerse. RIZA-werkdocument 2003.128x. Rijkswaterstaat-RIZA. Lelystad, December 2003.

[Geerse et al, 2002]
Wind-waterstandstatistiek Hoek van Holland. C.P.M. Geerse (RIZA), M.T. Duits (HKV), H.J. Kalk (HKV), I.B.M. Lammers, (HKV). RIZA/HKV rapport, Lelystad, July 2002.

[Geerse, 2004]
Bivariate correlatiemodellen met exponentiële en asymptotisch exponentiële marginale verdelingen. C.P.M. Geerse. RIZA-werkdocument 2002.104x. Rijkswaterstaat-RIZA. Lelystad, May 2004.

[Geerse en Diermanse, 2006]
Correlaties en meerdimensionale statistiek. C.P.M. Geerse en F.L.M. Diermanse. HKV LIJN IN WATER en WL|Delft Hydraulics, rapport PR1175, Lelystad, November 2006.

[Geerse, 2006]
Hydraulische Randvoorwaarden 2006 Vecht- en IJsseldelta - Statistiek IJsselmeerpeil, afvoeren en stormverlopen voor Hydra-VIJ. C.P.M. Geerse. RIZA-werkdocument 2006.036x. Rijkswaterstaat-RIZA. Lelystad, January 2006.

[Geerse, 2010]
Overzichtsdocument probabilistische modellen zoete wateren. Hydra-VIJ, Hydra-B en Hydra-Zoet. C.P.M. Geerse (HKV), met medewerking van Herbert Berger en Robert Slomp (Waterdienst). HKV Lijn in Water, Lelystad, July 2010. Client: RWS Waterdienst.

[Goda, 1969]
Reanalysis of laboratory data on wave transmission over breakwaters. Y. Goda. Report of the Port and Harbour Research Institute, Vol. 18, No 3, September 1969.

[HR, 2006]
Hydraulische Randvoorwaarden 2006 voor het toetsen van primaire waterkeringen. Ministerie van Verkeer en Waterstaat. Netherlands, Delft, september 2007.

[Huisman, 2004]
Water in the Netherlands, Managing Checks and Balances. Peter Huisman. Netherlands Hydrological Society, Utrecht, 2004.

[Hydra-M, 1999]
Achtergronden Hydraulische Belastingen Dijken IJsselmeergebied. RIZA Lelystad, March 1999. Een ontwerpmethodiek, RIZA rapport 99.037. R. Westphal, J. Hartman.

- Deelrapport 1: Gebruikershandleiding Hydra-M, RIZA rapport 99.038. E.J. Blaakman, R. Lisman.
- Deelrapport 2: Meerpeilstatistiek. RIZA rapport 99.039. E.J. Blaakman, H. Buiteveld, H.C. van Twuiver, A. Van Agthoven.
- Deelrapport 3: Windstatistiek. RIZA rapport 99.040. H.C. van Twuiver, C.P.M. Geerse.
- Deelrapport 4: Probabilistische rekenmethode. RIZA rapport 99.041. E.J. Blaakman.
- Deelrapport 5: Modellering waterbeweging (WAQUA). RIZA rapport 99.042. C.I. Bak, D.P. Vlag.
- Deelrapport 6: Modellering windgolven. RIZA rapport 99.043. D. Beyer, Q. Gao, D.P. Vlag.
- Deelrapport 7: Productiesommen waterbeweging en windgolven. RIZA rapport 99.044. D.P. Vlag, C.I. Bak, R. Westphal.
- Deelrapport 8: Reproductiefuncties. RIZA rapport 99.045. D. Beyer, E.J. Blaakman.
- Deelrapport 9: Modellering dammen, voorlanden en golfoploop. RIZA rapport 99.046. J.P. de Waal.
- Deelrapport 10: Beoordeling betrouwbaarheid Hydra-M. RIZA rapport 99.047. R. Westphal, J. Hartman.

[
Klopstra en Duits, 1999]
Methodiek voor vaststelling van de vorm van de maatgevende afvoergolf van de Rijn bij Lobith. D. Klopstra, M.T. Duits. HKV Lijn in water, December 1999.

[Leidraad rivierdijken deel 1, 1985]
Leidraad voor het ontwerpen van rivierdijken. Deel 1 – Bovenrivierengebied. Technische Adviescommissie voor de Waterkeringen. Staatsuitgeverij 's Gravenhage, September 1985.

[Leidraad rivierdijken deel 2, 1989]
Leidraad voor het ontwerpen van rivierdijken. Deel 2 – Benedenrivierengebied. Technische Adviescommissie voor de Waterkeringen. Staatsuitgeverij 's Gravenhage, 1989.

[LR, 2007]
Leidraad Rivieren. Directoraat-Generaal Rijkswaterstaat, Expertise Netwerk Waterkeren, Leidraad teksten door Rijkswaterstaat, HKV Lijn in Water, Arcadis, Met Andere Woorden. Den Haag, July 2007.

[Rijkoort, 1983]
A compound Weibull model for the description of surface wind velocity distribution. Rijkoort P.J. Koninklijk Nederlands Meteorologisch Instituut (KNMI). De Bilt, 1983.

[Ris, 1997]
Implementatie windopzet ENDEC. R.C. Ris. Memo.

[Seelig, 1979]
Effect of breakwaters on waves: laboratory tests of wave transmission by overtopping. W.N. Seelig. Proc. Coastal Structures 1979, p. 941 – 961.

[Stijnen et al, 2008]
Overzichtsdocument statistiek en probabilistische modellering. Jan Stijnen (HKV), Nadine Slootjes (HKV), Chris Geerse (HKV), Ferdinand Diermanse (WL|Delft Hydraulics), Henri Steenbergen (TNO B&O). Opdrachtgever Rijkswaterstaat Waterdienst, HKV-rapport PR1403.10, Lelystad, April 2008.

[TAC, 1998]
Fundamentals on Water defences (English translation of the Dutch Guidelines 'Grondslagen voor Waterkeren'). Technical Advisory Committee on Flood defences, The Netherlands, January 1998. Available on: http://www.enwinfo.nl.

[Van Velzen en Beyer, 2007]
Technisch Rapport Ontwerpbelastingen voor het rivierengebied (Behorend bij Leidraad Rivieren). E.H. van Velzen en D. Beyer. Ministerie van Verkeer en Waterstaat, May 2007.

[Vrouwenvelder et al, 2003]
Theoriehandleiding PC-Ring, versie 3.0, deel A t/m C. A.C.W.M. Vrouwenvelder, H.M.G.M. Steenbergen, K.Slijkhuis. TNO-rapport 2003-CI-R0020. TNO-Bouw, April 2003.

[Vrouwenvelder en Courage, 2010]
Belastingmodellen / Rekentechnieken toekomstig TOI. Concept, versie 5. A.C.W.M. Vrouwenvelder en W.M.G. Courage. TNO, Delft, August 2010.

[VTV, 2007]
De veiligheid van de primaire waterkeringen in Nederland. Voorschrift Toetsen op Veiligheid voor de derde toetsronde 2006-2011 (VTV). Ministerie van Verkeer en Waterstaat, September 2007.

[De Waal, 1999]
Achtergronden Hydraulische Belastingen Dijken IJsselmeergebied. Deelrapport 9: Modellering dammen, voorlanden en golfoploop. J.P. de Waal. RIZA-rapport 99.046. Rijkswaterstaat-RIZA. Lelystad, March 25, 1999.

[De Waal, 2003]
Windmodellering voor bepaling waterstanden en golven. Een analyse van de bouwstenen. J.P. de Waal. RIZA-werkdocument 2003.118x. Rijkswaterstaat-RIZA. Lelystad, 2003.

[De Waal, 2007]
Achtergrondrapport HR2006 voor de Benedenrivieren. Thermometerrandvoorwaarden 2006. RWS-RIZA rapport 2007.023. J.P. de Waal.

[De Waal, 2008]
Windgolven in HR2011 voor rivieren. Voorstudie naar noodzaak modelverbetering. Hans de Waal. Deltares, 2008.

[De Waal, 2010]
Spatial wind input for HBC production runs. SBW-Belastingen: Phase 3 and conclusions of sub-project "Wind modelling". J.P. de Waal. Deltares, February 2010.

[Wieringa en Rijkoort, 1983]
Windklimaat van Nederland. J. Wieringa en P.J. Rijkoort. Koninklijk Nederlands Meteorologisch Instituut (KNMI), De Bilt. Staatsuitgeverij Den Haag, 1983.

[Wilson, 1965]
Numerical prediction of ocean waves in the North Atlantic for December 1959. In: Deutsche Hydrographische Zeischrift, Jahrgang 18, 1965, Heft 3.
[Waterwet, 2009]
Wet van 29 januari 2009, houdende regels met betrekking tot het beheer en gebruik van watersystemen (Waterwet).

[Wwk, 1996]
Wet op de Waterkeringen. Wet, houdende algemene regels ter verzekering van de beveiliging door waterkeringen tegen overstromingen door het buitenwater en regeling van enkele daarmee verband houdende aangelegenheden. Staatsblad 304.

[Young en Verhagen, 1996]
The growth of fetch limited waves in water of finite depth, Part 1: Total energy and peak frequency. Coastal Engineering 29, p47-78.

Part 4: Appendices

Appendix A: Relation between year maximum and exceedance frequency

In applications, the probability that the year maximum of a random variable X exceeds the number x, is often approximated by the exceedance frequency of that number, where it is tacitly assumed that the underlying stochastic process is stationary. In what follows, a relation between the year maximum and the exceedance frequency is treated, from which this approximation follows.

Some definitions are needed. Consider a stationary stochastic process $\{X_t\}$. Here the stationarity (roughly) means that its joint probability distributions do not change when shifted in time. Define X_{year} as the maximum of the values X_t, for the t-values constituting a period of a year; X_{year} is called the year maximum. Also, define F(x) as the average number of exceedances of the level x, in times per year.

To obtain a relation between $P(X_{year}>x)$ and F(x), it is assumed, as an approximation, that the number of exceedance peaks of x, in a period of a year, follows a Poisson distribution with Poisson parameter F(x). In that case, the probability that no peak is present during the year equals $P(X_{year}<x) = \exp(-F(x))$, implying

$$P(X_{year} > x) = 1 - e^{-F(x)} \tag{A.1}$$

Because for small numbers y we have $1-\exp(-y) \cong y$, we obtain for small values of F(x) the approximation

$$P(X_{year} > x) \cong F(x), \qquad \text{if } F(x) \cong 0 \tag{A.2}$$

In practical applications, one often uses the approximation is $F(x)<0.1$, in which case the error is smaller than 5%.

Formula (A.1) is exact under the assumption of a Poisson process. There is, however, a relation between $P(X_{year}>x)$ and F(x) that holds in general. This relation is given by

$$P(X_{year} > x) = \frac{F(x)}{F(x \mid \#\text{peaks} \geq 1)} \leq F(x) \tag{A.3}$$

where $F(x|\#\text{ peaks} \geq 1)$ denotes the average number of exceedances of x in years where there is at least one peak present. Note that the first two terms of this relation are dimensionless, whereas the last term seems to have dimension 1/year. The latter is not really true, since we have divided by a number equal to 1, but with dimension 1/year.

year	# peaks > x
1	0
2	3
3	0
4	0
5	2
6	0
7	0
8	0
9	0
10	3
total of 10 years:	8 peaks

Table A-1: Example of exceedance peaks during a period of 10 years.

Below, a proof of relation (A.3) is given, but first an example is provided, illustrating this relation. Assume a period of 10 years is considered, with 8 peaks occurring in 3 of those years (see Table A-1). We then obtain

$$\begin{aligned} F(x) &= 8/10 &= 0.8 \quad &\text{peaks/year} \\ F(x \mid \#\text{peaks} \geq 1) &= 8/3 &= 2.67 \quad &\text{peaks/year} \\ F(x)/F(x \mid \#\text{peaks} \geq 1) &= 0.8/2.67 &= 0.3 \quad &[-] \end{aligned} \tag{A.4}$$

According to (A.3) we should have $P(X_{year}>x) = 0.3$. This probability could also be calculated directly, without the use of (A.3): there are 3 years out of 10 for which the year maximum exceeds x, yielding (indeed) a probability of 0.3.

The approximation of the year probability by the exceedance frequency appears to be a valid one if $F(x|\#\text{ peaks} \geq 1) \cong 1$. If the number of peaks follows a Poisson process, which process has the property that peaks occur independently from each other in time, this will be satisfied if $F(x) \cong 0$. For in that case the probability on more than one peak in a year becomes negligible, yielding $F(x|\#\text{ peaks} \geq 1) \cong 1$. In that case, relation (A.3) indeed implies (A.2).

Proof of (A.3)
Define the random variable Y_x as the number of exceedances of x during a period of a year. Because an exceedance of level x is equivalent to having $X_{year} > x$, we obtain

$$\begin{aligned} P(X_{jaar} > x) &= P(Y_x \geq 1) \\ F(x) &= E(Y_x) \\ F(x \mid \geq 1) &= E(Y_x \mid Y_x \geq 1) \end{aligned} \tag{A.5}$$

We can write

$$E(Y_x) = P(Y_x = 0)\ E(Y_x \mid Y_x = 0) + P(Y_x \geq 1)\ E(Y_x \mid Y_x \geq 1) \tag{A.6}$$

Since the condition $Y_x = 0$ implies that the conditional expectation of Y_x becomes zero, we then obtain

$$E(Y_x) = P(Y_x \geq 1)\ E(Y_x \mid Y_x \geq 1) \tag{A.7}$$

Using (A.5), this implies (A.3).

Appendix B: Formulas for the contributions to the exceedance frequency

Appendix B.1: Introduction

In the main text, formulas for the contributions to the exceedance frequency are given: for the tidal rivers in section 12.2, and for the Vecht and IJssel delta in section 16.2. Some of the statements were left without proof. These proofs are given in this appendix.

We note that the general structure of the formulas for the contributions is alike for both water systems, although the formulas for the Vecht and IJsseldelta are a bit more complicated than those for the tidal rivers. Reason for this is that the model for the Vecht and IJsseldelta uses two slow variables (discharge and lake level), whereas the model for the tidal rivers uses only one slow variable (discharge). Since the proofs for the statements concerning the tidal rivers are simpler versions from the proofs of the statements for the Vecht and IJsseldelta, we may, and will, restrict ourselves in this appendix to the proofs of the statements for the Vecht and IJsseldelta.

We note that this appendix requires more mathematical skills from the reader then required in the main text.

Appendix B.2: Formula for the contributions using an integral over time

The setting in the remainder of this appendix will be the one for the Vecht and IJsseldelta as in section 16.2. We will derive a formula for the contributions $F_H(h;[q_1,q_2], [m_1,m_2], [u_1,u_2],r,\omega)$ stated in (16.9). To that purpose, we first derive a version of this formula related to the base duration B, denoted by

$$A(h;[q_1,q_2],[m_1,m_2],[u_1,u_2],r,\omega) = \text{simultaneous contributions to the failure probability } P_B(H>h), \text{ of discharges in } [q_1,q_2], \text{ lake levels in } [m_1,m_2], \text{wind speeds in } [u_1,u_2], \text{wind direction } r \text{ and barrier state } \omega. \quad \text{(B.1)}$$

The relation between this variable and $F_H(h;[q_1,q_2], [m_1,m_2], [u_1,u_2],r,\omega)$ is simply

$$F_H(h;[q_1,q_2],[m_1,m_2],[u_1,u_2],r,\omega) = N_{trap} A(h;[q_1,q_2],[m_1,m_2],[u_1,u_2],r,\omega) \quad \text{(B.2)}$$

where $N_{trap} = 6$ denotes the number of trapezia within the winter half year.

To obtain the formula for (B.1), we first the simpler case where m,u,r,ω are left out. So we consider $A(h;[q_1,q_2])$ first. This situation is in fact already dealt with in section 12.2.3. From (12.18), (12.14), (12.15) and (12.17) we obtain

$$A\big(h;[q_1,q_2]\big) = \int dk\, f(k) A\big(h;[q_1,q_2] \mid k\big) \quad \text{(B.3)}$$

where the version of $A(h;[q_1,q_2])$ conditional on k is given by

$$A\big(h;[q_1,q_2]\,|\,k\big) = G_B\big(H>h\,|\,k\big)\,\frac{\displaystyle\int_{\tau\in[0,n(B)]:\,\alpha(\tau,k)\in[q_1,q_2]} d\tau\,P\big(H>h\,|\,\alpha(\tau,k)\big)}{\displaystyle\int_0^{n(B)} d\tau\,P\big(H>h\,|\,\alpha(\tau,k)\big)} \tag{B.4}$$

We can interpret this formula as follows. The number $A(h;[q_1,q_2]|k)$ equals the failure probability $P_B(H>h|k)$, apart from the fraction on the r.h.s., which serves as a correction on this failure probability. This correction accounts for the fact that (a) during failure no definite value can be ascribed to the discharge during failure, and (b) that several failure events during a trapezium wave can occur in different time blocks (see, if necessary, section 12.2.1 for more explanation).

We want to include the lake level m in the formulas. To extend (B.4) with the lake level, we use the following considerations. Note that the numerator on the r.h.s. of (B.4) restricts the time integral to those moments where the discharges in the trapezium $\alpha(\tau,k)$ belong to the interval $[q_1,q_2]$. The denominator consists of the time integral without any restriction on the discharges in the trapezium. These considerations motivate the following formula for the situation including the lake level m:

$$A\big([q_1,q_2],[m_1,m_2]\,|\,k,s\big) = G_B(H>h\,|\,k,s)\,\frac{\displaystyle\int_{\substack{\tau\in[0,n(B)]:\,\alpha(\tau,k)\in[q_1,q_2],\\ \beta(\tau,s)\in[m_1,m_2]}} d\tau\,P\big(H>h\,|\,\alpha(\tau,k),\beta(\tau,s)\big)}{\displaystyle\int_{\tau\in[0,n(B)]} dt\,P\big(H>h\,|\,\alpha(\tau,k),\beta(\tau,s)\big)} \tag{B.5}$$

where we recall from section 16.2.1 that the lake level trapezium with peak value s, as a function of time τ, is denoted by $\beta(\tau,s)$. We also recall that the probability $G_B(H>h|k,s)$ is given by (16.1), and that $P(H>h|\alpha(\tau,k),\beta(\tau,s))$ can be calculated with (15.9) or (15.14). Note that the integration over τ in the numerator of the r.h.s. of (B.5) is restricted to discharges and lake levels in the intervals $[q_1,q_2]$ and $[m_1,m_2]$, as graphically explained in Figure B-1.

To write (B.5) in a more compact form, we recall the definitions (16.5) and (16.6):

$$\overline{G}_B(H>h\,|\,k,s) = \int_0^{n(B)} d\tau\,P\big(H>h\,|\,\alpha(\tau,k),\beta(\tau,s)\big) \tag{B.6}$$

$$J(k,s) = \frac{G_B(H>h\,|\,k,s)}{\overline{G}_B(H>h\,|\,k,s)} \tag{B.7}$$

implying that (B.5) can be written as

$$A\big([q_1,q_2],[m_1,m_2]\,|\,k,s\big) = J(k,s)\int_{\substack{\tau\in[0,n(B)]:\,\alpha(\tau,k)\in[q_1,q_2],\\ \beta(\tau,s)\in[m_1,m_2]}} d\tau\,P\big(H>h\,|\,\alpha(\tau,k),\beta(\tau,s)\big) \tag{B.8}$$

We recall from (15.9) that $P(H>h|q,m)$ can be written as

$$P(H>h\,|\,q,m) = \sum_{r=1}^{16}\sum_{\omega=0}^{1}\int_{u\geq 0} du\,P(H>h\,|\,q,m,u,r,\omega)g(u,r,\omega\,|\,q,m) \tag{B.9}$$

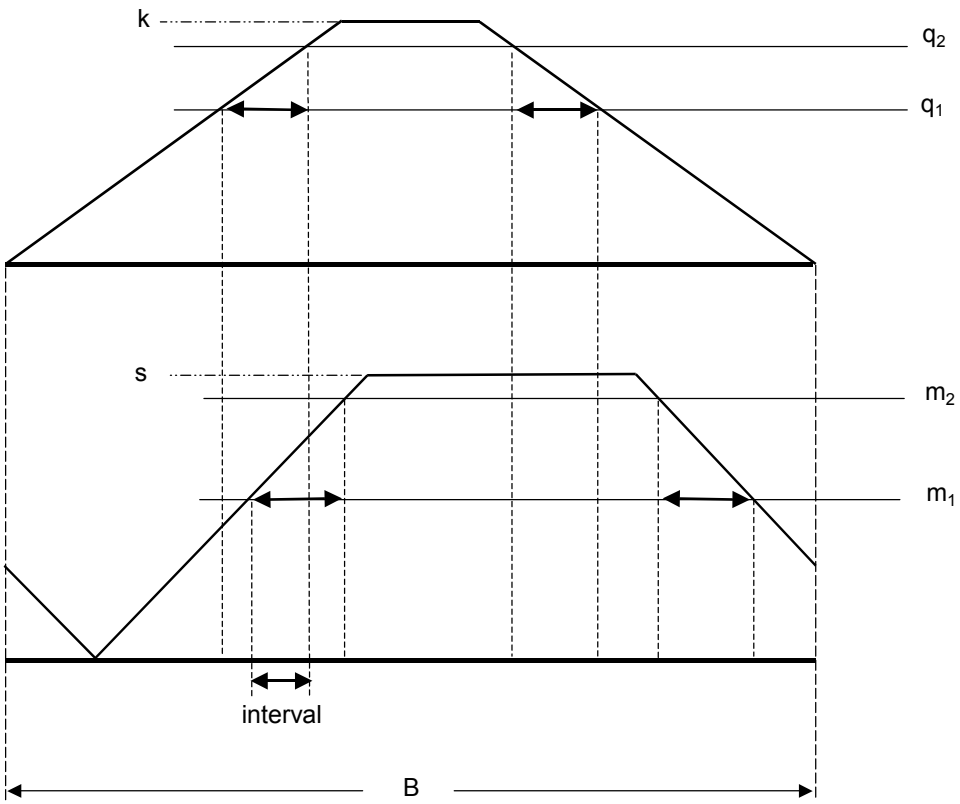

Figuur B-1: Illustration of the τ-values for which $\alpha(\tau,k) \in [q_1,q_2]$ and $\beta(\tau,s) \in [m_1,m_2]$: these values belong to the interval indicated in the figure.

As explained after (15.9), P(H>h|q,m,u,r,ω) is an indicator function, that either equals 0 or 1. Using (15.10), (15.11) and (15.15) it is observed that

$$P(H > h \mid q,m,u,r,\omega) = \begin{cases} 1 & \text{if } H\left(q,m,u,r,\lambda(\omega)\right) > h \\ 0 & \text{if } H\left(q,m,u,r,\lambda(\omega)\right) \le h \end{cases} \tag{B.10}$$

This means that (B.9) can be written as

$$P(H > h \mid q,m) = \sum_{r=1}^{16} \sum_{\omega=0}^{1} \int_{u \ge 0} du\, g(u,r,\omega \mid q,m) \chi_G(q,m,u,r,\omega) \tag{B.11}$$

where χ_G(q,m,u,r,ω) denotes the characteristic function of the failure region, introduced in (16.8). Formula (B.8) then takes the form

$$A\left([q_1,q_2],[m_1,m_2] \mid k,s\right) = J(k,s) \sum_{r=1}^{16} \sum_{\omega=0}^{1} \int_{\substack{\tau \in [0,n(B)]: \alpha(\tau,k) \in [q_1,q_2], \\ \beta(\tau,s) \in [m_1,m_2]}} d\tau \int_{u \ge 0} du\, g\left(u,r,\omega \mid \alpha(\tau,k),\beta(\tau,s)\right) \chi_G\left(\alpha(\tau,k),\beta(\tau,s),u,r,\omega\right) \tag{B.12}$$

This formula makes it evident that the formula for the 'most detailed' contributions should be:

$$A\left([q_1,q_2],[m_1,m_2],[u_1,u_2],r,\omega\,|\,k,s\right) = J(k,s) \int\limits_{\substack{\tau\in[0,n(B)]:\ \alpha(\tau,k)\in[q_1,q_2],\\ \beta(\tau,s)\in[m_1,m_2]}} d\tau \int_{u_1}^{u_2} du\, g\left(u,r,\omega\,|\,\alpha(\tau,k),\beta(\tau,s)\right)\chi_G\left(\alpha(\tau,k),\beta(\tau,s),u,r,\omega\right) \tag{B.13}$$

To obtain the contributions unconditional on k and s, the latter variables are integrated out, yielding

$$A\left(h;[q_1,q_2],[m_1,m_2],[u_1,u_2],r,\omega\right) = \int dk\, f(k,s)J(k,s) \int\limits_{\substack{\tau\in[0,n(B)]:\ \alpha(\tau,k)\in[q_1,q_2],\\ \beta(\tau,s)\in[m_1,m_2]}} d\tau \int_{u_1}^{u_2} du\, g\left(u,r,\omega\,|\,\alpha(\tau,k),\beta(\tau,s)\right)\chi_G\left(\alpha(\tau,k),\beta(\tau,s),u,r,\omega\right) \tag{B.14}$$

This is the formula for the contributions to the failure probability $P_B(H>h)$ as in (B.1). Formula (B.2) then provides the formula for the contributions to the failure frequency $F_H(h)$, which we here (loosely) characterise as a formula in terms of a time integration.

Appendix B.3: Formula for the contributions using an integral over q and m instead of time

The aim of this section is to prove formula (16.10), with which the contributions $F_H(h;[q_1,q_2],[m_1,m_2],[u_1,u_2],r,\omega)$ can be calculated, using, among other things, an integral over the slow variables q and m instead of an integral over τ. To that purpose, we will show that (B.14) can also be calculated as

$$A\left(h;[q_1,q_2],[m_1,m_2],[u_1,u_2],r,\omega\right) = \int_{q_1}^{q_2} dq \int_{m_1}^{m_2} dm \int_{u_1}^{u_2} du\ \tilde{v}(q,m)g(u,r,\omega\,|\,q,m)\chi_G(q,m,u,r,\omega) \tag{B.15}$$

with $\tilde{v}(q,m)$ given by (16.7), which is repeated here:

$$\tilde{v}(q,m) = \frac{\partial^2}{\partial q\partial m}\int_q^\infty dk \int_m^\infty ds\, f(k,s)J(k,s)L(q,k,m,s) \geq 0 \tag{B.16}$$

Formula (16.10) then immediately follows by multiplying (B.15) with N_{trap}, i.e. the number of trapezia in the winter half year. So, we are done once (B.15) has been proven.

To prove (B.15), we start with a simplified situation, and assume:

1. For the phase φ between the discharge and the lake level trapezia we will take $\varphi = 0$, implying that the centres of the discharge and lake level trapezia coincide.
2. Only the situation $q_2 = \infty$ and $m_2 = \infty$ is considered.
3. The trapezia will have a strictly increasing front flank, ranging from $\tau = 0$ to $\tau = n(B)/2$, and a strictly decreasing back flank, ranging from $\tau = n(B)/2$ to $\tau = n(B)$.

The situation for general phases and arbitrary values of q_2 and m_2 will be treated further on. The third assumption is not really a limitation, for if trapezia do not satisfy this condition,

arbitrarily small changes to them will bring us in the third situation. Such changes can be made so small that no physical distinction can be made compared to the original (undistorted) trapezia, while mathematically it is achieved that every discharge in the front flank then uniquely corresponds to a value of τ, while the same is true for every discharge in the back flank. Also, values of the lake level in the front and back flank then correspond to unique values of τ. This unique correspondence between discharges, lake levels and values of τ, will be used in the (version of) the proof we will provide.

In the proof we need the function A_W defined by

$$A_W(q_1,m_1)=\int_{q_1}^{\infty} dk \int_{m_1}^{\infty} ds\, f(k,s)J(k,s) \int_{\tau\in[0,n(B)]:\alpha(\tau,k)\geq q_1,\ \beta(\tau,s)\geq m_1} d\tau\, W\left(\alpha(\tau,k),\beta(\tau,s)\right) \tag{B.17}$$

where W(q,m) is an arbitrary bounded function of q and m, where the boundedness is used to guarantee that the integral on the r.h.s. of (B.17) exists as a finite number.[26] In the proof of (B.15), the following proposition is used.

Proposition
For all bounded functions W(q,m), the function A_W of (B.17) satisfies

$$A_W(q_1,m_1)=\int_{q_1}^{\infty} dq \int_{m_1}^{\infty} dm\, W(q,m)\tilde{v}(q,m) \tag{B.18}$$

with $\tilde{v}(q,m)$ given by (B.16).

We postpone the proof of this proposition for a moment. First we show that, using this proposition, the proof of (B.15) will be easy.

Consider the specific (bounded) function W = W_{contr}, where the subscript "contr" is a shorthand for "contributions", defined by

$$W_{contr}(q,m)=\int_{u_1}^{u_2} du\, g(u,r,\omega\,|\,q,m)\chi_G(q,m,u,r,\omega) \tag{B.19}$$

and the variables on the r.h.s. are the ones used in the previous section. Note that $W_{contr}(q,m)$ not only depends on q and m, but also on u_1, u_2, r and ω. But since the latter four variables in this context are fixed, there is no need to denote them explicitly.

We will show that the specific choice W_{contr} yields the contributions $A(h;[q_1,q_2],[m_1,m_2],[u_1,u_2],r,\omega)$. Substituting W_{contr} into (B.17), we obtain

$$A_{W_{contr}}(q_1,m_1)=\int_{q_1}^{\infty} dk \int_{m_1}^{\infty} ds\, f(k,s)J(k,s) \int_{\tau\in[0,n(B)]:\alpha(\tau,k)\geq q_1,\ \beta(\tau,s)\geq m_1} d\tau \int_{u_1}^{u_2} du \\ g(u,r,\omega\,|\,\alpha(\tau,k),\beta(\tau,s))\chi_G(\alpha(\tau,k),\beta(\tau,s),u,r,\omega) \tag{B.20}$$

[26] We mention boundedness here as a sufficient condition to garantee the eistence of the integral as a finite number. But actually, throughout this report we don not worry about technical details such as existence of integrals and derivatives, or whether interchanging the order of integrals is allowed, etcetera. The mere fact that boundedness is mentioned here, should not be interpreted as if all other mathematical manipulations have been rigorously proven.

In this formula, the lower integration bounds q_1 and m_1 both can be replaced by $-\infty$ (or by their minimum values q_{min} and m_{min}), since the restrictions $\alpha(\tau,k) \geq q_1$ and $\beta(\tau,s) \geq m_1$ imply that the integrand becomes zero for $k<q_1$ and $s<m_1$. Formula (B.14) then shows

$$A_{W_{contr}}(q_1,m_1) = A\left(h;[q_1,\infty],[m_1,\infty],[u_1,u_2],r,\omega\right) \tag{B.21}$$

So indeed, the specific choice W_{contr} in (B.17) leads to the contributions. On the other hand, from the above proposition, see (B.18), we obtain

$$A_{W_{contr}}(q_1,m_1) = \int_{q_1}^{\infty} dq \int_{m_1}^{\infty} dm \;\; \tilde{v}(q,m) \int_{u_1}^{u_2} du\, g(u,r,\omega \mid q,m)\chi_G(q,m,u,r,\omega) \tag{B.22}$$

So (B.15) has been proven once the proposition has been proven, at least for the specific choices $q_2 = \infty$ and $m_2 = \infty$ and phase $\varphi = 0$ considered here.

Proof of the proposition, for $q_2 = \infty$, $m_2 = \infty$, $\varphi = 0$[27]

Some definitions are needed. Consider a discharge trapezium $\alpha(\tau,k)$ and a lake level trapezium $\beta(\tau,s)$ as before. The unique value of τ attaining discharge q in the front flank of the discharge trapezium will be denoted by $\tau^{up}(q,k)$, i.e. $\alpha(\tau^{up}(q,k),k) = q$. An analogous definition for the back flank is used: $\tau^{down}(q,k)$ is the value of τ attaining q in the back flank of the discharge trapezium. For the lake level trapezium, similar definitions are used: the values of τ in the front and back flank are denoted as $\tau^{up}(m,s)$ and $\tau^{down}(m,s)$.

Also define

$$\begin{aligned} A(q,k) &= \left\{\tau \in [0,n(B)] \mid \alpha(\tau,k) \geq q\right\} \\ B(m,s) &= \left\{\tau \in [0,n(B)] \mid \beta(\tau,s) \geq m\right\} \end{aligned} \tag{B.23}$$

and denote the characteristic functions of these sets by $\chi_{A(q,k)}(\tau)$ and $\chi_{B(m,s)}(\tau)$. (E.g. $\chi_{A(q,k)}(\tau) = 1$ if τ belongs to A(q,k) and 0 otherwise.)

To prove (B.18), consider, for an arbitrary bounded function W(q,m), the number

$$\int_{\tau\in[0,n(B)/2]:\alpha(\tau,k)\geq q_1,\ \beta(\tau,s)\geq m_1} d\tau\; W\left(\alpha(\tau,k),\beta(\tau,s)\right) \tag{B.24}$$

which is a function of q_1, k, m_1 and s. This function appears, when considering only the front flank of the trapezia, as a part in the definition of $A_W(q_1,m_1)$ in (B.17). Using the characteristic functions of the sets in (B.23) and the Dirac delta function $\delta(\tau-t)$, (B.24) can be rewritten as

$$\begin{aligned} &\int_{\tau\in[0,n(B)/2]:\alpha(\tau,k)\geq q_1,\ \beta(\tau,s)\geq m_1} d\tau\; W\left(\alpha(\tau,k),\beta(\tau,s)\right) \\ &= \int_0^{n(B)/2} d\tau\, \chi_{A(q_1,k)}(\tau)\chi_{B(m_1,s)}(\tau) W\left(\alpha(\tau,k),\beta(\tau,s)\right) \\ &= \int_0^{n(B)/2} d\tau \int_0^{n(B)/2} dt\, \delta(\tau-t)\,\chi_{A(q_1,k)}(\tau)\chi_{B(m_1,s)}(t) W\left(\alpha(\tau,k),\beta(t,s)\right) \end{aligned} \tag{B.25}$$

[27] Essentially, the proof entails nothing more then a change of the integration variable τ to the pair of integration variables (q,m). Perhaps a simpler version of our rather awkward proof can be given, using some kind of a general transformation theorem.

We now change from the respective variables t and τ to m and q, using the 'substitutions' $\beta(t,s)=m$ and $\alpha(t,k)=q$, and rewrite (B.25) as

$$\begin{aligned}
&\int_{\tau\in[0,n(B)/2]:\alpha(\tau,k)\geq q_1,\ \beta(\tau,s)\geq m_1} d\tau\ W\left(\alpha(\tau,k),\beta(\tau,s)\right) \\
&= \int_0^{n(B)/2} d\tau \int_{m_1}^{s} dm\, \delta\left(\tau-\tau^{op}(m,s)\right)\chi_{A(q_1,k)}(\tau)W\left(\alpha(\tau,k),m\right)\frac{\partial\tau^{up}(m,s)}{\partial m} \\
&= \int_{q_1}^{k} dq \int_{m_1}^{s} dm\ \delta\left(\tau^{op}(q,k)-\tau^{op}(m,s)\right)W\left(q,m\right)\frac{\partial\tau^{up}(m,s)}{\partial m}\frac{\partial\tau^{up}(q,k)}{\partial q}
\end{aligned} \tag{B.26}$$

If we consider the analogue of the integral (B.24) for the situation where the front and back flank are considered collectively, then in a similar way, we obtain

$$\begin{aligned}
&\int_{\tau\in[0,n(B)]:\alpha(\tau,k)\geq q_1,\ \beta(\tau,s)\geq m_1} d\tau\ W\left(\alpha(\tau,k),\beta(\tau,s)\right) \\
&= \int_{q_1}^{k} dq \int_{m_1}^{s} dm\ W\left(q,m\right)\left\{\delta\left(\tau^{up}(q,k)-\tau^{up}(m,s)\right)\frac{\partial\tau^{up}(m,s)}{\partial m}\frac{\partial\tau^{up}(q,k)}{\partial q}\right. \\
&\qquad\left.+\delta\left(\tau^{down}(q,k)-\tau^{down}(m,s)\right)\frac{\partial\tau^{down}(m,s)}{\partial m}\frac{\partial\tau^{down}(q,k)}{\partial q}\right\}
\end{aligned} \tag{B.27}$$

As a shorthand for the part of the integral containing the delta-functions, we define

$$\begin{aligned}
D^{up}(q,k,m,s) &= \delta\left(\tau^{up}(q,k)-\tau^{up}(m,s)\right)\frac{\partial\tau^{up}(m,s)}{\partial m}\frac{\partial\tau^{up}(q,k)}{\partial q} \\
D^{down}(q,k,m,s) &= \delta\left(\tau^{down}(q,k)-\tau^{down}(m,s)\right)\frac{\partial\tau^{down}(m,s)}{\partial m}\frac{\partial\tau^{down}(q,k)}{\partial q}
\end{aligned} \tag{B.28}$$

Now (B.27) can also be written as

$$\begin{aligned}
&\int_{\tau\in[0,n(B)]:\alpha(\tau,k)\geq q_1,\ \beta(\tau,s)\geq m_1} d\tau\ W\left(\alpha(\tau,k),\beta(\tau,s)\right) \\
&\qquad= \int_{q_1}^{k} dq \int_{m_1}^{s} dm\ W\left(q,m\right)\left\{D^{up}(q,k,m,s)+D^{down}(q,k,m,s)\right\}
\end{aligned} \tag{B.29}$$

Using this formula, the function $A_W(q_1,m_1)$ of (B.17) can now be written as

$$\begin{aligned}
A_W(q_1,m_1) &= \int_{q_1}^{\infty} dk \int_{m_1}^{\infty} ds\, f(k,s)J(k,s)\int_{q_1}^{k} dq \int_{m_1}^{s} dm\ W\left(q,m\right)\left\{D^{up}(q,k,m,s)+D^{down}(q,k,m,s)\right\} \\
&= \int_{q_1}^{\infty} dq \int_{m_1}^{\infty} dm\ W\left(q,m\right)\int_{q}^{\infty} dk \int_{m}^{\infty} ds\, f(k,s)J(k,s)\left\{D^{up}(q,k,m,s)+D^{down}(q,k,m,s)\right\}
\end{aligned} \tag{B.30}$$

Next, since $A_W(q_1,m_1)$ tends to zero if q_1 and/or m_1 tend to ∞, we have the general property

$$\begin{aligned} A_W(q_1,m_1) &= \int_{m_1}^{\infty} dm \left\{ -\frac{\partial}{\partial m} A_W(q_1,m) \right\} \\ &= \int_{m_1}^{\infty} dm \left\{ -\frac{\partial}{\partial m} \left[\int_{q_1}^{\infty} dq \left\{ -\frac{\partial}{\partial q} A_W(q,m) \right\} \right] \right\} \\ &= \int_{q_1}^{\infty} dq \int_{m_1}^{\infty} dm \left\{ \frac{\partial^2}{\partial q \partial m} A_W(q,m) \right\} \end{aligned} \tag{B.31}$$

Since (B.30) and (B.31) hold for all values of q_1 and m_1, we conclude

$$\frac{\partial^2}{\partial q \partial m} A_W(q,m) = W(q,m) \int_q^{\infty} dk \int_m^{\infty} ds\, f(k,s) J(k,s) \left\{ D^{up}(q,k,m,s) + D^{down}(q,k,m,s) \right\} \tag{B.32}$$

We also have, from the very definition of $A_W(q_1,m_1)$ in (B.17),

$$\frac{\partial^2}{\partial q \partial m} A_W(q,m) = \frac{\partial^2}{\partial q \partial m} \int_q^{\infty} dk \int_m^{\infty} ds\, f(k,s) J(k,s) \int_{\tau \in [0,n(B)]: \alpha(\tau,k) \geq q,\ \beta(\tau,s) \geq m} d\tau\, W\left(\alpha(\tau,k), \beta(\tau,s)\right) \tag{B.33}$$

Now note that the function L(q,k,m,s) defined in section 15.2.2 can be calculated as

$$L(q,k,m,s) = \int_{\tau \in [0,n(B)]: \alpha(\tau,k) \geq q,\ \beta(\tau,s) \geq m} d\tau \tag{B.34}$$

Since (B.32) and (B.33) hold for arbitrary bounded functions W(q,m), we can take the specific choice W(q,m) = 1. We then obtain, using (B.33), (B.16) and (B.32),

$$\begin{aligned} \tilde{v}(q,m) &= \frac{\partial^2}{\partial q \partial m} A_{W=1}(q,m) \\ &= \int_q^{\infty} dk \int_m^{\infty} ds\, f(k,s) J(k,s) \left\{ D^{up}(q,k,m,s) + D^{down}(q,k,m,s) \right\} \end{aligned} \tag{B.35}$$

Now, considering arbitrary functions W again, (B.30) shows

$$A_W(q_1,m_1) = \int_{q_1}^{\infty} dq \int_{m_1}^{\infty} dm\, W(q,m) \tilde{v}(q,m) \tag{B.36}$$

This concludes the proof of the proposition for the case $q_2 = \infty$, $m_2 = \infty$, $\varphi = 0$.

Extension of the proof of the proposition to $\varphi \neq 0$ (again $q_2 = \infty$, $m_2 = \infty$)

Arbitrary phases φ satisfy $\varphi \in [-n(B)/2, n(B)/2]$. We first consider positive phases in the interval $\varphi \in (0, n(B)/2)$.

In the proof of the proposition, the base duration of the trapezia was split up in the intervals (0, n(B)/2) and (n(B)/2, n(B)), as a means to calculate the integral (B.27). This resulted in the introduction of the functions $D^{up}(q,k,m,s)$ and $D^{down}(q,k,m,s)$ appearing in (B.28) and (B.29). For $\varphi \in (-0, n(B)/2)$ the base duration will be split into four instead of two intervals. Recall that, perhaps after arbitrarily small changes, trapezia consist of strictly increasing front flanks and strictly decreasing back flanks, and that positive phases mean that the lake trapezium is delayed w.r.t. the discharge trapezium. We now consider the following four time intervals:

- (0, φ) on which the discharge increases and the lake level decreases (as illustrated in Figure 15-2);
- (φ, n(B)/2) on which the discharge increases and the lake level increases;
- (n(B)/2, n(B)/2+φ) on which the discharge decreases and the lake level increases;
- (n(B)/2+φ, n(B)) on which the discharge decreases and the lake level decreases;

In the proof of the proposition for the case $\varphi = 0$, the following expression occurs in (B.29):

$$\begin{aligned} &D^{up}(q,k,m,s)+D^{down}(q,k,m,s) \\ &=\delta\left(\tau^{up}(q,k)-\tau^{up}(m,s)\right)\frac{\partial\tau^{up}(m,s)}{\partial m}\frac{\partial\tau^{up}(q,k)}{\partial q}+\delta\left(\tau^{down}(q,k)-\tau^{down}(m,s)\right)\frac{\partial\tau^{down}(m,s)}{\partial m}\frac{\partial\tau^{down}(q,k)}{\partial q} \end{aligned} \quad \text{(B.37)}$$

So there are two terms, corresponding to the intervals (0, n(B)/2) and (n(B)/2, n(B)), that have to be added. When considering $\varphi \in$ (0, n(B)/2), this becomes an expression of four terms that have to be added, where these terms correspond to the ones just listed. (The terms consist of various combinations of τ^{up}(q,k), τ^{down}(q,k), τ^{up}(m,s), τ^{down}(m,s).) Inspection of the proof for this new situation shows that the essence of the proof does not change at all. So, with small alterations, the above proof remains valid.

Arbitrary phases satisfy $\varphi \in$ [-n(B)/2, n(B)/2]. The case $\varphi = 0$ has been dealt with before, just as the case $\varphi \in$ (0, n(B)/2). The cases φ = -n(B)/2 and φ = n(B)/2 are rather similar to the case $\varphi = 0$, with the base duration split into two intervals. The case $\varphi \in$ (-n(B)/2, 0) is similar to the one for $\varphi \in$ (0, n(B)/2), with the base duration split into four intervals. This means that the proposition is valid for arbitrary phases φ.

Extension of the proof of the proposition to arbitrary q_2 and m_2 (with φ arbitrary)
Consider arbitrary q_2 and m_2, with $q_2 > q_1$ and $m_2 > m_1$. With (B.14) it can be verified that

$$\begin{aligned} &A\left(h;[q_1,q_2],[m_1,m_2],[u_1,u_2],r,\omega\right) \\ &\quad=A\left(h;[q_1,\infty],[m_1,\infty],[u_1,u_2],r,\omega\right)-A\left(h;[q_1,\infty],[m_2,\infty],[u_1,u_2],r,\omega\right) \\ &\quad\quad-\left\{A\left(h;[q_2,\infty],[m_1,\infty],[u_1,u_2],r,\omega\right)-A\left(h;[q_2,\infty],[m_2,\infty],[u_1,u_2],r,\omega\right)\right\} \end{aligned} \quad \text{(B.38)}$$

Using this, (B.36) then shows the validity of (B.15). This concludes the proof of (B.15) for the most general case.